TARGETING CANCER THERAPY: USING PROTEASE CLEAVAGE SEQUENCES TO DEVELOP MORE SELECTIVE AND EFFECTIVE CANCER TREATMENTS

by

MATTHEW T. BASEL

B.S., Kansas State University, 2007

AN ABSTRACT OF A DISSERTATION

submitted in partial fulfillment of the requirements for the degree

DOCTOR OF PHILOSOPHY

Department of Chemistry
College of Arts and Sciences

KANSAS STATE UNIVERSITY
Manhattan, Kansas

2010

Abstract

This paper describes two methods for utilizing cancer associated proteases for targeting cancer therapy to the tumor. The first method is designing a drug delivery system based on liposomes that are sensitive to cancer associated proteases. Upon contact with the protease, the liposome releases its contents. The second method is designing a prodrug that is based on a porin isolated from *Mycobacterium smegmatis*. The porin is modified with protease consensus sequences, inhibiting its toxicity. Upon contact with the protease, the drug is activated.

Protease sensitive liposomes were synthesized that were sensitive to urokinase plasminogen activator. This was done by synthesizing a cholesterol-anchored, uPA consensus – sequence-containing, acrylic acid block copolymer and using it to form a covalently bound polymer cage around the outside of a hypertonic liposome. Liposomes were synthesized that had a diameter of 136 nm. Upon addition of the polymer the diameter increased by 2.69 nm, indicating it had successfully embedded into the liposome membrane. After crosslinking with either a short peptide containing a lysine (so that it is a diamine) or ethylenediamine, the diameter increased between 5.33 nm and 14.1 nm (depending on the type and amount of the crosslinked). Fluorescence release assays showed that the polymer cage could add in excess of thirty atmospheres of osmotic pressure resistance, and, under isobaric conditions, would prevent release of much of the liposomal contents. Upon treatment with uPA, the polymer caged liposomes released a significantly larger amount of their contents making the liposomes protease sensitive.

MspA was shown to be a very stable protein able to be imaged by AFM. AFM imaging demonstrated that MspA is able to form native pore structures in membranes making it a good imitator of the membrane attack complex. MspA was demonstrated to be highly cytotoxic, but poor at distinguishing between cells. Pro-MspA was synthesized by adding a hydrophilic peptide to MspA that prevents insertion. A uPA cleavage sequence embedded causes the MspA to become activated at the cancer site. This was demonstrated in tests against uPA and non-uPA producing cell lines.

TARGETING CANCER THERAPY: USING PROTEASE CLEAVAGE SEQUENCES TO DEVELOP MORE SELECTIVE AND EFFECTIVE CANCER TREATMENTS

by

MATTHEW T. BASEL

B.S. Kansas State University, 2007

A DISSERTATION

submitted in partial fulfillment of the requirements for the degree

DOCTOR OF PHILOSOPHY

Department of Chemistry
College of Arts and Sciences

KANSAS STATE UNIVERSITY
Manhattan, Kansas

2010

Approved by:

Major Professor
Stefan H. Bossmann

Copyright

Abstract

This paper describes two methods for utilizing cancer associated proteases for targeting cancer therapy to the tumor. The first method is designing a drug delivery system based on liposomes that are sensitive to cancer associated proteases. Upon contact with the protease, the liposome releases its contents. The second method is designing a prodrug that is based on a porin isolated from *Mycobacterium smegmatis*. The porin is modified with protease consensus sequences, inhibiting its toxicity. Upon contact with the protease, the drug is activated.

Protease sensitive liposomes were synthesized that were sensitive to urokinase plasminogen activator. This was done by synthesizing a cholesterol-anchored, uPA consensus – sequence-containing, acrylic acid block copolymer and using it to form a covalently bound polymer cage around the outside of a hypertonic liposome. Liposomes were synthesized that had a diameter of 136 nm. Upon addition of the polymer the diameter increased by 2.69 nm, indicating it had successfully embedded into the liposome membrane. After crosslinking with either a short peptide containing a lysine (so that it is a diamine) or ethylenediamine, the diameter increased between 5.33 nm and 14.1 nm (depending on the type and amount of the crosslinked). Fluorescence release assays showed that the polymer cage could add in excess of thirty atmospheres of osmotic pressure resistance, and, under isobaric conditions, would prevent release of much of the liposomal contents. Upon treatment with uPA, the polymer caged liposomes released a significantly larger amount of their contents making the liposomes protease sensitive.

MspA was shown to be a very stable protein able to be imaged by AFM. AFM imaging demonstrated that MspA is able to form native pore structures in membranes making it a good imitator of the membrane attack complex. MspA was demonstrated to be highly cytotoxic, but poor at distinguishing between cells. Pro-MspA was synthesized by adding a hydrophilic peptide to MspA that prevents insertion. A uPA cleavage sequence embedded causes the MspA to become activated at the cancer site. This was demonstrated in tests against uPA and non-uPA producing cell lines.

Table of Contents

List of Figures

List of Tables

Acknowledgements

First, I would like to thank my major professor, Dr. Stefan Bossmann, and Dr. Deryl Troyer for encouragement, guidance, suggestions, and support throughout my doctoral program. Their mentorship has been extremely valuable to my development as a scientist.

Special thanks go to the members of my committee, Dr. Stefan Bossmann, Dr. Duy Hua, Dr. Kenneth Klabunde, Dr. Eric Maatta, and Dr. Deryl Troyer for devoting their time to mentoring me during my doctoral program.

Special thanks goes to Dr. Tej Shrestha who has given immeasurable help in suggestions and support for various organic synthesis during my doctoral program, especially his suggestions for how to synthesize the protease sensitive polymer and his work on optimizing the reaction conditions. Recognition goes to the other members of the Bossmann group as well, Thilani Samarkoon, Ayomi Perara, Dr. Hongwang Wang, and Dr. Pubudu Gamage who have each given me various amounts of support and friendship during my doctoral program.

I would like to thank Marla Pyle for constantly providing cells and for making excellent suggestions in cell culture experiments and for support in general on many research projects. I would like to thank our departmental technicians, James Hodgson, Tobe Eggers and Ron Jackson. These men have often taken crazy ideas that I've had and made them reality, and without them, many of my research projects would have floundered.

Special thanks go to Dr. Michael Niederweis and his laboratory at University of Alabama, Birmingham for supplying MspA for the MspA studies.

Finally, I would like to thank my lovely wife. She has given me immeasurable support and encouragement during all of my education and has been incredibly understanding during long hours, late nights and getting less of my time than she deserves.

1. Targeting Cancer

1.1. Current Cancer Therapy

Cancer is actually a collection of similar diseases that are marked by an uncontrolled proliferation of certain cells. Usually, this is caused by a series of genetic disruptions that prevent proper control of either cell division or apoptosis (Figure 1.1.1). This leads to rapidly increasing cell populations that invade the rest of the body, disrupting normal functions and producing toxic byproducts. Eventually, the disruption of normal functions and/or toxic byproducts grows to a point where the uncontrolled proliferation becomes lethal.

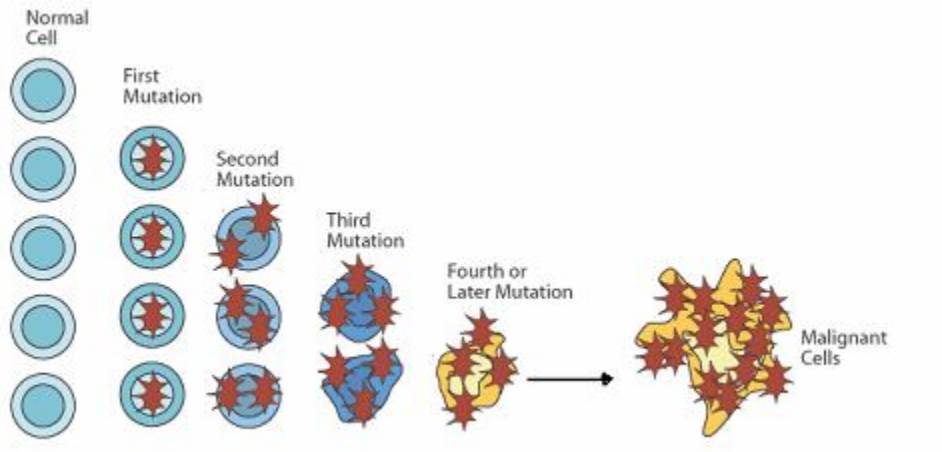

Figure 1.1.1 Cancer is caused by a build up of mutations in a cell line. Most healthy humans start with 0-1 mutations from the germ line. Over time mutagens add more mutations to various cell lines. Mutations that do not kill the cell, but provide a survival advantage can build up and cause cancer.

Although much advancement has been made in cancer therapy in the last several decades, cancer is still a poorly controlled disease with unsatisfactory treatment options. According to the NIH, nearly 1.5 million Americans will be newly diagnosed with cancer this year and over half a million will die from cancer, a mortality rate of almost 40%.[1] Malignant cancer was the second

leading cause of death in the United States in 2005 (the last year statistics are available), led only by cardiovascular disease.[2] The need for more effective treatment options is evident.

Current cancer treatments are focused mainly on targeting rapidly dividing cells, the common symptom of almost all cancers. The goal is that a short treatment with a drug that kills dividing cells will catch most of the cancer cells dividing, thus killing them, while only a small fraction of the body's normal cells will be dividing, sparing them from the drug's lethality (Figure 1.1.2).[3] Unfortunately, although most of the body's cells are dividing quite slowly, there

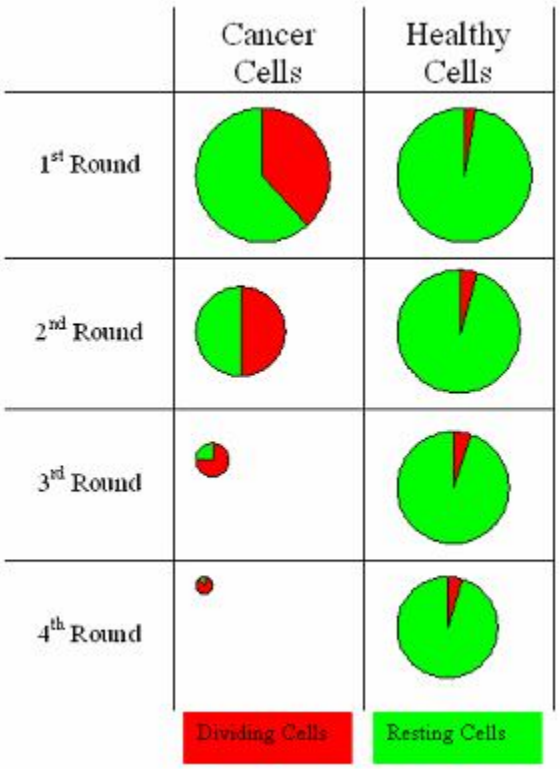

Figure 1.1.2 Many cancer therapies target cancer by targeting rapidly dividing cells. Since most cancers have a much higher percent of their population dividing at any given time versus healthy cells, a drug that kills dividing cells will select against cancer cells.

are certain cell types which do naturally divide very rapidly, including blood cell precursors (red and white), cells lining the mouth and digestive track, hair follicles and reproductive cells. These cells are also targeted by most current cancer chemotherapy

techniques, causing most of the well known cancer chemotherapy side effects – killing blood cell precursors leads to susceptibility to infection and lethargy, killing digestive track cells leads to upset stomach and diarrhea, killing the cells lining the mouth leads to loss of appetite and ability to taste, killing hair follicles leads to hair loss, and killing reproductive cells leads to sterility.[4]

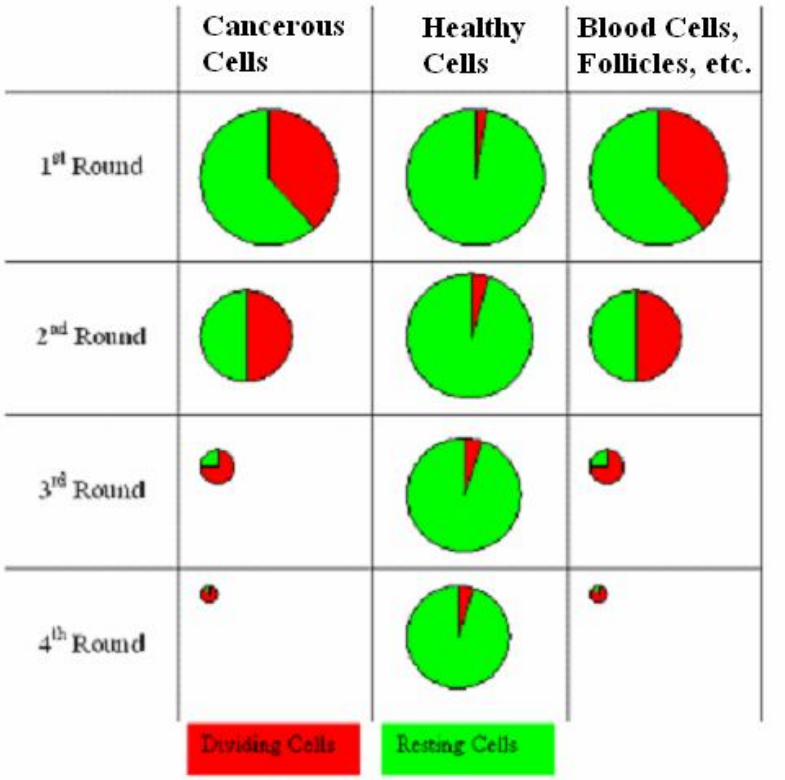

Figure 1.1.3 Although most healthy cells are not dividing rapidly, some subpopulations of healthy cells (e.g. blood precursors, follicles, etc.) do divide relatively rapidly. Thus, standard cancer therapy also selects against these cells causing many of the well known side effects.

Targeting cancer chemotherapy to the cancer cell better is a major goal of cancer therapy research today. Many techniques are being used to do this including drug delivery systems (delivering the drug more specifically to the tumor site), antibody targeted treatment (using antibodies to direct the drug to an antigen upregulated at the tumor site), metabolism targeted treatment (tagging the treatment with metabolites that are needed by the cancer cell to trigger

uptake), and proteome targeted treatment (targeting the protein signature of the cancer cell – either over or under expression of various proteins).

1.2. Cancer Markers – Differentiating Between Cells

One of the biggest challenges in cancer therapy is that cancer is a disease of the body's own cells. Because of this, it is often very challenging to diagnose cancer until the disease is quite progressed. This also affects treatment efficiency – since the cancer cells have the same enzymes, replication equipment, structural features, etc. as healthy cells, treatments that delineate cancer cells from healthy cells are hard to come by. This is why (as mentioned above), cancer is usually treated based on the symptom, rapidly growing cells and/or leaky vessels, rather than specifically targeting the cancer. Therefore, determining ways to distinguish cancerous cells from healthy cells is a large area of research in cancer therapy.

Many tumor biomarkers have been determined to date, and have been used mostly to diagnose cancer, to determine the prognosis (how far advanced is the tumor, what chance is there of curing it), and to determine the effectiveness of the treatment methods. Recently, though, cell surface antigens (proteins or protein fragments that are expressed on the outside of the cell membrane) that are cancer cell markers have been used to target antibody-drug conjugates to the tumor cells.

Most classic cancer biomarkers are not useful for targeting treatment to the cancer cell. This is because most classic cancer biomarkers are soluble markers, used for blood or serum tests. Also, classic biomarkers are usually proteins that are naturally occurring at a low level in the body (often proteins that are upregulated in the developing fetus and then downregulated in adulthood). Because there is some level of the biomarker naturally in the body, high occurrences of false positives and false negatives occur, making them unsuitable for treatment. One of the best cancer biomarkers known is prostate specific antigen (PSA). Associated with prostate cancer, PSA is a serine protease that is found in low levels in healthy men. Men with prostate tumors, either benign or malignant, show a large spike in blood concentration of PSA, making

PSA a very useful tool for early detection of prostate cancer. Unfortunately, since PSA is not attached to the cancer cells in any way, it can't be used for antibody targeted treatment. Another biomarker that has been effective in cancer treatment is cancer antigen 125 (CA-125). CA-125 is associated with ovarian cancer and, to a lesser degree, with breast cancer and is a cell surface protein that regulates adhesion of the cell. Over 80% of ovarian cancer patients show elevated levels of CA-125 in the serum. Although, CA-125 does not have the diagnostic power of PSA, due to the high range of values found in healthy women, the concentration of CA-125 can be used to develop a prognosis of the cancer, to determine the effectiveness of the treatment regimen, and to monitor for recurrence of the tumor after remission. CA-125 cannot be used as an antibody target, even though it is a cell surface antigen, because of the high concentrations often found in healthy women indicating that healthy cells express the protein as well. Other well known biomarkers include carcinoembryonic antigen (CEA), alpha-fetoprotein and human chorionic gonadotropin, although none of these has found a use in targeting treatments to the cancer cell, and are only useful for diagnosis or prognosis of the disease.[5,6,7]

Antibody targeting of tumors has found some success in cancer therapy, although, not by specifically targeting the cancer cells, but simply the tissue that the cells come from. The FDA has approved eight monoclonal antibody treatments for cancer: Rituximab targets CD20 (a surface antigen on B cells, for treatment of Non Hodgkin's Lymphoma), Trastuzumab targets HER2 (a metastatic breast cancer marker, for treatment of metastatic breast cancer), Alemtuzumab targets CD52 (a surface antigen on B and T cells, for treatment of Chronic Lymphocytic Leukemia), Bevacizumab targets VEGF (vascular endothelial growth factor, for treatment of metastatic colorectal carcinoma), Cetuximab targets EGFR (epidermal growth factor receptor, for treatment of metastatic colorectal caner), Tositumomab and Ibritumomab targets CD20 (a surface antigen on B cells, for treatment of Non Hodgkin's Lymphoma), and Gemtuzumab ozogamicin targets CD33 (a monomyeloid hematopoetic progenitor cell marker, for treatment of acute myeloid leukemia). All except the last three are pure antibody treatment, that is, the antibody is given alone and causes an immune reaction to the cancer cell. The last

three are antibody's conjugated to either a radioisotope (Tositumomab, Ibritumomab) or an immunotoxin (Gemtuzumab ozogamicin).[8]

Although, these antibody targeted treatments have been approved, they are not that effective for several reasons. First, the monoclonal antibodies, themselves, are not very cytotoxic and rely upon the immune system to recognize them and kill the cancer cell. Unfortunately, this only happens in ~5-15% of cases, making these treatments not very favorable. Also, the monoclonal antibodies are (by necessity) produced in non-humans (usually mice). This causes the body to recognize the antibody as foreign, which can lead to either simply removal from the body (rendering it ineffective) or causing an allergic reaction (which can prove fatal). Much work has been done on this, though, by making chimeric antibodies, where the F_{AB} fragment is from a mouse but the F_C fragment is human or various variations thereof. Finally, the antibodies are not cancer specific antibodies, but tissue specific antibodies. This means, the antibody does not target the cancer specifically, it targets the tissue that the cancer came from. Therefore, the antibody can also attack healthy non-cancerous tissue that comes from the same tissue as the cancer.[8, 9]

Since the main drawback to monoclonal treatment is the lack of cytotoxicity, the obvious answer is to conjugate something cytotoxic to the antibodies. This has been tried several times, but has yet to show excellent outcomes. The best outcomes come from conjugating a radioisotope to the antibody (Tositumomab, Ibritumomab). This is not that effective, though, because the amount of time the antibody spends in circulation before becoming trapped at the tumor site is quite long and allows a large portion of the radioisotope to break down before reaching the tumor, delivering unwanted radiation to the rest of the body and decreasing the dose of radiation that reaches the tumor. Conjugating a toxin to the antibody has been tried as well (Gemtuzumab ozogamicin). Again, since the antibody spends a lot of time in circulation before becoming trapped at the tumor site, the toxin can interact with many things, because the antibody does not prevent it from acting. This can have drastic side effects, up to and including death, depending on how powerful the toxin is. Finally, attaching chemotherapy drugs to the antibody

have failed miserably to this point, although attempts are still being made. This is primarily due to immune responses against the conjugate. Chemotherapy drugs are, for the most part, small molecules that should be highly immunoreactive, but are too small to be noticed by the immune system. Once they are conjugated to an antibody, they become considerably larger and they are easily recognized by the immune system, often with violent results.[8]

Although much more work can and is being done on antibody targeted treatments, they are not going to easily be the magic bullets in the fight against cancer. Other methods for targeting treatments to the cancer cell need to be found.

1.3. Proteases – Targeting the Proteome of the Cancer Cell

Although most tumor biomarkers have failed to produce a reliable and effective antibody targeted treatment, one class of biomarkers has the potential for a different type of targeted treatments – proteases (Figure 1.3.1). Proteases are a class of enzyme that catalyzes the cleavage of the peptide bond in other proteins. They can be very specific (only being able to degrade one peptide bond in one protein) or extremely broad (being able to cleave the peptide bond every time there is a lysine). Quite a few proteases are known to be necessary for cancer development and progression including Matrix Metalloproteinases (MMPs), Tissue Serine Proteases, and the

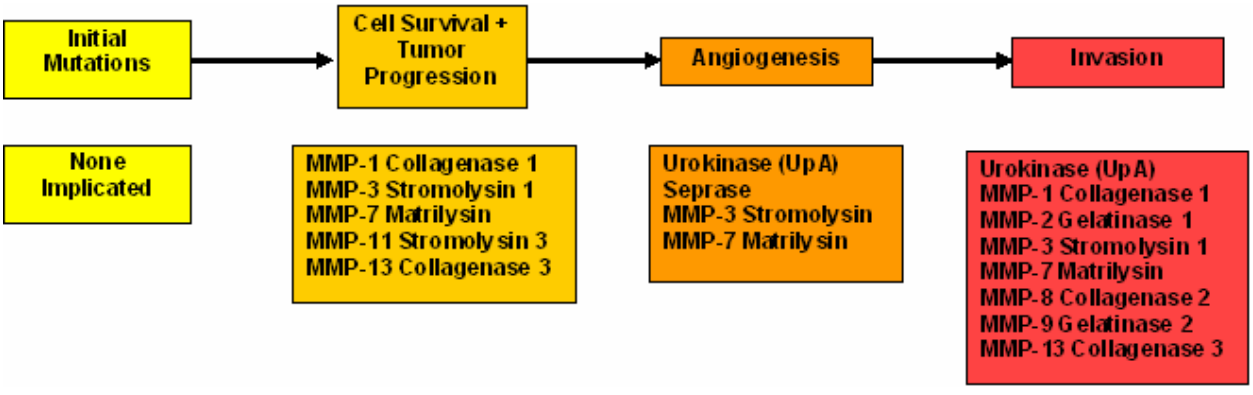

Figure 1.3.1 Proteases known in the progression of cancer

Cathepsins. Many of these proteases are either upregulated in cancer (that is they have a much higher activity in the tumor than in healthy tissue), are misexpressed (that is they are found in compartments where they should not be found), or are proteases that are involved in embryonic development, but are not found to any significant extent in an adult.[10]

Matrix metalloproteinases are the classic cancer associated proteases (Figure 1.3.2). MMPs are a family of zinc proteases that are named for the zinc and calcium ions that are required as cofactors. There are 21 different known MMPs that are grouped into families based on their substrates: collagenases, gelatinases, stromelysins, matrilysin, metalloelastase, enamelysin, and membrane-type MMPs. As can be seen from the family names, MMPs degrade the proteins that make up the extracellular matrix (ECM) and the basement membrane (BM). Interestingly, MMPs are usually not produced by the cancerous cells themselves, but by the stromal cells surrounding the tumor. This is because the cancerous cells give off a variety of cell

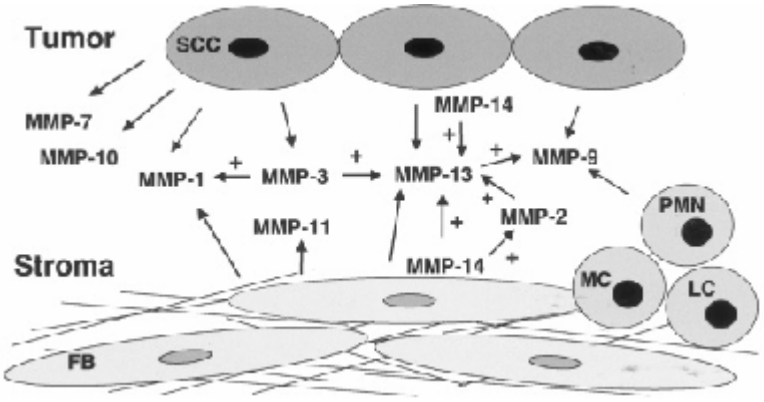

Figure 1.3.2 MMP upregulation by the tumor and surrounding cells

signals that cause the surrounding stromal cells to highly upregulate their production of MMPs. MMPs are vital to cancer survival and progression for several reasons – they cleave cell surface bound growth factors from the stromal and epithelial cells and release them to interact with the cancer cells to stimulate growth, they play a role in angiogenesis by opening the ECM to new vessel development and by releasing pro-angiogenic factors and starting pro-angiogenic

protease cascades, and they play a major role in tumor metastasis by degrading the ECM and the BM allowing the cells to pass through and releasing ECM and BM fragments which stimulates cell movement. MMPs are not perfectly specific, they usually cleave several related proteins, but consensus sequences (the sequence of amino acids that a protease targets) have been determined for several MMPs and are shown in table 1.3.1, allowing peptides to be created that are selectively cleaved by the target MMP.[10, 11, 12, 13, 14, 15]

Several serine proteases have well-documented roles in cancer as well, especially urokinase plasminogen activator (uPA) and plasmin (Figure 1.3.3). uPA has actually been used with excellent success as a prognostic marker for breast cancer. uPA is a very specific protease that binds to its receptor, uPAR, and cleaves the inactive plasminogen to the active plasmin. This is the first step in a well known cascade that causes angiogenesis and uPA is associated with angiogenesis in tumors, although it is also very active in tumor metastasis. Plasmin is a somewhat non-specific protease that goes on to cleave many things including activating procollagenases, degrading the ECM, and releasing/activating growth factors. Although plasmin is somewhat non-specific and a consensus sequence is hard to determine, uPA does have a well defined consensus sequence shown in table 1.3.1.[10, 11, 15, 16, 17]

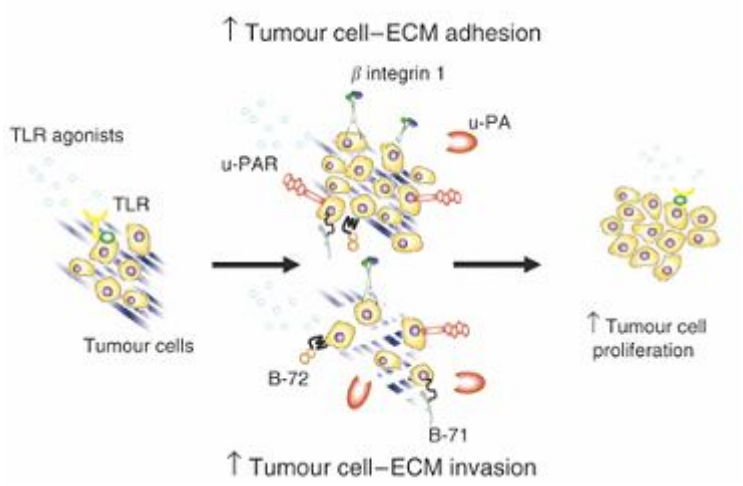

Figure 1.3.3 Urokinase Plasminogen Activator and Cancer Progression

Cathepsins, with a few exceptions, are cysteine proteases. Often found in the lysosomal/endosomal pathway, cathepsins usually operate at low pH values, but some are still active at neutral pH. Three of the cathepsins (B, D, and L) that are active at neutral pH are often misexpressed in cancer, causing activation outside of the cells. This activation outside of the cell can cause ECM degradation, initiate known ECM degradation cascades, cathepsin B is known to activate uPA, and cathepsin D is known to activate Insulin-like Growth Factors. Consensus sequences have been found for cathepsins B, D and L and are shown in table 1.3.1.[10, 11, 18, 19]

The proteases with known consensus sequences that are activated at the tumor site can be used to target therapy. To date this has been primarily done with pro-drug activation through cleavage by one of the proteases. In 2001, Liu et. al. demonstrated an anthrax toxin that was made sensitive to uPA by replacing the cleavage sequence for furin with the cleavage sequence for uPA. This caused the anthrax toxin to only be activated by uPA producing cells.[17] In 2003, Thor proposed a ricin toxin that could be activated by many of the proteases depending on the sequence inserted. Ricin A-chain was connected to the B-chain through the protease consensus sequence. Only at protease producing cells would the A-chain and B-chain be separated, activating the toxin.[18] In 2007, Warnecke et. al. demonstrated a modified form of methotextrate that could be cleaved and activated by plasmin or cathepsin B.[20] The initial success of targeting cancer treatment to the cancer cell through the proteases the cancer cell expresses invites more interest in this topic.

Table 1.3.1 Consensus Sequences of Several Well Characterized Cancer Associated Proteases

MMP	Consensus
MMP-1	VPMS-MRGG
MMP-2	IPVS-LRSG
MMP-3	RPFS-MIMG
MMP-7	VPLS-LTMG
MMP-9	VPLS-LYSG
MMP-11	HGPEGLRVGFYESDVMGRGHARLVHVEEPHT
MMP-13	GPQGLA-GQRGIV
MT1-MMP	IPES-LRAG
uPA	SGR-SA
Cathepsin B	SLLKSR-MVPNFN
Cathepsin D	SLLIFR-SWANFN
Cathepsin L	SGVVIA-TVIVIT

2. Protease Sensitive Liposomes

2.1. Literature Review

2.1.1. Liposome Discovery

Liposomes were first described in 1961 (published 1964) by Alec Bangham while trying to determine a valid way to view lipid leaflets in the electron microscope. Bangham prepped various mixtures of ovolecithin (a mixture of phospholipids derived from egg yolk), lysolecithin (lecithins that have been hydrolyzed to lack the C2 carbon chain, thus they posses lyctic activity against lipid bilayers), cholesterol, and/or saponin (any of a variety of plant derived sterols) (Figure 2.1.1) by dissolving the various mixtures in cholesterol, drying, hydrating in water and then suspending the lipids through either hand shaking or sonication.

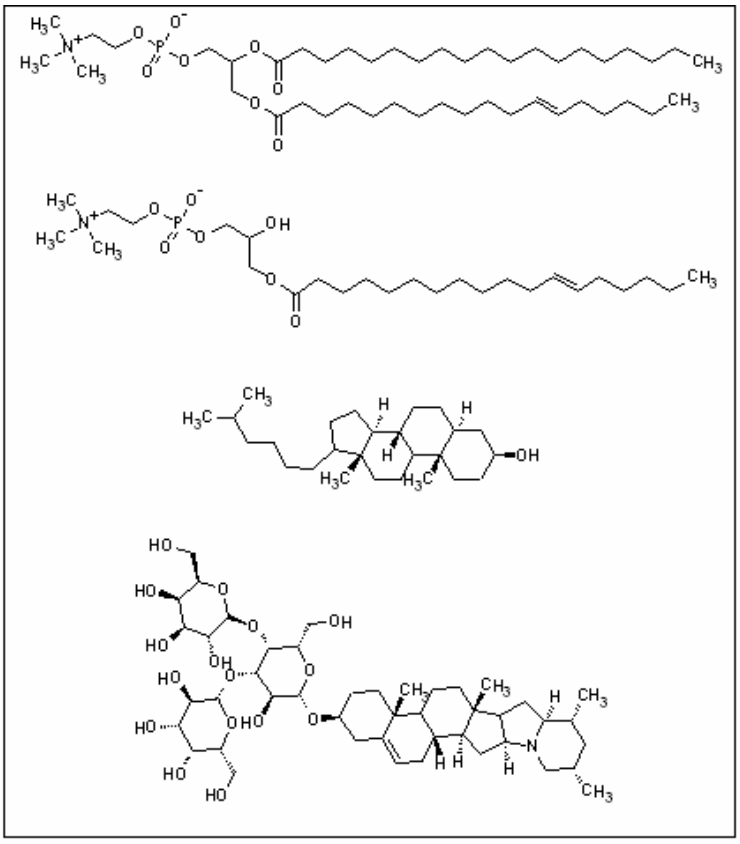

Figure 2.1.1 From top to bottom: 2-Palmitoyl 3-oleoylphosphatidylcholine, a common component of ovolecithin; 3-oleoylphosphatidylcholine, a common lysolecithin, cholesterol, and saponin.

When viewed in the electron microscope (negatively stained with potassium phosphotungstate), Bangham found that the lecithin and mixtures of lecithin and cholesterol formed spherical, multilayered particles of approximately 120 nm, similar to an onion (Figure 2.1.2). Lysolecithin did not show these multi-lamellar spheres, but rather homogenous 7 nm spheres, very typical of micelles, indicating that the lecithin structures were, in fact, significant and different from micelles.[1]

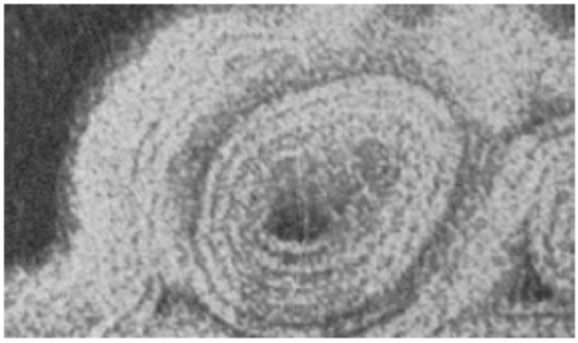

Figure 2.1.2 Bangham's lecithin only preparation as viewed in the electron microscope showing a multilamellar spherulite

Bangham called the spherical, onion-like particles, spherulites, and determined that they were three-dimensional, enclosed, multi-walled spheres of lipid with water entrapped inside (Figure 2.1.3). Treating these spherulites with lysolecithin or saponin broke down the structure and reverted to something more like micelles.[1]

Bangham's spherulites quickly became popular and were renamed liposomes. Liposomes (Figure 2.1.4) consist of a double layered membrane of phospholipids (often containing up to 50% cholesterol) that form in the presence of excess water. The membrane wraps around to form a closed, sphere defining an interior and an exterior compartment.[2] Bangham showed that the interior compartment would have the same composition (solutes, etc.) as the exterior compartment which it was made in, as long as the solute is small enough to fit in the interior compartment.[1] Liposomes were quickly shown to be substantially similar to

naturally occurring membranes[3,4] and thus resistant to leakage of polar molecules (that is, molecules that could not easily adapt to the hydrophobic interior of the membrane).[5,6]

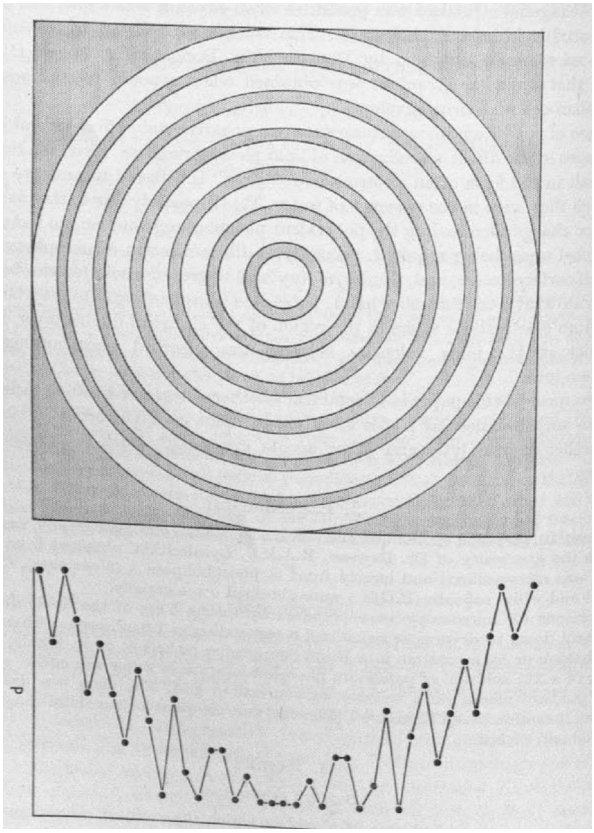

Figure 2.1.3 Bangham's drawing of the multi-lamellar membranes enclosing multiple compartments. The graph shows the densities across the spherulites, demonstrating that they are three dimensional

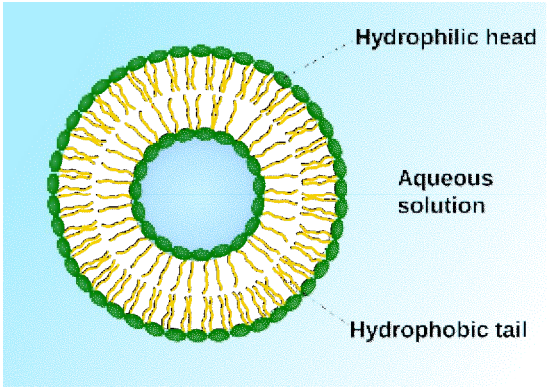

Figure 2.1.4 Phospholipids arrange themselves into a spherical bilayer to form a liposome.

2.1.2. Biological Uses of Liposomes

Since liposomes (and the solutes that they trapped inside), could be separated from smaller, drug-like molecules simply by gel filtration or dialysis, the medical usefulness of the liposome soon became evident.[2,7] Liposomes could regulate how quickly their contents were cleared from the body and where they ended up in the body, thus making excellent dosing and targeting regulators.[8,9] Studies showed that the liposomes were stable in blood, not releasing their contents,[10, 11, 12, 13, 14, 15] and when incubated with plasma constituents, they retained their spherical shape,[16] although some small molecules (such as 5-fluoruracil or penicillin-G) were able to leak out through the membrane.[17]

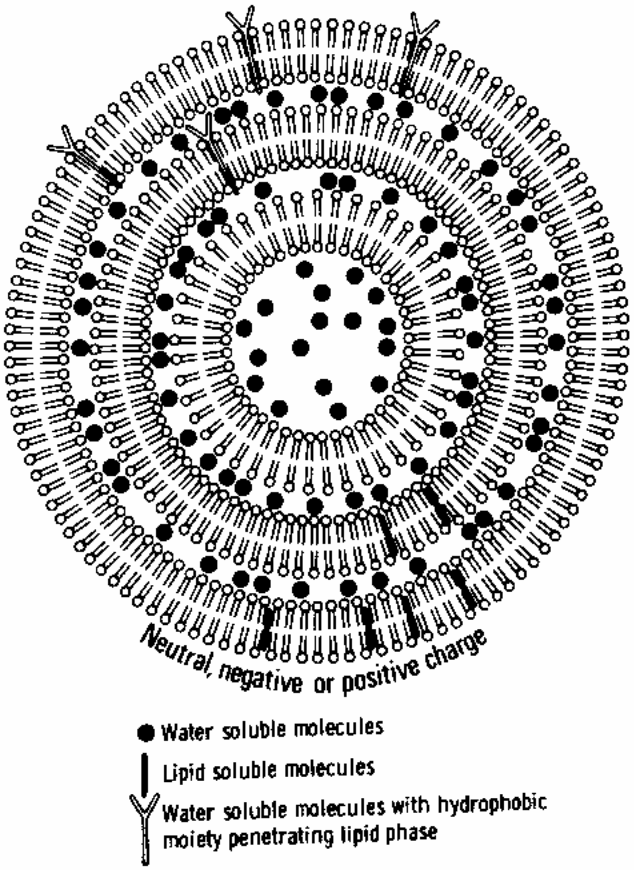

Figure 2.1.5 A multilamellar liposome with entrapped hydrophilic or hydrophobic molecules.

Some problems with *in vivo* use became evident, though, because the liposomes were quickly removed from the body, primarily by the reticuloendothelial system.[10, 17, 18, 19] However, liposomes made with positively charged lipids lasted much longer *in vivo* than liposomes made with neutral or negatively charged lipids. When delivered intravenously, liposomal contents primarily ended up in the liver and the spleen, with smaller concentrations being delivered to the kidneys and lung, although, in some tests, this accounted for less than one percent of the delivered drug, with the majority being excreted in the feces.[10, 20, 21, 22, 23, 24, 25, 26]

Some of the problems of quick removal were solved by using better defined preparations of lipid to make the liposomes. Liposomes made from dipalmitoylphosphatidylcholine delivered a greater dosage of their contents than those made from undefined ovolecithin and this was hypothesized to be due to lower rates of hydrolysis of the dipalmitoylphosphatidylcholine compared to ovolecithin.[27] Also, quick removal of the liposomes by the macrophages and monocytes of the reticuloendothelial system could be prevented by attaching a polyethylene glycol coating to the outside of the liposome (Figure 2.1.6). Polyethylene glycol apparently creates a steric block around the outside of the liposome that does not interact with recognition molecules. Since the polyethylene glycol does not interact with recognition molecules and it prevents the recognition molecules from reaching the liposomal surface, the liposomes are ignored by the reticuloendothelial system. This preparation (liposomes coated in polyethylene glycol) has come to be known as stealth liposomes because of their ability to evade the reticuloendothelial system.[28]

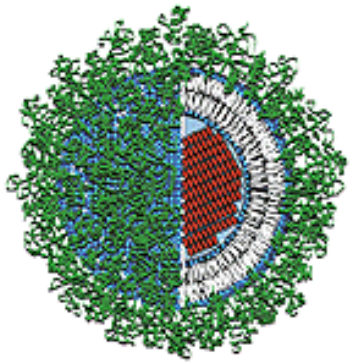

Figure 2.1.6 A stealth liposome showing the polymer coating

Although liposomes made from bovine brain phospholipids have been shown to have various unwelcome side-effects, liposomes made from most standard lipids do not show negative side effects in the body.[30]

2.1.3. Drug Delivery Systems

Many very useful drugs are generally toxic to the body, and can cause havoc when they interact with systems other than what they are targeted for. An obvious solution to this problem would be to deliver the drug directly to the desired site, not allowing it to come in contact with the rest of the body, insuring that there is no indiscriminate toxicity. To do this, drug delivery systems have been developed.[31,32]

Drug delivery systems can overcome a variety of delivery and pharmacokinetic problems including poor pharmacokinetics, quick clearance or breakdown of the drug, poor solubility, unwanted general toxicity, or unwanted specific toxicity.[32] A well known drug delivery system is Nicoderm, which, along with Nicotrol and Prostep are transdermal patches which release nicotine into the body creating a much better pharmacokinetic profile for cessation of smoking.[33,34] Other drug delivery systems include Zolodex (an injectable polymer rod), Lupron, and Decapeptyl (both injectable polymer spheres), which have all been approved for use in long term delivery (better pharmacokinetics) of LHRH analogs to prostrate cancer.[35, 36, 37] Oncaspar, PEG intron, and Neulasta are pegylated drugs (l-asparaginase, α-interferon, G-CSF) that allow the drug to stay in circulation for a much longer period of time.[32] Gliadel, an implantable wafer doped with BCNU, is used to control drug delivery to malignant gliomas.[38]

All of the above drug delivery systems have no targeting effect, they are physically placed where the drug is desired (or, for the transdermal patches, the drug is delivered systemically). In some cases, a targeting effect of the delivery system is desired because it is impractical or impossible to physically place a delivery device next to the target area. The optimal drug delivery system would: 1) target the desired area, delivering the drug to the target

area and not systemically; 2) be easily administratable; and 3) release the drug in a way to maximize pharmacokinetic efficiency.

2.1.4. Liposomes as Drug Delivery Systems

Liposomes can make excellent drug delivery systems.[39, 40, 41] They can carry large payloads of both hydrophilic (in the interior) or hydrophobic drugs (in the membrane) drugs. The membrane makes it very hard for the drug to diffuse out of the liposome, so they deliver very little of the drug systemically. Liposomes are, themselves, non-toxic, and fortunately they naturally target tumor sites. This build up, known as the EPR (Enhanced Permeation Retention) effect (Figure 2.1.7), is due to the leakiness of the blood vessels surrounding the tumor allowing the liposomes to extravagate into the tumor site. The tumor is leaky because its nutritional needs lead it to rapidly develop new blood vessels without much quality control. The tumor does not develop the lymphatic drainage system, though, meaning substances that enter the tumor site get trapped there. This becomes like a small pool off of a big river – as debris floats down the river, it can float into the little pools to the side of the river and get stuck there, because there is no longer any current to continue moving the debris. Thus, to reduce general toxicity, highly toxic chemotherapy drugs can be encapsulated in a liposome, where they will be prevented from interacting with healthy tissue and build up in cancerous tissue.[31]

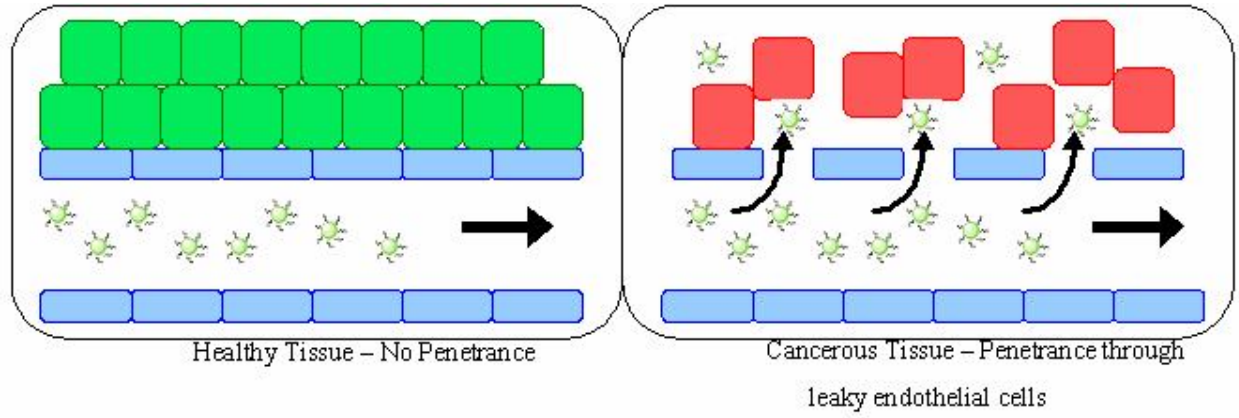

Figure 2.1.7 EPR Effect. Blue cells are endothelial cells lining the blood vessels. Red cells are cancer cells and green cells are healthy cells.

Although, liposomes demonstrate potential as drug delivery systems for cancer chemotherapy, there are a few continuing challenges. First, although the drug builds up in the tumor, it is still encapsulated in the liposome. The liposome must release the drug and let it interact with the cells to be of much use. Although, this does eventually happen, it is a slow process, and hampers the effectiveness of the drug, leading to increased dosages to achieve the target level of the drug. This slow leaking also happens in the rest of the body, so the drug is still delivered at low doses to the rest of the body. Increased dosages leads to increased non-discriminate leakage, which can cause the side effects that liposomes were created to prevent. Second, the liposome is not targeted specifically to the tumor. Although, less prevalent than at tumor sites, liposomes are able to leak through the blood vessels at non-cancerous sites, delivering the drug to unwanted parts of the body.[42, 43]

Extensive research has been done trying to solve these problems, especially focusing on immunoliposomes – liposomes conjugated to an antibody that recognizes the tumor cell. The antibody causes the liposomes to become trapped at the cancer site, because they are targeted to a cancer antigen. The antibody also encourages uptake of the liposomes by the cancer cells. Although, this method sounds good on paper, finding antibodies that distinguish healthy cells from cancer cells is quite challenging and, even if suitable antibodies are found, the antibodies themselves become a target of the RES system.[44, 45] Other targeting techniques have been tried including, heat sensitive liposomes, pH sensitive liposomes, and metabolism targeted liposomes, although, the 'magic bullet' has not yet been found.[45, 46, 47]

2.1.5. Tonicity and Osmotic Pressure

Due to the tendency of systems to move toward equilibrium, solutions with high solute concentrations will tend to move solute molecules to solutions with low solute concentrations when they are in contact with each other. When movement of the solute particles is inhibited, the solvent will move from one solution to the other to move the systems toward equilibrium.

This movement of water is called osmosis. Because osmosis is a thermodynamically favored event, water, in osmosis, can actually flow against pressure gradients, until the entire system is at equilibrium; this is called osmotic pressure. This can be easily demonstrated (Figure 2.1.8) by placing a semipermeable membrane (a membrane that is permeable to water, but impermeable to most solutes) in a U shaped tube and placing a concentrated solution on one side of the membrane and a dilute solution on the other. Water from the dilute solution will flow through the membrane to the concentrated solution diluting it (and concentrating the dilute solution) until the osmotic pressure of the water is equal to the gravitational pressure of the water due to the height difference on either side of the tube.[48]

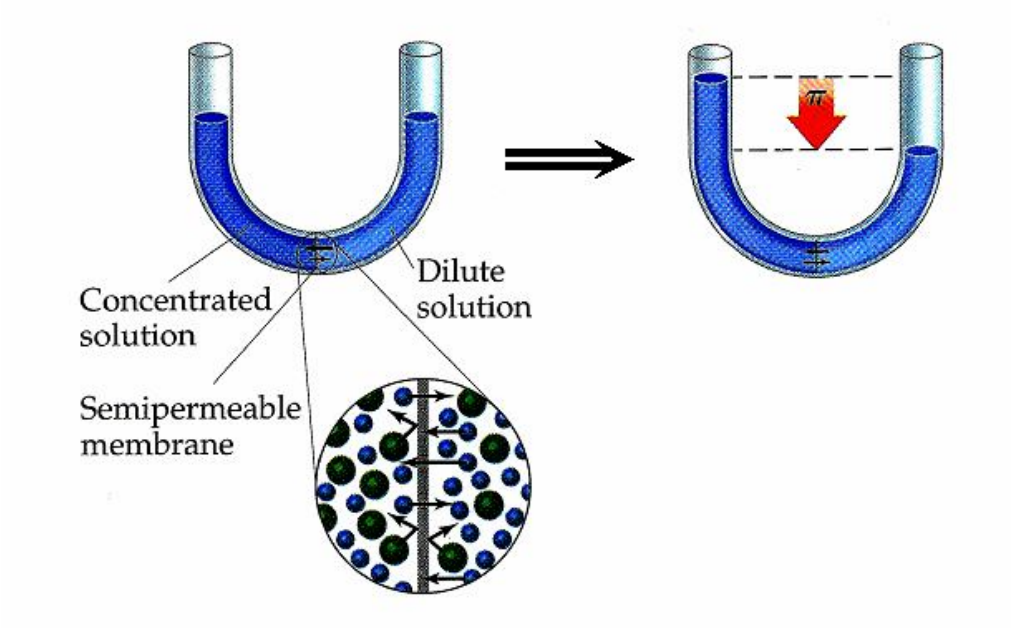

Figure 2.1.8 A demonstration of osmotic pressure. The tube on the left is pre-equilibrium. The tube at the right is in equilibrium, showing that, at equilibrium, the system has developed gravitational pressure that balances the osmotic pressure

The osmotic pressure of a system can be calculated using the equation:

$$\Pi = RT \Sigma (i_x M_x) \quad (1)$$

where Π is the 'absolute' osmotic pressure, R is the gas constant, T is the absolute temperature, i is the van't hoff factor which, usually, equals the number of discrete particles the substance dissolves into, and M is the molarity of the solution. The actual pressure exerted across a semipermeable membrane can be calculated by subtracting the 'absolute' osmotic pressure of the higher concentration from the 'absolute' osmotic pressure of the lower concentration side, $\Pi_1 - \Pi_2$.[49]

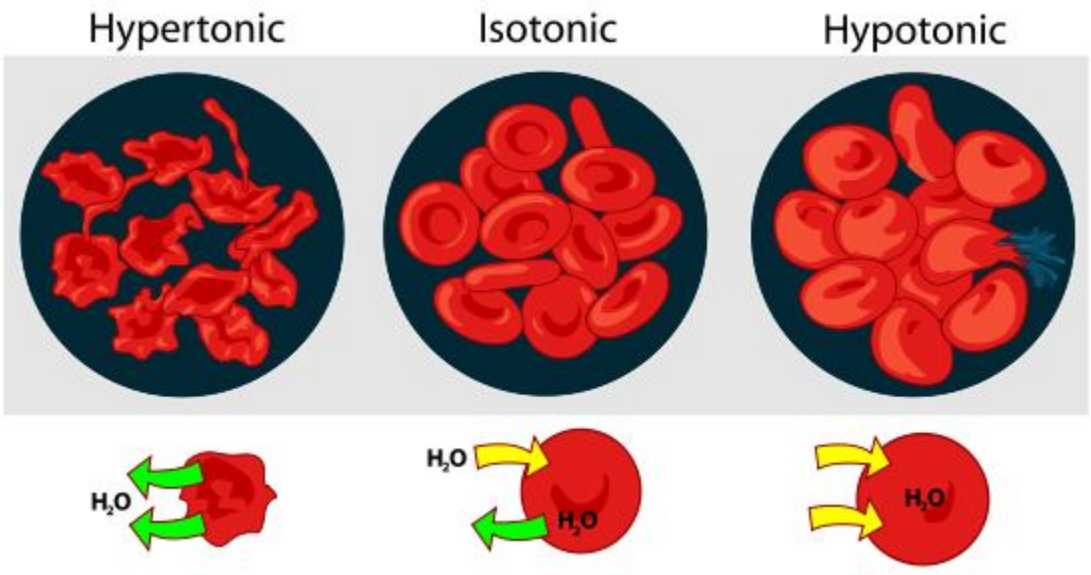

Figure 2.1.9 Red blood cells in hypertonic, isotonic and hypotonic solutions, demonstrating how they shrink or swell

Osmotic pressure is very important in biological systems as they are filled with high solute concentrations and semipermeable membranes. Phospholipid membranes act as semipermeable membranes because they are resistant to ionic and polar compounds and large compounds, but allow small, non-polar compounds to cross freely. Due to the large concentration of water and its small size, water can cross phospholipid membranes in biological systems, but most normal biological solutes cannot. Since cells are defined by a phospholipid membrane, they must be very careful to regulate the osmotic pressure across their membranes. If the osmotic pressure becomes too high either direction, it can destroy the cell (Figure 2.1.9).

When the cell is hypertonic (higher concentration of solutes unable to cross the membrane) compared to the interstitial fluid, the cell can swell and burst due to the pressure of the water flowing in pushing out on the membrane. When a cell is hypertonic compared to the interstitial fluid, the cell can shrivel do to loss of interior pressure on the membrane from the water flowing out.[49]

2.1.6. Liposomes and Osmotic Pressure

The outer membrane of a liposome acts as a semipermeable membrane that allows water to pass through, but resists letting most hydrophilic solute molecules pass through, similar to a cell membrane. Thus, liposomes are sensitive to osmotic pressure. Liposomes that are hypotonic comparatively to the exterior compartment will shrink, while liposomes that are hypertonic will expand and may burst.[50]

Theoretical studies on liposome swelling, pore formation, and bursting have determined that total destruction of a liposome is very unlikely. More likely is the formation of pores in the membrane which allow efflux of the osmotically active substance, balancing the osmotic pressure. The pressure at which this should occur can be derived theoretically from equation 1 above. Taking $\Delta\Pi$ to equal $\Pi_1 - \Pi_2$, the influx of water into a hypertonic liposome should be:

$$q_{inf} = L_p S(\Delta\Pi - \Delta P) \quad (2)$$

where q_{inf} is the influx of water, L_p is the permeability coefficient of the membrane to water, S is the membrane area, and ΔP is pressure from the membrane being stretched.[50]

ΔP can be determined from the following equation:

$$\Delta P = 4\,(\Gamma/R_0)\,(\Delta S/S_0) \quad (3)$$

where Γ is the elastic constant for the membrane (~100 - 1000 dyn/cm), R_0 is the initial radius, ΔS is the change in membrane area, and S_0 is the initial membrane area. When $\Delta P = \Delta\Pi$, the influx of water stops because the pressure exerted by the membrane equals the excess osmotic pressure. To relieve strain, on the membrane, the membrane may form pores. When and how these pores are formed can be calculated theoretically as well.[50]

Influx of water can also be expressed as:

$$q_{inf} = d\Delta V/dt \quad (4)$$

where ΔV is the change in volume of the liposome and t is time. Taking into account equations 2 and 3 above, ΔV can be calculated with respect to time:

$$\Delta V = (\Pi/2)\ (R_0^4 \Delta\Pi / \Gamma)\ [1-\exp(-8\ L_p\ \Gamma\ t / R_0^2)] \quad (5)$$

From the equation, the maximum expansion of the membrane (ΔV_{max}) and the time it takes to expand (t_{max}) can be determined:

$$\Delta V_{max} = \Pi\ R_0^4 \Delta\Pi / 2\ \Gamma \quad (6)$$

$$t_{max} = R_0^2 / -8\ L_p\ \Gamma \quad (7)^{50}$$

In cases with large excess osmotic pressure, though, the membrane is unable to expand to the size necessary for $\Delta P = \Delta\Pi$ without breaking. The energy of an expanded membrane can be calculated from:

$$\omega = \Gamma\ (\Delta S)^2/S_0 \quad (8)$$

where ω is the energy of the membrane. Formation of a pore also requires energy, because the pore must either expose the hydrophobic core of the membrane to water, or have a very sharp curvature to prevent water from reaching the hydrophobic core. The energy of pore formation can also be calculated from:

$$\omega_p = 2\pi\gamma r \quad (9)$$

where ω_p is the energy of the curvature of the pore, γ is the linear tension of a pore (~2 x 10^{-6} dyn), and r is the radius of the pore.[50]

The energy of a membrane (ϕ) that is originally expanded ΔS and then forms a pore with area A has the following energy:

$$\phi = \Gamma\ (\Delta S - A)^2/S_0 + 2\ \gamma\ \mathrm{sqrt}(\pi A) \quad (10)$$

being equation 8, modified by the loss of area of the pores, plus equation 9. If ΔS is known, then the only unknown is A, the area of the pore. The system 'chooses' A in order to minimize the energy of the system.[50]

Calculations show that at low ΔS values, pore formation is always unfavorable (curve 1 above). At larger ΔS values, a minimum appears on the ϕ vs. A curve, indicating that the formation of pores is favorable (Figure 2.1.10).

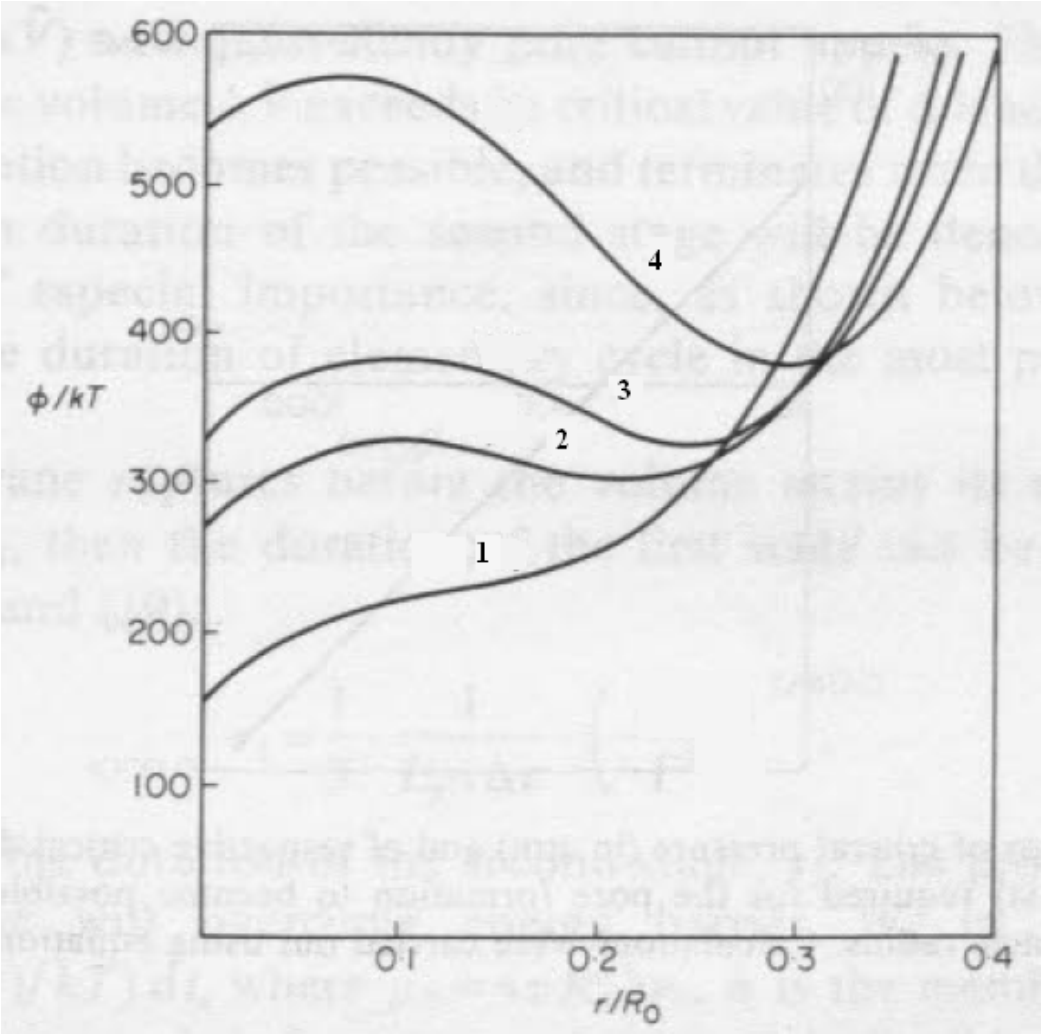

Figure 2.1.10 The dependence of the vesicle energy on the pore radius for a vesicle of the radius of 40 nm, Γ =0.1 J/m^2, γ =2 X10^{-11} N; curves are parameterized by the relative excessive volume: (1) ΔV/Vo=2.25%, (2) ΔV/Vo=3%, (3) ΔV/ Vo=3.3%, (4) ΔV Vo=4.2%.

A minimum value of ΔS (and thus ΔV) and A (and thus r) have to be met for pore formation to be favorable. The minimum values are given by:

$$\Delta S_{min}/S_0 = (3/4)\,(\gamma / \Gamma R_0)^{2/3} \quad (11)$$

$$\Delta V_{min}/S_0 = (9/8)\,(\gamma / \Gamma R_0)^{2/3} \quad (12)$$

$$A_{min}/S_0 = (1/4)\,(\gamma / \Gamma R_0)^{2/3} \quad (13)$$

$$r_{min}/S_0 = (\gamma / \Gamma R_0)^{1/3} \quad (14)$$[50]

Using these equations, the membrane pressure at which pore formation can happen (ΔP_{min}) is given by:

$$\Delta P_{min} = (3\,\Gamma / R_0)\,(\gamma / \Gamma R_0)^{2/3} \quad (15)$$

If $\Delta\Pi > \Delta P_{min}$ then it would be expected that the liposome would form pores (as long as the liposome can temporarily absorb enough energy from the surroundings to overcome the barrier energy of pore formation, given by:

$$\omega_0 = (3\pi / 4)\,(\gamma^4 R_0^2 / \Gamma)^{1/3} \quad (16)$$

where ω_0 is the barrier energy).[50]

Pore formation does not instantly bring the system into equilibrium, though. The residual membrane pressure (ΔP_r), causes the osmotically active substance to leak out through the pores, returning the system to equilibrium:

$$\Delta P_r = 2\,\gamma / R_0\,r \quad (17)$$

$$q_{eff} = \Delta P_r\,r^3 / \eta \quad (18)$$

where q_{eff} is the efflux of the osmotically active substance and η is the viscosity of the solution.[50]

Thus, if $\Delta\Pi > \Delta P_{min}$ then the entrapped osmotically active substance will leak out of the liposome into the solution. To prevent leakage, $\Delta\Pi \leq \Delta P_{min}$ or an external pressure source pushing in on the liposome must be introduced with:

$$P_{ext} \geq \Delta\Pi - \Delta P_{min} \quad (19)$$

and thus:

$$\Delta\Pi \leq \Delta P_{min} + P_{ext} \quad (20)$$

2.1.7. Osmotic Pressure and Drug Delivery

Acquired drug resistance is a major obstacle in cancer therapy. Acquired drug resistance is when the drug being used was once effective against the cancer, but the cancer has developed a resistance to the drug, rendering it ineffective. A major mechanism of acquired drug resistance is drug transport, either a mechanism where the cell transports the drug out of the cell once it penetrates, or a mechanism where the cell does not allow the transport of the drug into the cell. Devising a mechanism to overcome this acquired drug resistance would greatly increase the effectiveness of chemotherapy.[51, 52]

An effective way to overcome both types of drug transport resistance would be to deliver the drug directly inside of the cancer cell in large enough doses to overwhelm the drug transporters. Liposomes are an excellent candidate to pursue for direct drug delivery because they have the potential to fuse membranes with the target cell, releasing the entrapped drug into the cell (Figure 2.1.12).[53]

Although liposomes do naturally fuse with cell membranes, fusion is very slow because it is a kinetically hindered process – both membranes are in kinetically locked states. In fact, it happens so slowly that most of the drug leaks out of the liposome before it fuses with any membranes, making this fusion useless to cancer therapy.

Liposomes can be made to swell when a sufficient osmotic gradient is applied across the membrane.[54, 55] In 1982, Cohen, et. al. demonstrated that causing a liposome to swell when it is near a planar membrane can cause rapid fusion with the membrane. This is because the kinetically locked state of the membrane is disturbed by the swelling, enhancing the rate of fusion (a thermodynamically favored process).[56] Two years later, Cohen demonstrated that swelling liposomes fused with cell membranes. It was determined that a gradient of at least 200 mosM was necessary for fusion and that the rate of fusion increased with increasing gradients to the point where the liposome burst. Thus, liposomes that can be made to swell at the cancer site could be excellent drug delivery vehicles to overcome a basic drug resistance mechanism.[57]

2.1.8. Polymer Caged Liposomes

Liposomes that deliver their contents when presented with a certain trigger are highly sought after for targeting various diseases. In 2007, Lee et. al. described a method for coating liposomes in a cross-linked polymer shell. The cross-linked polymer shell caused the liposomes to be sensitive to pH, delivering their contents at low pHs. Lower pH is known to be associated with cancer cells due to their irregular glycolysis and respiration. Unfortunately, the polymer caged liposomes (PCLs) did not release their contents until pH 2, while most tumor sites rarely get below 1 pH unit below physiological pH (~7.4).[58]

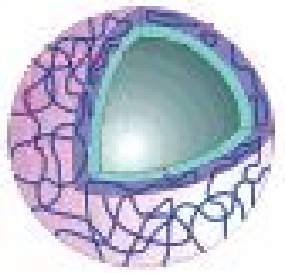

Figure 2.1.11 Polymer Caged Liposome

The polymer cage was not a total loss, though. The cross-linked polymer did make the liposomes much more stable including preventing dissociation of the polymer from the membrane, preventing liposome degradation upon freezing or drying, and drastically slowed the natural leak of contents from the liposome. PCLs may have a future in drug delivery due to their extremely stable properties. If a suitable trigger can be found, PCLs could be the perfect delivery mechanism.[58]

2.1.9. Protease Sensitive Liposomes

In 2008, D. K. Srivasta's group at North Dakota State University and Sanku Mallik's group at University of North Dakota published a method for preparing liposomes that were sensitive to MMP-9 (gelatinase). Shorts sequences of collagen were covalently modified with

lipids on their N-terminal ends and incorporated into liposomes through absorption. MMP-9 was shown to trigger release of the liposomal contents.[59] It is theorized that this release is triggered by MMP-9 distorting the triple helical structure of collagen during cleavage, distorting the membrane at the base of the sequences. The distortion caused micropores to form in the membrane, releasing the contents.[60]

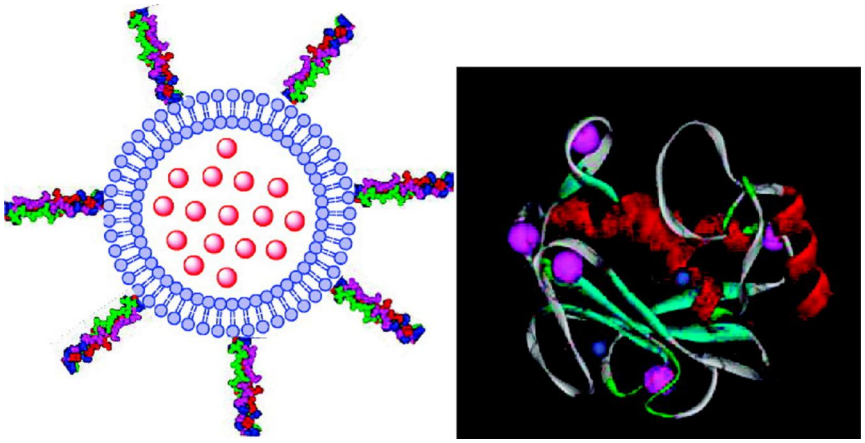

Figure 2.1.12 MMP-9 sensitive liposome showing the triple helical structure extending from the surface of the liposome. Inset – MMP-9

Due to the mechanism of release, this method can only be used for collagenases (including gelatinases). Other cancer associated proteases will not be able to use this mechanism because they cannot cleave multiple strands at once and do not cause major distortions in the three dimensional structure of short peptides during cleavage.

2.2. Methods and Theory

2.2.1. Liposome Preparation

Liposome preparation has remained, for the most part, substantially similar to the preparation used by Bangham when he discovered liposomes. The basic process has five steps (Figure 2.2.1). First, dissolve the lipids and cholesterol in an organic solvent in the desired ratios. Next, evaporate the solution to dryness, making sure to fully remove all of the organic solvent, leaving a thin layer of mixed lipid/cholesterol on the bottom/sides of the container. Third, add an aqueous solution containing any molecules that are to be trapped in the liposome. Fourth, disperse the lipid film into the aqueous solution. Finally, separate the liposomes from the unentrapped solution.[1]

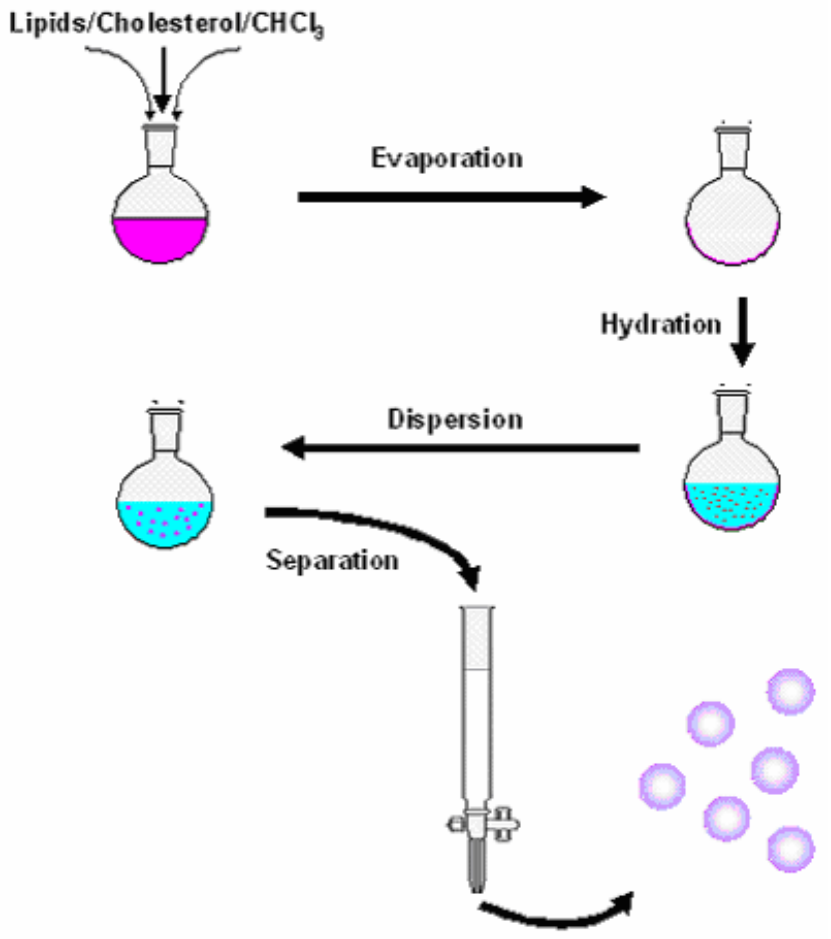

Figure 2.2.1 The basic scheme of liposome synthesis

The first two steps are still done nearly universally with very little deviation. The third and the last step have a couple of variations, but are substantially the same. The fourth step, though, dispersing the lipid film into aqueous solution, has many different variants, depending on the desired liposome characteristics.[1]

The dispersion step is the most important step for determining many of the important properties of the liposomes including size, lamellarity, and monodisperseness. The methods can be broken down into three broad categories based on how the liposomes are dispersed: mechanical dispersion, solvent dispersion, and detergent solubilization.[1]

2.2.1.a. Mechanical Dispersion

Mechanical dispersion was the first method used to prepare liposomes and is still the most widely used. It also has the most variations in order to get different types of liposome preparations, primarily focused on determining whether multilamellar vesicles (MLVs), large unilamellar vesicles (LUV) or small unilamellar vesicles (SUV) are prepared, whether these preparations are monodisperse or polydisperse, and what the average size of the liposomes are.1,2

The first method, used by Bangham, is simply hand shaking the hydrated lipid film. This is a very simple procedure, but the small mechanical agitation caused by shaking is enough to disperse thin enough lipid films into the aqueous solution. If the film is too thick (as might happen if the vessel is too small that the lipid was dried in, or if the temperature of drying was too high), glass beads can be added to the preparation during shaking. Shaking at approximately 60 RPM for 30 minutes will provide suitable liposome preparations. Liposomes prepared by this method are MLVs and usually very polydisperse.1,2,3

A similar method is called non-shaken vesicles. The hydrated film is simply left to sit for a long period of time (two or more hours), and the lipid film swells into the solution. After

swelling, the preparation is very gently agitated (swirled) to disperse the swelled lipid film into the solution. This method can be used to prepare LUVs that are usually polydisperse.1,4

In order to create somewhat more monodisperse, size defined MLVs, a method called pro-liposomes can be used. Before drying the lipid/chloroform solution, a water soluble dry powder (such as sodium chloride) is added. After drying, the lipid film is hydrated and shaken rapidly for less than a minute. As the lipid film coating the particles swells and the particles dissolve in the aqueous solution, MLVs are created. The MLVs size is influenced by the size of the substrate particles used, leading to more monodisperse preparations.1,5

Another method for creating more monodisperse preparations is freeze drying. The lipids, instead of being dissolved in chloroform are dissolved in an organic solvent suitable for freeze drying. The solution is then freeze dried, leaving a foam-like film of lipid. Upon hydration, the film is hydrated and shaken rapidly. This forms MLV whose size is somewhat dependant on the size of the pores in the foam-like lipid film, leading to more monodisperse preparations.1,2

To prepare small unilamellar vesicles, one method is to use a microemulsifier. MLV are prepared by one of the methods above, and then the suspension is introduced in the microemulsifier. The microemulsifier runs the solution at very high pressure through tubing. At one point the channel splits into two, and then the device brings the channels back together at nearly right angles, causing the solutions to collide with each other at very high speeds. The shearing forces causes the MLVs to break apart forming SUVs. The size of the SUVs can be somewhat controlled by how many passes the MLVs take through the emulsifier. The more passes the suspension makes, the smaller the SUVs' size.1,6

Another simple method for creating SUVs is to use a sonicator. The hydrated lipid film is placed in a sonicator bath and sonicated for up to an hour with occasional shaking. This method produces SUVs of extremely small sizes, and thus usually very monodisperse. Unfortunately, this method is often destructive to many samples. It can destroy biological and

organic molecules, and at longer sonication times can even hydrolyze the lipid used to form the liposomes.1,2,7

To create the most size defined SUVs two methods can be employed. The first is using a French Press to shear already prepared multilamellar liposomes. The high pressures of the French Press (up to 40,000 psi) create enormous shearing forces across the orifice. These shearing forces create very monodisperse SUVs and the size can be regulated by the pressure used – the higher the pressure the smaller the size.1,2,8,9

The second method is to do membrane extrusion with MLVs. A polymer membrane (such as polycarbonate) is created that has well defined straight pores bored in it. The MLV suspension is then pushed through this membrane at high pressure (500 psi or more). The high pressure forces the larger MLVs to contort and break to fit through the pores. After passing through the membrane several times (5-10), monodisperse SUVs are prepared with the average diameter being the pore size of the membrane.1,2,10

A final mechanical method called freeze-thaw is used to create LUVs that entrap up to 30% of the solution. Liposomes are created by short sonication and then alternatively frozen and thawed several times (approximately ten times). The freeze-thaw cycle causes the small unilamellar vesicles to fuse together creating larger and larger unilamellar vesicles. Using this method, the largest LUVs can be prepared.1,11,12,13,14

2.2.1.b. Solvent Dispersion

Solvent dispersion is used in place of mechanical dispersion when either the lipids or the entrapped substance cannot withstand the high forces associated with mechanical dispersion. All the mechanical dispersion methods, except hand-shaking and non-shaken liposomes, involve extremely high forces that can destroy some biological samples.[1]

The easiest solvent dispersion method is ethanol injection. The lipids are dissolved in ethanol instead of chloroform. The ethanol solution is then rapidly pushed into an aqueous solution through a fine needle (ethanol concentration cannot exceed 7.5%). This method gives

SUVs of about 25 nm in diameter. Because of the low solubility of most lipids in ethanol, though, and the low maximum ethanol concentration of the final preparation, the liposomes formed by this method are extremely dilute. Also, ethanol is often very hard to remove from the lipids.[1,15]

A similar method is ether injection. The lipids are dissolved in ether and then slowly pushed into an aqueous solution at a temperature at which the ether quickly evaporates off. This method creates monodisperse LUV with size dependant on the speed of injection. It does not have the problems associated with ethanol injection because the ether is evaporated off and does not stay in the solution.[1,16,17]

2.2.1.c. Detergent Solubilization

Detergent solubilization can give extremely monodisperse SUV and thus is sometimes used to create well defined liposome preparations. The general method is to dissolve the desired lipids and a detergent in chloroform and then evaporate to dryness. The film is then hydrated and micelles are formed. The micelle suspension is then placed in dialysis tubing, and the free detergent removed by dialysis. As the free detergent concentration drops, the micelles lose detergent into the solution. As this continues, the micelles eventually run out of enough detergent to be stable and combine to form liposomes. The size of the liposomes can be determined by the original lipid to detergent ratio.[1,2]

2.2.2. Liposome Concentration

There are several methods for assaying the concentration of a liposomal preparation. Nearly all are based on assaying the phosphate concentration from the phospholipids making up the liposome. The three main methods of determining liposome concentration are the Bartlett assay, the Stewart assay, and optical emission spectroscopy (OES).[2]

Each of these assays gives phospholipid concentration, not liposome concentration. To get liposome concentration, the size of the liposomes must also be known and can be calculated from size and phospholipids concentration.[2]

2.2.2.a. Phospholipid Concentration

Bartlett Assay

The Bartlett assay is based on the molybdenum blue method for determining inorganic phosphate first introduced in 1914. The assay is performed by hydrolyzing the phosphoester bonds (with perchloric acid), liberating inorganic phosphate from the lipids. The inorganic phosphate is then converted to phosphomolybdic acid and then the molybdenum VI is reduced to molybdenum V to form a blue colored complex. The reduction does not happen without the presence of the phosphate in the phosphomolybdic acid, so the intensity of the color formed is proportional to the concentration of the phosphate. The concentration can then be assayed colorimetrically at 830 nm.[2,18,19]

The procedure is as follows:

Put liposome solution containing approximately 30 nmol of phospholipids in a test tube.

Add .4 mL of perchloric acid.

Incubate for 30 min at 180°C and then cool to room temperature.

Add 1.2 mL of water, .2 mL of 5% (w/w) ammonium molybdate and 50uL amino-naphthyl-sulfonic acid.

Vortex the tube and then boil seven minutes.

Read the absorbance at 830 nm.

The Bartlett assay can be very precise, but is also easily interfered with. The strengths of the assay are the preciseness of the assay, the disregard for type of lipid, and the low sample amount needed. The drawbacks are extreme interference of that assay by other forms of inorganic phosphate in the system or other molybdenum active ions (sulfate, etc.), the time required for the assay, and the extreme preciseness needed in time, concentration and volume measurements needed for highly accurate results.[2]

Stewart Assay

The Stewart assay was introduced by J.C.M. Stewart in 1980 to compensate for the drawbacks of the Bartlett assay. The Stewart assay is not sensitive to other forms of phosphate in the system and is much faster and easier to perform. The drawback of the system is, though, that different phospholipids do give different results, so the precise phospholipid make-up of the liposome must be known in order to get accurate results.[2,20]

The procedure is based on the interaction of phosphate with ferrothiocyanate, which is a deep blood red color. Ammonium ferrothiocyanate is very water soluble and partitions completely to the aqueous phase of an aqueous-organic mixture. Phospholipids, on the other hand, partition nearly completely to the organic phase of an aqueous-organic mixture and can carry phosphate associated ferrothiocyanate into the organic phase. The absorbance of the organic phase is proportional to the concentration of phospholipids in the system.[2]

The procedure is as follows:

Put liposome solution containing approximately .2 mg of phospholipids into a test tube.

Add 2 mL of chloroform and 2 mL of 0.1 M ferrothiocyanate.

Vortex vigorously for 30 seconds.

Centrifuge at 1000 r.p.m. for 5 minutes.

Remove the lower (organic) layer and take the absorbance at 485 nm.

Optical Emission Spectroscopy

A third method for determine the phospholipids concentration is OES. To run OES, an aliquot of the liposome solution is simply diluted and put into the OES machine. The phosphorus emission is recorded and translated back into phospholipids concentration.[21]

The benefit of OES is that it is extremely simple, there are no reaction steps involved, and it is extremely accurate. The drawbacks are that the assay uses an enormous amount of sample relative to the Bartlett or Stewart assays and requires special equipment (an ICP-OES machine or equivalent) that is often quite expensive.[21]

2.2.2.b. Calculation of Liposome Concentration

Once the phospholipids concentration and the size of the liposomes have been determined, the liposome concentration can be calculated. The calculation is done by calculating the number of lipid molecules in a liposome. The number of lipid molecules in a liposome can be calculated by taking the area of the membrane (both the exterior and interior membrane) and dividing it by the area taken up by one lipid. The surface area of the exterior membrane is given by:

$$A_e = 4 \pi r^2$$

where r is the radius of the liposome. The surface area of the interior membrane is given by the same expression, but the radius is determined by subtracting the membrane thickness (h, ~ 5 nm) from the exterior radius:

$$A_i = 4 \pi (r-h)^2$$

Thus the number of lipid molecules per liposome is given by:

$$N = (A_e + A_i)/a$$

where a is the head group area of the phospholipids. The head group area is a property of the head group of the lipid (choline, ethanolamine, etc.), thus the lipid make-up must be known for this equation to be accurate.[22]

The concentration of liposomes in the solution can then be found by dividing the concentration of phospholipids in the solution by the number of phospholipids per liposome:

$$C_L = C_{pl} / N$$

where C_L is the liposome concentration and C_{pl} is the phospholipid concentration.[22]

2.2.3. Dynamic Light Scattering

There are several methods for determining the size of a liposome preparation, but by far the most useful is dynamic light scattering. Dynamic light scattering is a system based on the Rayleigh scattering of light (elastic scattering, as opposed to Raman scattering which is

inelastic). By measuring fluctuations in the light scattering, the size of particles in the field can be calculated.[23]

When an electromagnetic wave impinges on matter, the wave interacts with and accelerates the electrons. The accelerated electrons in turn produce new electromagnetic waves which, in the absence of any actual electronic change in the particle, should be of the same wavelength as the incident wave but may be in a different direction or phase from the incident wave. This is called elastic (Rayleigh) scattering. Thus, when light interacts with matter, some of the light should be 'redirected' from its original course. The intensity of light in any direction (except the direction of the incident beam) will be the sum of the scattered light in that direction from each particle in the incident beam.[23]

It can be shown that, for optically homogenous matter (that is matter where the dielectric constant is exactly the same at any position), the sum of the scattered light in any direction (except the forward direction) is equal to zero, and thus, although the particles are scattering light, the total light scatter is zero. This is because, in homogenous media, for every particle that scatters light in direction D with phase P, another particle can be paired with it that scatters light in direction D but with phase P + ½ period and the waves cancel out. Thus, any observable light scatter must be from differences of dielectric constant within the media.[23]

Because all particles in a fluid are constantly in motion, even in macroscopically homogenous media, the microscopic dielectric constants are not homogenous across the media. Thus, even macroscopically homogenous media can scatter light do to the distortion of microscopic domains of the dielectric constant by the movement of the particles. This scattering is not constant, though, and changes rapidly as the particles move. Thus the intensity of scattering in direction D at time T is a property of the instantaneous state of the system at time T and how fast the scatter in direction D changes is related to how fast the instantaneous state of the system is changing, and thus is related to how quickly the particles are moving.[23]

Measuring the scattering intensity (E_s) in direction D will thus give an average value A plus a time dependent value A_t, with A_t being the change in E_s due to the random motion of

particles in the scattering area. In a truly random system, A_t would be totally random and the correlation between any two time points, t_1 and t_2 would be zero. In actual systems, though, although the motion of the particles appears totally random (due to the enormous number of collisions they may experience) the starting point of that movement is dependant on the previous state. Thus, A_t is not a totally random variable and some correlation should be seen in the value of E_s from t_1 to t_2 if Δt (t_1-t_2) is small. Eventually, as Δt becomes larger, the correlation between E_s at t_1 and E_s at t_2 will become zero because the random motion of the particles will erase the systems 'memory' of its starting position. As above, how quickly this 'memory' is lost is a function of how quickly the particles are moving.[23]

It can be shown that the bulk property of a measured variable that is fluctuating around an average value and the average value is independent of when the measurement is taken is equal to:

$$\langle A \rangle = \lim_{T \to \infty} \frac{1}{T} \int_0^T dt A(t)$$

where <A> is the average value, T is the length of time over which it is averaged, A(t) are the values measured at time t, and dt is the infinitely small spacing between measurements. In this system, the correlation between two time points, t and t + τ can be given by the expression:

$$\langle A(0)A(\tau) \rangle = \lim_{T \to \infty} \frac{1}{T} \int_0^T dt A(t)A(t+\tau)$$

where <A(0)A(τ)> is the correlation between the measurement A(0) at time 0 and the measurement A(τ) at time 0 + τ, for any time 0, T is the length of time over which the correlation is measured, A(t) and A(t+τ) are the values measured at time t and t+τ, and dt is the infinitely small spacing between measurements. For measurements that are not infinitely close together, this becomes:

$$\langle A(0)A(\tau) \rangle \cong \lim_{N \to \infty} \frac{1}{N} \sum_{j=1}^{N} A_j A_{j+n}$$

where N is the number of measurements taken, j represents the measurement at time t and j+n represents the measurement at time t+τ.[23]

This function can be plotted against τ, and, as long as the variation around the average value is not periodic, the correlation function can be shown to have a maximum at $\tau = 0$ where $\langle A(0)A(\tau)\rangle = \langle A(0)A(0)\rangle$ or $\langle A^2\rangle$. The function also has a minimum at τ = infinity where $\langle A(0)A(\tau)\rangle = \langle A(0)\rangle\langle A(\tau)\rangle$ or $\langle A\rangle^2$. Thus the correlation function is an exponential decay which follows the equation:

$$\langle A(0)A(\tau)\rangle = \langle A\rangle^2 + \left\{\langle A^2\rangle - \langle A\rangle^2\right\}\exp\frac{-\tau}{\tau_r}$$

where τ_r is the correlation time of the function.[23]

Making the definition:

$$\delta A(t) \equiv A(t) - \langle A\rangle$$

the exponential decay function reduces to:

$$\langle \delta A(0)\delta A(\tau)\rangle = \langle \delta A^2\rangle \exp\frac{-\tau}{\tau_r}$$

This formula can be used to mathematically represent the correlation between A_t (the time dependent change in E_s) from above. Thus the scattering of light by particles can be defined by correlation time, τ_r. The value of τ_r determines how quickly the exponential function decays. Since, as shown above, the correlation of A_t between any two time points gets smaller as the particles lose their 'memory' of where they started, the speed of decay in the correlation is dependant on how quickly the particles are moving. Thus τ_r is dependant on the speed of motion of the particles.[23]

In a fluid, particles have rapid, random motion due the massive number of collisions they have with other particles in the fluid; this motion is called Brownian motion. The speed of Brownian motion can be shown to depend on the size of the particle. Consider a colloidal suspension with small solvent molecules and large colloid particles, thousands of times larger

than the solvent. The small solvent molecules will interact with several other solvent molecules at any given instant. A disproportion in interaction on one side or the other will impart a new momentum to the solvent molecule. The same happens for the colloid particles, but because of their larger size, they interact with hundreds of thousands more solvent molecules that a single solvent molecule does. Thus, the random averaging of the collisions in more close to zero and the ratio of the disproportionate force to the mass of the particle is much smaller. Also, the larger particle has more drag through solvent molecules which also retards Brownian motion. The summation of the lower force/mass ratio and the larger drag shows that the Brownian motion of spherical particles is only related to their radius (it is not related to mass because the mass term is a multiplier in the friction term and a divisor in the applied force term, in low Reynolds's number situations, these terms cancel). Thus particles with larger radius move slower than particles with slower radius.[23]

In a colloidal suspension, the dielectric constant changes at the interface between the solvent and the suspended particle, making suspended particles very good scatterers. Thus, in a colloidal suspension, nearly all of the scattered light is due to the larger suspended particles. Since the properties of the scattered light can be represented by the correlation time, τ_r, and the correlation time is a function of the speed of the particles, the scattered light can determine the size of the suspended particles based on how quickly they are moving.[23]

This is mathematically modeled with the following equation:

$$\frac{1}{\tau_r} = \left[\frac{4\pi n_0}{\lambda}\sin\left(\frac{\theta}{2}\right)\right]^2 D_t$$

where n_0 is the refractive index of the suspension, λ is the wavelength of light used for scattering, θ is the angle at which the scattering was measured, and D_t is the diffusion constant.[24]

D_t in turn can be related to the mobility of the particle by the following:

$$D_t = \mu\ k_B\ T$$

where μ is the mobility of the particle (or the terminal drift velocity in an applied force), k_B is the Boltzmann constant, and T is the absolute temperature. Mobility, in turn, is the reciprocal of the drag coefficient (γ):

$$\gamma = 6\ \pi\ \eta\ R_H$$

where η is the viscosity of the sample and r is the hydrodynamic radius of the particle. Thus the radius can be found by:[24]

$$R_H = \frac{k_B T}{6\pi\eta}\left[\frac{4\pi\ n_0}{\lambda}\sin\left(\frac{\theta}{2}\right)\right]^2 \tau_r$$

2.2.4. Liposome Integrity and Delivery

One of the most important aspects to measure when using liposomes as a drug delivery device is when, where, and why they deliver their contents. This can be modeled using a variety of assays to determine how much of the liposomal contents have leaked out in response to some variable. Early assays for liposome leaking were based on simple colorimetrically active substances. The absorbing species was incorporated into the liposome during synthesis and any unincorporated absorbing species were removed by gel filtration or dialysis. The liposomes were then exposed to whatever variable was desired and then the liposomes were separated from the leaked contents, often by centrifugation. The concentration of the leaked contents was determined colorimetrically and the amount of leaking was determined. The marker was chosen to have the following properties:

it does not pass through intact membranes

it is highly water soluble

it has low solubility in organic media

it does not associate with the membrane in any way so as to destabilize or aggregate them

it can be easily separated from liposomes[2]

Currently, simple colorimetric assays are used less often because they are time consuming and the separation techniques (centrifugation) themselves can cause the liposomes to

leak, making it hard to separate leaking from the applied variable and leaking from the separation. There are three main methods for assaying the leak rate of liposomes without having a separation step involved: dye interaction, fluorescence self-quenching and enzymatic determination.[2]

2.2.4.a. Dye Interaction

The dye interaction application is the closest to the earlier colorimetric assays. A colorimetric dye is trapped in the liposomes that changes its absorbance properties in response to another substance that obeys the rules above. The prime example of this is Arsenazo III. Under standard conditions Arsenazo III has an absorbance maximum at 560 nm, but in the presence of calcium, the absorbance maximum shifts to a doublet at 606 and 660 nm. Arsenazo III is incorporated into liposomes without calcium. The liposomes are then diluted into a buffer containing calcium and whatever variable is being tested is applied. The absorbance at 660 nm is then measured to determine the amount of released Arsenazo III that has been able to interact with calcium. This method works well, because it does not require any separation step, but sometimes (as in the case of calcium) the interaction partner can induce its own changes in many membranes, thus occluding the actual effect of the variable.[2]

2.2.4.b. Fluorescence Self Quenching

Certain fluorescent dyes at high concentrations will form stable homocomplexes that change the absorbance profile of the dye and quench the fluorescence. This can be used to create liposomes that will only fluoresce once the entrapped dye is released. The two most common fluorescent dyes used for this are carboxyfluorescein (CF, with similar fluorescence properties to fluorescein, but more soluble in water allowing it to obtain quenching concentrations) and calcein. To prepare self-quenched liposomes with CF, the liposomes are prepared in the presence of 100mM or more CF (at concentrations above 3mM, carboxyfluorescein shows almost no fluorescence). Unentrapped CF is removed by gel filtration and the liposomes are diluted to a dilution where total CF is between 3 and 30uM. The desired variable is then applied

and fluorescence can be measured from the CF. In the absence of leaking, the CF remains trapped inside the liposomes at concentrations exceeding 100mM and shows no fluorescence. Upon leaking, the CF is drastically diluted and fluoresces strongly. Thus the percent released is proportion to the total fluorescence of the sample.[2]

This method is extremely useful, because it can nearly instantly determine the amount of contents released without any separation step or need for secondary reactants outside the liposome that may interfere with the liposome or variable being tested.[2]

2.2.4.c. Enzymatic Assays

A final method for percent release assays is enzymatic determination. Either an enzyme or an enzymatically active substance is entrapped inside the liposome. Once the liposomes are purified, they are diluted into a solution containing the counterpart enzyme or substrate. Upon leaking of the liposomes, the enzyme and substrate come together and the product is formed. If the product is colorimetrically active, the increase in absorbance can be directly measured.[2]

A common example is glucose and hexokinase/glucose-6-phosphate dehydrogenase. Glucose is entrapped in the liposomes. Upon leaking, the glucose is converted to 6-phosphogluconate with the reduction of NADP to NADPH. The increase in concentration of NADPH can be measured at 340nm. This method is useful for measurements that do not require separation, but require many reactants and enzymes to be used outside the liposome that may interfere with the variable being tested. It is also not instantaneous as the carboxyfluorescein is above, and thus is unsuitable for kinetic measurements.[2]

2.3. Experimental

2.3.1. Materials

All lipids obtained for liposome synthesis were of greater than 99% purity. 1,2-dipalmitoyl-sn-glycero-3-phosphocholine (DOPC) was purchased from Avanti Polar Lipids, Inc. (Alabaster, AL). 1,2-dioleoyl-sn-glycero-3-phosphocholine (DPPC) was purchased from Sigma Life Science. Cholesterol was purchased from Pfaltz and Bauer (Waterbury, CT). Lipids were dissolved in chloroform upon receipt and stored at -20°C to prevent degradation or absorption of water.

10X HEPES buffered saline (10X HBS) was prepared as .012M 4-(2-hydroxyethyl)-1-piperazineethanesulfonic acid (HEPES), 1.36M sodium chloride and .045M potassium chloride. HEPES (4-(2-hydroxyethyl)-1-piperazineethanesulfonic acid, >99.5% purity) was purchased from Sigma Life Science. Sodium chloride and potassium chloride (>99% purity) was purchased from Fisher Scientific. 5(6)-carboxyfluorescein (CF, >99% pure) was purchased from Sigma Life Science and was stored at -20°C upon receipt.

Peptides GSGRSAGC and GSGRSAGK (synthetic, >80% pure) were purchased from GenScript (Piscataway, NJ). 3-(ethyliminomethyleneamino)-N,N-dimethyl-propan-1-amine hydrochloride (EDC∗HCl) was purchased from Sigma Life Science. 3-(ethyliminomethylene-amino)-N,N-dimethyl-propan-1-amine methyliodide (EDC∗MeI) was purchased from MP Biomedicals (Solon, OH). Hydroxybenzotriazole (HOBt) was purchased from Fisher Scientific. Both peptides and all coupling reagents were stored at 4°C upon receipt. Sodium polyacrylate (average mass 5100 Da) was purchased from Aldrich.

2.3.2. Synthesis of Cholesterol-Tagged, Protease-Sensitive Polyacrylic Acid

2.3.2.a. Acid Functionalized Cholesterol

1.15 g of cholesterol (3 mmol, 1 eq.) was dissolved in 30 mL of THF along with 0.72 g NaH (30 mmol, 10 eq.) and the reaction was stirred one hour. At the end of one hour, 10 mL of diethyl ether was added and the reaction was stirred 1.5 hours. After stirring, 1.76 g of tertiary butyl 2-bromoacetate (9 mmol, 3 eq.) was added to the solution and the solution was refluxed for 15 hours. After refluxing, 20 mL of water was added and the product was extracted with 3 x 25 mL diethyl ether. After extracting, the ether was evaporated off, and the sample was dissolved in 10:1 hexane:ethylacetate (vol/vol) and run over a 0.5 in. x 15 in. silica gel column. The product eluted after 40 mL. NMR was taken to confirm product and can be seen in Appendix A.

To deprotect the acid group, 3 mL of formic acid (79.5 mmol, 26.5 eq.) was added to the product isolated above with 7 mL of diethyl ether. The solution was refluxed for 2 hours and then the diethyl ether and formic acid was evaporated. NMR was taken to confirm product and can be seen in Appendix A.

2.3.2.b. Amine Functionalized Polyacrylic Acid

5 g of sodium polyacrylate (5100 Da average weight, 1 equivalent) and .38 mL 2-(2-chloroethyl)oxirane (5 equivalents) were dissolved in 20 mL of dry DMF. The mixture was stirred for 72 hours at room temperature and then 1 mL of 18M NH_4OH (18 equivalents) was added drop wise to the mixture. The solution was then stirred another 24 hours at room temperature and then rotovapped to dryness. Once dry, the powder was put under high vacuum for 72 hours to remove any remaining solvent. The resulting white powder was stored under nitrogen.

2.3.2.c. Condensation

2.5 mg (1 equivalent) of the acid derivatized cholesterol from 2.3.2.a was dissolved in 500 μL dry DMF and cooled to 0°C. 1.7 mg (1 equivalent) EDC*HCl was added and the solution was stirred at 0°C for 30 minutes. 1 mg (1.33 equivalents) HOBt was then added and

the solution was stirred at room temperature for three hours. 4 mg (1 equivalent) of the peptide GSGRSAGC was added to the mixture and the solution was stirred overnight to give the cholesterol-peptide complex (not purified).

After 24 hours, the mixture was again cooled to 0°C. 1.7 mg (1 equivalent) EDC*HCl was added and the solution was stirred at 0°C for 30 minutes. 1 mg (1.33 equivalents) HOBt was then added and the solution was stirred at room temperature for three hours. 29 mg (1 equivalent) amine functionalized polyacrylic acid from 2.3.2.b was added to the mixture and the mixture was stirred overnight. The mixture was then rotovapped to dryness and the resulting powder was put under high vacuum for 72 hours to remove any solvent remaining.

2.3.3. Liposome Preparation

2.3.3.a. Bare Liposomes

Bare liposomes were prepared according to standard methods.[1] To prepare bare liposomes (BL), DPPC or DPPC and DOPC (various ratios) was dissolved in 600 μL of chloroform along with cholesterol (various ratios). The solution was vortexed for 30 seconds to insure even distribution of the lipids. The chloroform was then evaporated off at 50°C under blowing air. Once the lipid film was dry, it was placed under high vacuum for 1 hour to remove any remain chloroform.

After drying, the lipid film was hydrated with 600 μL of nX HBS (prepared by diluting 10X HBS) with or without 100 mM CF. The hydrated film was vortexed for 3 minutes, sonicated for 1 minute, and then vortexed again for two minutes to suspend the lipid film in the HBS. The suspension was then put through ten freeze-thaw cycles, 8 minutes/cycle (4 cold/4 hot) with the high temperature being 50°C and the low temperature being -80°C.

After the last freeze-thaw cycle, the suspension was warmed to 50°C. The suspension was then forced through two polycarbonate membranes with 200 nm pores using an Eastern Scientific, Inc. mechanical extruder. After passing through the membranes ten times, the liposome preparation was purified from the unentrapped analytes by passing through a 15 cm x 1

cm Sephadex G-50 gel filtration column. The cloudy fraction that comes out with the void volume was collected. Liposome preparation was verified by dynamic light scattering of the resulting suspension. The suspension was stored at 4°C until used.

2.3.3.b. Polymer Incorporated Liposomes

Polymer incorporated liposomes were prepared similarly to the procedure in Lee, et. al.[2] To prepare polymer incorporate liposomes (PIL), protease sensitive polyacrylic acid from 2.3.2 (various amounts) was added to BL from 2.3.3.a. The mixture was heated to 37.5°C and rocked overnight. The PIL were then separated from unincorporated polymer by passing over a 15 cm x 1 cm Sephadex G-50 gel filtration column. The cloudy fraction that comes out with the void volume was collected. PIL preparation was verified by dynamic light scattering. The suspension was stored at 4°C until needed.

2.3.3.c. Polymer Caged Liposomes

Polymer caged liposomes were prepared similarly to the procedure in Lee, et. al.[2] To prepare polymer caged liposomes (PCL), PIL from 2.3.3.b were heated to 37.5°C. One equivalent of EDC*MeI (in relation to the polyacrylic acid residues, assuming 100% incorporation) was added to the suspension and the suspension was rocked for two hours at 37.5°C. The peptide GSGRSAGK or ethylene diamine was then added to the suspension (various ratios to polyacrylic acid residues), and the suspension was rocked at 37.5°C overnight. The PCL were separated from reagents by passing over a 15 cm x 1 cm Sephadex G-50 gel filtration column. The cloudy fraction that comes out with the void volume was collected. PCL preparation was verified by dynamic light scattering. The suspension was stored at 4°C until needed.

2.3.4. Liposome Concentration

Liposome concentration was assayed by determining the phospholipid concentration of the suspension using the Stewart Assay or ICP-OES.

2.3.4.a. ICP-OES

The liposome sample was diluted to approximately 5 mg/L phosphate content. Standards were prepared at 1, 2, 4, 6, 8, and 10 mg/L phosphate from DPPC. 25 mL of the standards and the samples were fed into an ICP-OES and the sample was compared to the standard curve to determine phosphate concentration.

2.3.4.b. Stewart Assay

The Stewart Assay was adapted from Lasch, et. al.[3] Iron (III) thiocyanate ion was prepared from 27.03 g (0.1 mol) $FeCl_3$ and 30.4 g (0.045 mol) NH_4SCN and diluted to 1 L in water to give 0.1 M $Fe(SCN)(H_2O)_5^{2+}$. One hundred microliters of either BL, PIL, or PCL were added to 2 mL of the $Fe(SCN)(H_2O)_5^{2+}$ solution and 2 mL of chloroform. Standard were made with DPPC to cover the range of possible concentrations. The mixtures were then vortexed vigorously for 1 minute and centrifuged at 2000 RPM for 10 minutes to separate the organic and aqueous layers. The lower organic layer was then removed and 725 μL of the organic layer was diluted to 1.45 mL with chloroform. The absorbance at 485 nm and 690 nm was taken. The value ABS(485) – ABS(690) was plotted against the standard curve to determine phospholipid concentration.

2.3.5. Liposome Sizing

Once the liposome concentration was found, liposomes were diluted to 1 mg P/L in isotonic buffer. The liposome suspension was allowed to stabilize to room temperature and dynamic light scattering measurements were taken with a Brookhaven ZetaPlus Particle Size Analyzer.

2.3.6. Carboxyfluorescein Concentration

A percent encapsulation procedure was adapted from Lasch et. al.[3] In order to determine percent encapsulation, 100 μL of the liposome suspension was added to 100 μL of 5M Brij-58. The solutions were mixed well and then diluted to 2 mL. Serial dilutions were made until the

absorbance at 480 nm was less than one. The absorbance at 480 nm and 690 nm were then measured. The concentration of carboxyfluorescein was determined by the $ABS_{480} - ABS_{690}$ as compared to a standard curve.

2.3.7. Carboxyfluorescein Release Assay

2.3.7.a. Pressure Sensitive Carboxyfluorescein Release

Bare liposomes, polymer incorporated liposomes, and polymer caged liposomes were prepared as above in 10 X HBS. Various dilutions of HBS were then made by diluting 10 X HBS with 0.012 M HEPES Buffer to make the solutions have the desired pressures against 10X HBS. The desired samples were then diluted so that the sample contained 2 μmol carboxyfluorescein in 2 mL in each sample. The diluted samples were incubated at 37.5°C for the desired time and then fluorescence measurements were taken to determine percent release. Carboxyfluorescein was excited at 450 nm and the fluorescence was recorded from 470 nm to 620 nm. Total fluorescence was determined by summing the fluorescence from 470 nm to 620 nm. Curves of total fluorescence verses pressure were fitted using a logistic function:

$$F(\Pi) = \frac{A}{B + Ce^{-D\Pi + E}}$$

where Π is the difference in osmotic pressure and A, B, C, D, and E are fitting constants. The fluorescence verses pressure curves were then compared to determine the difference in pressure sensitivity of various liposome preparations.

2.3.7.b. Urokinase Sensitive Carboxyfluorescein Release

Using the results from the pressure sensitivity studies, the ideal osmotic pressure was determined for various liposome preparations. Bare liposomes, polymer incorporated liposomes and polymer caged liposomes were prepared as above in a concentration of HBS that would give the ideal osmotic pressure for that preparation versus 1X HBS ($\Pi_{nx\ HBS} - \Pi_{1x\ HBS}$ = ideal osmotic pressure or $\Pi_{1x\ HBS}$ + ideal osmotic pressure = $\Pi_{nx\ HBS}$). These liposome preparations were then diluted into HBS with various amounts of uPA so that the final concentration of HBS was 1x and

the final content of carboxyfluorescein was 2 μmol in 2 mL. The diluted samples were incubated at 37.5°C for the desired time and then fluorescence measurements were taken to determine percent release. Carboxyfluorescein was excited at 450 nm and the fluorescence was recorded from 470 nm to 620 nm. Total fluorescence was determined by summing the fluorescence from 470 nm to 620 nm.

2.4. Results and Discussion

2.4.1. Goals

The goal of the current study is to prepare a drug delivery system that will more selectively target cancer cells through their protease signature. This will be done by synthesizing a block copolymer composed of a short peptide sequence sensitive to a cancer specific peptidase and polyacrylic acid. An anchor (either a fatty acid or cholesterol) will be attached to the polymer and the polymer will be incorporated into liposomes. The polymer will be cross-linked with a cross-linker that is also sensitive to the peptidase. When formed under hypertonic conditions, liposomes can swell and burst, rapidly releasing their contents into the surrounding media. The cross-linked polymer will be able to stabilize the hypertonic liposome. Upon reaching the cancer cell, the cancer specific peptidase will degrade the cross-links and cleave the polymer from the liposome, causing the liposome to swell from the osmotic pressure. The swelling will cause the liposome to either fuse with nearby cell membranes, delivering the drug directly into the cell, or burst, delivering the drug at the cancer cell site.

To accomplish this goal, the following steps must be accomplished:

1. Bare liposomes must be successfully prepared
2. Polymer incorporated liposomes must be successfully prepared
3. Polymer caged (crosslinked) liposomes must be successfully prepared
4. Polymer caged liposomes must show significant resistance to osmotic pressure induced leakage verses bare liposomes
5. Polymer caged liposomes must show significant increase in percent release when exposed to urokinase plasminogen activator

2.4.2. Polymer Caged Liposomes

2.4.2.a. Bare Liposomes

Bare liposomes were initially prepared with 5.2 mg DPPC (55.4 mol%) and 2.1 mg Cholesterol (44.6 mol%). The lipids were dissolved in 300 μL chloroform and dried under argon at 50 °C. The lipids were then hydrated in 300 μL of 1x PBS (1x Phosphate Buffered Saline, 0.136 M NaCl, 0.0045 M KCl, .012 M PO_4^{3-} buffered to pH 7.4. 1x PBS is isotonic with blood serum and thus is a commonly used buffer for biological studies) and prepared as detailed above in 2.3.3.a. The liposomes were then diluted to 10% of the concentration post-preparation in 1x PBS and dynamic light scattering measurements were taken to verify liposome preparation. Four separate samples were measured (Table 2.4.1) with a mean diameter of 136.72 nm and a standard deviation of 0.82 nm (0.60%) indicating that liposomes were successfully prepared by this method. Considering the very low standard deviation across samples, this would indicate that the liposomes are very monodisperse.

Table 2.4.1 Dynamic Light Scattering Results: Bare Liposome Synthesis

	Correlation Time (ms)	Diameter (nm)
1	0.8023	137.73
2	0.79227	136.01
3	0.79839	137.06
4	0.79275	136.09
Mean	0.79642	136.72
St. Dev.	0.00480	0.82
% St. Dev.	0.60%	0.60%

2.4.2.b. Liposome Concentration

Initial liposome concentration measurements were attempted by HPLC using a reverse phase C-18 column with solvent A being water and solvent B being chloroform. Standards were prepared for DPPC in chloroform (330 μg/mL, 230 μg/mL, 130 μg/mL, 33 μg/mL, and

17 μg/mL) and for cholesterol in chloroform (140 μg/mL, 98 μg/mL, 56 μg/mL, 14 μg/mL and 7 μg/mL). The prepared liposome sample was diluted 50 times with chloroform to a maximum (considering 100% capture of cholesterol and DPPC in the liposomes) of 330 μg/mL DPPC and 140 μg/mL. Unfortunately, the available HPCL did not show a linear response to the DPPC or cholesterol standards, so the HPLC as a concentration measurement had to be abandoned.

ICP-OES (Inductively Coupled Plasma – Optical Emission Spectroscopy) has been used before to determine lipid concentration in water by measuring the phosphorous signal (nearly every biological lipid (except cholesterol) is a phospholipid, thus the concentration of lipid in the sample can be measured by measuring the phosphate signal). To use ICP-OES, though, there needs to be no other source of phosphate in the system, so a phosphate buffered system (such as PBS) is unsuitable as the phosphate in the buffer will overwhelm any signal from the phosphorous in the lipids. To correct for this, liposome samples were hydrated in 1x HEPES Buffered Saline (1x HBS, 0.136 M NaCl, 0.0045 M KCl, .012 M HEPES buffered to pH 7.4, still isotonic with blood serum) instead of 1x PBS for the remainder of the studies.

Standards were prepared for ICP-OES at 0, 4, 8, 12, 16, and 20 mg Phosphorous/L using DPPC in 1x HBS and samples were prepared by diluting in 1x HBS until the maximum phosphorous concentration (assuming 100% capture of DPPC) was 14 mg/mL. ICP-OES showed a linear curve with DPPC concentration and worked well for measuring the lipid concentrations. Due to lack of access to an easily available ICP-OES (inducing extra time and expense) and the enormous sample sizes needed (50 mL for each standard and each sample, also inducing extra time and expense), the deviation in capture over several liposome preparations was studied to determine if the lipid concentration needed to be measured each time. As can be seen in Table 2.4.2, the standard deviation in the concentration was very high (26.91 %). Thus, ICP-OES was also abandoned as a lipid measurement technique in favor of easier, cheaper and quicker methods.

Table 2.4.2 Deviation in Liposome Concentrations

Sample	Counts 177.434nm (arbitrary units)	mg/L Phosphorous	mol/L DPPC
Standard 1	0.00	0.00	0.00E+00
Standard 2	20.00	4.00	1.29E-04
Standard 3	40.00	8.00	2.58E-04
Standard 4	60.00	12.00	3.87E-04
Standard 5	80.00	16.00	5.17E-04
Standard 6	100.00	20.00	6.46E-04
Sample 1	28.72	5.74	1.85E-04
Sample 2	50.26	10.05	3.25E-04
Sample 3	44.88	8.98	2.90E-04
Sample 4	57.97	11.59	3.74E-04
Sample 5	62.46	12.49	4.03E-04
Sample Mean	48.86	9.77	3.16E-04
Standard Deviation	13.15	2.63	8.49E-05
% Standard Deviation	26.91%	26.91%	26.91%

Another method for quantifying the lipid concentration in a sample based on the phosphate in phospholipids is the Stewart Assay as described above in the experimental (2.3.4.b). Standards were prepared with 0, 2.5, 5, 7.5, 10, 11, 22, 33, 44, 50, 75, 150, 225, and 300 mg Phosphorous/L with DPPC in 1x HBS. Samples were prepared by adding 100 μL of the liposome preparation or standard to 2 mL of the $Fe(SCN)(H_2O)_5^{2+}$ solution and 2 mL of chloroform (as above). Absorbance of the $Fe(SCN)(H_2O)_5^{2+}$ complex was taken at 480 nm and to construct a better curve, the absorbance was corrected by subtraction out background absorbance of the sample as measured at 690 nm. The curve of $ABS_{480} - ABS_{690}$ versus concentration was linear over the entire concentration range (Figure 2.4.1).

Figure 2.4.1 Stewart Assay Standards

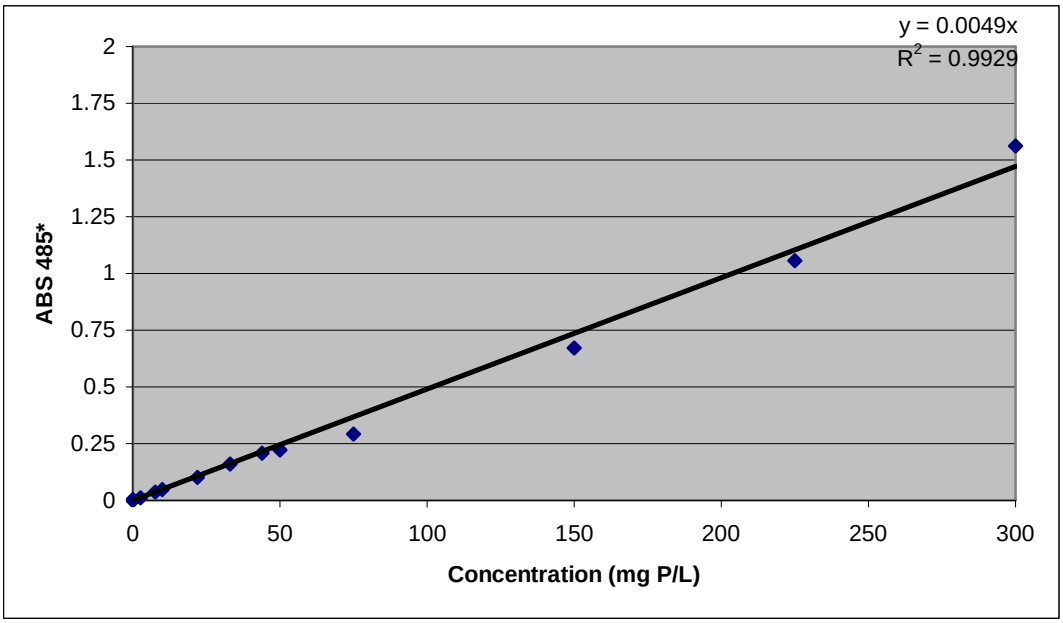

The Stewart Assay uses much less sample (50 – 100 µL versus 500 µL) and can be performed on the bench with a simple spectrometer. Thus, the Stewart Assay was used for the rest of the studies in this paper for liposome concentration.

2.4.2.c. Polymer Integrated Liposomes

A block copolymer (Figure 2.4.2) containing a cholesterol anchor, a short peptide sequence comprised of the uPA consensus sequence and some spacer peptides, and polyacrylic acid was synthesized as described above in the experimental (2.3.2).

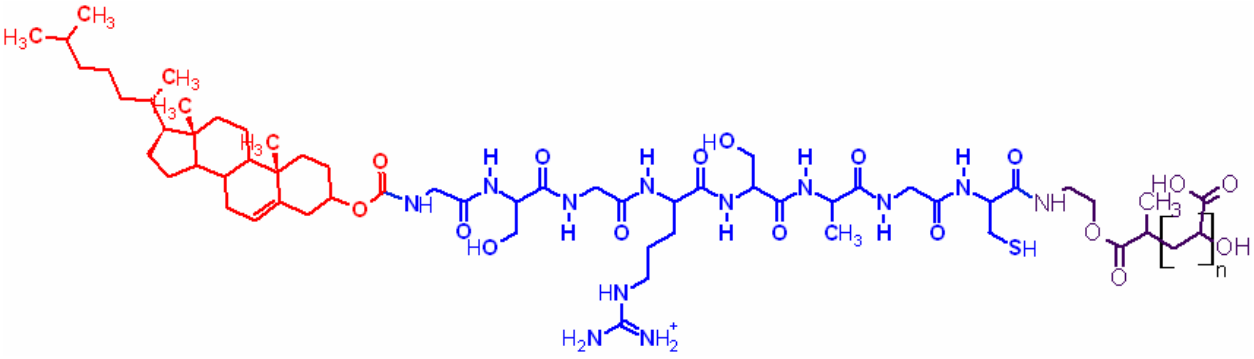

Figure 2.4.2 The synthesized block copolymer. Red is the cholesterol anchor, blue is the uPA consensus sequence, purple is the polyacrylic acid.

The block copolymer was integrated into bare liposomes made in 10x HBS + 100 mM carboxyfluorescein as described above in 2.3.3.b by adding bare liposomes constituting 2 μmol of DPPC (1 equivalent) to 20 μL of the prepared polymer at .2 mg/μL (4 mg, 0.32 equivalents) and diluting to 600 μL with 10x HBS. A control batch was also made by adding bare liposomes constituting 2 μmol of DPPC to 20 μL 10x HBS and diluting to 600 μL with 10x HBS. Three preparations of the sample and the control were made. After incubating and purifying and taking concentration measurements, the preparations were diluted to 1 mg phosphorous/L and DLS measurements were taken. Each sample was sampled four times for DLS measurements. The polymer integrating into the liposome should increase the hydrodynamic diameter because it adds size and drag to the liposome.

As can be seen in Figure 2.4.3, the sample containing the polymer did register slightly larger than the control. Doing a t-test on the results shows $p = 0.03$, indicating that there is a very low probability that the samples are the same. Considering the increase in size was in the expected direction and the significance indicated by the t-test, it can be safely said that the polymer incorporated liposomes were successfully prepared.

Figure 2.4.3 Polymer Incorporated Liposome DLS Measurements

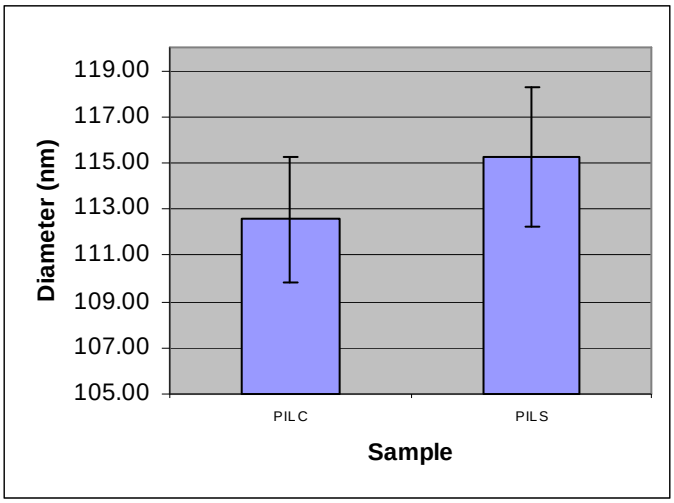

Table 2.4.3 Polymer Incorporated Liposome DLS Measurements.

Sample	Measurement 1	2	3	4	Mean	St Dev	% St Dev
Control 1	112.55	111.76	113.38	117.30	113.75	2.46	2.16%
Control 2	114.06	114.37	108.70	114.42	112.89	2.80	2.48%
Control 3	107.32	113.34	113.17	110.48	111.08	2.83	2.54%
Sample 1	116.03	118.80	115.48	115.73	116.51	1.54	1.32%
Sample 2	116.03	110.92	113.83	121.69	115.62	4.56	3.94%
Sample 3	113.25	113.38	111.46	116.56	113.66	2.12	1.87%

Table 2.4.4 PIL DLS Summary

Sample	Mean	St Dev	% St Dev
PIL C	112.57	2.70	2.40%
PIL S	115.26	3.01	2.61%

2.4.2.d. Polymer Caged Liposomes

The cross-linker used was another short peptide sequence, GSGRSAKG, that contains two amines (the N-terminal amine and the lysine amine) and the uPA consensus sequence between them (GSGRSAGC). This was used so that uPA should be able to cleave both the polymer and the cross-links to more fully degrade the polymer cage. To prepare polymer caged liposomes, PILs were prepared as above (2.4.2.c) and the integrated polymers were crosslinked as described in 2.3.3.c. PILs constituting 640 nmol DPPC (1 equivalent) were added to 5.8 mg EDC*MeI (19.5 μmol, 30 equivalents) and incubated 2 hours. After incubating, 20 μL of crosslinker at 40 mg/mL (36 nmol, .056 equivalents, 34% crosslinking assuming 100% reaction) was added and the preparation was incubated overnight. A control batch was also made by adding PILs constituting 640 nmol DPPC (1 equivalent) to 5.8 mg EDC*MeI (19.5 μmol, 30 equivalents) and incubating 2 hours. After incubating, 20 μL 1x HBS was added and the preparation was incubated overnight. Three preparations of the sample and the control were made. After incubating and purifying and taking concentration measurements, the preparations

were diluted to 1 mg phosphorous/L and DLS measurements were taken. Each sample was sampled four times for DLS measurements. Cross-linking the polymer should increase the hydrodynamic radius of the liposomes because it increases the rigidity of the polymer cage which increases both size and drag.

As can be seen in figure 2.4.4, the cross-linking did register substantially larger than the control. Doing a t-test on the results shows $p < 0.0001$, indicating that there is an extremely low probability that the samples are the same. Considering the increase in size was in the expected direction and the significance indicated by the t-test, it can be safely said that the polymer caged liposomes were successfully prepared.

Figure 2.4.4 Polymer Caged Liposomes DLS Measurements

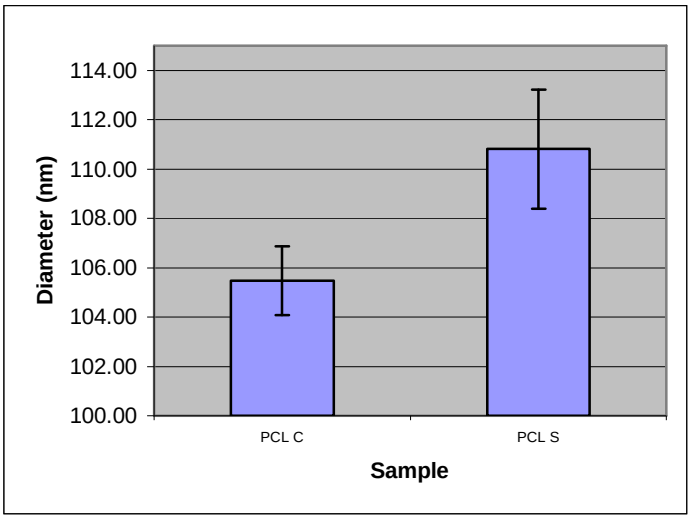

Table 2.4.5 Polymer Caged Liposome DLS Measurements

Sample	Measurement 1	2	3	4	Mean	St Dev	% St Dev
Control 1	104.15	103.13	104.77	105.03	104.27	0.84	0.81%
Control 2	104.98	107.08	106.05	107.20	106.33	1.04	0.97%
Control 3	107.44	105.99	106.09	103.77	105.82	1.52	1.44%
Sample 1	112.16	110.67	113.24	114.06	112.53	1.47	1.30%
Sample 2	113.85	107.53	107.18	111.42	110.00	3.21	2.92%
Sample 3	107.87	109.26	110.65	111.77	109.89	1.69	1.54%

Table 2.4.6 PCL DLS Summary

Sample	Mean	St Dev	% St Dev
PCL C	105.47	1.40	1.33%
PCL S	110.81	2.41	2.17%

As will be discussed below (2.4.3.b), although the polymer caged liposomes were successfully prepared with the synthesized polymer and the peptide cross-linker, the resultant liposomes did not have any added resistance to osmotic pressure. In order to correct this problem, polymer caged liposomes were also synthesized by cross-linking with ethylenediamine instead of the short peptide sequence. Bare liposomes were synthesized as above (2.3.3.a) using 27.5 mg DPPC (37.5 μmol, 47.5 mol%), 3.1 mg DOPC (3.9 μmol, 5.0 mol%), and 14.5 mg cholesterol (37.5 μmol, 47.5 mol%) hydrated in 10x HBS with 100 mM carboxyfluorescein (see below 2.4.3.a for a discussion of the change in lipid composition). Bare liposomes constituting 4 μmol DPPC + DOPC (1 equivalent) were added to either 25 nmol (0.006 equivalent, average 9 nm between polymers), 53 nmol (.013 equivalents, average 6 nm between polymers), or 212 nmol (.053 equivalents, average 3 nm between polymers) of the synthesized polymer and diluted to 600 μL. These were designated low (L), medium (M), or high (H) samples respectively.

After incubating overnight to prepare polymer incorporated liposomes, EDC*MeI and ethylenediamine were added without a purification step (one-pot procedure) in order to increase

yield. To the low sample, either 146 nmol (0.036 equivalents, 50% crosslinking), 219 nmol (0.055 equivalents, 75% crosslinking), or 292 nmol (0.073 equivalents, 100% crosslinking) were added along with EDC*MeI at 1500:1 EDC:ethylenediamine. These were designated L50, L75, and L100 respectively. To the medium sample, either 313 nmol (0.078 equivalents, 50% crosslinking), 470 nmol (0.117 equivalents, 75% crosslinking), or 626 nmol (0.157 equivalents, 100% crosslinking) of ethylenediamine were added along with EDC*MeI at 1500:1 EDC:ethylenediamine. These were designated M50, M75, and M100 respectively. To the high sample either 1250 nmol (0.313 equivalents, 50% crosslinking), 1880 nmol (0.470 equivalents, 75% crosslinking), 2500 nmol (0.626 equivalents, 100% crosslinking) of ethylenediamine were added along with EDC*MeI at 1500:1 EDC:ethylenediamine. These were designated H50, H75 and H100 respectively.

Figure 2.4.5 Ethylenediamine Cross-linked PCL DLS Measurements

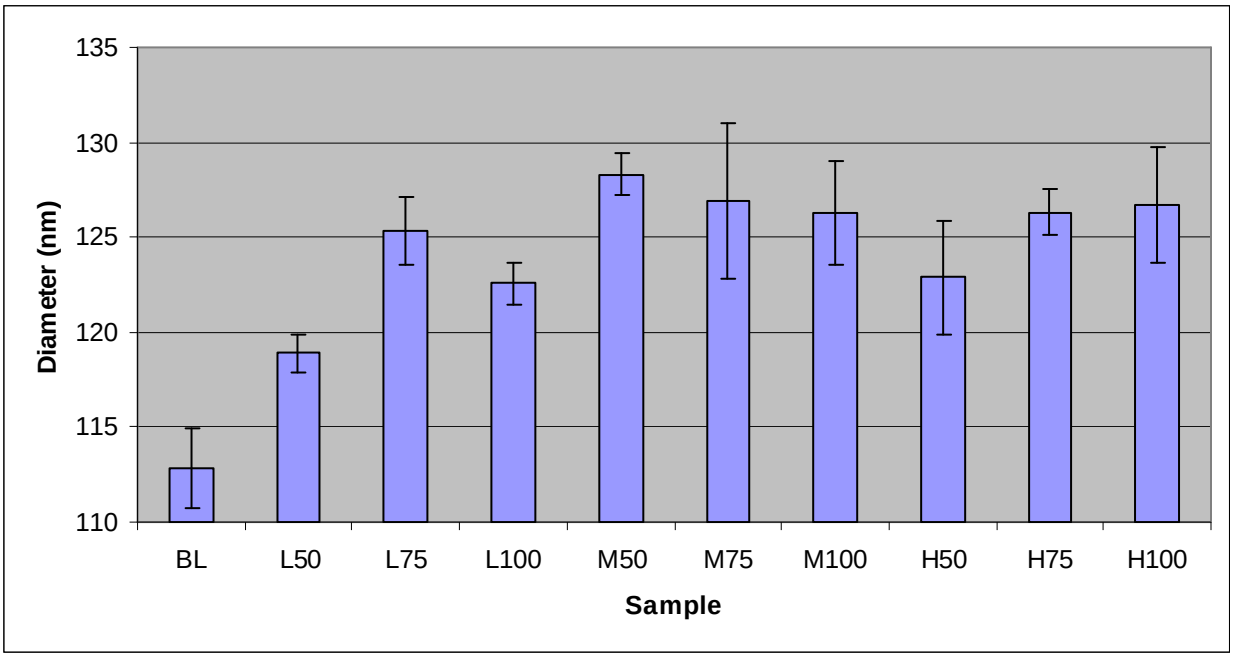

As can be seen in figure 2.4.5, each of the polymer caged liposomes showed an increase in average diameter verses the control (Bare Liposomes). The values ranged from a minimum of + 6.1 nm for L50, to +15.5 nm for M50. P values were calculated for each sample verses the

control and the values can be seen in table 2.4.7. All P values were less than 0.01, indicating that there is very little probability of any of the samples being the same as the control. Considering the increase in size was in the expected direction and the significance indicated by the t-test, it can be safely said that the polymer caged liposomes were successfully prepared.

Table 2.4.7 Ethylenediamine Cross-linked PCL DLS Measurements

	Mean	St Dev	P value vs. BL
BL	112.8	2.1	--
L50	118.9	1	0.0063
L75	125.3	1.8	0.0001
L100	122.6	1.1	0.0004
M50	128.3	1.1	< 0.0001
M75	126.9	4.1	0.0036
M100	126.3	2.7	0.0002
H50	122.9	3	0.0027
H75	126.3	1.2	0.0001
H100	126.7	3	0.0006

Each sample was compared to other samples in its set (sets being all the L samples, M samples, or H samples, and then also all the 50 samples, all the 75 samples and all the 100 samples) and p values were calculated using two sample t-tests. The p values can be seen in table 2.4.8.

With low amounts of integrated polymer (average 9 nm between polymers), adding more crosslinker made a significant difference in the size (although the 75% crosslinking was on the verge of not being significantly different from the 100% crosslinking). With medium and high amounts of integrated polymer (average 6 nm and 3 nm respectively), adding different amounts of crosslinker made no significant difference in size. This would indicate that at low polymer integration levels, the polymer probably has high mobility along the chain and can lay flat

against the liposome reducing added size and added drag. Therefore, adding rigidity through crosslinking makes a significant difference in the measured size of the liposomes, up to the point where the system is 100% crosslinked. For medium to high polymer integration levels, because of the close packing, the polymer probably has less mobility along the chain and cannot lay flat against the liposome. Therefore, adding rigidity through crosslinking makes little difference to the measured size of the liposomes.

Table 2.4.8 T-test P Values within Each Subgroup

	L50	L75	L100
L50	*	0.0016	0.0025
L75	0.0016	*	0.0507
L100	0.0025	0.0507	*

	L50	M50	H50
L50	*	<.0001	0.0647
M50	<.0001	*	0.0278
H50	0.0647	0.0278	*

	M50	M75	M100
M50	*	0.5566	0.2420
M75	0.5566	*	0.8166
M100	0.2420	0.8166	*

	L75	M75	H75
L75	*	0.5143	0.3977
M75	0.5143	*	0.7927
H75	0.3977	0.7927	*

	H50	H75	H100
H50	*	0.1031	0.1234
H75	0.1031	*	0.8166
H100	0.1234	0.8166	*

	L100	M100	H100
L100	*	0.0641	0.0622
M100	0.0641	*	0.8494
H100	0.0622	0.8494	*

No significant trends were seen across the 50, 75, or 100% crosslinking groups. This may indicate that the amount of cross linking is a larger factor in the measured size of liposomes than the amount of integrated polymer. This makes sense at non-vanishingly small concentrations of integrated polymer. The polymer has a certain length fully stretched and the liposomes have a certain radius. At concentrations where the integrated polymer extends all the way around the liposome, the new radius should be the initial radius plus the length of the

polymer. How rigid the polymer is is going to be the main factor in how large the measured diameter is, so cross-linking amount ends up being more important than polymer density.

2.4.3. Osmotic Pressure Resistance

2.4.3.a. Initial Test

Bare liposomes were prepared as described above (2.4.2.a) and polymer incorporated liposomes were prepared as described above (2.4.2.c). Polymer caged liposomes were made by adding polymer incorporated liposomes constituting 640 nmol DPPC (1 equivalent) and adding it to 5.8 mg EDC*MeI (19.5 μmol, 30 equivalents) and incubated 2 hours. After incubating, 20 μL of peptide crosslinker at 40 mg/mL (36 nmol, .056 equivalents, 34% crosslinking assuming 100% reaction) was added and the preparation was incubated overnight.

After incubating and purifying, both the sample and the control were diluted to a final tonicity of 5x HBS which induces 33.81 atm of osmotic pressure inside the liposomes (caused by the difference in tonicity of the solution trapped inside the liposome (10x) verses the tonicity of the of the solution outside the liposome (5x)). The solutions were incubated overnight at 37.5 °C and fluorescent intensity was measured as described above (2.3.7.a) as shown in figure 2.4.6 and figure 2.4.7.

Visual inspection of the samples indicated that neither the bare liposomes nor the polymer caged liposomes had leaked any of their contents. (Leakage and subsequent dilution of carboxyfluorescein (see 2.2.4.b) causes a noticeable visual change in the color of solution. The concentrated carboxyfluorescein inside the liposomes is a dark red color, and at low concentrations of liposomes appears orange. Upon leaking and dilution of the carboxyfluorescein, the solution turns bright fluorescent green.) The initial hypothesis of this experiment (guided by theory from 2.1.6) was that a much smaller osmotic pressure would cause the bare liposomes to leak nearly all of their contents, so this result was unexpected.

Taking the equation $\Delta P_{min} = (3\,\Gamma / R_0)\,(\gamma / \Gamma\, R_0)^{2/3}$, and average values for Γ (0.1 - 1 J/m^2) and γ (0.02 - 0.2 nJ),[1] and the radius measured above in 2.4.2.a (68.36 nm), the minimum

osmotic pressure needed for leaking should be as low as 0.89 atm or as high as 8.9 atm, four to forty times lower than the actual applied pressure. Assuming that the values of Γ and γ are closely related (being measurements of the cohesive force between the lipid molecules), to get a liposome at this radius that would resist over 33 atm of osmotic pressure, the values of Γ and γ must be raised 4 times to 4 J/m^2 and 0.8 nJ, values much higher than reported average values for biological membranes.

To further explore these extremely pressure resistant liposomes, the liposomes were diluted to a final concentration of 5x HBS and 1M Brij-58 (a strong detergent used to disrupt them membrane). Visual inspection of this solution also showed no leakage of carboxyfluorescein from the membranes (no change from orange to green).

A literature review of detergent resistant membranes and membrane elasticity revealed that detergent resistant membranes are a current research interest in membrane biology. Of interest to this research is the identification that membrane rafts (which have sometimes been associated with detergent resistant membranes) and detergent resistant membranes often consist of high concentrations of saturated phospholipids and cholesterol and low concentration of mono- or polyunsaturated phospholipids.[2,3] Also, lipid membranes made with high concentrations of saturated phospholipids and cholesterol and low to no unsaturated phospholipids have much higher elasticity constants than ovolecithin or other standard biological membranes that contain unsaturated and saturated phospholipids.[4,5,6] Adding cholesterol greatly increases the membrane elasticity up to 55 mol% cholesterol in the membrane, at which point, the elasticity of pure cholesterol starts to decrease the elasticity of the membrane. In fact, a sphingomyelin membrane with 55 mol% cholesterol can have 1.73 J/m^2 elasticity constant.[5] Sphingomyelin is still monounsaturated, and saturated, long-chain phospholipids increase the membrane elasticity more. A membrane that is pure DPPC + nearly 55 mol% cholesterol could conceivable have a membrane elasticity of 2 – 3 J/m^2. Although, this is not the 4 J/m^2 needed to make sense of the data above, it is quite a bit closer. Other research has shown that membranes made entirely out of unsaturated lipid and cholesterol will have very low water permeability.[7,8]

Increasing concentration of cholesterol in any membrane will reduce the water permeability,[8] perhaps because water permeability is closely linked to the area/lipid molecule and cholesterol reduces the area/lipid molecule by making the lipids pack together better.[7]

Between an increase in the elasticity of the membrane caused by having solely DPPC and cholesterol in nearly 50 mol% each, and a decrease in the permeability of water (which will, in turn, decrease the effective osmotic pressure), the result above can be considered reasonable. Therefore, for the following tests, an unsaturated phospholipid (DOPC) was added to decrease the elasticity of the membrane and increase the water permeability.

2.4.3.b. Peptide Crosslinker + DOPC

Bare liposomes were prepared as described above (2.3.3.a) using 27.5 mg DPPC (37.5 μmol, 51.5 mol%), 2.7 mg DOPC (3.4 μmol, 4.7 mol%) and 12.3 mg cholesterol (31.8 μmol, 43.8 mol%) hydrated in 10x HBS + 100 mM carboxyfluorescein. Bare liposomes constituting 2 μmol of DPPC (1 equivalent) were added to 20 μL of the prepared polymer at 200 mg/mL (4 mg, 0.32 equivalents) and diluting to 600 μL with 10x HBS. A control batch was also made by adding bare liposomes constituting 2 μmol of DPPC to 20 μL 10x HBS and diluting to 600 μL with 10x HBS. The integrated polymers were then crosslinked as described in the experimental (2.3.3.c). PILs constituting 640 nmol DPPC + DOPC (1 equivalent) were added to 5.8 mg EDC*MeI (19.5 μmol, 30 equivalents) and incubated 2 hours. After incubating, 20 μL of crosslinker at 40 mg/mL (36 nmol, .056 equivalents, 34% crosslinking assuming 100% reaction) was added and the preparation was incubated overnight.

After incubating and purifying, the concentration of carboxyfluorescein in the polymer caged liposomes and the bare liposomes were measured as described above (2.3.6). Both the sample and the control were diluted to 4 μM carboxyfluorescein and a final tonicity of either 10x, 9.75x, 9.5x, 9.25x, 9x, 8.5x, 8.25x, 8x, or 7.75x HBS (the solutions were marked by the difference in concentration (0, 0.25, 0.5, 0.75, 1, 1.5, 1.75, 2, and 2.25 respectively). The osmotic pressure against the 10x HBS inside the liposomes can be calculated and is 0, 1.69, 3.38,

5.07, 6.76, 10.14, 11.83, 13.52, 15.21 atm respectively. The solutions were incubated overnight at 37.5 °C and fluorescent intensity was measured as described above (2.3.7.a) as shown in figure 2.4.6 and figure 2.4.7.

Figure 2.4.6 Fluorescent Intensity of Bare Liposomes

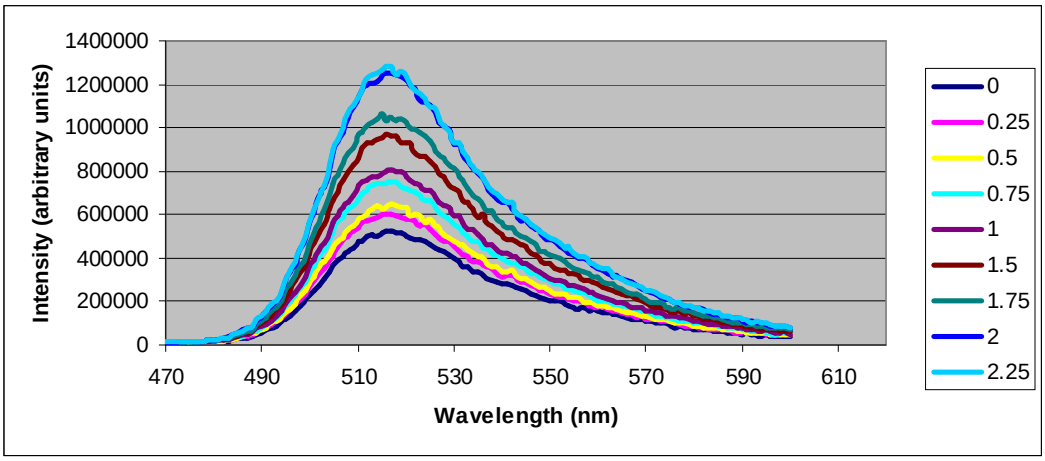

Figure 2.4.7 Fluorescent Intensity of Polymer Caged Liposomes

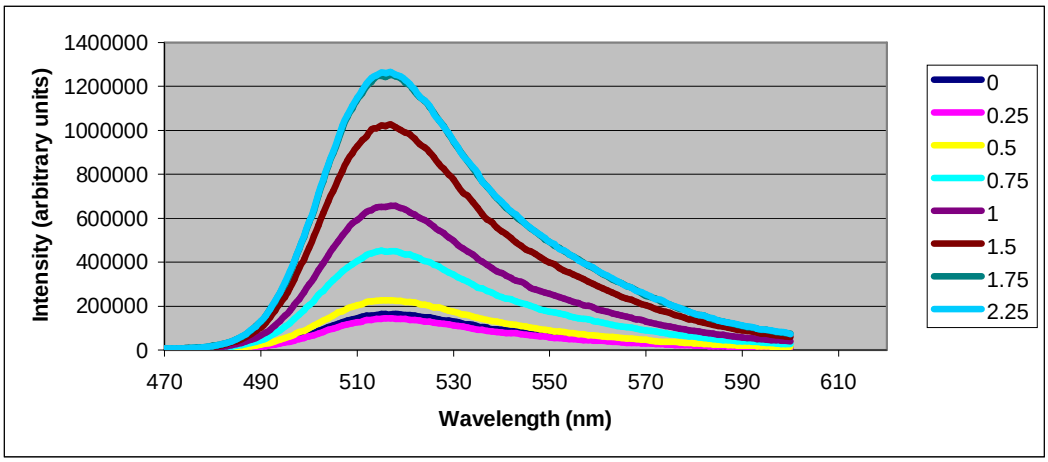

The total fluorescent intensity was scaled to a maximum of 100% and the percent release (which equals the scaled fluorescence values) was plotted against the osmotic pressure and the fitting constants were calculated (table 2.4.9, figure 2.4.8). The difference in percent release as a function of pressure was calculated by subtracting the percent release curve of the bare

liposomes from the percent release curve of the polymer caged liposomes. The zero value line of the bare liposome curve minus the bare liposome curve is also shown (figure 2.4.9).

As can be seen in figure 2.4.8 and 2.4.9, there is very little difference in the percent release at any osmotic pressure between the polymer caged liposomes and the bare liposomes. This means that this liposome preparation is not useful for the stated goals of this project (see 2.4.1). Ideally a large change would be seen in the pressure resistance of the polymer caged liposomes that would show itself as a rightward shift in the fitting curve. Thus at intermediate pressures, a substantial difference in the percent release of the carboxyfluorescein would be seen.

Table 2.4.9 Fitting Constants for % Release verses Osmotic Pressure

	BL	PCL
A	2.9171	2.6778
B	2.8325	2.6524
C	228.4391	228.4444
D	-0.3448	-0.5774
E	-1.4654	-0.2378
R^2	0.99998953	0.99999502

Figure 2.4.8 Fitting Curves for Bare Liposomes and Polymer Caged Liposomes

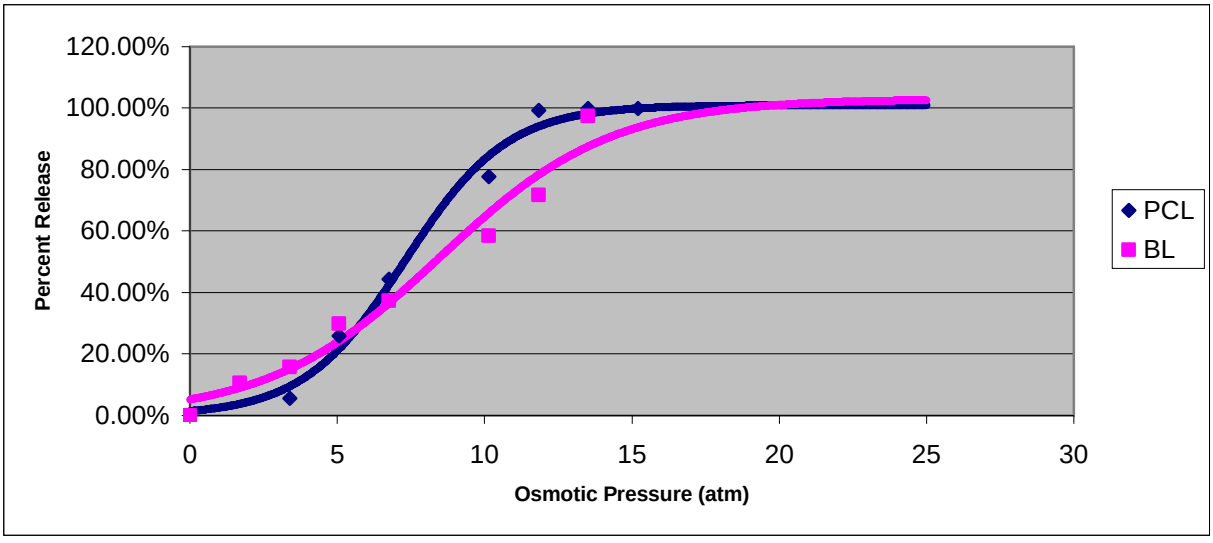

Figure 2.4.9 Difference in Percent Release versus Osmotic Pressure

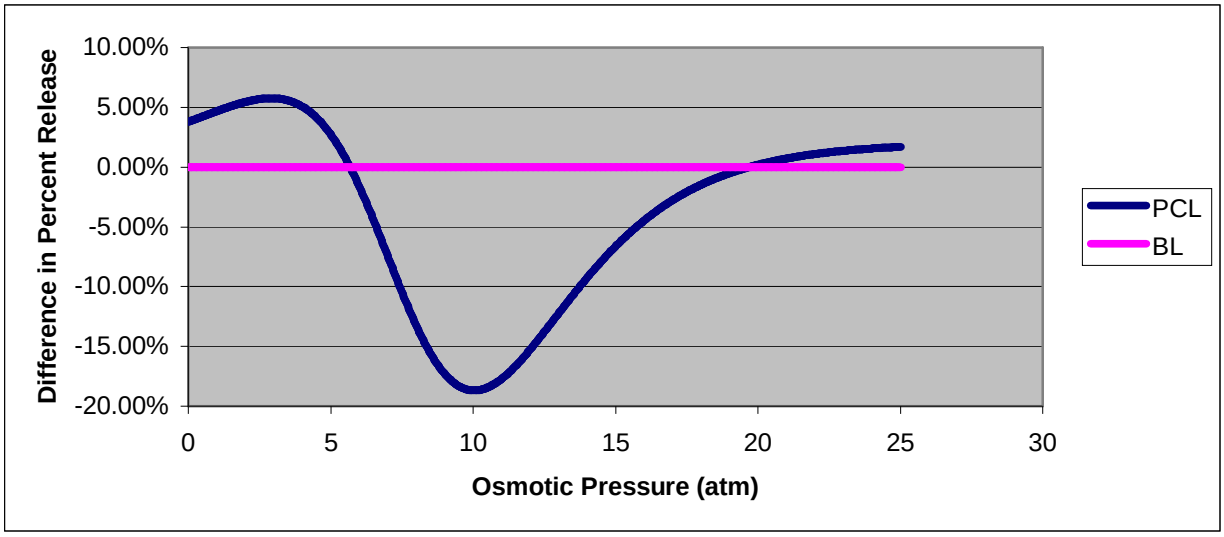

The maximum pressure the polymer cage can withstand can be estimated from the fitting curves (figure 2.4.8). As explained in the literature review (2.1.6), bare liposomes should start to release their entrapped contents at ΔP_{min}. ΔP_{min} can be estimated from the graph, and for most reliable results, the half maximum (when the carboxyfluorescein is 50% released) is the best point for estimating. In the same way, the polymer caged liposomes should start to release their entrapped contents at $\Delta P_{min} + P_{ext}$, or the pressure needed to break the liposome membrane plus the pressure needed to overcome the polymer shell. Again, this can be estimated from the graph as osmotic pressure at the half maximum of the polymer caged liposome release curve. P_{ext}, the added maximum pressure resistance from the polymer cage can be calculated by subtracting the osmotic pressure at half height of the bare liposome curve from the osmotic pressure at half height of the bare liposome curve. For this system, the osmotic pressure at half maximum for the bare liposomes is 13.17 atm; the osmotic pressure at half height for the polymer caged liposomes is 12.16 atm. Subtracting the two gives a maximum added pressure resistance from the polymer cage as -1.01 atm, or no significant added pressure resistance.

2.4.3.c. Ethylenediamine Crosslinker + DOPC

To create a polymer cage that does add significant pressure resistance, it was hypothesized that the crosslinking needs to be tightened. If the crosslinking is too loose, the polymer cage may still allow the membrane to expand past its maximum expansion point, allowing the liposome to release its contents before it interacts significantly with the polymer cage. In order to make tighter crosslinking, a shorter crosslinker was used, namely ethylenediamine.

Bare liposomes were prepared as described above (2.3.3.a) using 27.5 mg DPPC (37.5 μmol, 51.5 mol%), 2.1 mg DOPC (2.67 μmol, 3.7 mol%), and 12.6 mg cholesterol (32.6 μmol, 44.8 mol%) in 10x HBS with 100 mM carboxyfluorescein. Bare liposomes constituting 3 μmol of DPPC (1 equivalent) were added to either 15 μL (3 mg, 0.17 equivalents), 30 μL (6 mg, 0.34 equivalents), or 45 μL (9 mg, 0.50 equivalents) of the prepared polymer at 200 mg/mL and diluting to 400 μL with 10x HBS. The resulting PILs, after incubating and purifying were added to either 46.5 μL (700 nmol, crosslinking percent depends on sample) or 70 μL (1000 nmol, crosslinking percent depends on sample) 1% ethylenediamine. This gives the following samples:

Table 2.4.10 Polymer Equivalents and Crosslinking in Samples

Sample	Polymer	Crosslinking
1	17%	80%
2	17%	120%
3	34%	40%
4	34%	60%
5	50%	27%
6	50%	40%

After incubating and purifying, the concentration of carboxyfluorescein in the polymer caged liposomes and the bare liposomes was measured as described above (2.3.6). Both the sample and the control were diluted to 4 μM carboxyfluorescein and a final tonicity of either

10x, 9.75x, 9.5x, 9x, 8.5x, 7.5x, or 5x HBS (the solutions were marked by the difference in concentration (0, 0.25, 0.5, 1, 1.5, 2.5, and 5 respectively). The osmotic pressure against the 10x HBS inside the liposomes is 0, 1.69, 3.38, 6.76, 10.14, 16.90, and 33.81 atm respectively. The solutions were incubated overnight at 37.5 °C and fluorescent intensity was measured as described above (2.3.7.a). Fluorescent intensity and percent release verses osmotic pressure can be seen in Appendix B. A summary graph compiling all of the calculated curves is shown in figure 2.4.10.

Figure 2.4.10 % Release verses Osmotic Pressure Fitting Curves

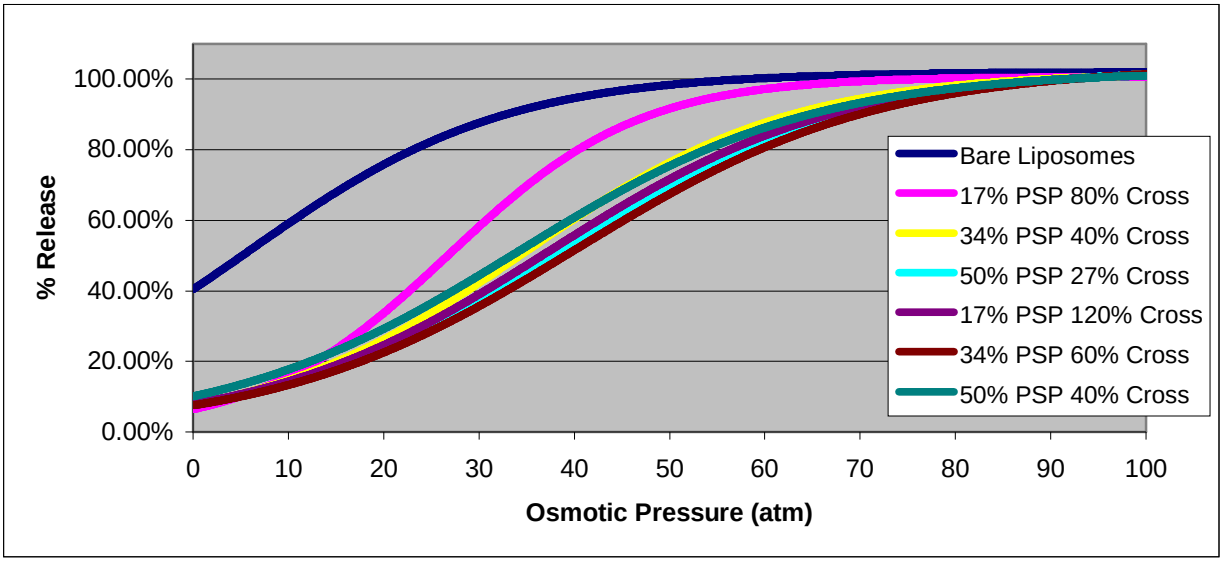

Table 2.4.11 Fitting Constants

	BL	1	2	3	4	5	6
A	11.0279	10.8532	10.9297	10.9988	10.9737	11.0182	10.9708
B	10.8009	10.7729	10.7139	10.6431	10.6710	10.6194	10.7066
C	236.3898	236.3994	236.3986	236.3986	236.3985	236.3987	236.3973
D	-0.0741	-0.1000	-0.0719	-0.0648	-0.0663	-0.0634	-0.0648
E	-2.6624	-0.4018	-0.5928	-0.5911	-0.6161	-0.5540	-0.8823
R^2	0.9999989	0.9999992	0.9999994	0.9999992	0.9999998	0.9999989	0.9999999

As can be seen in figure 2.4.10, the polymer caged curves shifted substantially to the right. This indicates that the polymer cage does add substantial resistance to osmotically induced leakage. Again, the amount of added resistance to pressure ($P_{Max\ ext}$) can be estimated by subtracting the pressure at half maximum of the bare liposomes ($P_{Half\ Max}$) from the $P_{Half\ Max}$ of the polymer caged liposomes. The $P_{Max\ ext}$ and the $P_{Half\ Max}$ are shown in table 2.4.12.

Table 2.4.12 Maximum Added Pressure Resistance

Sample	$P_{Half\ Max}$ (atm)	$P_{Max\ ext}$ (atm)
BL	5.20	0.00
1	26.70	21.50
2	34.25	29.05
3	37.75	32.55
4	36.60	31.40
5	39.10	33.90
6	33.40	28.20

The $P_{Max\ ext}$ calculations represent a horizontal line across figure 2.4.10. For this research though, the 'isorelease' lines are not nearly as important as the 'isobaric' lines. This is because the premise of the research is that a protease can degrade the polymer shell. When this happens, the osmotic pressure stays the same (isobaric) but the liposome looks more like a bare liposome post-degradation than the polymer caged liposome. This means that the liposome would release its contents after the polymer cage has been degraded. The isobaric difference in release between the bare liposomes and the polymer caged liposomes can be calculated for each sample by subtracting the percent release curve for bare liposomes from the percent release curve for the sample. The isobaric difference curves are shown in figure 2.4.11. The isobaric difference represents the maximum amount of entrapped solute that can be released by protease degradation, so higher values are preferential.

Sample 4 (0.34 equivalents polymer, 60% crosslinking) showed the greatest difference in % release with a maximum % release of 53.84% at 23.5 atm, although sample 5 (0.50 equivalents polymer, 40% crosslinking) did not show a substantially large difference. The smallest difference in % release was sample 1 (0.17 equivalents polymer, 80% crosslinking), which probably simply represents the very low amount of polymer and crosslinking.

Figure 2.4.11 Differences in Percent Release versus Osmotic Pressure

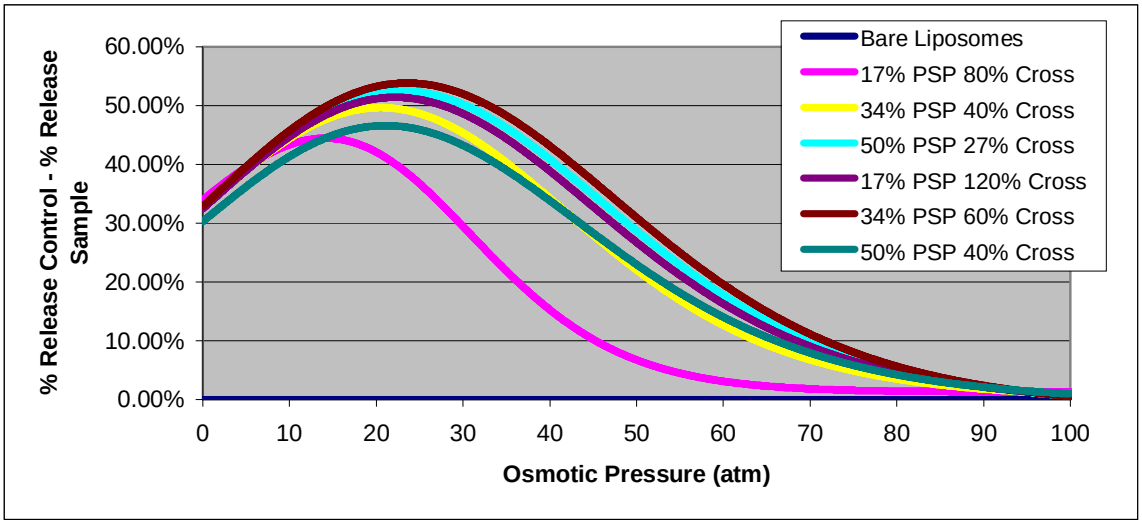

Figure 2.4.12 Comparison to Figure 2.4.9

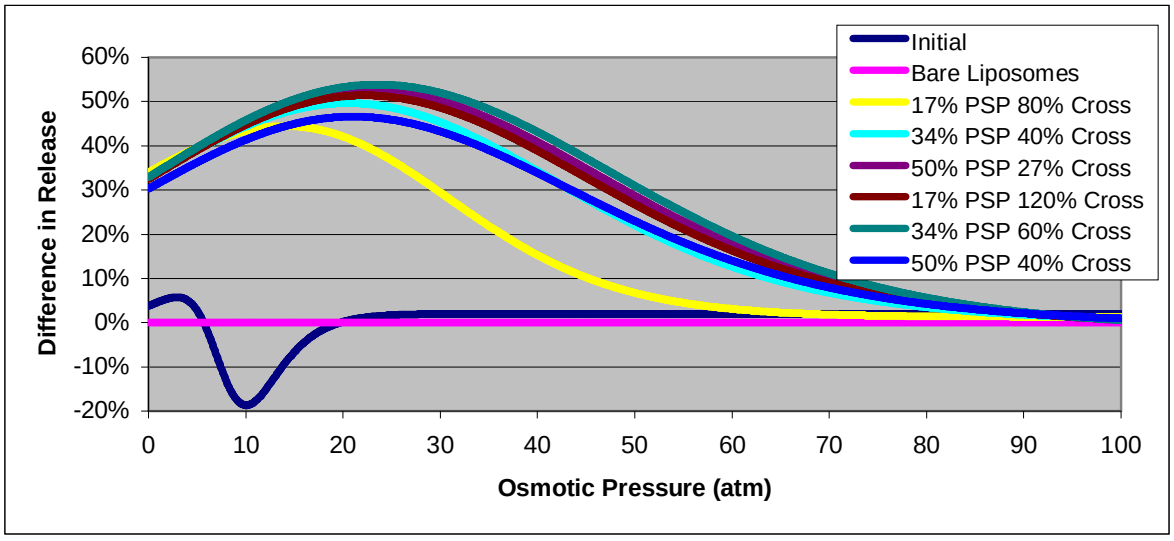

To show the increase in effectiveness of the ethylenediamine compared to the peptide crosslinker, figure 2.4.9 was overlaid on figure 2.4.11 and is shown in figure 2.4.12. Ethylenediamine as a crosslinker dramatically increased the $P_{Max\ ext}$, lending credence to the theory that the earlier polymer caged liposomes with peptide crosslinker was simply not tight enough to keep the liposome from swelling and bursting.

2.4.3.d. Kinetics of Liposome Swelling

Although the swelling of the liposomes and the subsequent release of contents should be very fast in the presence of large osmotic pressures, this swelling and releasing is a transient state as discussed in 2.1.6. This means that the liposome will swell, form pores, release some contents, and then the pores will seal again. If the pressure gradient is not minimized enough to prevent swelling the process starts again. Thus, even though each swelling and releasing process is very quick, it is conceivable that the total release of contents may happen over a much longer time period.

To determine how quickly the contents of the liposomes are released in response to osmotic pressure bare liposomes were prepared as described above (2.3.3.a) using 27.5 mg DPPC (37.5 μmol, 51.5 mol%), 2.1 mg DOPC (2.67 μmol, 3.7 mol%), and 12.6 mg cholesterol (32.6 μmol, 44.8 mol%) in 10x HBS with 100 mM carboxyfluorescein. Bare liposomes constituting 3 μmol of DPPC (1 equivalent) were added to 30 μL (6 mg, 0.34 equivalents) of the prepared polymer at 200 mg/mL and diluting to 400 μL with 10x HBS. The resulting PILs, after incubating and purifying were added to 70 μL 1% ethylenediamine (1000 nmol, 60% crosslinking).

After incubating and purifying, the concentration of carboxyfluorescein in the polymer caged liposomes and the bare liposomes was measured as described above (2.3.6). Both the sample and the control were diluted to 4 μM carboxyfluorescein and a final tonicity of either 10x, 9.5x, 9x, 8x, 7x, 6x or 5x HBS (the solutions were marked by the difference in

concentration (0, 0.5, 1, 2, 3, 4 and 5 respectively). The osmotic pressure against the 10x HBS inside the liposomes is 0, 3.38, 6.76, 13.52, 20.28, 27.04 and 33.81 atm respectively. The solutions were incubated at 37.5 °C and fluorescent intensity was measured at time 0 (15 min), 2 hours, 5 hours, 24 hours, 47 hours and 71 hours as described above (2.3.7.a). Fluorescent intensity and percent release verses osmotic pressure can be seen in Appendix C. A summary graph compiling all of the calculated curves is shown in figure 2.4.13 for the bare liposomes and 2.4.14 for the polymer caged liposomes.

Figure 2.4.13 Bare Liposomes % Release verses Osmotic Pressure Fitting Curves

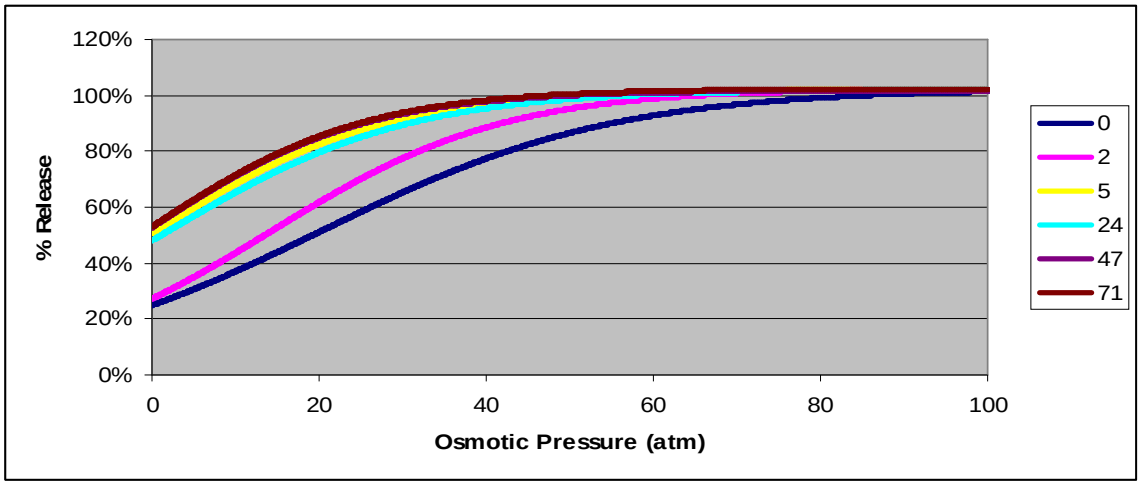

Figure 2.4.14 Polymer Caged Liposomes % Release verses Osmotic Pressure Fitting Curves

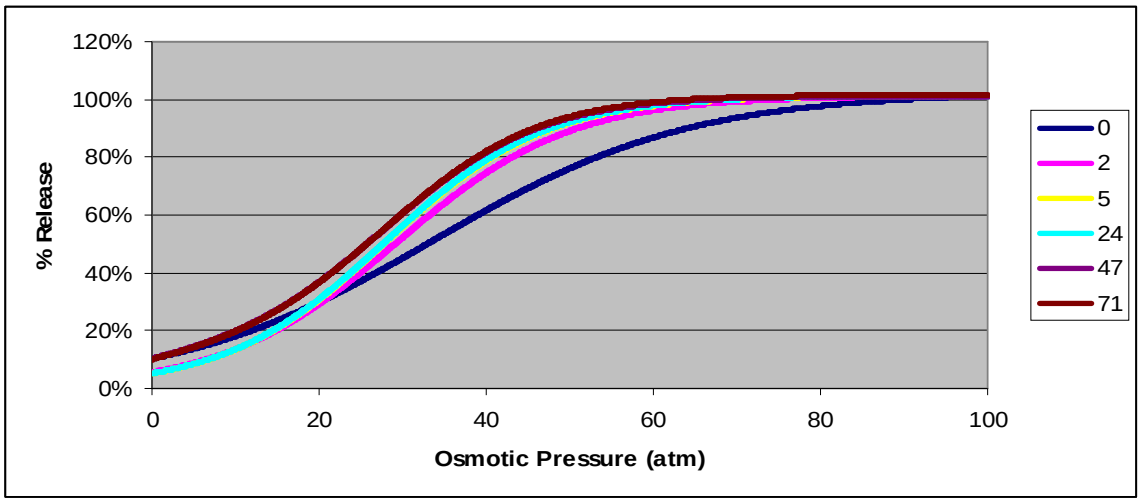

As can be seen from figure 2.4.13, it takes more than 2 hours but less than 5 hours for the bare liposomes to reach osmotic equilibrium (no more increase in % release). In figure 2.4.14, the polymer caged liposomes take more than 15 minutes but less than 2 hours to reach osmotic equilibrium. The difference in time can be easily understood in the difference between what is happening to each sample. In the bare liposomes, the osmotic pressure causes the liposome to swell and form pores releasing some of the contents and the pores close again. This continues to happen over time, and each time it happens, the osmotic pressure goes down. As the osmotic pressure goes down, the speed of pore formation also slows down. Thus the bare liposomes will take some time to reach equilibrium because their progress towards equilibrium is slowed. At higher pressures, the liposomes will reach equilibrium faster and at lower pressures the liposomes will reach equilibrium slower because of less initial rate, which can be seen in the curve at 2 hours.

On the other hand, polymer caged liposomes start out the same. They swell for a moment and release a little bit of their contents. They would continue in the bare liposome trend of swell, pore, release, close, repeat, but they quickly expand into the polymer cage and are trapped. Thus the point of equilibrium is not equalizing the osmotic pressure inside and out, but rather running into the polymer cage. Since the time it takes to expand into the polymer cage is much less than the time it takes to release all of the contents, the polymer caged liposomes reach equilibrium much faster.

The difference in percent release at each pressure at each time can be calculated again by subtracting the sample curve from the control curve at the same time. Because of the difference in rate of how quickly the bare liposomes reach equilibrium at high and low pressures, the difference graph not only grows larger over time but also moves to the left (to lower osmotic pressures).

Figure 2.4.15 Differences in Percent Release versus Osmotic Pressure

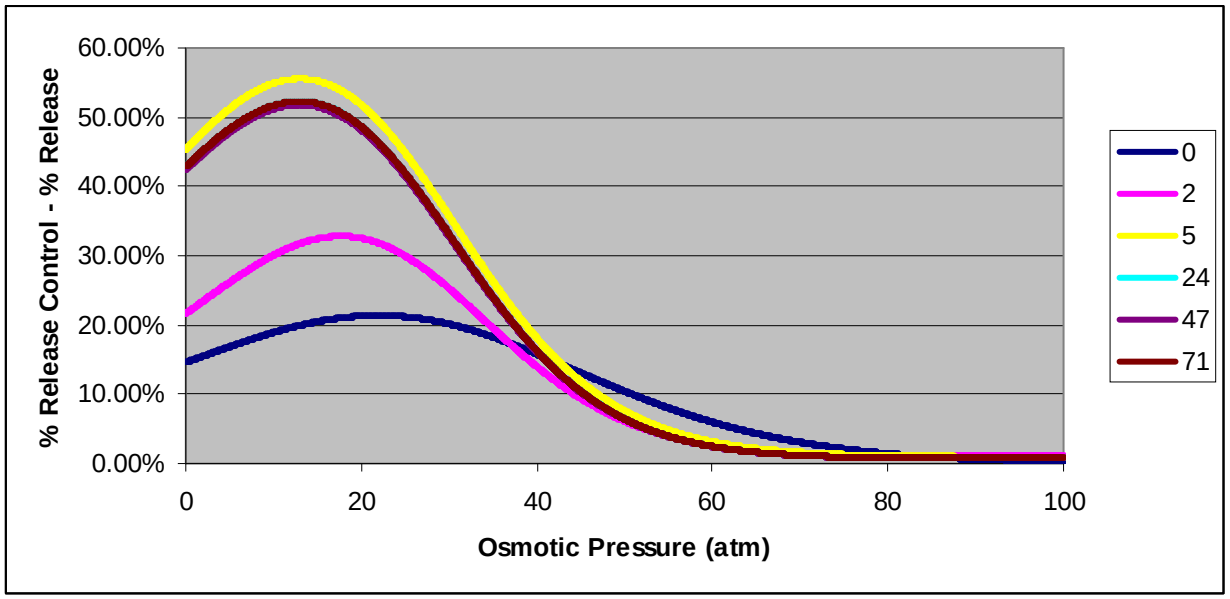

The change in both of the variables (maximum difference in release and pressure at maximum difference in release) can be graphed verses time. These are shown in figure 2.4.16 and figure 2.4.17.

Figure 2.4.16 Maximum Difference in Release verses Time

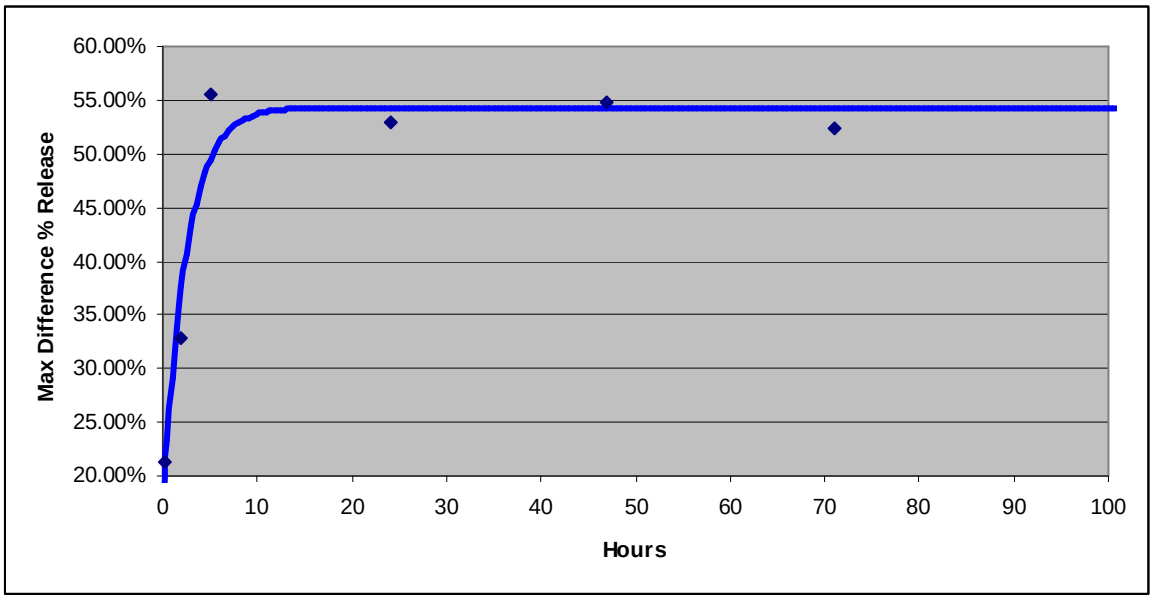

Figure 2.4.17 Optimal Pressure verses Time

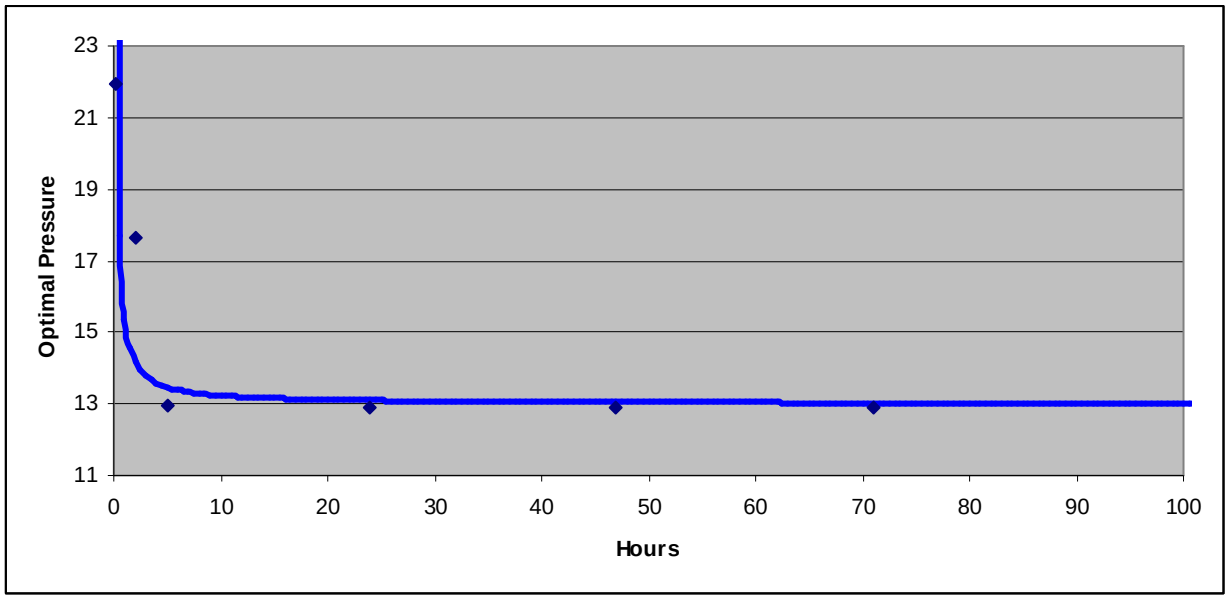

Because of the time that it takes for the liposomes to reach osmotic equilibrium, all further fluorescence measurements were taken at least 16 hours after starting the experiment. This is enough time to ensure that both the bare liposomes and the polymer caged liposomes have reached osmotic equilibrium but is well within the tested window for stability of results (results stay stable for at least three days, the maximum testing period).

2.4.3.e. Membrane Composition

In order to maximize the pressure resistance of the polymer caged liposomes, the next variable looked at was the composition of the membrane. The membrane consists of three parts: DPPC which is the main lipid component of the membrane, cholesterol which is added to give fluidity and elasticity to the membrane, and DOPC which is added to increase water permeability and to prevent elasticity from becoming too large. The DPPC is considered the main component of the membrane, so the other two components, DOPC and cholesterol, were changed in concentration to determine their effect on $P_{Max\ ext}$.

Oleic Acid Content

To determine how oleic acid concentration affects $P_{Max\ ext}$, bare liposomes were prepared as described above (2.3.3.a) using either:

- 27.5 mg DPPC (37.5 μmol, 51.5 mol%), 2.1 mg DOPC (2.67 μmol, 3.7 mol%), and 12.6 mg cholesterol (32.6 μmol, 44.8 mol%)
- 28 mg DPPC (38.1 μmol, 52.6 mol%), 1.4 mg DOPC (1.78 μmol, 2.5 mol%) and 12.6 mg cholesterol (44.9 mol%)
- 28.5 mg DPPC (38.8 μmol, 53.7 mol%), 0.7 mg DOPC (0.89 μmol, 1.2 mol%) and 12.6 mg cholesterol (45.1 mol%)

in 10x HBS with 100 mM carboxyfluorescein. Bare liposomes constituting 3 μmol of DPPC (1 equivalent) were added to 30 μL (6 mg, 0.34 equivalents) of the prepared polymer at 200 mg/mL and diluting to 400 μL with 10x HBS. The resulting PILs, after incubating and purifying were added to 70 μL 1% ethylenediamine (1000 nmol, 60% crosslinking).

After incubating and purifying, the concentration of carboxyfluorescein in the polymer caged liposomes and the bare liposomes was measured as described above (2.3.6). Both the sample and the control were diluted to 4 μM carboxyfluorescein and a final tonicity of either 10x, 9.5x, 9x, 8x, 7x, 6x or 5x HBS (the solutions were marked by the difference in concentration (0, 0.5, 1, 2, 3, 4 and 5 respectively). The osmotic pressure against the 10x HBS inside the liposomes is 0, 3.38, 6.76, 13.52, 20.28, 27.04 and 33.81 atm respectively. The solutions were incubated at 37.5 °C overnight and fluorescent intensity was measured as described above (2.3.7.a). Fluorescent intensity and percent release verses osmotic pressure can be seen in Appendix D. A summary graph compiling all of the calculated curves is shown in figure 2.4.18 for the bare liposomes and 2.4.19 for the polymer caged liposomes.

Figure 2.4.18 Bare Liposomes % Release verses Osmotic Pressure Fitting Curves

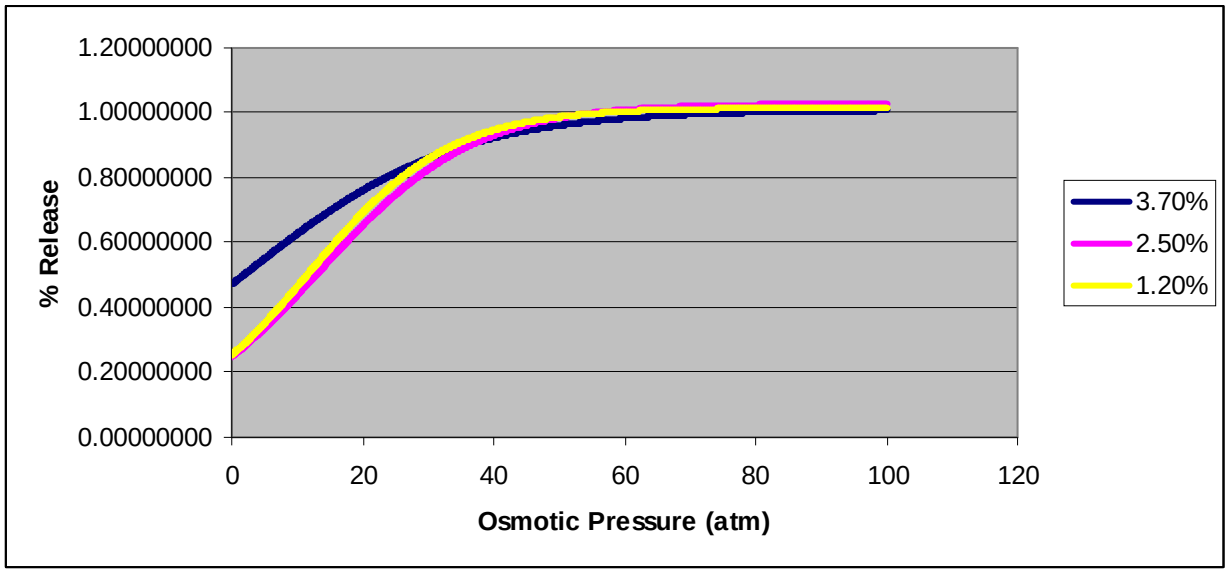

Figure 2.4.19 Polymer Caged Liposomes % Release verses Osmotic Pressure Fitting Curves

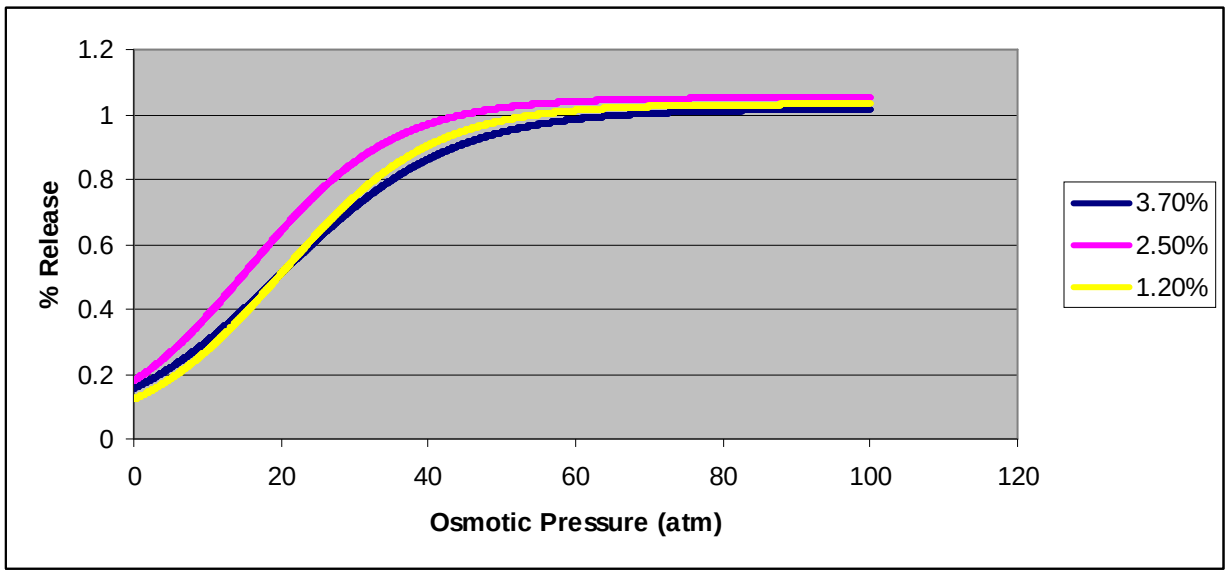

As can be seen in figure 2.4.18, lower concentrations of DOPC lowered the percent release at lower osmotic pressures. This is consistent with the earlier findings that DOPC is necessary to allow water permeability and reduce membrane elasticity. As the amount of DOPC is lowered, the pressure needed to cause effective pressure in the membrane becomes larger,

making the lower pressures reduce their percent release. As can be seen in figure 2.4.19, lowering the concentration of DOPC did not affect the percent release of the polymer caged liposomes significantly. This also fits into earlier findings. The polymer caged liposomes are not dependent on membrane elasticity as the main pressure resistance. Thus, changing the elasticity and water permeability of the membrane does not significantly change the percent release.

Because the bare liposomes have lower percent release with lower DOPC concentrations, the isobaric difference curves are also going to be smaller at lower DOPC concentrations, indicating that there is less content available for release upon protease degradation (figure 2.4.20). Therefore, keeping the DOPC at 3.7%, or even increasing it slightly will give the best results for this project.

Figure 2.4.20 Differences in Percent Release versus Osmotic Pressure

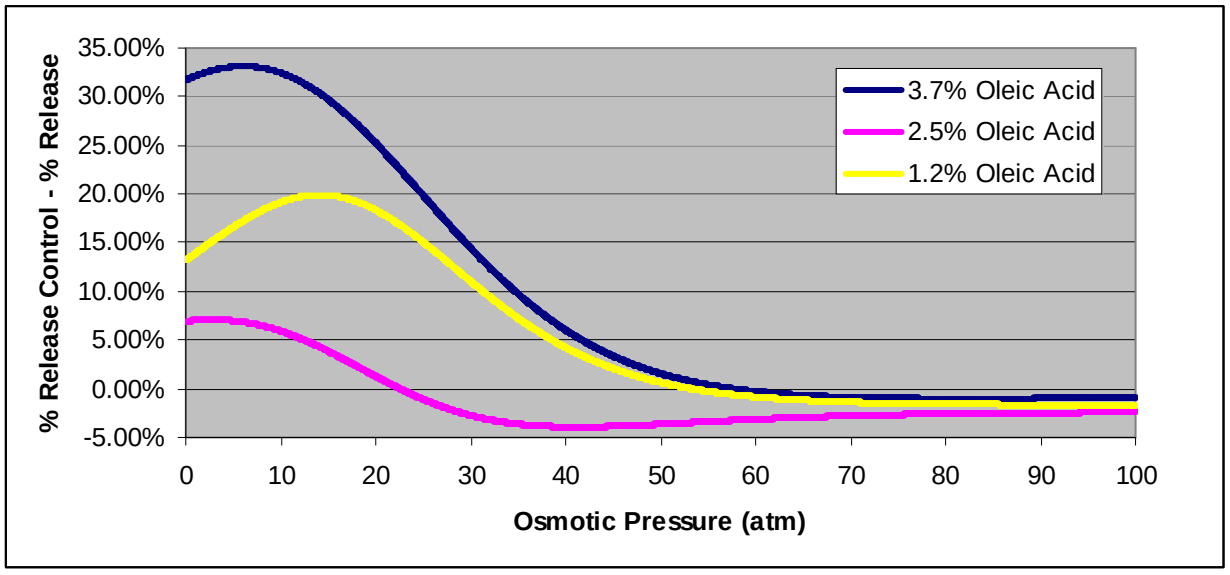

Cholesterol Content

To determine how cholesterol concentration affects $P_{Max\ ext}$, bare liposomes were prepared as described above (2.3.3.a) using either:

- 27.5 mg DPPC (37.5 μmol, 51.5 mol%), 2.1 mg DOPC (2.67 μmol, 3.7 mol%), and 12.6 mg cholesterol (32.6 μmol, 44.8 mol%)
- 27.5 mg DPPC (38.1 μmol, 74.6 mol%), 2.1 mg DOPC (1.78 μmol, 5.3 mol%) and 3.9 mg cholesterol (10.1 μmol, 20.1 mol%)

in 10x HBS with 100 mM carboxyfluorescein. Bare liposomes constituting 3 μmol of DPPC (1 equivalent) were added to 30 μL (6 mg, 0.34 equivalents) of the prepared polymer at 200 mg/mL and diluting to 400 μL with 10x HBS. The resulting PILs, after incubating and purifying were added to 70 μL 1% ethylenediamine (1000 nmol, 60% crosslinking).

After incubating and purifying, the concentration of carboxyfluorescein in the polymer caged liposomes and the bare liposomes was measured as described above (2.3.6). Both the sample and the control were diluted to 4 μM carboxyfluorescein and a final tonicity of either 10x, 9.5x, 9x, 8x, 7x, 6x or 5x HBS (the solutions were marked by the difference in concentration (0, 0.5, 1, 2, 3, 4 and 5 respectively). The osmotic pressure against the 10x HBS inside the liposomes is 0, 3.38, 6.76, 13.52, 20.28, 27.04 and 33.81 atm respectively. The solutions were incubated at 37.5 °C overnight and fluorescent intensity was measured as described above (2.3.7.a). Fluorescent intensity and percent release verses osmotic pressure can be seen in Appendix E. A summary graph compiling all of the calculated curves is shown in figure 2.4.21 for the bare liposomes and 2.4.22 for the polymer caged liposomes.

Since the cholesterol level was already nearly saturated, a higher concentration of cholesterol was not test, only a lower concentration of cholesterol. As can be seen in figures 2.4.21 and 2.4.22, lowering the cholesterol level shifts $P_{Half\ Max}$ of both the bare liposomes and the polymer caged liposomes to the left. The change is approximately the same for both bare liposomes and polymer caged liposomes, so the $P_{Max\ ext}$ value does not change. The optimal

osmotic pressure does shift to the left, though. $P_{Half\ Max}$, $P_{Max\ ext}$ and optimal pressure values are shown in Table 2.4.13.

Figure 2.4.21 Bare Liposomes % Release verses Osmotic Pressure Fitting Curves

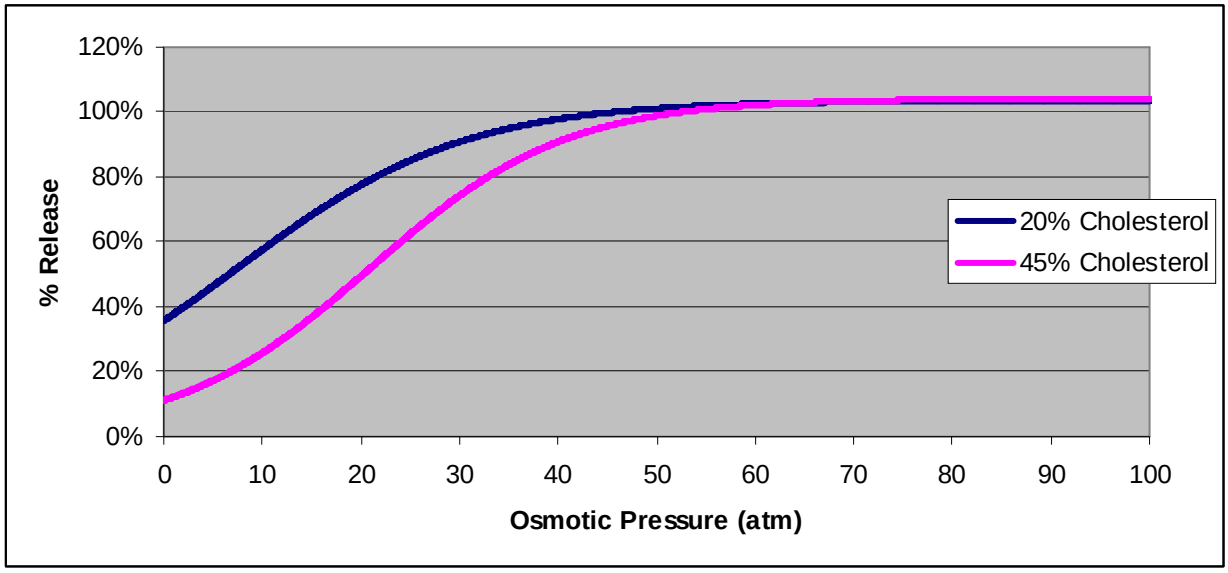

Figure 2.4.22 Polymer Caged Liposomes % Release verses Osmotic Pressure Fitting Curves

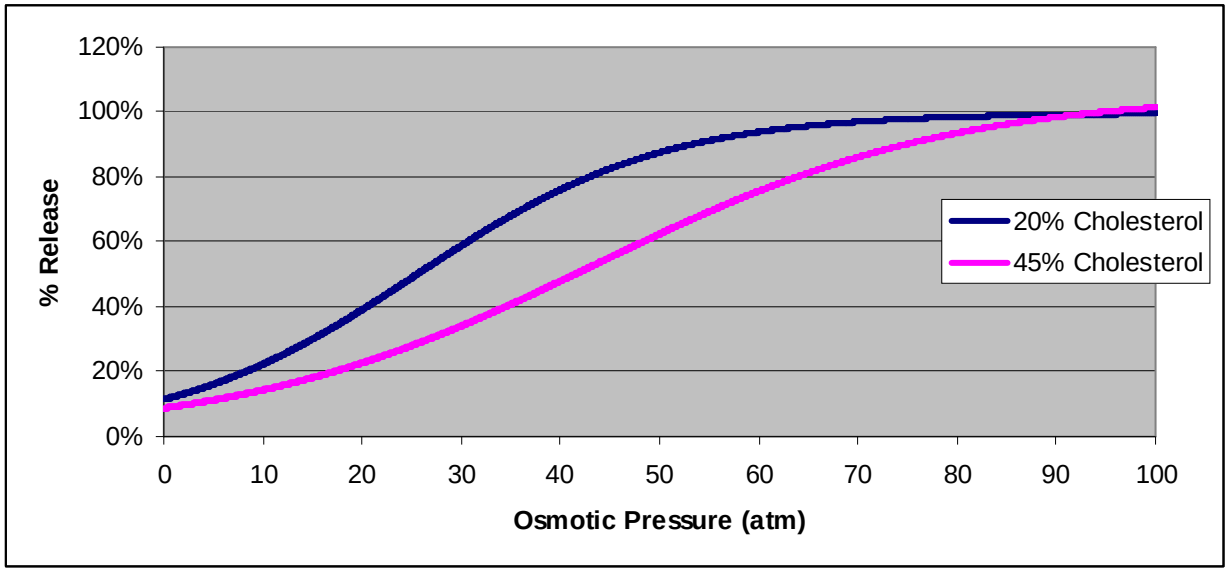

Table 2.4.13 $P_{Half\ Max}$, $P_{Max\ ext}$, and Optimal Pressure

	20% Chol	45% Chol
BL	6.55	20.2
PCL	25.5	41.4
$P_{max\ ext}$	18.95	21.2
Opt P	17.95	37.25

Taking these results with the results above for differences in oleic acid concentration, the activities of cholesterol and oleic acid can be determined. Oleic acid concentration affects only the bare liposomes and not the polymer caged liposomes. Cholesterol concentration affects both bare liposomes and polymer caged liposomes. This can be explained by oleic acid having more effect on the elasticity of the membrane while cholesterol has more effect on the water permeability of the membrane. The elasticity of the membrane is going to affect the bare liposomes more than the polymer caged liposomes because the polymer caged liposomes do not depend on membrane elasticity to prevent release. Rather, they depend on the 'elasticity' of the polymer cage as their main resistance to osmotic leakage. On the other hand, water permeability will affect both bare liposomes and polymer caged liposome approximately the same because decreased water permeability reduces the effective osmotic pressure of the system. Reducing the effective osmotic pressure will increase $P_{Half\ Max}$ for both bare liposomes and polymer caged liposomes.

The isobaric difference in release can also be calculated for the different cholesterol concentrations and is shown in figure 2.4.23. As would be expected from the $P_{Half\ Max}$ and $P_{Max\ ext}$ values, the maximum difference in release is not much different between low and high concentrations of cholesterol in the membrane. The pressure at the maximum difference does shift to the right with increasing cholesterol concentration, though.

Figure 2.4.23 Differences in Percent Release versus Osmotic Pressure

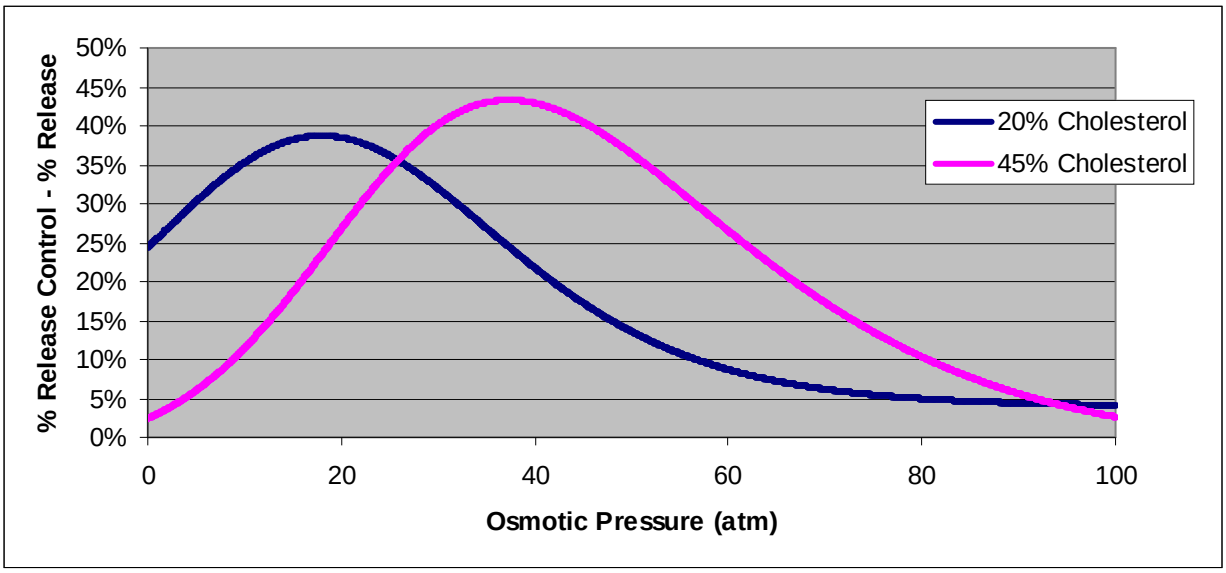

2.4.3.f. Revisiting Polymer Content and Concentration

In 2.4.3.c, several different polymer contents and crosslinking % were tried. The polymer content tested spanned a wide range of equivalence values verses the lipid content, but did not span a wide range of distances between polymer molecules. In fact, 0.017 equivalents of polymer equals an average of 5.3 nm between polymers in the membrane, 0.034 equivalents of polymer equals an average of 3.7 nm, and 0.050 equivalents of polymer equals an average of 3.1 nm between polymers. Since the polymer fully stretched is nearly 12 nm long, these values allow substantial, if not excessive overlap. To see if a less overlapped (and thus a polymer that was already more stretched out) would increase the isobaric difference between bare liposomes and polymer caged liposomes and/or $P_{Max\ ext}$, polymer equivalents were added to bare liposomes so that there would be, on average, either 3 nm, 6 nm, or 9 nm between the liposomes (increasing the range tested by 50%).

Also, because the crosslinker in 2.4.3.c was chosen as an equivalent to lipid content and not as an equivalent to acrylic acid residue concentration, somewhat random (and sometimes irrational) percent crosslinking was calculated for the liposomes. To more methodically

determine ideal percent crosslinking, crosslinker was chosen as an equivalent to acrylic acid residue content at either 25% (50% crosslinking because each crosslinker crosslinks two residues), 37.5% (75% crosslinking), or 50% (100% crosslinking).

Bare liposomes were synthesized as above (2.3.3.a) using 27.5 mg DPPC (37.5 μmol, 47.5 mol%), 3.1 mg DOPC (3.9 μmol, 5.0 mol%), and 14.5 mg cholesterol (37.5 μmol, 47.5 mol%) hydrated in 10x HBS with 100 mM carboxyfluorescein. Bare liposomes constituting 4 μmold DPPC + DOPC (1 equivalent) were added to either 25 nmol (0.006 equivalent, average 9 nm between polymers), 53 nmol (.013 equivalents, average 6 nm between polymers), or 212 nmol (.053 equivalents, average 3 nm between polymers) of the synthesized polymer and diluted to 600 μL. These were designated low (L), medium (M), or high (H) samples respectively.

After incubating overnight to prepare polymer incorporated liposomes, EDC*MeI and ethylenediamine were added without a purification step (one-pot procedure) in order to increase yield. To the low sample, either 146 nmol (0.036 equivalents, 50% crosslinking), 219 nmol (0.055 equivalents, 75% crosslinking), or 292 nmol (0.073 equivalents, 100% crosslinking) were added along with EDC*MeI at 1500:1 EDC:ethylenediamine. These were designated L50, L75, and L100 respectively. To the medium sample, either 313 nmol (0.078 equivalents, 50% crosslinking), 470 nmol (0.117 equivalents, 75% crosslinking), or 626 nmol (0.157 equivalents, 100% crosslinking) of ethylenediamine were added along with EDC*MeI at 1500:1 EDC:ethylenediamine. These were designated M50, M75, and M100 respectively. To the high sample either 1250 nmol (0.313 equivalents, 50% crosslinking), 1880 nmol (0.470 equivalents, 75% crosslinking), 2500 nmol (0.626 equivalents, 100% crosslinking) of ethylenediamine were added along with EDC*MeI at 1500:1 EDC:ethylenediamine. These were designated H50, H75 and H100 respectively.

After incubating and purifying, the concentration of carboxyfluorescein in the polymer caged liposomes and the bare liposomes were measured as described above (2.3.6). Both the sample and the control were diluted to 4 μM carboxyfluorescein and a final tonicity of either

10x, 9.5x, 9x, 8x, 7x, 6x, 5x, 3x, 1x, or 0.5x HBS (the solutions were marked by the difference in concentration (0, 0.5, 1, 2, 3, 4, 5, 7, 9, and 9.5 respectively). The osmotic pressure against the 10x HBS inside the liposomes is 0, 3.38, 6.76, 13.52, 20.28, 27.05, 33.81, 47.33, 60.85, and 64.23 atm respectively. The solutions were incubated at 37.5 °C overnight and fluorescent intensity was measured as described above (2.3.7.a). Fluorescent intensity and percent release verses osmotic pressure can be seen in Appendix F. A summary graph compiling all of the calculated curves is shown in figure 2.4.24 and the isobaric difference curves are shown in figure 2.4.25.

Figure 2.4.24 % Release verses Osmotic Pressure Fitting Curves

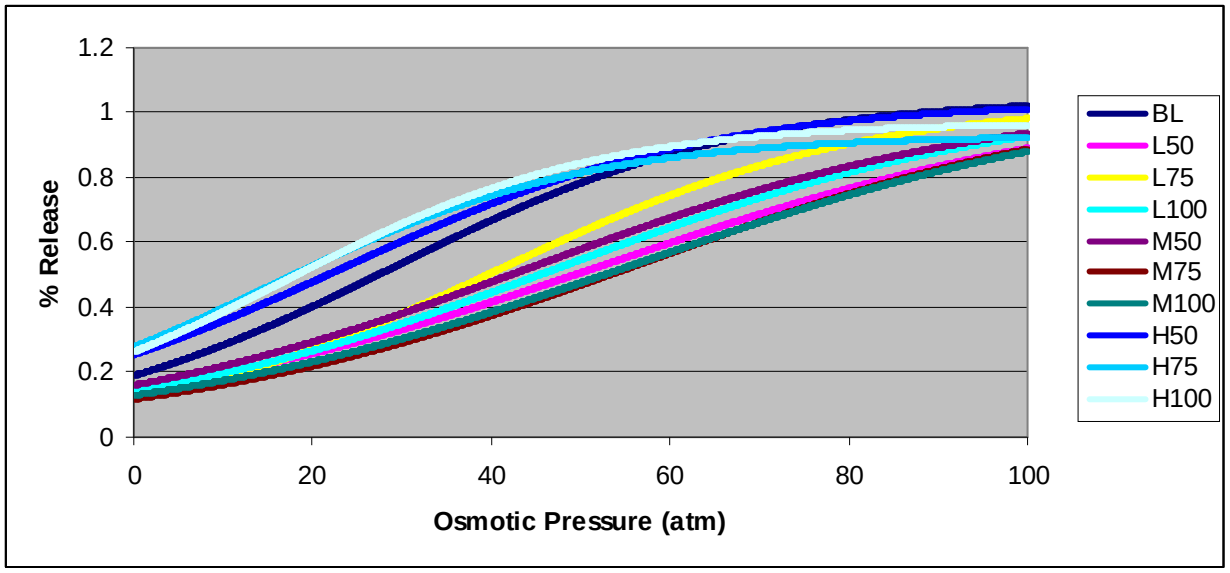

The top six values for maximum difference in percent release verses control were all from samples with spacing farther apart (lower percent polymer) than 2.4.3.c. This would indicate that having less overlap between the polymers is a good thing. This is a reasonable result, because polymers that start out more stretched out are going to have less expansivity than loose polymers (and polymers that have to stretch farther to crosslink will be more stretched out). Thus, the membrane will expand less due to osmotic pressure before interacting with the

polymer cage and will thus release less of the liposomal contents in the expansion process. The drawback could be a weaker polymer cage, but the data does not support this. The lower polymer integration level liposomes start out at low osmotic pressures with lower leakage and continue to be lower when the osmotic pressure is raised. There does seem to be a drop off in polymer cage strength in the very low integration levels (spacing average 9 nm apart).

Table 2.4.14 $P_{Half\ Max}$ and $P_{Max\ ext}$ Values

	$P_{Half\ Max}$	$P_{Max\ ext}$	Area under Difference Curve
BL	27.3	0	0
L50	49.25	21.95	393
L75	39.5	12.2	222
L100	45.35	18.05	331
M50	42.1	14.8	282
M75	53.2	25.9	451
M100	52.55	25.25	441
H50	21.65	-5.65	-68
H70	17.85	-9.45	-48
H100	18.15	-9.15	-90

Figure 2.4.25 Differences in Percent Release versus Osmotic Pressure

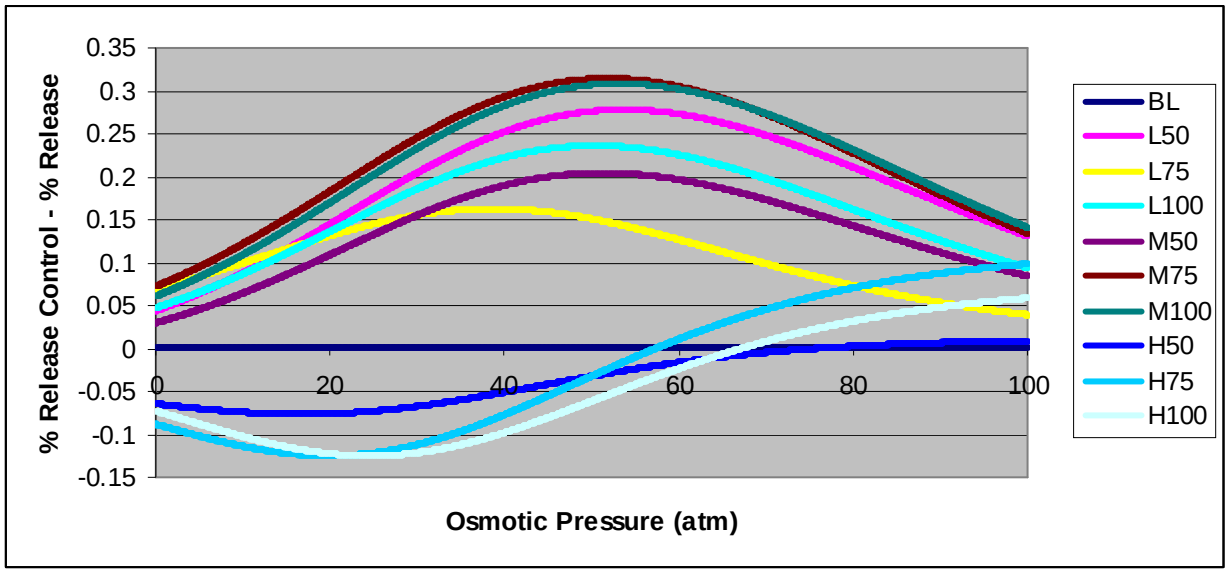

The very high concentration of polymer (average spacing 3 nm apart) actually shows very little difference from bare liposomes. This is probably due to a very large expansivity of the polymer cage before it will resist osmotic pressure. Although the polymer cage is well crosslinked, since the polymer is very close together, it can be stretched apart a little bit before the crosslinking is truly tight. In very high concentrations of polymer, the expansivity appears to be greater than the maximum membrane expansivity, so the liposomes will leak out all of their contents before the polymer shell will provide resistance to osmotic pressure.

Thus, the optimal spacing between polymers appears to be between 5 and 6 nm on average (1.3% - 1.9% polymer). These values of polymer integration have consistently had the highest isobaric pressure differences and the highest $P_{Max\ ext}$ values. The optimal value of crosslinking seems to depend strongly on polymer integration level. At higher integrations, less crosslinking seems to be preferred, while at lower integrations, more crosslinking seems to be preferred.

2.4.4. Urokinase Release of Contents

Initial Test

Bare liposomes were prepared as described above (2.3.3.a) using 27.5 mg DPPC (37.5 μmol, 51.5 mol%), 2.1 mg DOPC (2.67 μmol, 3.7 mol%), and 12.6 mg cholesterol (32.6 μmol, 44.8 mol%) in 4.75x HBS with 100 mM carboxyfluorescein. Bare liposomes constituting 3 μmol of DPPC (1 equivalent) were added to 30 μL (6 mg, 0.34 equivalents) of the prepared polymer at 200 mg/mL and diluting to 400 μL with 4.75x HBS. The resulting PILs, after incubating and purifying were added to 70 μL 1% ethylenediamine (1000 nmol, 40% crosslinking). This is the same as sample 4 from 2.4.3.c except in 4.75x HBS instead of 10x HBS. It was prepared in 4.75x HBS so that when diluted into 1x HBS (for uPA studies) they would be at the optimal pressure for maximum difference in percent release calculated above.

After incubating and purifying, the concentration of carboxyfluorescein in the polymer caged liposomes was measured as described above (2.3.6). The liposomes were diluted to 4 μM carboxyfluorescein and a final tonicity of 4.75x HBS and the sample had either no uPA added or 25 μg/mL uPA added. The osmotic pressure against the 4.75x HBS inside the liposomes is 25 atm, the optimal pressure for maximum difference in 2.4.3.c. The solutions were incubated overnight at 37.5 °C and fluorescent intensity was measured as described above (2.3.7.a). Fluorescent intensity can be seen in Appendix G. A summary graph showing average total fluorescent intensity is shown in figure 2.4.26.

Figure 2.4.26 Total Fluorescent Intensity

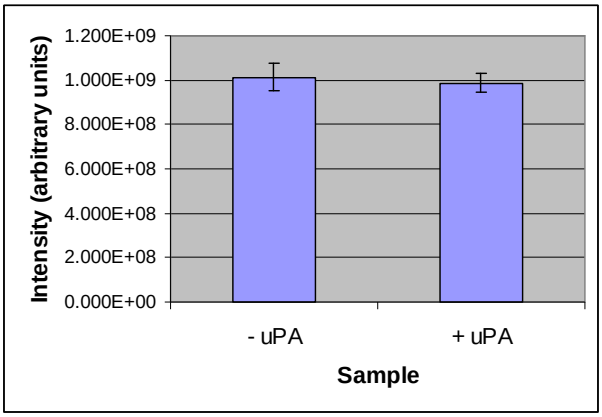

As can be seen in figure 2.4.26, there was very little difference between the no uPA sample and the uPA sample, indicating that the polymer caged liposome is not sensitive to uPA as was desired. The p value between the two samples was 0.5173, again indicating that there is no difference between the samples. There are three instantly obvious reasons why this could be happening: 1) the liposomes are not sensitive to uPA and the experiment failed; 2) there is not enough uPA to effectively degrade the polymer cage; or 3) the uPA that was used was not active for some reason. Of these three possibilities, #2 can be discounted immediately because 25 μg/mL is a very high concentration relative to biological systems, so needing a higher concentration that 25 μg/mL would be impractical for the desired effects. Of the remaining two possibilities, #3 is by far the easiest to fix. Therefore a fresh batch of uPA was ordered.

Second Test

While waiting for the new uPA to arrive, the polymer caged liposomes were optimized as described above. Once the uPA arrived, bare liposomes were synthesized as above (2.3.3.a) using 27.5 mg DPPC (37.5 μmol, 47.5 mol%), 3.1 mg DOPC (3.9 μmol, 5.0 mol%), and 14.5 mg cholesterol (37.5 μmol, 47.5 mol%) hydrated in 8x HBS with 100 mM carboxyfluorescein. Bare liposomes constituting 4 μmold DPPC + DOPC (1 equivalent) were added to 53 nmol (.013 equivalents, average 6 nm between polymers)) of the synthesized polymer and diluted to 600 μL.

After incubating overnight to prepare polymer incorporated liposomes, EDC*MeI and ethylenediamine were added without a purification step (one-pot procedure) in order to increase yield. To the PILs 470 nmol (0.117 equivalents, 75% crosslinking) of ethylenediamine were added along with EDC*MeI at 1500:1 EDC:ethylenediamine.

After incubating and purifying, the concentration of carboxyfluorescein in the polymer caged liposomes and the bare liposomes were measured as described above (2.3.6). Both the bare liposomes and polymer caged liposomes were diluted to 4 μM carboxyfluorescein and a final tonicity of 1x HBS without uPA (for a positive and negative control). The polymer caged

liposomes were also diluted to 4 μM carboxyfluorescein and a final tonicity of 1x HBS with 25 μg/mL uPA (as the sample). Finally, the polymer caged liposomes were also diluted to 4 μM carboxyfluorescein and a final tonicity of 8x HBS without uPA (as a baseline value). The osmotic pressure in 1x HBS against the 8x HBS inside the liposomes is 47.33 atm (8x verses 8x is 0 atm). The solutions were incubated at 37.5 °C overnight and fluorescent intensity was measured as described above (2.3.7.a). Fluorescent intensity can be seen in Appendix H. A summary graph showing average total fluorescent intensity is shown in figure 2.4.27. T-test P values for each comparison are given in table 2.4.15

Figure 2.4.27 Total Fluorescent Intensity

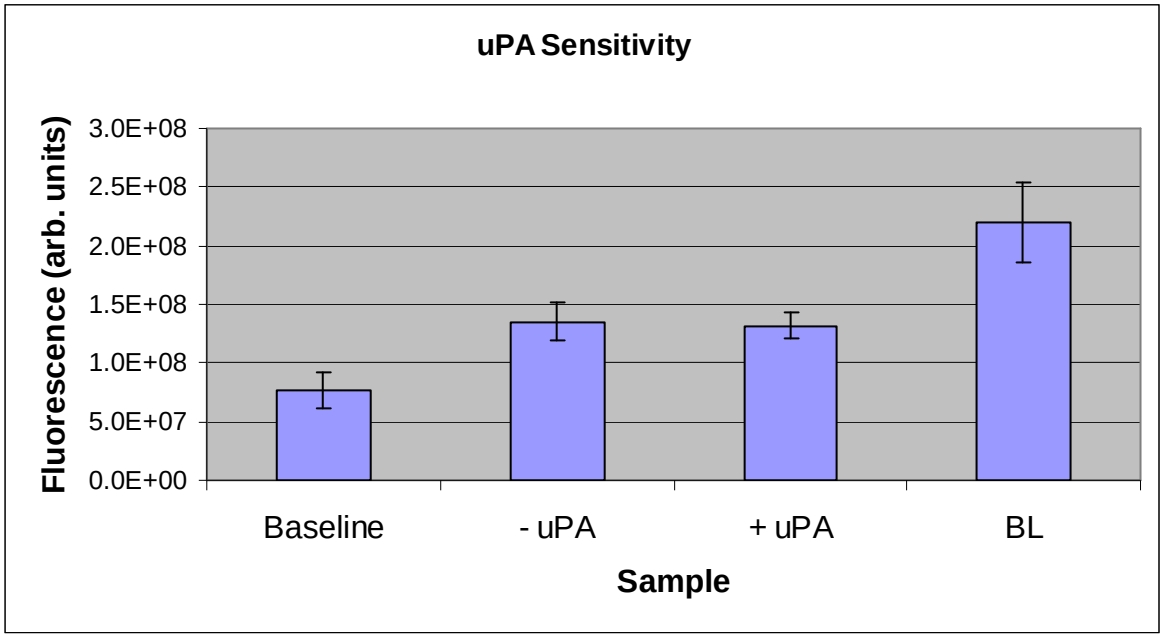

Table 2.4.15 T-test P Values

t test	Base vs. - uPA	Base vs. + uPA	- uPA vs. + uPA	Base vs. BL	- uPA vs. BL	+ uPA vs. BL
p value	<.0001	0.0001	0.6617	0.0001	0.0009	0.0009
Significant	Yes	Yes	No	Yes	Yes	Yes

As expected, the – uPA value was somewhat above baseline, indicating a small amount of leakage with osmotic stress but significantly lower than the BL at the same osmotic pressure. The most important result is the comparison of the + uPA and – uPA samples. They show very little difference in total intensity and the p value is 0.6617 between the two, indicating that they are not different. Thus, the polymer caged liposomes are still not sensitive to uPA and the new uPA did not solve the problem.

Third Test

The last possible option, barring the experiment having failed, is that there was nothing wrong with the uPA of either batch, except that it had become denatured during storage. To test this last possibility, the same liposomes were prepared as in the second test above. The same fluorescent test samples were prepared as well, with the exception of the baseline sample (which was considered unnecessary). Thus there is a – uPA sample as a negative control, a BL sample as a positive control, and a + uPA sample as the test sample. A fourth sample was also introduced that had renatured uPA in it. A sample of uPA was renatured by heating to 90°C for 5 minutes and then cooling to room temperature and repeating twice. This sample of uPA was also used to make a + uPA sample, so that there are two +uPA samples one with non-renatured uPA and one with renatured uPA. Fluorescent intensities can be seen in figure 2.4.28 and a summary graph of total fluorescent intensity can be seen in figure 2.4.29 and a table of p values can be seen in table 2.4.16.

Figure 2.4.28 Fluorescent Intensity

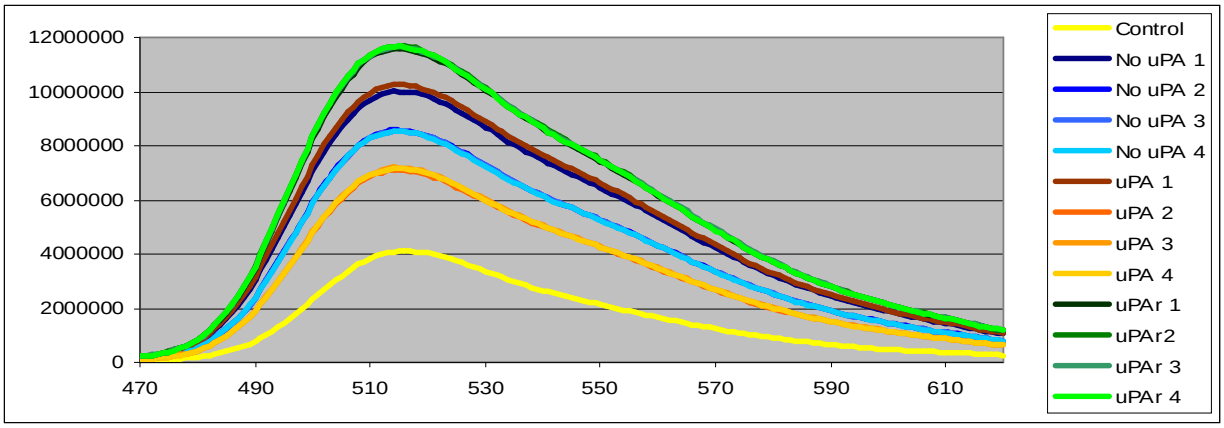

Figure 2.4.29 Total Fluorescent Intensity

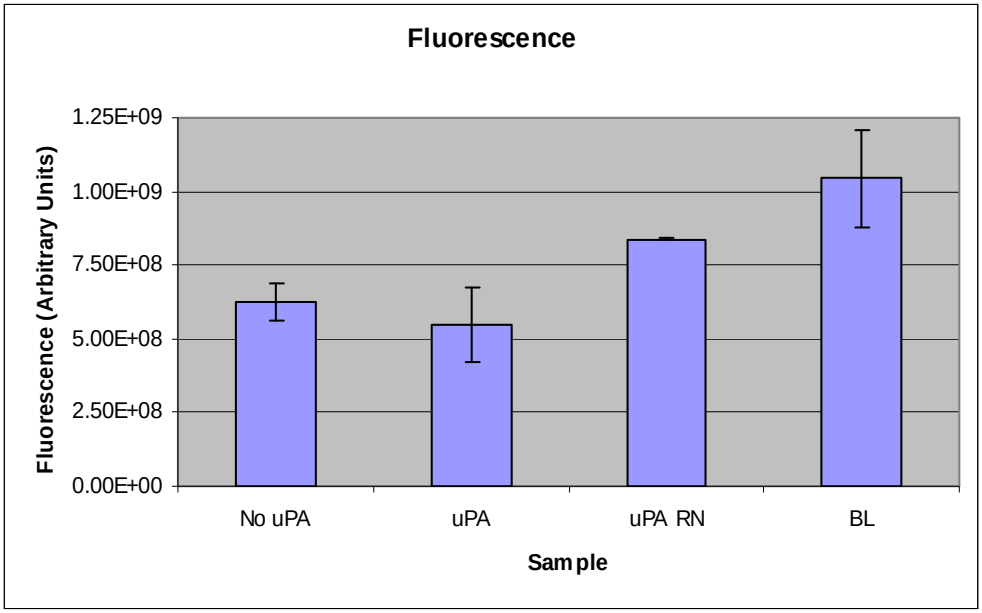

Table 2.4.16 T Test P Values

t test	No uPA / uPA	No uPA / uPA RN	uPA / uPA RN	uPA RN / BL	uPA / BL	No uPA / BL
p value	0.3426	0.0071	0.0203	0.0888	0.0032	0.0093
Significant	No	Yes	Yes	No	Yes	Yes

As can be seen in figure 2.4.29, there is a difference between the uPA and uPA renatured sample, which would indicate that the uPA that was used before was denatured. More importantly, there is a difference between the no uPA sample and the uPA sample with the uPA sample being significantly higher (p value 0.0071). Compared to the BL sample, the uPA RN

mean is lower, but it is on the verge of not being statistically significant (p value 0.0888) indicating there is a small possibility that the uPA RN and the BL are the same. Whether it is the same or not, though, the polymer caged liposomes are sensitive to the renatured uPA and release their contents in response to uPA. This concludes the last necessary step in proving that the polymer caged liposomes are a valid possibility for protease sensitive treatments.

2.5. Conclusion

2.5.1. Summary

The purpose of this study was to develop a drug delivery device that would quickly release its contents upon interaction with a specific protease, but would be stable until then. The proposed method (figure 2.5.1) was to prepare liposomes in a high tonic buffer so that they are intrinsically unstable in low tonic buffers. The intrinsically unstable liposomes would then be stabilized by forming a covalently bound polymer cage around the liposome. This would be done by synthesizing a cholesterol anchored protease sensitive block copolymer and then allowing the cholesterol anchor to diffuse into the membrane of the bare liposomes. The integrated polymer would then be crosslinked with a diamine (since one of the blocks of the polymer is acrylic acid, a diamine will crosslink the polymer) to give polymer caged liposomes.

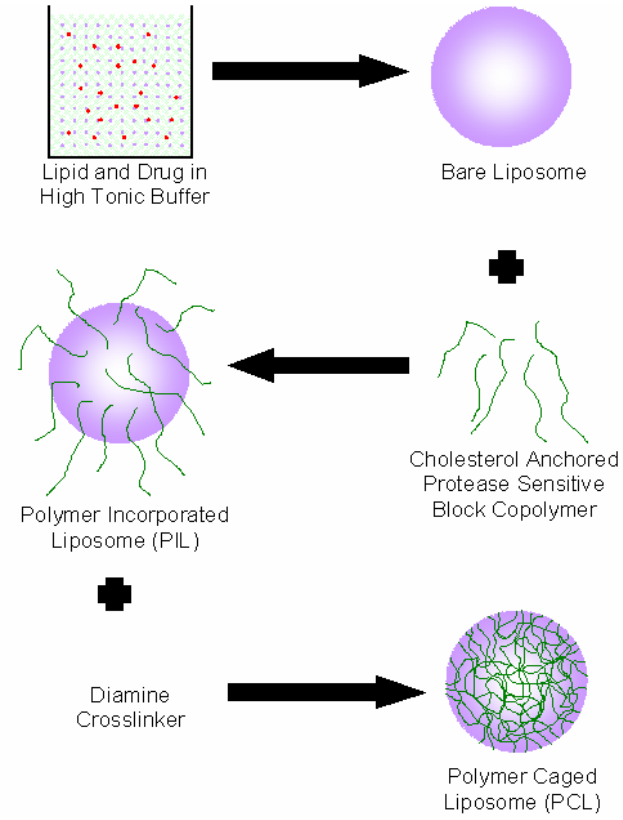

Figure 2.5.1 Proposed Method for Developing a Protease Sensitive Drug Delivery System

Each of these steps has been successfully accomplished. A cholesterol-anchored, protease-sensitive, block copolymer containing polyacrylic acid was synthesized (2.3.2). Bare liposomes were successfully prepared in high tonic buffer (2.4.2.a) and the synthesized polymer was successfully integrated into them (2.4.2.c). The polyacrylic acid in the polymer was successfully crosslinked with both a short peptide sequence containing a lysine to make a diamine and ethylenediamine (2.4.2.d).

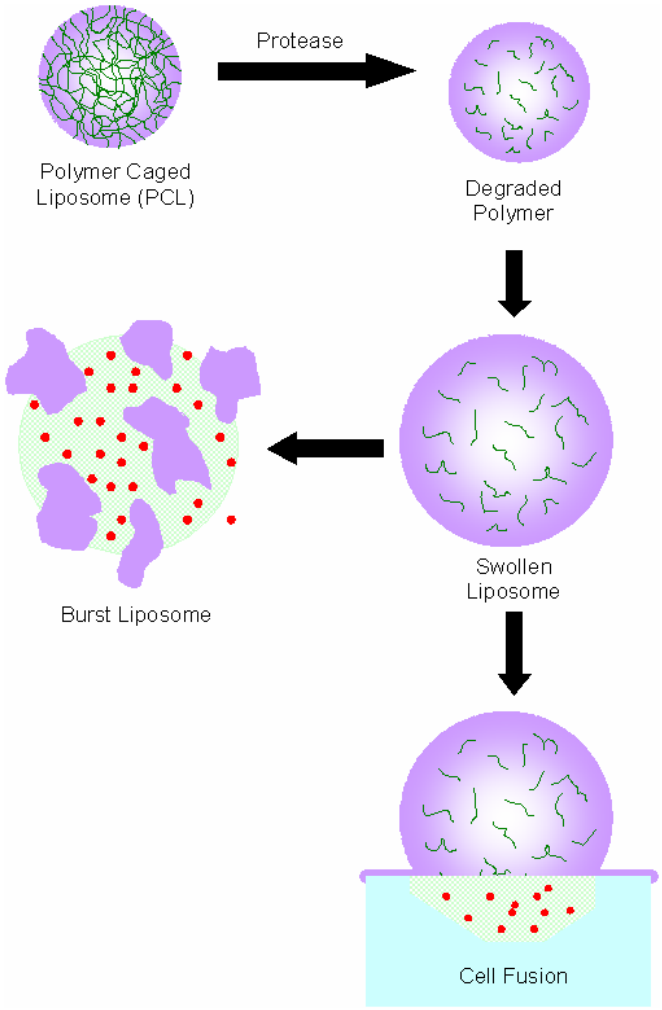

Figure 2.5.2 Proposed Method for Releasing the Contents of the Polymer Caged Liposomes

The proposed method of release was by protease degradation of the polymer. This was accomplished by incorporating a peptide sequence containing the consensus sequence for uPA as

one of the blocks of the synthesized copolymer (2.3.2). The polymer cage was shown to confer substantial osmotic pressure resistance (2.4.3) and the factors affecting how much pressure resistance the polymer cage confers were studied. It was then shown that uPA can degrade the polymer cage and release the contents of the polymer caged liposomes (2.4.4).

As mentioned above (2.4.1), to provide proof of concept of the protease sensitive polymer caged liposome as a usable drug delivery system, the following needs to be proved:

1. Bare liposomes must be successfully prepared
2. Polymer incorporated liposomes must be successfully prepared
3. Polymer caged (crosslinked) liposomes must be successfully prepared
4. Polymer caged liposomes must show significant resistance to osmotic pressure induced leakage verses bare liposomes
5. Polymer caged liposomes must show significant increase in percent release when exposed to urokinase plasminogen activator
6. Each of these steps has been accomplished, so, as a proof of concept, this is a workable system.

Quod erat demonstrandum

2.5.2. Protease Sensitive Liposome Potential and Significance

The system demonstrated above holds enormous potential as a drug delivery system for cancer therapy and perhaps many other diseases as well (as long as there are specific proteases associated with the disease, such as Alzheimer's disease). Liposomes already have some selectivity towards cancer (2.1.4) because of the EPR effect. Adding sensitivity to cancer associated proteases can increase the specificity of the liposome as a drug delivery device, minimizing unwanted side effects from general delivery and increasing the drug delivery to the site (figure 2.5.3). This system could also be stacked to provide multiple layers of specificity by making liposomes sensitive to different proteases. By filling one liposome with a prodrug and another liposome with an activator, three levels of specificity can be obtained (figure 2.5.4).

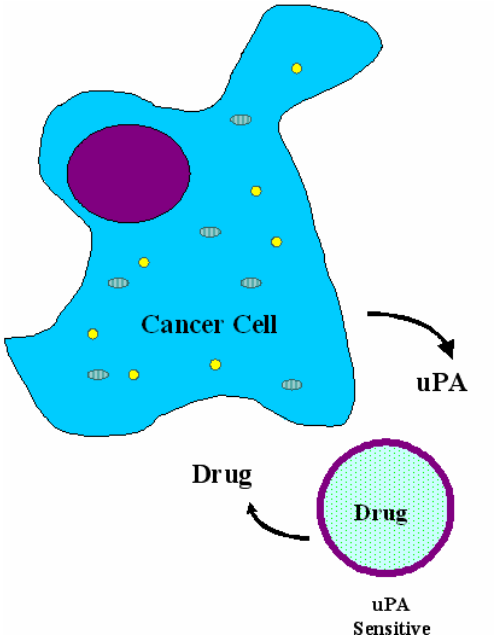

Figure 2.5.3 A schematic showing how protease sensitive liposomes would target cancer. This system would have two levels of specificity: the EPR effect and sensitivity to uPA.

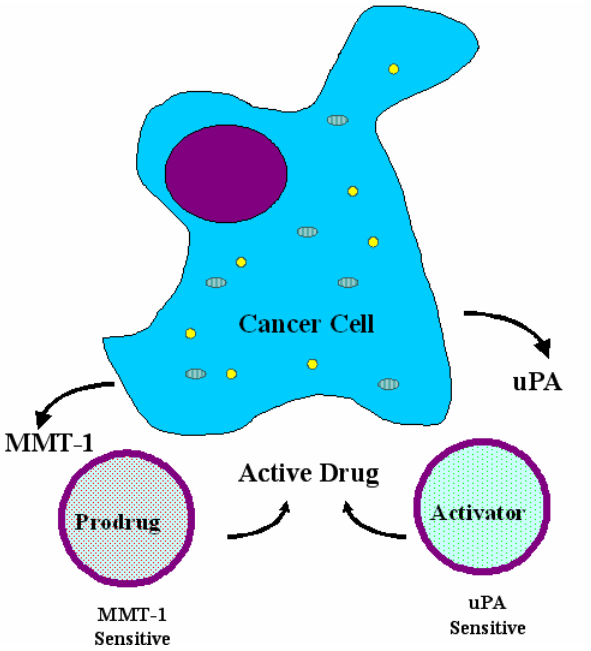

Figure 2.5.4 A schematic showing how protease sensitive polymers could be stacked to provide extra specificity. This system would have three layers of specificity: the EPR effect, sensitivity to uPA and sensitivity to MMT-1.

A major reason cancer therapy sometimes fails is that the undesired side effects of the drug limit the amount of the drug that can be delivered systemically and thus the amount of drug that can be delivered to the tumor. A more specific method of delivery could decrease systemic delivery (and thus unwanted side effects) and increase tumor delivery (increasing effectiveness of the drug). Thus the cancer therapy would be much less likely to fail because of low dosages or stopped because of overwhelming side effects.

2.5.3. Future Work

As a proof of concept study, much more work needs to be done to make the protease sensitive liposomes a useable system. As a next step, three things are proposed: 1) synthesize a block-copolymer with an embedded consensus sequence for another cancer associated protease and use this to make protease sensitive liposomes to a different protease; 2) test the protease sensitive liposome on cell lines known to express the desired cancer associated protease and on cell lines known not to express the desired cancer associated protease; and 3) test the liposomes in small animals for biosystem compatibility and effectiveness as a treatment for cancer.

To provide a layered system such as the one shown in figure 2.5.4, multiple different protease sensitive liposomes need to be developed to target different proteases. Also, not all cancers express uPA so other protease targets would expand the range of cancers that the single layer treatment would be useful for as well. So, the first proposal is to develop another protease sensitive liposome to a different cancer associated protease by going through the procedure detailed above with a different consensus sequence. As a list of consensus sequences is already known (table 1.3.1), the procedure for synthesizing the cholesterol-anchored block copolymer is already optimized and the procedures for preparing and testing the protease sensitive liposomes have already been developed, many new consensus sequences could be tested in a relatively short period of time.

Although the uPA sensitive liposomes worked in a test tube, biological systems often produce unexpected results. Thus the second proposal is to test the liposomes against a range of

cells expressing different proteases *in vitro*. This will show that the liposome system is stable under biological conditions, is effective against biological concentrations of uPA (or other proteases), and resists other proteases that it is not targeted against. Also, how the drug is delivered could also be determined, whether it is simply releasing the drug in the extracellular matrix upon coming in contact with the protease or if it is fusing with the membrane (see 2.1.7).

The third proposal, to test the liposomes *in vivo*, will demonstrate that the liposomes are stable in the blood and can be delivered to the cancer site. It will also demonstrate that the polymer shell does not produce unwanted side effects in the body. The third proposal will also test the true effectiveness of the drug delivery system in cancer therapy. By testing in mice (or other small animals) with known tumors, the liposomes, containing a cancer therapy drug, can be tested for their ability to slow, stop, or reverse the growth of the tumor. This would be the end goal of this project, a drug delivery system that is effective at delivering therapeutic (toxic) agents to tumors that reduces or eliminates the tumor.

3. Protease Sensitive Pro-MspA

3.1. Literature Review

3.1.1. The Complement System

The complement system is a subset of the innate immune system that was discovered in 1896 by Jules Bordet. Bordet demonstrated that there were two components of blood serum that were responsible for its antibacterial properties. When heated, blood serum looses its antibacterial properties. Bordet demonstrated that this was only due to the loss of activity of one of the components by heating blood serum and then adding fresh serum that had the antibodies removed. The antibody depleted serum by itself was not able to lyse cells, nor was the heated serum, but together, the activity was restored. Bordet concluded that the first component of blood serum was the antibodies, and these were resistant to heat. The second component of blood serum was heat labile, and must be added back in after heating for blood serum to retain its antibacterial properties. Several years later, Paul Ehrlich designated the system "complement" because it complemented the activity of the antibodies in blood serum.[1]

The complement system makes up nearly 5% of the protein content in blood serum. There are fourteen known components in the complement system, and most of these components are proenzymes that have no activity until a trigger (such as an activated antibody complex) causes the complement cascade. In the cascade (Figure 3.1.1), either C1, C3 or MASP 1 + 2, are activated from a proenzyme to an active protease (either by self-cleavage, or association). Then C1 or MASP 1 + 2 cleave C2 and C4, which bind together and form another protease (C3 associates with Factor B, which is cleaved by Factor D to become an active protease), called C3 convertase. C3 convertase cleaves C3 which causes it to bind to C3 convertase changing it to C5 convertase another active protease. C5 convertase binds C5 and cleaves it, producing C5a and C5b. C5b can recruit C6, C7, C8 and multiple units of C9 to form the membrane attack complex.[1]

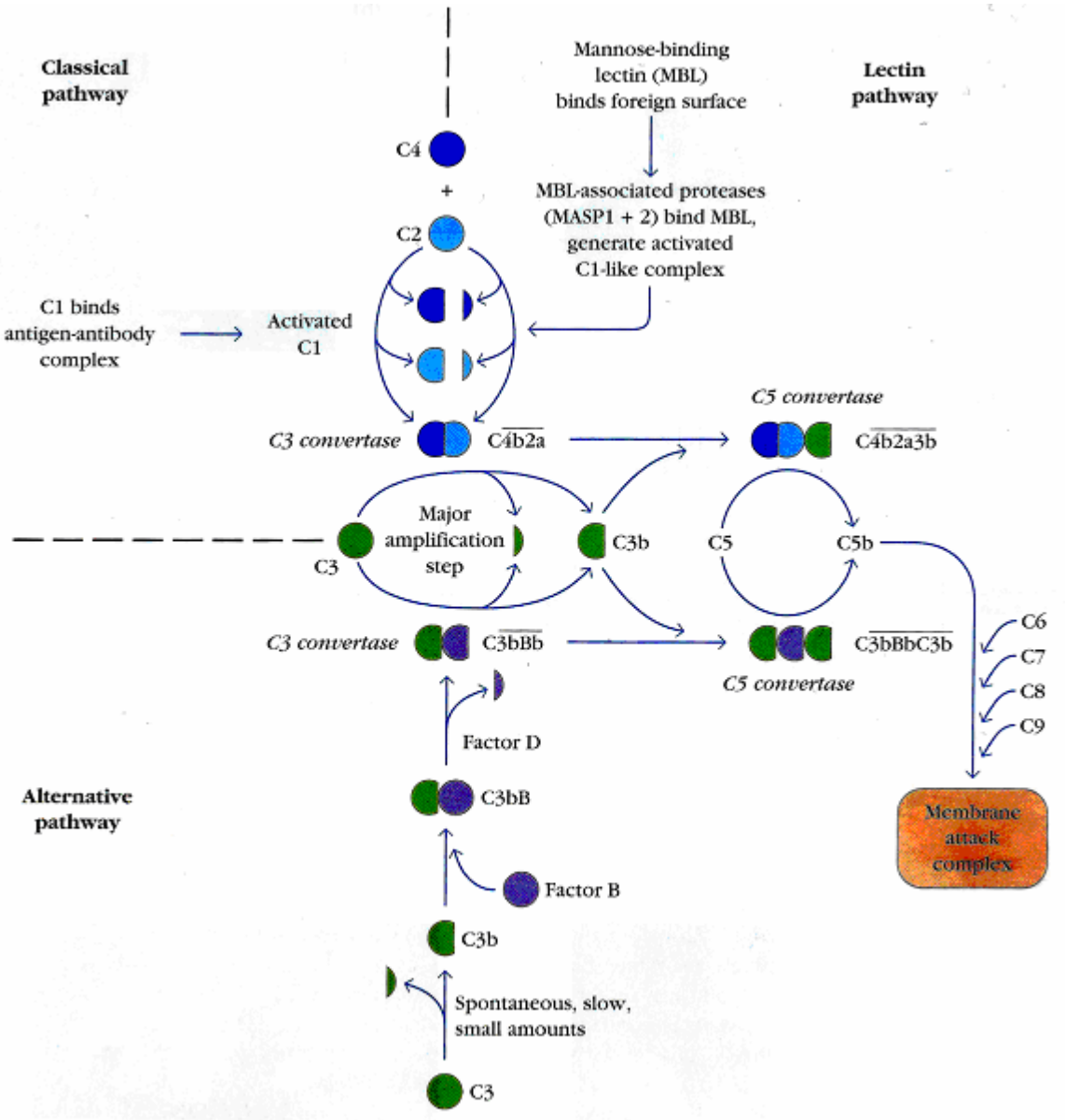

Figure 3.1.1 The Complement Cascade

The main effecter of the complement cascade is the membrane attack complex. C5 when it is cleaved forms a C5a and C5b fragment. The C5a fragment simply diffuses away, but the C5b complex binds to the surface of the offending membrane. C6 binds to C5b on the surface to stabilize C5b (which otherwise would become inactive in less than two minutes). C7 then binds to C5b6 and causes a change in the C5b67 complex that exposes a hydrophobic region to make the C5b67 complex ampiphilic allowing it to insert into the membrane. C8 then binds to the

C5b67 complex and also undergoes a hydrophilic-ampiphilic transition which causes a small pore to form in the membrane (~1 nm). C5b678 then recruits up to 17 C9 proteins to form the membrane attack complex. The C9 proteins form a much larger pore in the membrane (~10 nm) and is much more damaging to the cell (Figure 3.1.2, Figure 3.1.3).[1]

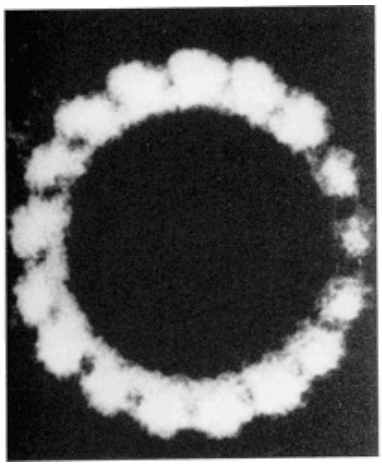

Figure 3.1.2 A photomicrograph of the membrane attack complex

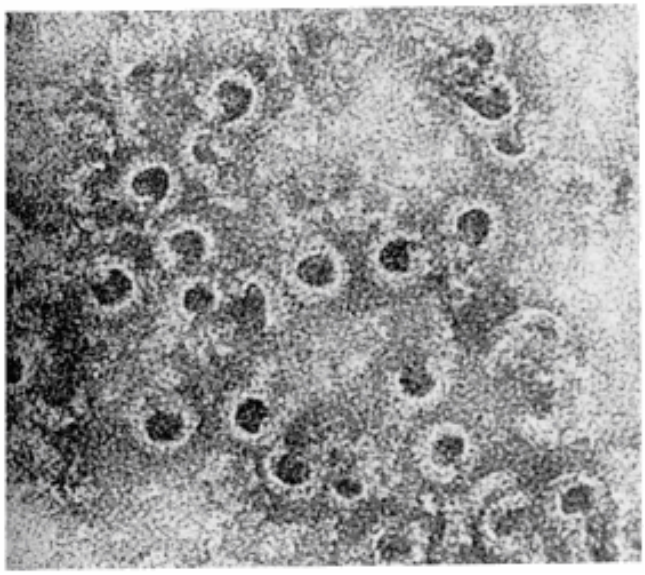

Figure 3.1.3 A photomicrograph of the MAC forming pores in a membrane

The pore formed by the membrane attack complex (MAC), disrupts the finely balanced ion concentrations on both sides of the membrane. Sodium ions rush into the cell, while potassium and chloride ions flow out of the cell. The net results is an influx of ions into the cell, which causes osmosis as water follows the sodium ions into the cell (Figure 3.1.4). The osmotic pressure causes the cell membrane to swell and burst, killing the cell.[1]

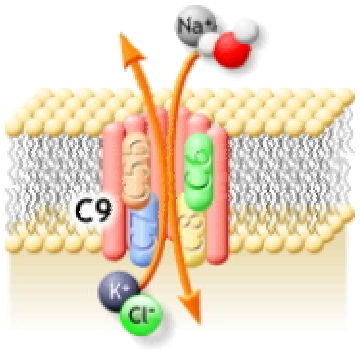

Figure 3.1.4 A schematic of the membrane attack complex showing it poking holes in the membrane. The careful balance of ions across the membrane is destroyed.

The complement system is very finely tuned to kill unwanted cells, and there is very little defense the attacked cell can offer once the membrane attack complex has been formed. Thus the complement system, or a similar system would be an ideal cancer therapy treatment. In fact, several systems have tried to exploit the complement system and activate it to kill cancer cells. For example, antibody treatments, such as trastuzumab and rituximab have had their F_c portions modified to increase complement activation and BCG has been applied to tumors of the walls of the urinary bladder (to induce complement activation) with some success. In most cases, though, cancer cells seem immune to complement and complement activation may, in fact, increase tumor growth.[2, 3]

Recently, several researchers have shown that cancerous cells often over express complement regulators such as CD46, CD55, and CD59.[3, 4] These regulators inhibit the formation of the MAC, and prevent complement from having a cytotoxic effect on the cancer

cell. CD46, CD55 and CD59 do not prevent the initial cascade of complement from happening, so activated C5b is often formed at cancer sites. C5b can cause the MAC to form on almost any membrane, and as such, it is often used as a damper to the immune system to keep it from jumping into hyperdrive and killing by hypercytokinemia. When a lot of MAC forms, it can lyse immune effector cells as well as the invading cells, thus providing a negative feedback loop and preventing the positive feedback loop of hypercytokinemia from killing the organism. Cancer exploits this negative feedback loop. Since cancer does not downregulate C5b production, only its effectiveness against the cancerous cells, cancer effectively nullifies the complement system and dampens the entire immune system response by causing lysis of other effector cells.[3]

Thus, complement would be a very good system to exploit for treating cancer, except cancer has already exploited it in the other direction. If a system similar to complement could be developed that would lyse the cancer cells by forming pores in the membrane without being subject to down regulation by complement regulators, it would make an excellent candidate for cancer therapy.

3.1.2. MspA

A possible MAC imitator is Mycobacterium smegmatis porin A (MspA). MspA is a porin isolated from *Mycobacterium smegmatis* a member of the mycobacterium genus, the most famous of which is *M. tuberculosis*, which, along with many other of the genus members, causes tuberculosis. Mycobacterium are somewhat of an oddity in the microbiology world. One of their best known oddities is their cell membrane and cell wall. Most bacteria have an inner cell membrane and an outer cell membrane of about the same size (roughly 6 nm), with a free peptidoglycan layer in between (Figure 3.1.5). Mycobacteria, on the other hand have a much larger outer membrane (~10 nm) that is covalently linked to the peptidoglycan layer underneath (Figure 3.1.6). The large size of the outer membrane is caused by mycolic acids, extremely long chain lipids synthesized by mycobacteria. This outer membrane makes mycobacteria notoriously

resistant to many standard antibiotics because of low diffusion through the large membrane and lack of free access to the peptidoglycan layer.[5,6,7]

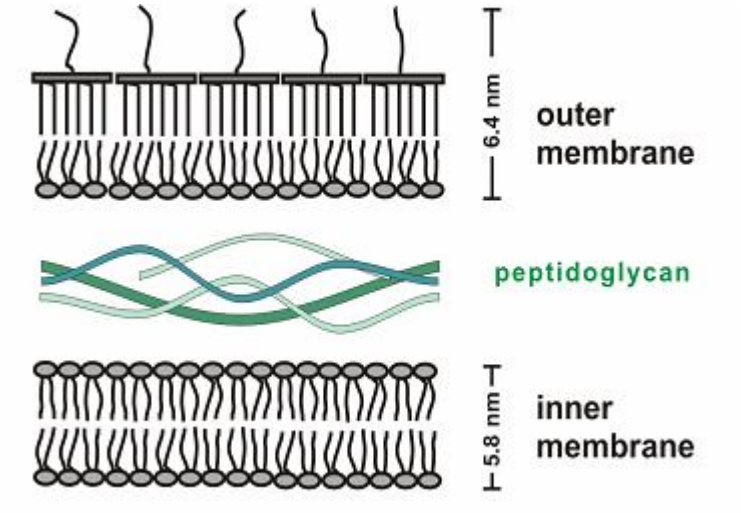

Figure 3.1.5 The membrane of *e coli* as a representative bacterial membrane.

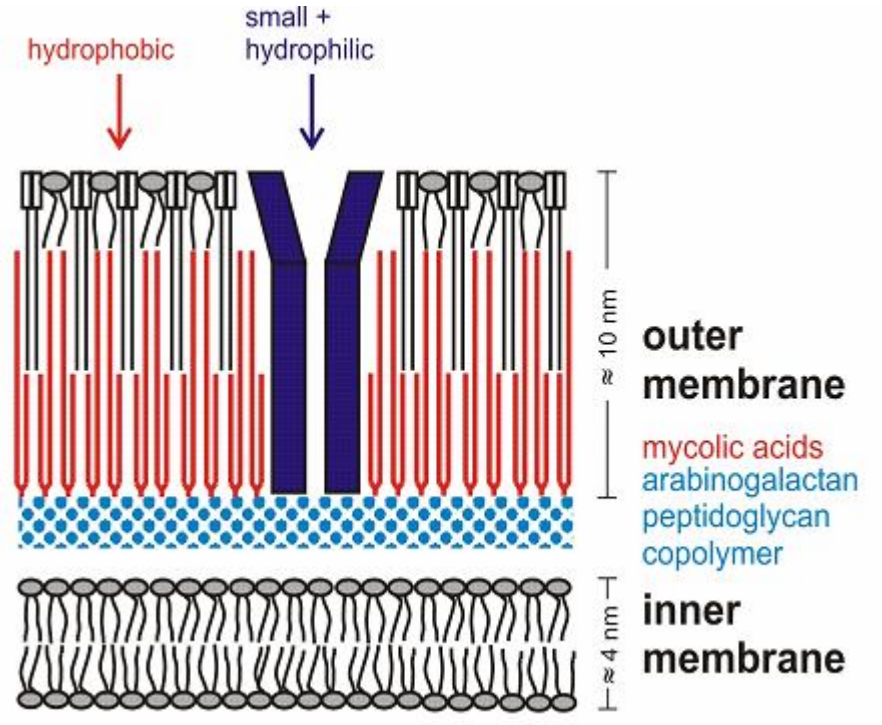

Figure 3.1.6 A membrane from *m. tuberculosis* as a representative mycobaterial membrane

As mycobacteria have very different outer membranes from other bacteria, it would be expected that the pores that are in the outer membranes would also be quite different. Standard bacterial porins are trimeric structures that form three pores in the membrane and are approximately 6 nm tall (Figure 3.1.7).[8]

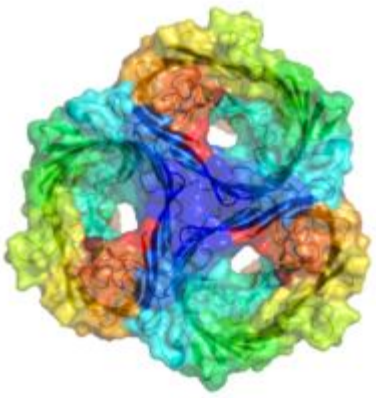

Figure 3.1.7 A sucrose specific porin from *Salmonella typhimurium* as a representative bacterial porin.

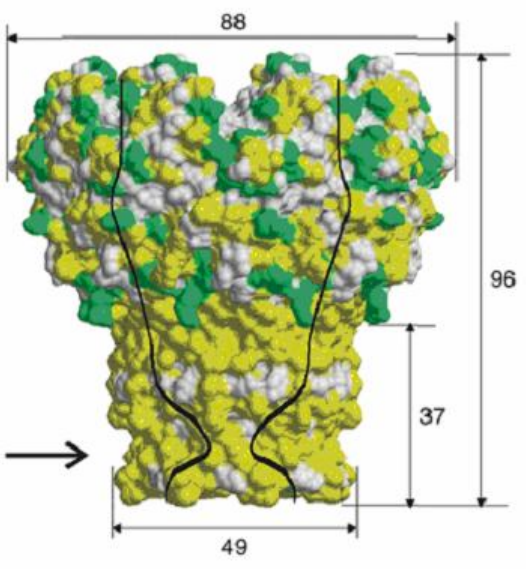

Figure 3.1.8 MspA. Green indicates hydrophilic residues, yellow hydrophobic residues. (dimensions are in Angstroms)

Several porins have been isolated from *M. smegmatis* that are all fairly similar. The most prevalent was named Mycobacterium smegmatis porin A (Figure 3.1.8). X-ray crystal studies

revealed that MspA is a homooctameric porin that forms a single pore in the membrane and is nearly 10 nm tall. MspA is an incredibly stable protein and resists denaturing even in conditions such as 100°C with 3% SDS. This stability allows it to be separated from the membrane and purified without denaturing it.[9]

MspA has several similarities to the MAC. It is multimeric protein that forms pores in membranes. It has a very hydrophobic region that desires to be buried in the hydrophobic membrane, and the energetics of burying the MspA should be strong enough to form pores in the membrane. It is also different in many ways. It should not interact with the complement regulatory proteins. It is very stable and should be able to be transported through the body (as opposed to formed on the spot). It does not exist as a pro-porin. If MspA is able to poke holes in membranes, there is no regulation on which membranes it will poke through.

Because of these similarities and differences, MspA makes a good candidate for a MAC replacement for use in cancer therapy. To be a good cancer therapy candidate it will need to be proven that: 1) MspA can poke holes in membranes; 2) the magnitude and multitude of these holes is enough to induce cell lysis or apoptosis; and 3) MspA can be modified somehow to select cancerous cells from non-cancerous cells.

3.2. Experimental

3.2.1. Materials

MspA and MspA A96C were obtained from the Michael Niederweis lab at University of Alabama Birmingham. MDA 231 and MatBIII cell lines were obtained from ATCC and were cultured in recommended media. The peptide (SRSRSRSRSRSGRSAGGGC) was purchased from GenScript (Piscataway, NJ). All other materials were obtained from Fisher Scientific.

3.2.2. Atomic Force Microscopy

Mica plates were cut into 1 cm^2 squares and cleaved by slowly removing the top layer of mica to expose a clean and microscopically smooth mica surface. The sample to be imaged was added to the mica plate and dried overnight. The sample was then imaged using a PicoScan AFM in MACmode (magnetic alternating current mode, similar to tapping mode (AC mode) but typically with less force applied on the sample) using a fresh MACmode tip stored under argon (to prevent oxidative destruction of the magnetic coating). Images were collected and analyzed with the PicoScan software.

3.2.3. Cell Assays

Cell lines were obtained from ATCC and were continually passaged in the recommended media in T75 flasks. To start a test, cells that were ready to passage were passaged into 12 well flat-bottom plates and allowed to come to 75% confluence. Testing conditions were then added. Post-testing conditions, the cells were counted using a hemocytometer. The cells were washed in PBS and then lifted by adding 100 μL trypsin and rocking for two minutes or until cells were visibly detached. 100 μL of media was then added to quench the trypsin activity and an equal volume of 0.4% trypan blue in PBS was added to stain non-viable cells. After staining, the cells were diluted until less than 100 but more than 50 cells were counted in the hemocytometer. The cells were then counted in the hemocytometer (discounting stained cells) and the counts were used to calculate total cells in the well.

3.2.4. Synthesis of Pro-MspA

MspA A96C was obtained from the Niederweis group at UAB at 60 μg/mL (37.5 μM) and the peptide SRSRSRSRSRSGRSAGGGC was obtained from GenScript and diluted to 2 mM. To reduce any currently existing cys-cys bonds, 15 μL of 120 μM DTT (1.5 eq.) was added to 400 μL of MspA (1 eq.). Separately, 150 μL of 120 μM DTT (15 eq.) was added to 6 μL of the peptide (10 eq.). Both reactions were incubated overnight at room temperature. The next day, both reactions were mixed together (1 eq. MspA, 10 eq. peptide, 1.25 eq. peptide/MspA cysteine) and 27.5 μL of 1.10 M NaOH and 150 μL of 132 μM Chloramine-t (88 equivalents) was added to the reaction mixture to oxidize the cysteine-cysteine bonds. Reactants and side-products (peptide-peptide cysteine bonds) were removed by adding 9 mL 1x PBS and ultrafiltrating using filters with MWCO of 15 kDa to 0.75 mL. The product was washed twice more using 9 mL 1x PBS and ultrafitered to 0.75 mL.

3.3. Results and Discussion

3.3.1. AFM Studies

Initially, it was desired to note the similarity between MspA and the MAC by getting high resolution images of the MspA pore and comparing them to the MAC complex. To do this, MspA stock (3 μM) was diluted to 3 nM using water/methanol (80%/20%). A 150 μL drop was

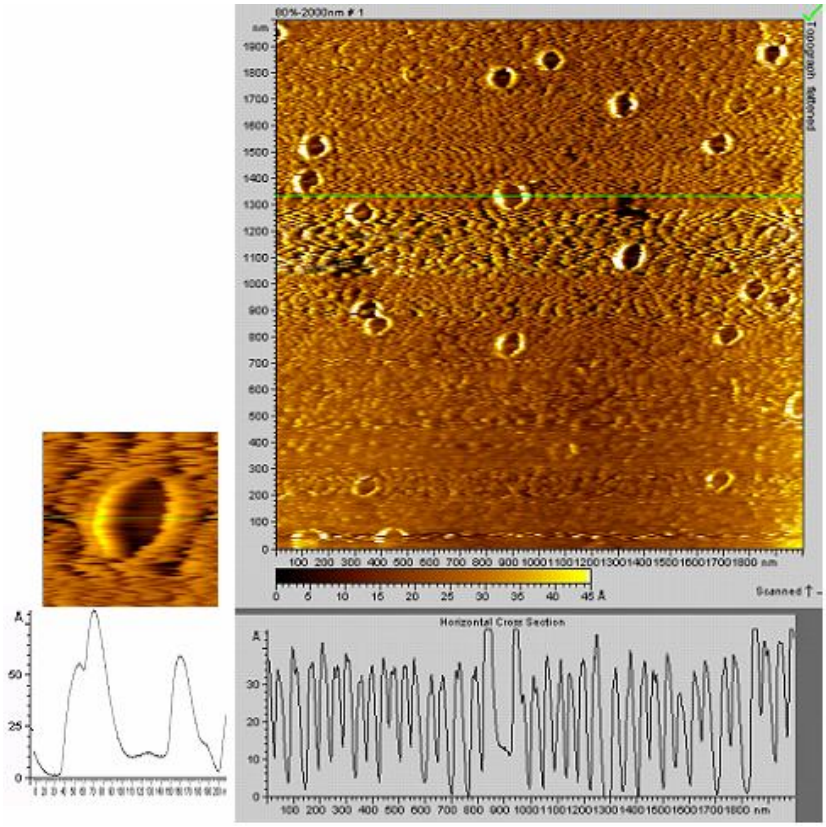

Figure 3.3.1 AFM image of MspA on mica.

put on a 1 cm^2 piece of cleaved mica and dried at 37.5°C overnight. The mica was then imaged using a PicoScan AFM in MACmode. As can be seen in Figure 3.3.1, MspA is stable enough to image, and the pore structure shows up clearly in AFM. The dimensions measured match closely the X-ray measurements (10nm x 10 nm x 10 nm). Comparing to Figure 3.1.2 shows that MspA has a very similar shape the MAC.

3.3.2. Membrane Insertion Studies

To prove that MspA could integrate into membranes, another AFM study was set up. A poly-N-isopropyl-amine (pNIPAM) synthetic membrane was prepared on cleaved mica by making a solution of 50 mg/mL pNIPAM in acetonitrile/water (50%/50%). A 50 uL drop of the pNIPAM solution was then dropped onto the center of the cleaved mica piece, and the mica was

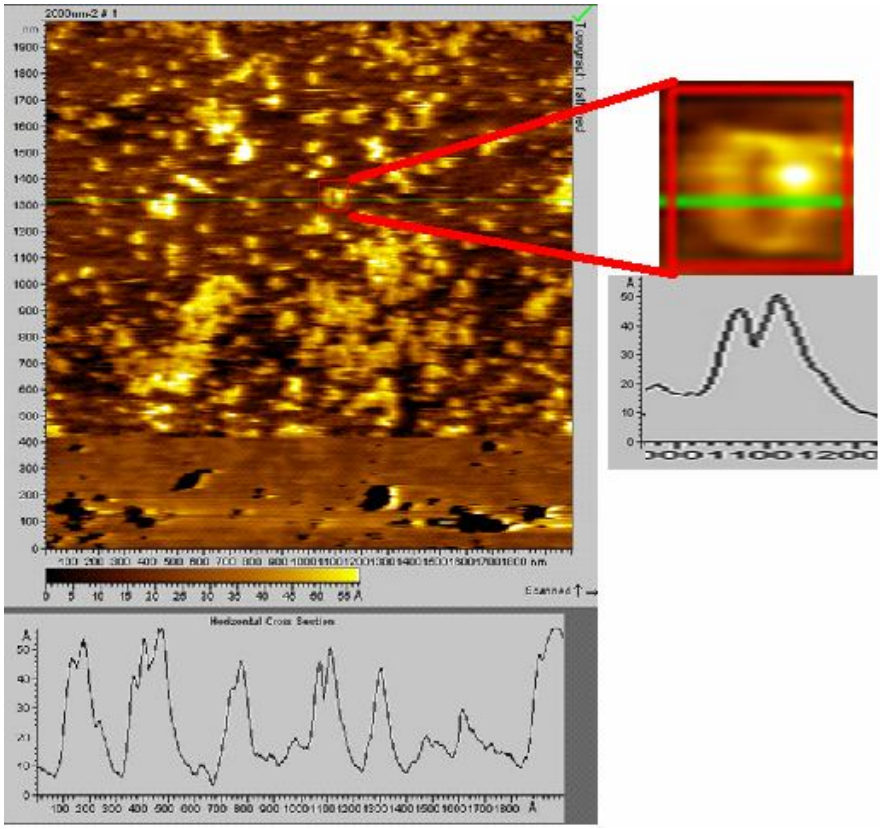

Figure 3.3.2 AFM image of MspA integrated into the pNIPAM membrane

spun at 3000 RPM for 45 seconds on an industrial spin coater to prepare a membrane that was approximately 5 nm thick. The membrane was dried at 37.5°C overnight and then 150 uL of 3 nM was dropped on to the membrane and left for one hour. The mica was then washed with distilled water to remove unbound MspA and dried at 37.5°C overnight. The mica was then imaged using a PicoScan AFM in MACmode.

As can be seen in Figure 3.3.2, the MspA does integrate into the membrane. There is an abundance of protein in the image, although the resolution is not excellent ('soft' samples such as pNIPAM drastically reduce the maximum resolution in AFM due to the force of the tip interacting with the sample). The porin with the best resolution was enlarged and is seen to the right. The pore structure is still evident, showing that the MspA retained its native conformation upon entering the membrane. Also, in the cross section view, the MspA is now only 5 nm tall, as opposed to 10 nm in Figure 3.3.1. This would indicate that the MspA is actually buried in the membrane (which is ~5 nm thick) and has inserted itself and is not merely interacting with the surface of the membrane as half of the height is below the surface of the membrane and is not imaged.

3.3.3. Cell Toxicity

Since AFM results indicate that the MspA can integrate into membranes and form pores, the toxicity of MspA against cultured cells was tested next. MDA231 cells (human metastatic breast cancer cell line), were cultured to 75% confluency in 12 well flat-bottom plates containing 1 mL of media. MspA was diluted to various concentrations in 1x PBS and added to the media. The cells were placed in the incubator for 36 hours and then live cell counts were taken. As can be seen in Figure 3.3.3 and Figure 3.3.4, MspA is extremely cytotoxic, with 100% cell death at approximately 2.5 nM. This is consistent with MspA acting similarly to the MAC. Not very many holes need to be poked in a membrane before the cell cannot compensate, so the toxicity of a pore forming toxin is quite high.

Figure 3.3.3 % Live Cells vs. [MspA]

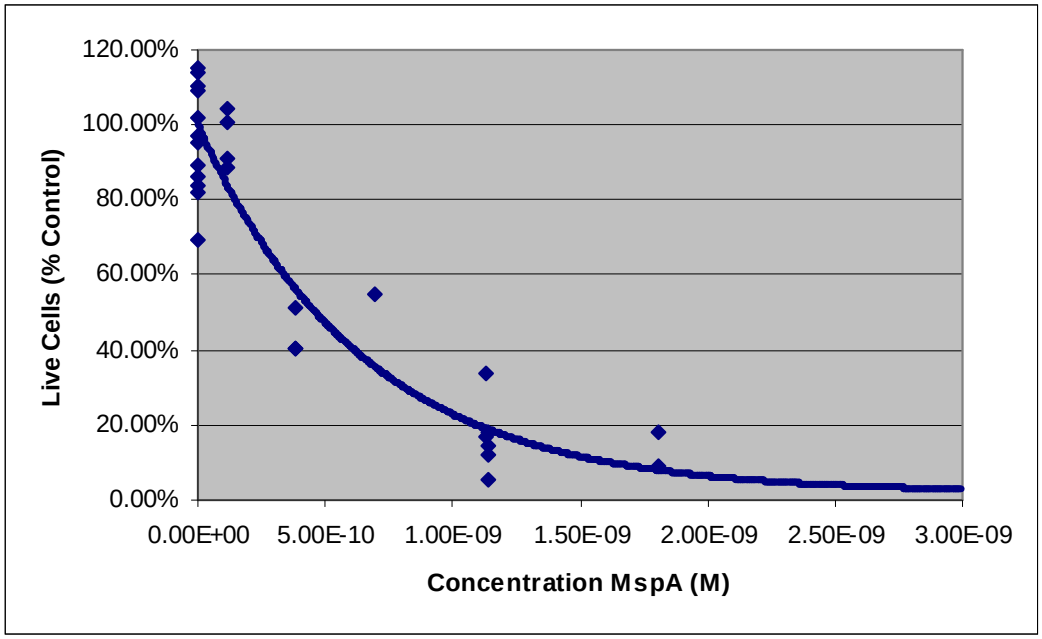

Figure 3.3.4 % Live Cells vs. log[MspA]

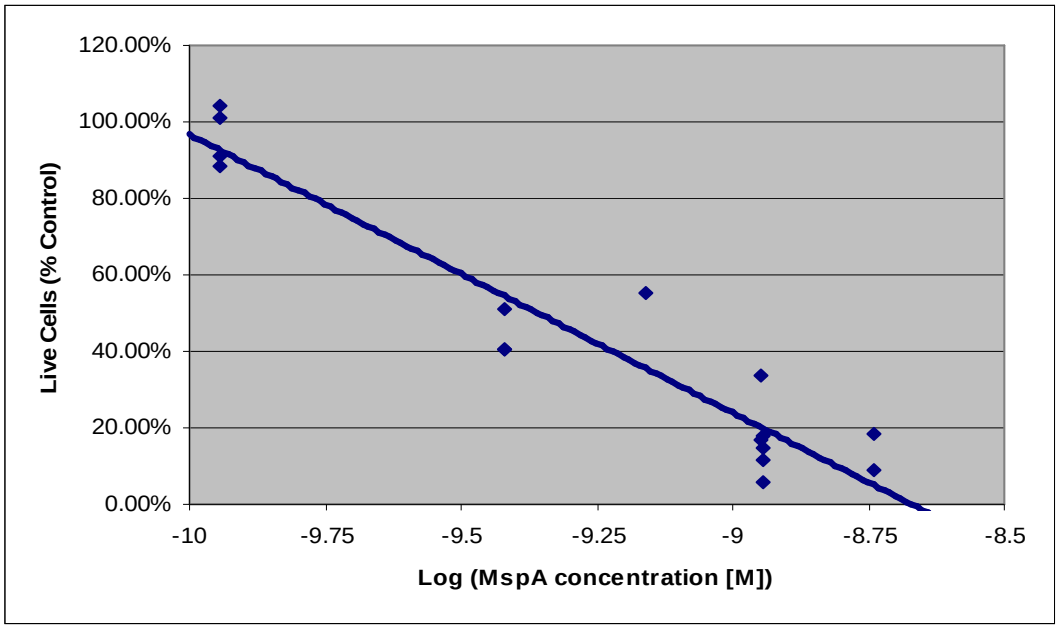

3.3.4. Mechanism of Toxicity

Once it was established that MspA was extremely cytotoxic, the mechanism of toxicity was looked into. The hypothesis was that MspA is a pore forming toxin similar to the MAC. If

MspA does form pores in the membrane, an excellent method of proving this would be to watch molecules that normally are excluded by live cells enter the cells.

3.3.4.a. Chromophore/Fluorophore Exclusion

To test increased membrane permeability post-MspA treatment, cells were cultured to 75% confluency in 12 well plates. Either 100 μL of MspA in PBS (for a final concentration of 0.4 nM, chosen to create some pores in the membrane without a large population of cell death), or 100 μL of PBS (no MspA) was added to the cells and the cells were incubated two hours. Then various dyes were added to both the sample (with MspA) and the control (without MspA) wells in 100 μL for a final concentration of 0.2% wt/vol dye. The cells were incubated one more hour and then were observed in the microscope or fluorescent microscope. For a successful test, the cells with MspA added should be stained, while those without MspA should not be stained. If both sets of cells are stained, it would indicate that the dye can cross the membrane readily, and is not useful for this study. If neither set of cells are stained, it could indicate one of two things: 1) MspA does not form pores in the membrane; or 2) the dye is too large to go through the pore formed by MspA.

The dyes tested include azo blue, trypan blue, trypan blue + $MgSO_4$, propidium iodide, ethylene bromide, and DAPI. None of these dyes produced a positive result (the MspA containing cells stained while the non-MspA cells unstained). Some stained all of the cells (azo blue, ethylene bromide, DAPI) and some stained none of the cells (trypan blue, trypan blue + $MgSO_4$, propidium iodide). As stated above, this could mean that either MspA does not kill cells by forming pores, or that the pore of MspA is too small to fit conventional dyes through.

3.3.4.b. Current Induction

To differentiate between the two possibilities above, other evidence of MspA forming pores in membrane was looked for. The first evidence is already detailed above in 3.3.2, demonstrating the MspA can enter the membrane and form pore-like structures in it. Also, from x-ray studies, it is known that the constriction zone of MspA is less than 1 nm in diameter and it

is defined by sixteen aspartate residues giving it a very negative charge.[1] The small size and large negative charge of the constriction zone would likely repulse most biological dyes.

The final piece of evidence was provided by the Niederweis group at UAB who were studying the effect of deleting residues from the periplasmic loop of MspA.[2] As part of this study, they tested the transmembrane conductance of a diphytanoylphosphatidylcholine membrane after adding MspA. Without any pores, the membrane blocks virtually all current flow, making the conductance zero. If MspA forms true pores in the membrane, the transmembrane conductance will increase because electrolytes are able to cross the membrane to connect the electrodes.

The channel activity of the protein was measured by preparing a diphytanoylphosphatidylcholine membrane across a pore that connected an aqueous circuit (containing 1 M KCl as the electrolyte). A voltage of -10 mV was applied to the circuit. 0.02 ng of freshly reconstituted MspA pores were added to both the cis and trans sides of the membrane and conductance was recorded against time.

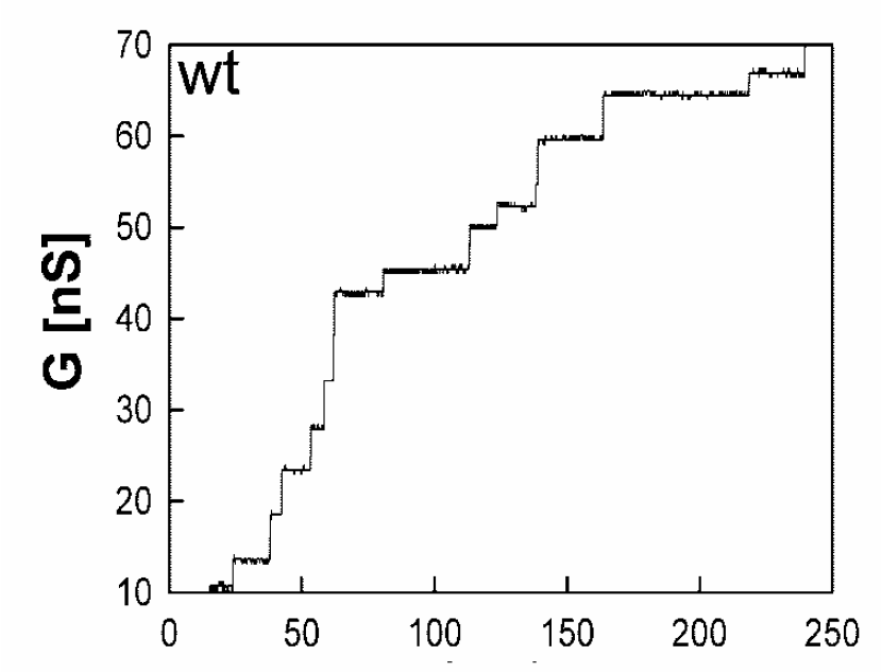

Figure 3.3.5 Conductance versus time.

As can be seen in Figure 3.3.5, addition of MspA caused discreet jumps in the transmembrane conductance. This would indicate that MspA does form true pores in the membrane that allow the KCl to pass through the membrane connecting the circuit. Thus, the hypothesis that MspA does not cause toxicity by pore formation was rejected.

3.3.5. Toxicity and Selectivity of Pro-MspA

Since MspA has been shown to be a suitable imitator of the MAC complex, to make a good cancer treatment, MspA's pore formation must be triggered by the cancer and not elsewhere. An obvious method for preventing MspA pore formation would be to simply preventing it from inserting into the membrane. As can be seen above (Figure 3.1.8), the lower half of MspA is very hydrophobic, which is what drives it insertion into the membrane. The upper half, on the other hand, is mixed hydrophobic and hydrophilic and will not insert nearly as readily as the lower half. Thus, to prevent insertion, the hydrophobicity of the lower half needs to be masked somehow.

To mask the hydrophobicity of the lower half, an MspA mutant (MspA A96C) was obtained from the Niederweis group. The alanine-cysteine switch does not affect the activity of the MspA, but it does provide a reactive group in the periplasmic loop of MspA. This cysteine was used to attach a peptide (SRSRSRSRSRSGRSAGGGC) by a disulfide bond between the cysteine in the periplasmic loop and the cysteine in the peptide. At 100% reaction, 8 peptides are added to the bottom of the MspA. The peptide was designed to be very hydrophilic (containing mostly serine and asparagines residues) and also contains the consensus sequence for uPA (SGRSA). Thus, when attached, the hydrophobicity of the lower half of the MspA is masked by the peptide. The peptide can be cleaved off, though, leaving only a short, nearly neutral peptide (SAGGGC), drastically increasing the hydrophobicity of the lower half.

To test the efficacy of the modified MspA, more cell tests were done. MDA231 cells, which are known to express uPA,[3] and Jurkat cells, which are known not to express uPA,[4] were cultured separately in 12 well flat-bottom plates to 75% confluency. Modified MspA (pro-

MspA) was diluted to various concentrations in 1x PBS and added to the media. The cells were placed in the incubator for 36 hours and then live cell counts were taken.

Figure 3.3.6 WT, A96C and A96C non-uPA Toxicity

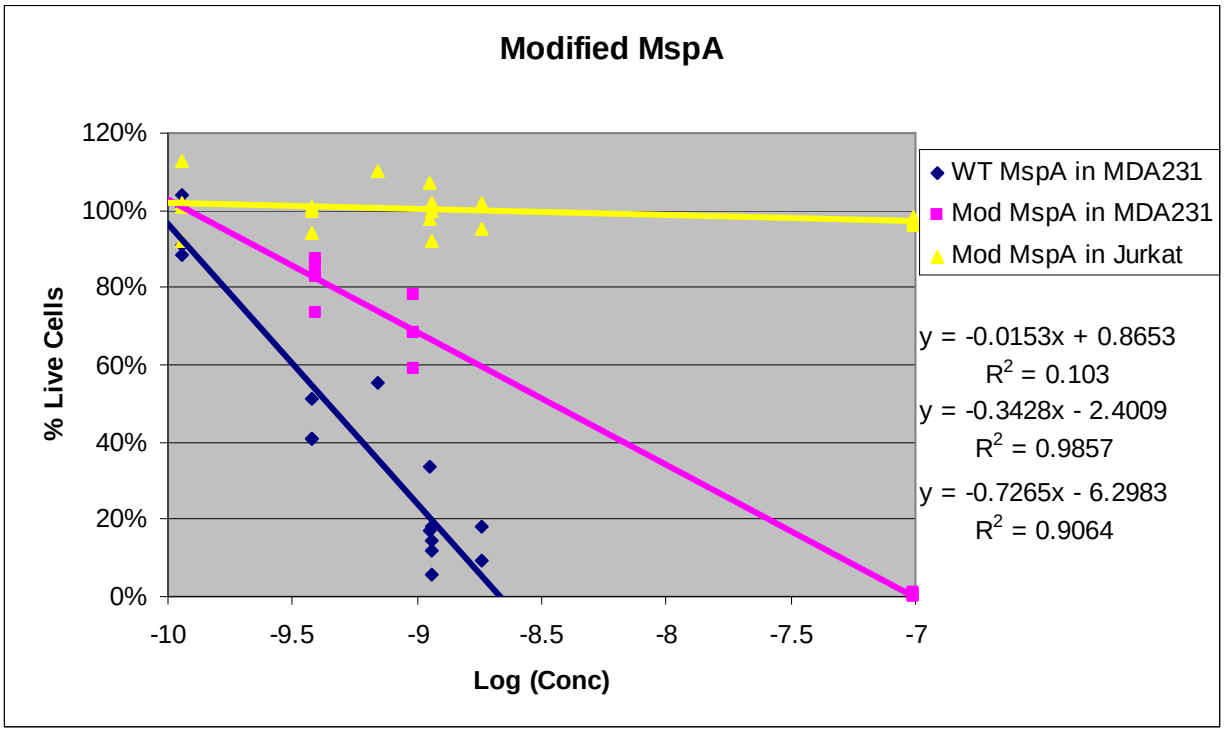

As can be seen in Figure 3.3.6, pro-MspA still retains a large degree of its toxicity against MDA231 (100% cell death at 100 nM), although it is slightly less. This may be explained by the remnant peptide left on after cleavage may reduce the efficiency of insertion into the membrane. Pro-MspA does not show any toxicity against Jurkat cells up to 100 nM. This would indicate that the peptide does prevent insertion and that insertion causes toxicity. Without uPA to cleave off the peptide, pro-MspA is non-toxic. Thus, pro-MspA can select for cells that are expressing uPA, and as a cancer associate protease, pro-MspA can select for cancer cells.

3.4. Conclusion

The above study demonstrates that MspA shows strong potential as a replacement protein for the MAC in cancer therapy. As discussed above, to demonstrate that MspA is a suitable MAC imitator three things must be proven: 1) MspA can poke holes in membranes; 2) the magnitude and multitude of these holes is enough to induce cell lysis or apoptosis; and 3) MspA can be modified somehow to select cancerous cells from non-cancerous cells. Each of these was demonstrated above. MspA pokes holes in artificial membranes that can be viewed with AFM or measured by current induction in electrochemical studies. MspA is a very powerful toxin, showing toxicity in the nanomolar or subnanomolar range. Finally, when modified with hydrophilic peptides, MspA can select which cells to kill based on protease production.

As a MAC imitator, MspA could be a very potent anticancer treatment. There is very little a cell can do to develop resistance to holes being poked in the membrane, so MspA could potentially be very effective even against multidrug resistance cancers. Also, being targeted independently of the rate of dividing of the cells (being targeted to a cancer associated protease) could alleviate many of the well known side effects of cancer allowing higher systemic dosages and, perhaps more effective treatments.

Many things still need to be considered, though. MspA is a foreign protein and may induce a strong immune response that could either hamper or improve its effectiveness as a cancer therapy. (The effectiveness would be hampered if the immune response removed the protein before it had a chance to act on the cancer. The effectiveness could be improved if the immune response happened once the MspA was at the tumor site. This could target the immune system to the cancer.) General biological compatibility of the pro-MspA has not been tested either, nor has deliverability of the MspA to the tumor site. To test all of these things, the next step would be to do *in vivo* tests of the MspA in a small animal model.

References

Chapter 1

1. National Cancer Institute: What is Cancer, Cancer Statistics. http://www.cancer.gov/cancertopics/what-is-cancer (6/21/2008)
2. Death Rates by Age and Race. http://www.disastercenter.com/cdc/Death%20rates%20for%20113%20selected%20causes%20by%20race%20and%20sex%202005.html (6/21/2008)
3. American Cancer Society: How Does Chemotherapy Work. http://www.cancer.org/docroot/ETO/content/ETO_1_4X_How_Does_Chemotherapy_Work.asp?sitearea=ETO (6/21/2008)
4. American Cancer Society: What Causes Side Effects. http://www.cancer.org/docroot/MBC/content/MBC_2_2X_What_Causes_Side_Effects.asp?sitearea=MBC (6/21/2008)
5. Jain, K. *Curr Opin Mol Ther* **2007,** *9,* 563.
6. Dalgleish, A; Pandha, H. *Adv Cancer Res.* **2006,** *96,* 175.
7. TC-Cancer.com: Tumor Markers. http://www.tc-cancer.com/tumormarkers.html (6/12/2008)
8. Waldman, T; Morris, J. *Adv Immunol.* **2006,** *90,* 84.
9. Buchegger, F; Antonescu, C; Delaloye, A; Helg, C; Kovacsovics, T; Kosinski, M; Mach, J; Ketterer, N. *Brit J Cancer.* **2006,** *94,* 1770.
10. Bogenrieder, T; Herlyn, M. *Oncogene.* **2003,** *22,* 6524.
11. Duffy, M. *Clin Cancer Res.* **1996,** *2,* 613.
12. Johansson, N; Ahonen, M; Kahari, V. *Cell Mol Life Sci.* **2000,** *57,* 5.
13. Turk, B; Huang, L; Piro, E; Cantley, L. *Nat Biotechnol.* **2001,** *19,* 661.
14. Khasigov, P; Podobed, O; Gracheva, T; Salbiev, K; Grachev, S; Berezov, T. *Biochemistry (Moscow).* **2002,** *68,* 869.
15. DeClerk, Y; Bajou, K; Luag, W. *Antiangiogenic Cancer Ther.* **2008,** 239.
16. Duffy, M. *Biochem Soc Trans.* **2002,** *30,* 207.
17. Liu, S; Bugge, T; Leppla, S. *J Biol Chem.* **2001,** *276,* 17976.
18. Thor, B. (Twinstrand Therapeutics, Inc.) Ricin-like Toxin Variants for Treatment of Cancer, Viral or Parasitic Infections. United States Patent 6593132. July 15, 2003.
19. Turk, V; Kos, J; Turk, B. *Cancer Cell.* **2004,** *5,* 409.
20. Warnecke, A; Fichtner, I; SaB, G; Kratz, F. *Arch Pharm Chem Life Sci.* **2007,** *340,* 389.

Chapter 2.1

1. Bangham, A. D.; Horne, R. W. *J. Mol. Biol.* **1964,** *8,* 660-668.
2. Gregoriadis, Gregory. *N. Engl. J. Med.* **1976**, *293* (13), 704-10.
3. Bangham, A. D. *Progr. Biophys. Mol. Biol.* **1968,** *18,* 29.
4. Sessa, G.; Weissmann, G. *J. Lipid Res.* **1968,** *9,* 310.
5. Kinsky, Stephen C. *Meth. Enym.* **1974,** *32,* 501.
6. H. Fricke, *Phys. Rev.* **1923,** *21,* 708.

7. Bangham, A. D.; Hill, M. W. Miller, N.G.A. Preparation and use of liposomes as models of biological membranes. In *Methods in Membrane Biology*. E.D. Korn, Ed. Plenium Press: New York, 1974, pp 1-68.
8. Gregoriadis, G. Structural requirements for the specific uptake of macromolecules and liposomes by target tissues. In *Enzyme Replacement Therapy of Lysosomal Storage Diseases.* J.M. Tager, G.J.M. Hooghwinkel, W.Th. Daems, Ed. North Holland Publishing Company, 1974, pp 131-148.
9. Gregoriadis, G; Ryman, B.E. Biochem J. 1971, 124 (5), 58P.
10. Gregoriadis, G; Ryman, B.E. Eur. J. Biochem. 1972, 24, 485-491.
11. Gregoriadis, G; Ryman, B.E. Biochem J. 1972, 129, 123.
12. Gregoriadis, G; Putnam, D. Louis L. Biochem J. 1974, 140, 323.
13. Neerunjun, E. D. Gregoriadis, G. Biochem. Soc. Trans. 1976, 4, 133.
14. Gregoriadis, G; Allison, A. C. FEBS Lett. 1974, 45, 71.
15. Juliano, R. L.; Stamp, D. Biophys. Res. Commun. 1975, 63, 651.
16. Black, C.D.V.; Gregoriadis, G. Biochem. Soc. Trans. 1976. 4, 253.
17. Segal, A.W.; Willis, E.J.; Richmond, J.E. Br. J. Exp. Pathol. 1974, 55, 320.
18. Wisse, E.; Gregoriadis, G. J. Reticuloendothel. Soc. 1975, 18, 10a.
19. Rahman, Y.E.; Wright, D.J. J. Cell Biol. 1975, 85, 112.
20. Tanaka, T.; Taneda, K.; Kobayahsi, H.; Chem. Pharm. Bull. 1975, 23, 3069.
21. Magee, W. E.; Miller, O.V. *Nature*, **1972**, *235*, 339.
22. Johan, M.M.; Cerny, E.A.; Rahman, Y.E. *Biochim. Biophys. Acta*, **1975,** *401*, 336.
23. Rahman, Y.E.; Ramanthal, M.W.; Ceray, E.A. *J. Lab. Clin. Med.* **1974,** *87*, 660.
24. McDougall, I.N.; Dunnick, J.K.; Mcnamee, M.G. *Proc. Natl. Acad. Sci. USA*, **1974**, *71*, 3487.
25. McDougall, I.N.; Dunnick, J.K.; Goris, M.L. *J. Nucl. Med.* **1975,** *16*, 488.
26. Kimelburg, H.K.; Mayhew, E.; Papahadjopoulos, D. *Life Sci.* **1975**, *17*, 715.
27. Kamp, J.A.F.; Kavertz, M.T.; Van Desern, L.L.M. *Biochim. Biophys. Acta*, **1975,** *406*, 169.
28. Papahadjopoulos, D; Allen, T; Gabizon, A; Mayhew, E; Matthay, K; Huang, S; Lee, K; Woodle, M; Lasic, D; Redemann, C; Martin, F. *Proc. Natl. Acad. Sci.* **1991,** *88*, 11460.
29. Bruni, A; Toffano, G; Leon, A. *Nature.* **1976,** *260*, 331.
30. Gregoriadis, G.; Swain, C.P.; Willis, E.J. *Lancet.* **1974,** *1*, 1313.
31. Allen, T; Cullis, P. *Science.* **2004,** *202*, 1818.
32. Moses, M; Brem, H; Langer, R. *Cancer Cell.* **2003**, *4*, 337.
33. Prausnitz, M., Mitragotri, S., and Langer, R. Nature Drug Discovery, in press.
34. Henningfield, J.E. *N. Engl. J. Med.* **1995**. *333*, 1196.
35. Dijkmana, G.A., del Moral, P.F., Plasman, J.W., Kums, J.J., Delaere, K.P., Debruyne, F.M., Hutchinson, F.J., and Furr, B.J. *J Steroid Biochem. Mol. Biol*. **1990**. *37*, 933.
36. Sartor, O., Dineen, M.K., Perez-Marreno, R., Chu, F.M., Carron, G.J., and Tyler, R.C. *Urology*. **2003**. *62*, 319.
37. Langer, R. *Nature*. **1998**. *392* Suppl., 5–10.
38. Peppas, N.; Langer, R. *Science*. **1994**. *263*, 1715.
39. Kaye, S; Richardson, V. *Cancer Chemother Pharmacol.* **1979,** *3*, 81.
40. Weinstein, John; Leserman, Lee. *Pharm. Ther.* **1984.** *24*, 207.
41. Allen, Theresa. *Science***. 2004.** *303*, 1818.

42. Gabizon, A; Shmida, H; Zalipsky, S. *J Liposome Res.* **2006**, *16*, 175.
43. Kaye, S. *Cancer Treatment Reviews.* **1981,** *8*, 27.
44. Shenoy, V; Vijay, I; Murthy, R. *J Pharm Pharmacol.* **2005,** *57*, 411.
45. Park, J; Benz, C; Martin, F. *Sem Oncol.* **2004,** *31(S13)*, 196.
46. Simoes, S; Moriera, J; Fonseca, C; Duzgunes, N; Pedroso de Lima; M. *Adv Drug Delivery Rev* **2004,** *56*, 947.
47. Gabizon, A; Shmeeda, H; Horowitz, A; Zalipsky, S. *Adv Drug Delivery Rev* **2004,** *56*, 1177.
48. Brown, Theodore L.; Lemay, Eugene Jr.; Bursten, Bruce E.; Burdge, Julia R. Chemistry: The Central Science; Pearson Education, Inc: Upper Saddle River, NJ, 2003.
49. Alberts, Bruce; Johnson, Alexander; Lewis, Julian; Raff, Martin; Roberts, Keith; Walter, Peter. Molecular Biology of the Cell, 4th Edition; Garland Science: New York, 2002.
50. Koslov, M.M.; Markin, V.S. *J. Theor. Biol.* **1984,** *109*, 17.
51. Hazlehurst, L; Dalton, W. De Novo and Acquired Resistance to Antitumor Alkylating Agents. In *Cancer Drug Resistance.* Teicher, B. Humana Press, Inc: Totowa, NJ, 2006; 377.
52. Sharma, R; Kacevska, M; London, R; Clarke, S; Liddle, C; Robertson, G. *Brit J Cancer.* **2008,** *98*, 91-97.
53. Kaye, S; Richardson, V. *Cancer Chemother Pharmacol.* **1979,** *3*, 81.
54. Ertel, A; Marangoni, A; Marsh, J; Hallett, F; Wood, J. *Biophys J.* **1993,** *64*, 426.
55. Hallett, F; Marsh, J; Nickel, B; Wood, J. *Biophys J.* **1993,** *64*, 435.
56. Cohen, F; Akabas, M; Finkelstein, A. *Science.* **1982,** *217*, 458.
57. Akabas, M; Cohen, F; Finkelstein, A. *J Cell Biol.* **1984,** *98*, 1063.
58. Lee, S; Chem, H; Dettmer, C; O'Halloran, T, Nguyen, S. *J Am Chem Soc.* **2007,** *129*, 15096.
59. Sarkar, Nihar; Banerjee, Jayati; Hanson, Andrea J.; Elegbede, Adekunle I.; Rosendahl, Theresa; Krueger, Aaron B.; Banerjee, Abir L.; Tobwala, Shakila; Wang, Rongying; Lu, Xiaoning; Mallik, Sanku; Srivastava, D.K. *Bioconjugate Chem.* **2008,** *19*, 57.
60. Elegbede, Adekunle I.; Banerjee, Jayati; Hanson, Andrea J.; Tobwala, Shakila; Ganguli, Bratati; Wang, Rongying; Lu, Xiaoning; Srivastava, D.K.; Mallik, Sanku. *J. Am. Chem. Soc.* **2008,** *130*, 10633.

Chapter 2.2

1. New, R.R.C. Preparation of Liposomes. In *Liposomes: A Practical Approach*; R.C.C. New, Ed. Oxford University Press: New York, 1990, pp 33-104.
2. Lasch, J.; Weissig, V.; Brandl, M. Preparation of Liposomes. In *Liposomes: A Practical Approach Second Edition.* V. Torchilin and V. Weissig, Ed. Oxford University Press: New York, 2003, pp.3-30.
3. Bangham, A.D.; Standish, M.M.; Watkins, J.C. *J. Mol. Biol.* **1965**, *13*, 238.
4. Reeves, J.P.; Dowben, R.M. *J. Cell Physiol.* **1969,** *73*, 49.
5. Payne, N.I.; Timmins, P.; Ambrose, C.V.; Ward, M.D.; Ridgeway, F. *J. Pharm. Sci.* **1986**, *75*, 325.
6. Mayhew, E.; Lazo, R.; Vail, W.J.; King, J.; Green, A.M. *Biochim. Biophys. Acta.* **1984**, *775*, 169.
7. Huang, C. *Biochemistry*. **1969**, *8*, 344.

8. Barenholtz, Y.; Amselem, S.; Lichtenberg, D. *GEBS Lett.* **1979**, *99*, 210.
9. Hamilton, R.L.; Goerke, J.; Guo, L.S.S.; Williams, M.C.; Havel, R.J. *J. Lipid Res.* **1980,** *21*, 981.
10. Olson, F.; Hunt, C.A.; Szoka, F.C.; Vail, W.; Mayhew, E.; Paphadjopoulos, D. *Biochim. Biophys. Acta.* **1980,** *601*, 559.
11. Mayer, L.D.; Hope, M.J.; Cullis, P.R. Janoff, A.S. *Biochim. Biophys. Acta*. **1985**, *817*, 193.
12. Castile, J.D.; Taylor, K.M.G. *Int. J. Pharm.* **1999**, *188*, 87.
13. Pick, U. *Arch. Biochem. Biophys.* **1981**, *212*, 186.
14. Kasahara, M.; Hinckle, P.C. *J. Biol. Chem.* **1977**, *252*, 7384.
15. Batzri, S.; Korn, E.D. *Biochim. Biophys. Acta.* **1973**, *298*, 1015.
16. Deamer, D.W.; Bangham, A.D. *Biochim. Biophys. Acta.* **1976**, *443*, 629.
17. Deamer, D.W. *Ann. N.Y. Acad. Sci.* **1978**, *308*, 250.
18. Taylor, A.E.; Miller, C.W. *J. Biol. Chem.* **1914**, *37*, 215.
19. Bartlett, G.R. *J. Biol. Chem.* **1959**, *234*, 446.
20. Stewart, J.C.M. *Anal. Biochem.* **1959**, *104*, 10.
21. Lee, S; Chem, H; Dettmer, C; O'Halloran, T, Nguyen, S. *J Am Chem Soc.* **2007,** *129,* 15096.
22. Huang, C.; Mason, J.T. *Proc. Natl. Acad. Sci. USA.* **1978**, *75*, 308.
23. Dynamic Light Scattering: With Applications to Chemistry, Biology, and Physics. John Wiley and Sons, Inc: New York, 1976.
24. Einstein, A.; *Annalen der Physik*. **1905**, *17*, 549.

Chapter 2.3

1. New, R.R.C. Preparation of Liposomes. In *Liposomes: A Practical Approach*; R.C.C. New, Ed. Oxford University Press: New York, 1990, pp 33-104.
2. Lee, S; Chem, H; Dettmer, C; O'Halloran, T, Nguyen, S. *J Am Chem Soc.* **2007,** *129,* 15096.
3. Lasch, J.; Weissig, V.; Brandl, M. Preparation of Liposomes. In *Liposomes: A Practical Approach Second Edition*. V. Torchilin and V. Weissig, Ed. Oxford University Press: New York, 2003, pp.3-30.

Chapter 2.4

1. Koslov, M.M.; Markin, V.S. *J. Theor. Biol.* **1984,** *109*, 17.
2. Lichtenberg, D.; Goni, F.; and Heerklotz, H. *TRENDS in Biochemical Science.* **2005,** *30* (8), 430.
3. Schuck, S.; Hansho, M.; Ekros, K.; Shevchenko, A.; and Simons, K. *PNAS.* **2003,** *100* (10), 5795.
4. Rawicz, W.; Olbrich, K.; McIntosh, T.; Needham, D.; and Evans, E. *Biophys. J.* **2000,** *79*, 328.
5. Needham, D.; Nunn, R. *Biophys. J.* **1990,** *58*, 997.
6. Rutkowski, C.; Williams, L.; Haines, T.; and Cummins, H. *Biochemistry.* **1991,** *30* (23), 5688.

7. Mathai, J.; Tristam-Nagle, S.; Nagle, J.; and Zeidel, M. *J. Gen. Physiol.* **2008,** *131* (1), 69.
8. Finklestein, A. and Cass, A. *Nature.* **1967,** *216,* 718.

Chapter 3.1

1. Goldsby, Richard A.; Kindt, Thomas J.; Osborne, Barbara A.; Kuby, Janis. *Immunology*, *5th Edition*; W.H. Freeman and Company: New York, 2003; pp. 299-318.
2. Loveland, B and Cebon, J. *Nat. Immunol.* **2008,** *9*(11), 1205.
3. Markiewski, M; DeAngelis, R; Benencia, F; Ricklin-Lichtsteiner, S; Koutoulaki, A; Gerard, C; Coukos, F; Lambris, J. *Nat. Immunol.* **2008,** *9*(11), 1225.
4. Gelerman, K; Blok, V; Fleuren, G; Gortor, A. *Lab Invest.* **2002,** *4*, 483.
5. Matias et al. (2003), *J. Bacteriol.* **185**, 6112–6118
6. Minnikin, D. E. (1982) in *The Biology of the Mycobacteria* (eds C. Ratledge and J. Stanford) (London:Academic Press, Inc) pp. 96–184.
7. Brennan and Nikaido (1995), *Annu. Rev. Biochem.* **64**, 29-63
8. Forst D, Welte W, Wacker T, Diederichs K. *Nat Struct Biol*. **1998**; *5*(1):37-46.
9. Faller M, Niederweis M, Schulz GE. *Science*. **2004**; *303*(5661):1189-92.

Chapter 3.3

1. Basel MT, Dani RK, Kang M, Pavlenok M, Chikan V, Smith PE, Niederweis M, Bossmann SH. *ACS Nano*. **2009**;*3*(2):462-6.
2. Huff, J.; Pavelenok, M.; Sukumaran, S.; Niederweis, M. *J. Biol. Chem.* **2009,** *284*(15), 10223.
3. Pakneshan, P.; Szyf, M.; Farias-Eisner, R.; Rabbani, S. *J. Biol. Chem.* **2004,** *279*, 31735.
4. Kramer, M.; Spring, H.; Todd, R.; and Vettel, U. *J. Leukocyte Biol.* **1994,** *56*, 110.

Appendix A NMR

Figure A.1 ^{1}H NMR Tert-butyl Cholesterol Acetate

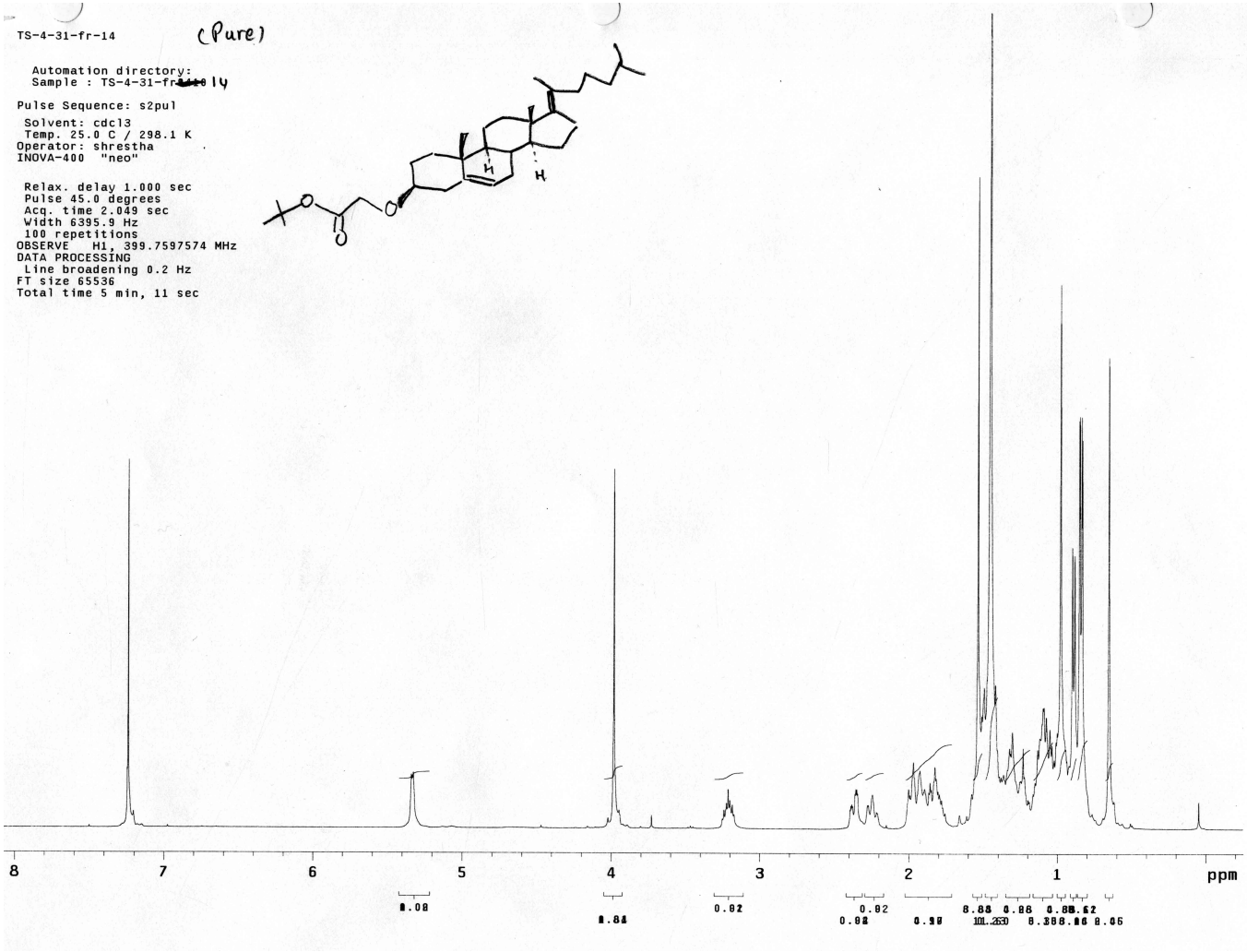

Figure A.2 ^{13}C NMR Tert-butyl Cholesterol Acetate

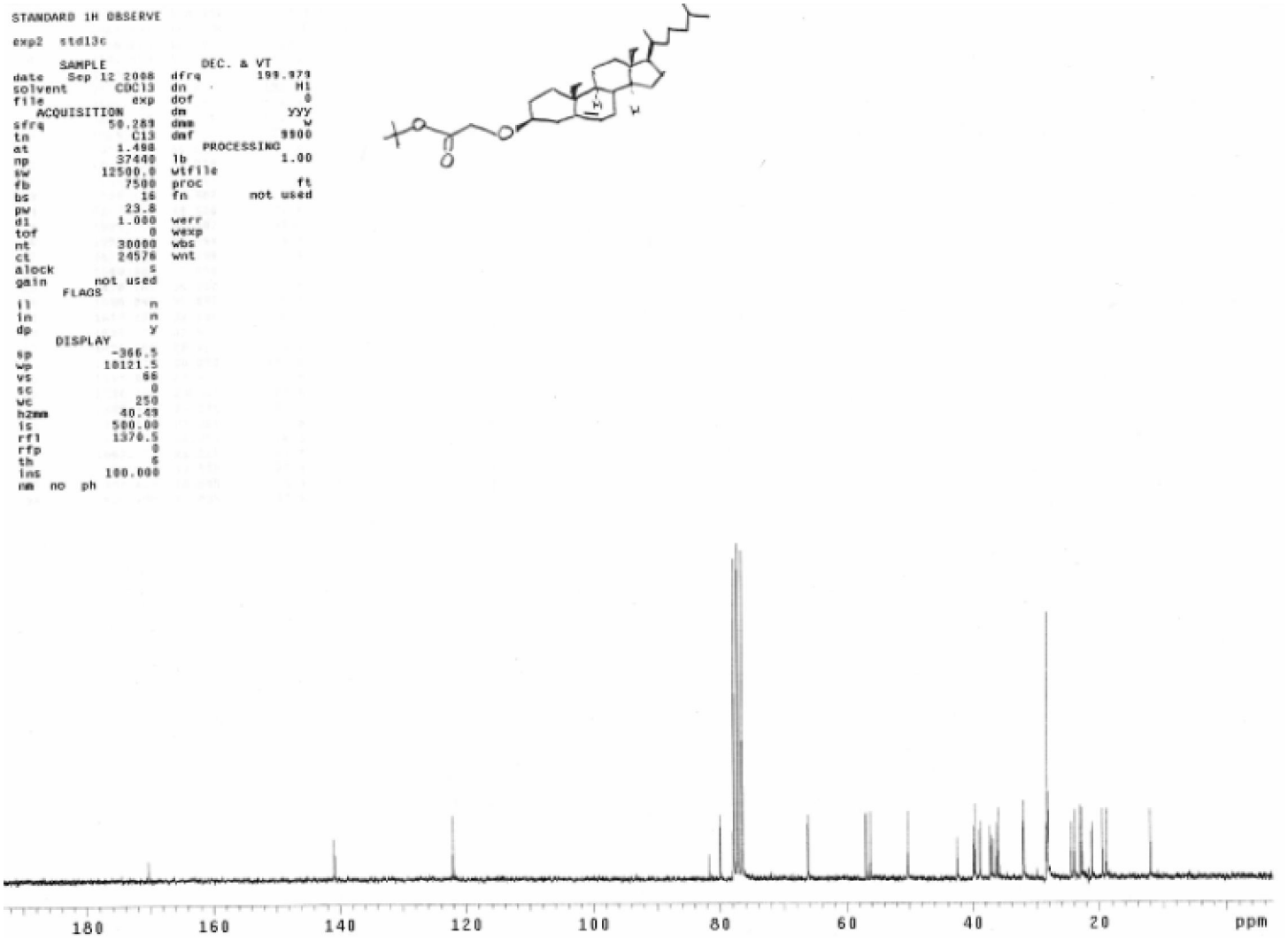

Figure A.3 ^{1}H NMR Cholesterol Acetic Acid

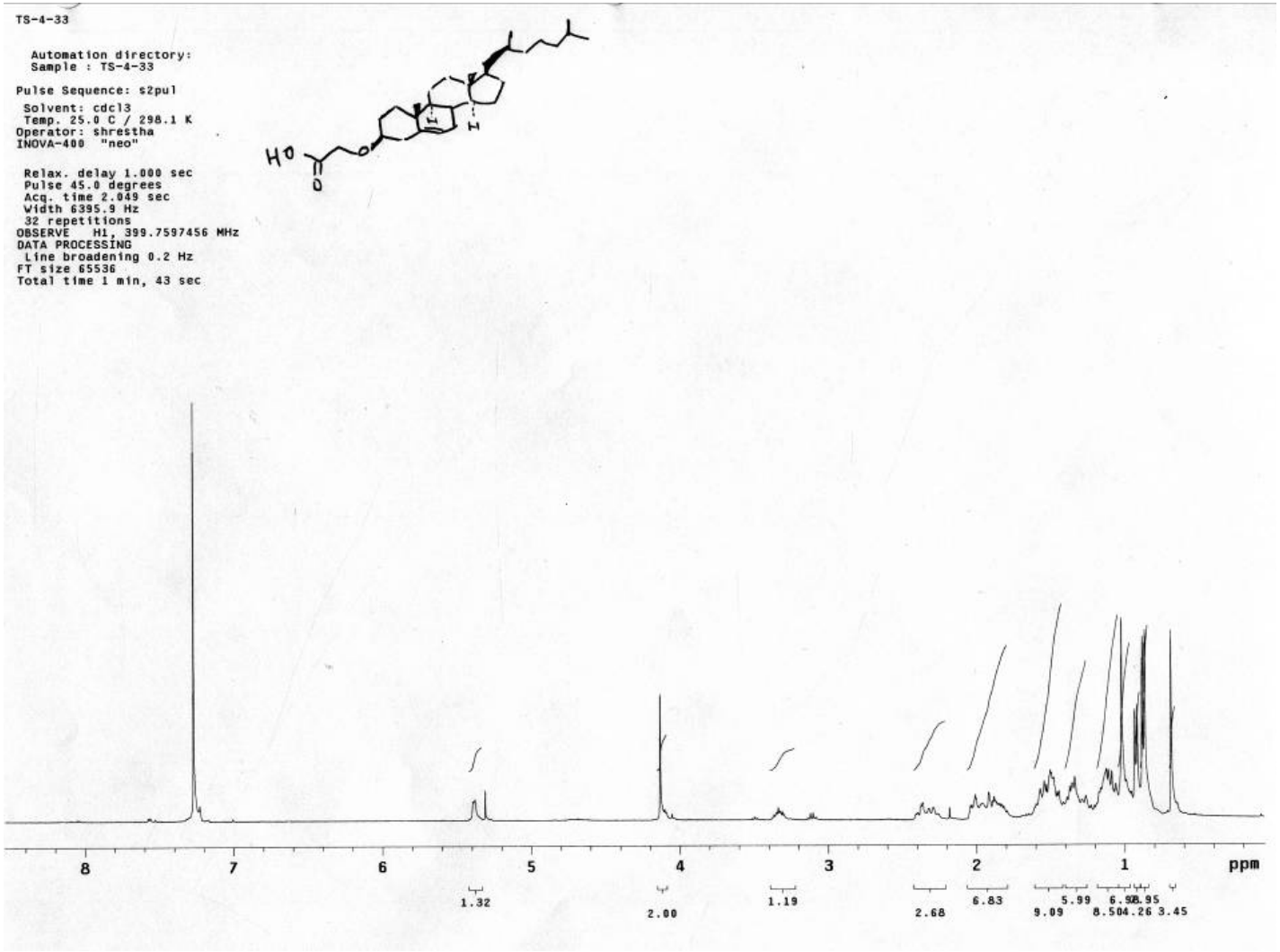

Figure A.4 ^{13}C NMR Cholesterol Acetic Acid

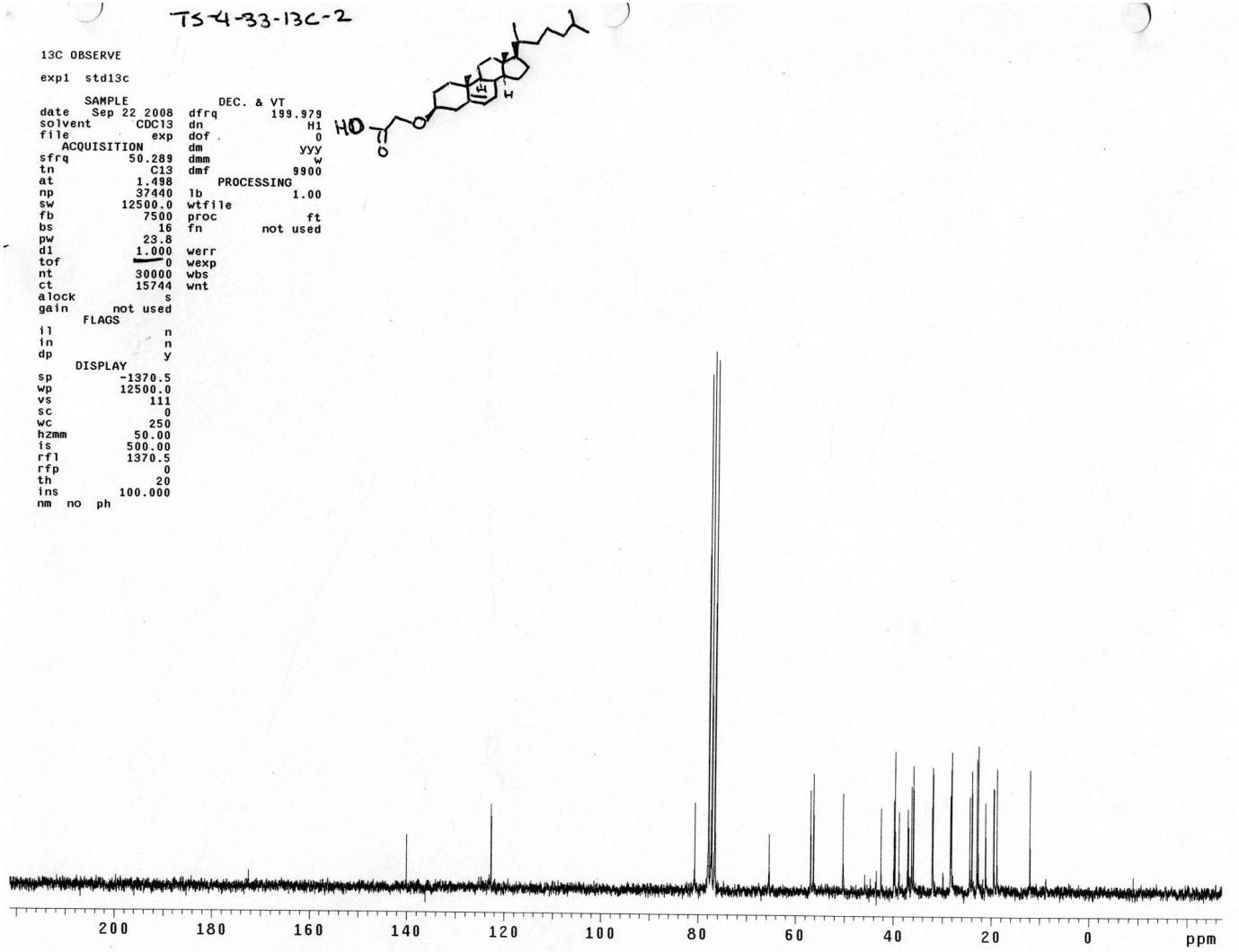

Appendix B PRESSURE Resistance Calculations

Figure B.1 Bare Liposomes Fluorescent Intensity

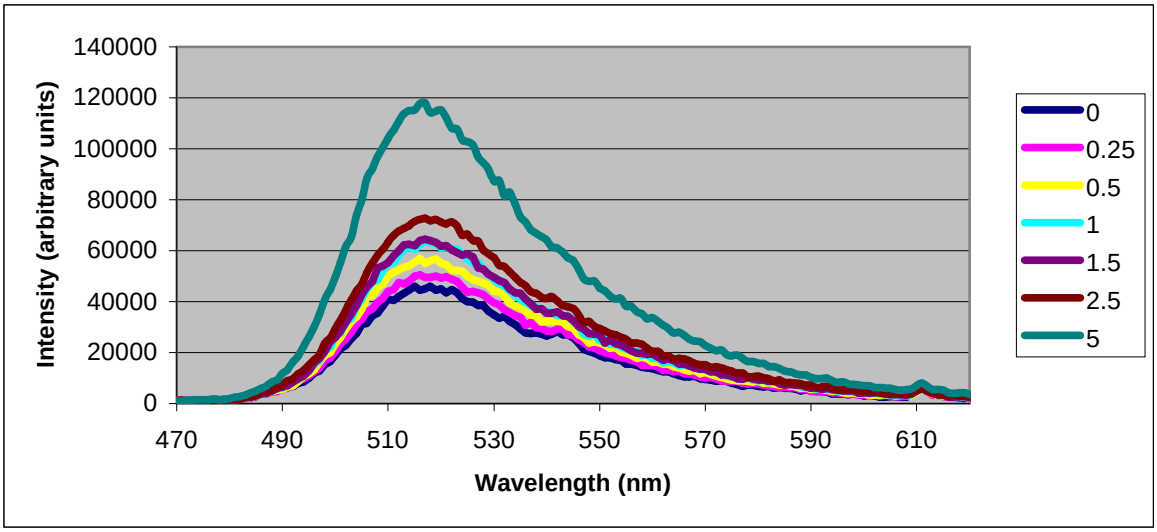

Figure B.2 Bare Liposomes Percent Release verses Osmotic Pressure Curve

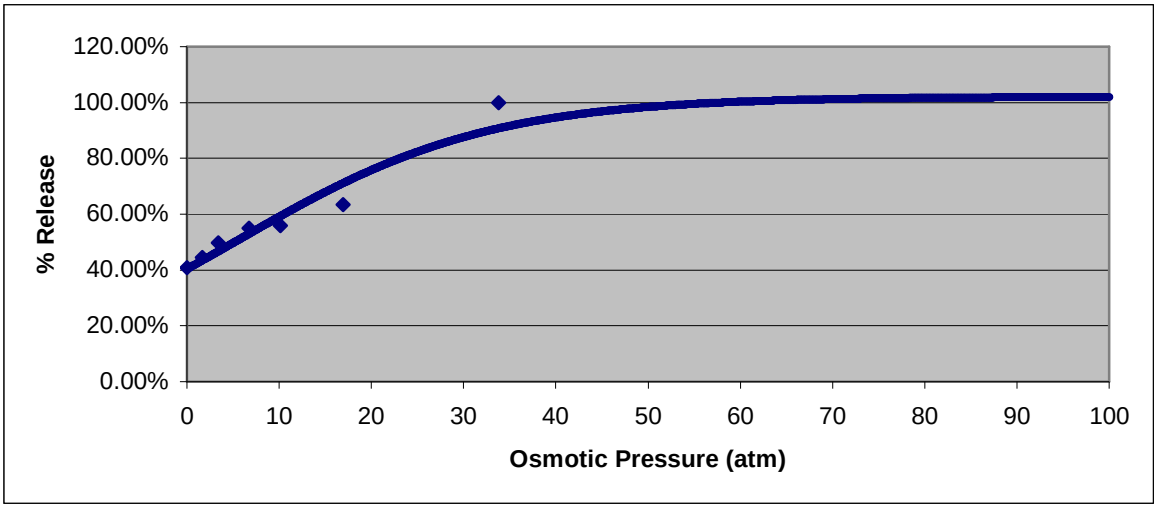

Table B.1 Bare Liposomes Fitting Constants

A	11.0279
B	10.8009
C	236.3898
D	-0.0741
E	-2.6624
R^2	0.999998992

Figure B.3 Sample 1 Fluorescent Intensity

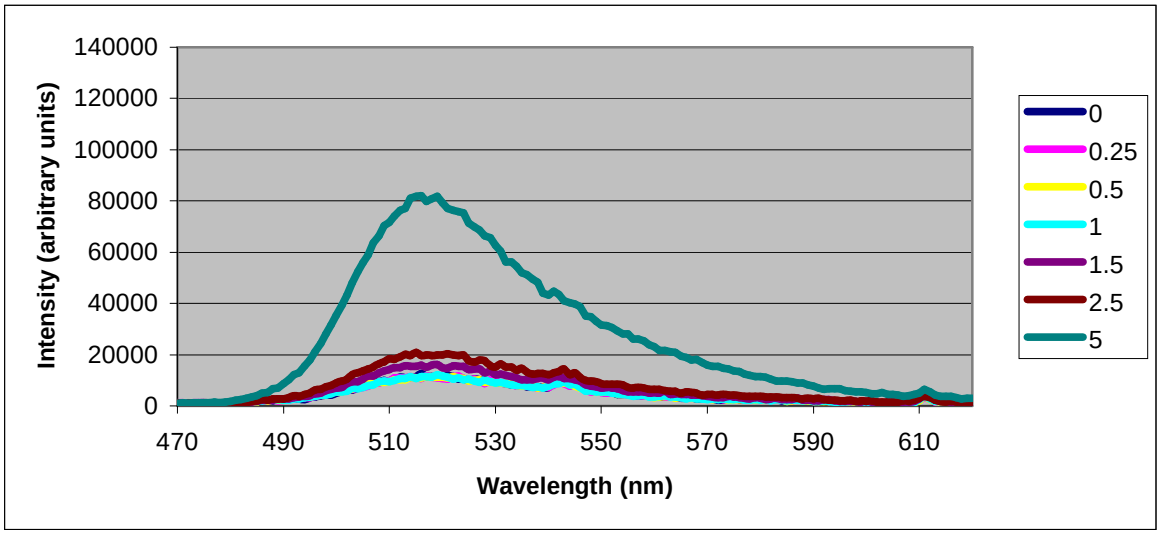

Figure B.4 Percent Release verses Osmotic Pressure Curve

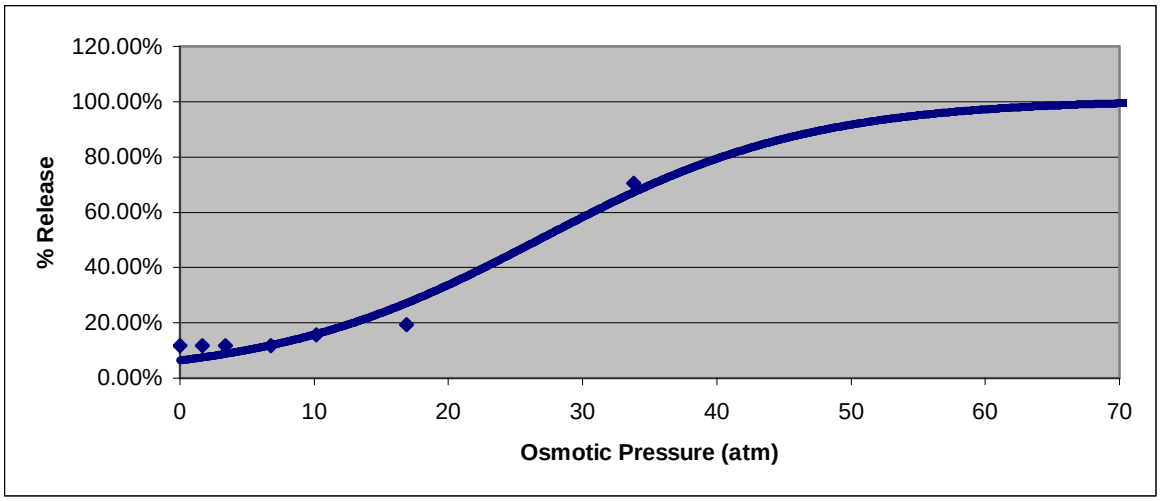

Table B.2 Fitting Constants

A	10.8532
B	10.7729
C	236.3994
D	-0.1000
E	-0.4018
R^2	0.999999279

Figure B.5 Sample 2 Fluorescent Intensity

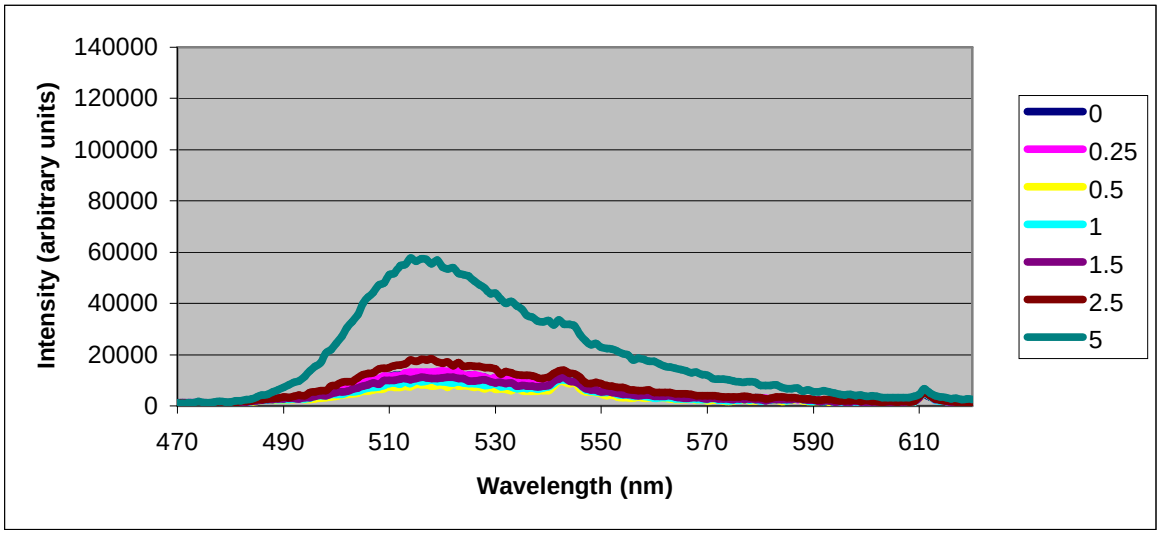

Figure B.6 Percent Release verses Osmotic Pressure Curve

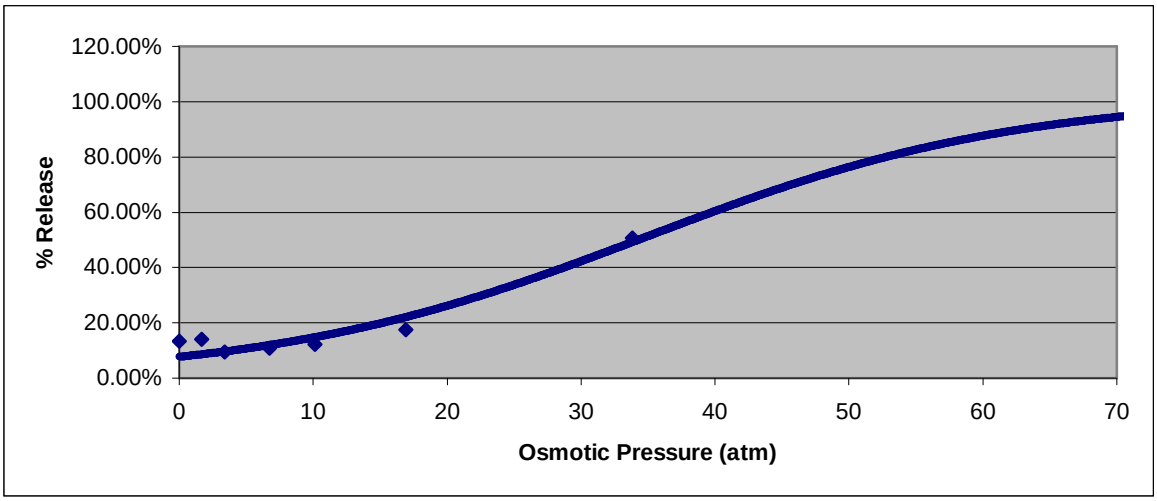

Table B.3 Fitting Constants

A	10.9297
B	10.7139
C	236.3986
D	-0.0719
E	-0.5928
R^2	0.999999435

Figure B.7 Sample 3 Fluorescent Intensity

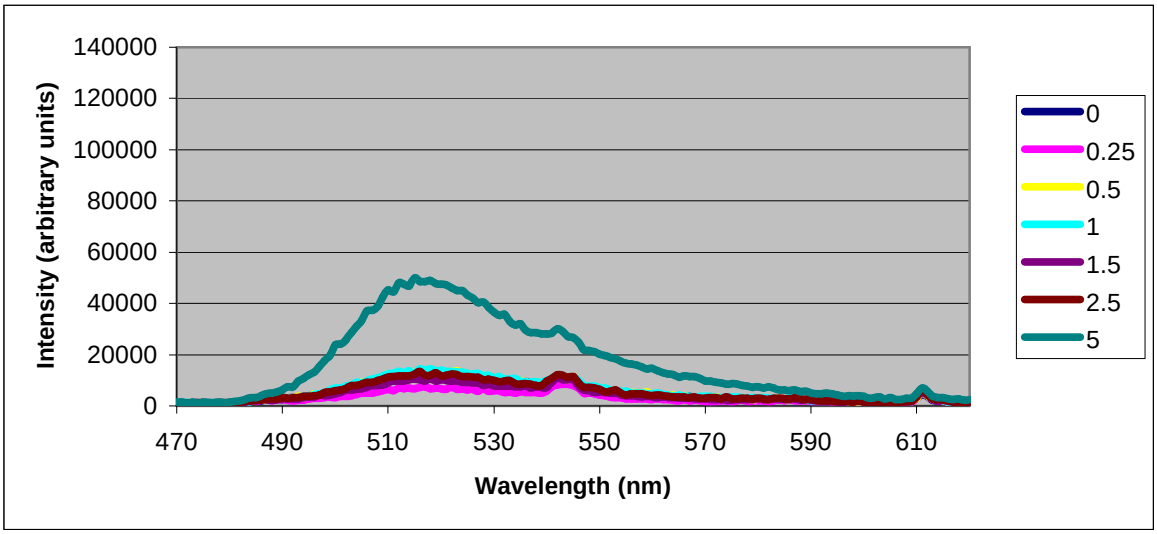

Figure B.8 Percent Release verses Osmotic Pressure Curve

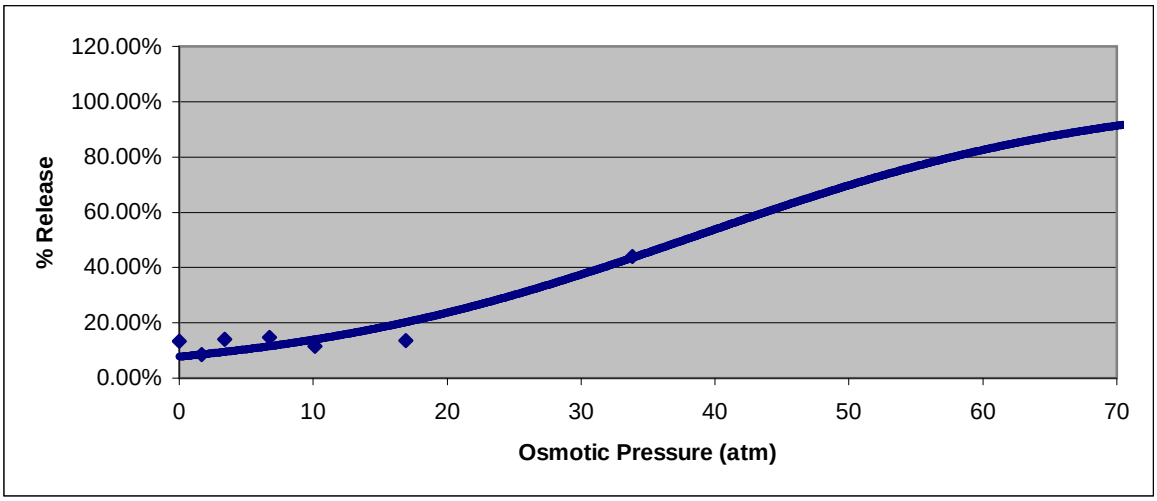

Table B.4 Fitting Constants

A	10.9988
B	10.6431
C	236.3986
D	-0.0648
E	-0.5911
R^2	0.999999259

Figure B.9 Sample 4 Fluorescent Intensity

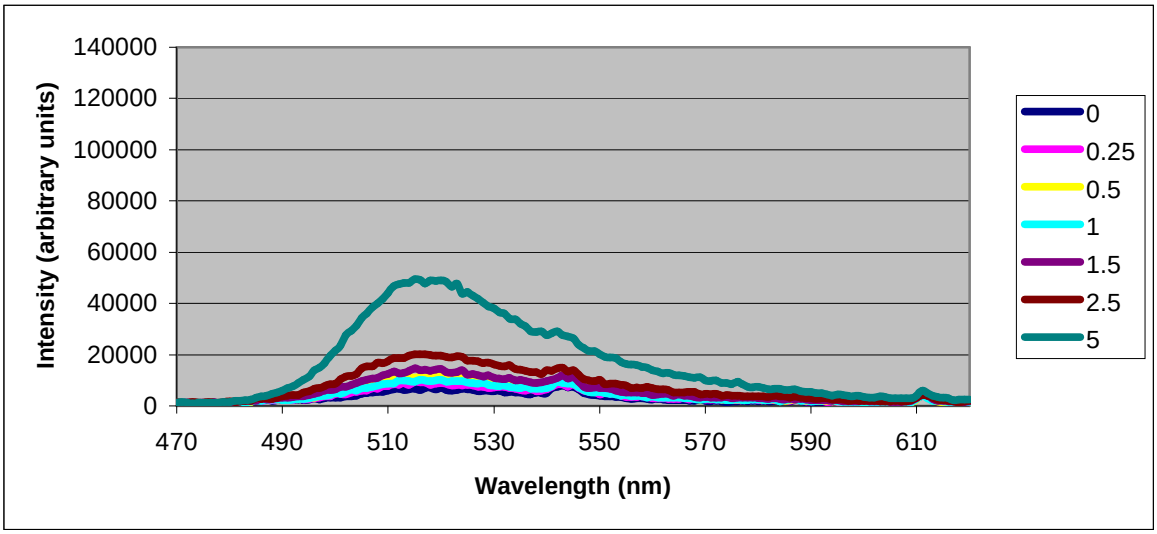

Figure B.10 Percent Release verses Osmotic Pressure Curve

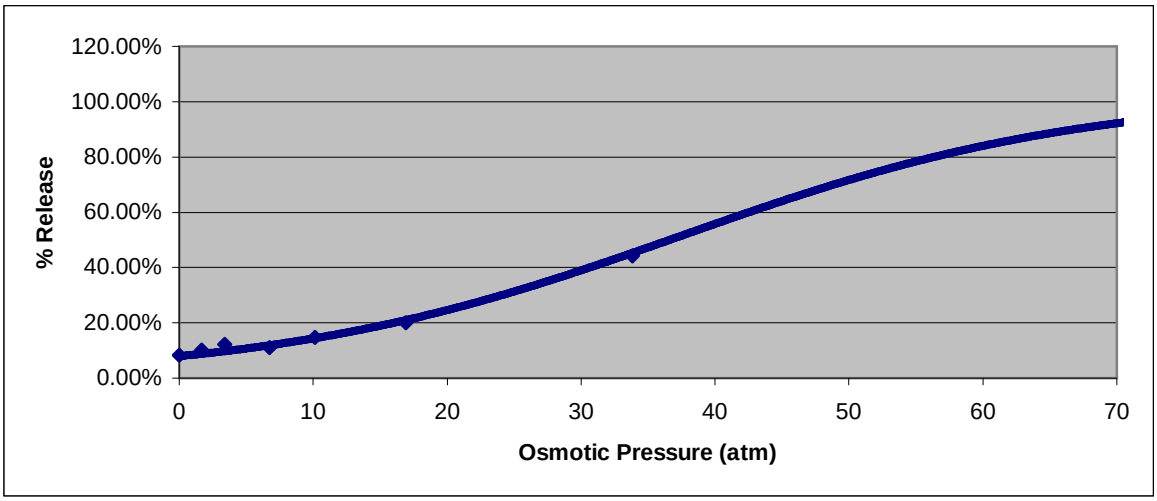

Table B.5 Fitting Constants

A	10.9737
B	10.6710
C	236.3985
D	-0.0663
E	-0.6161
R^2	0.999999856

Figure B.11 Sample 5 Fluorescent Intensity

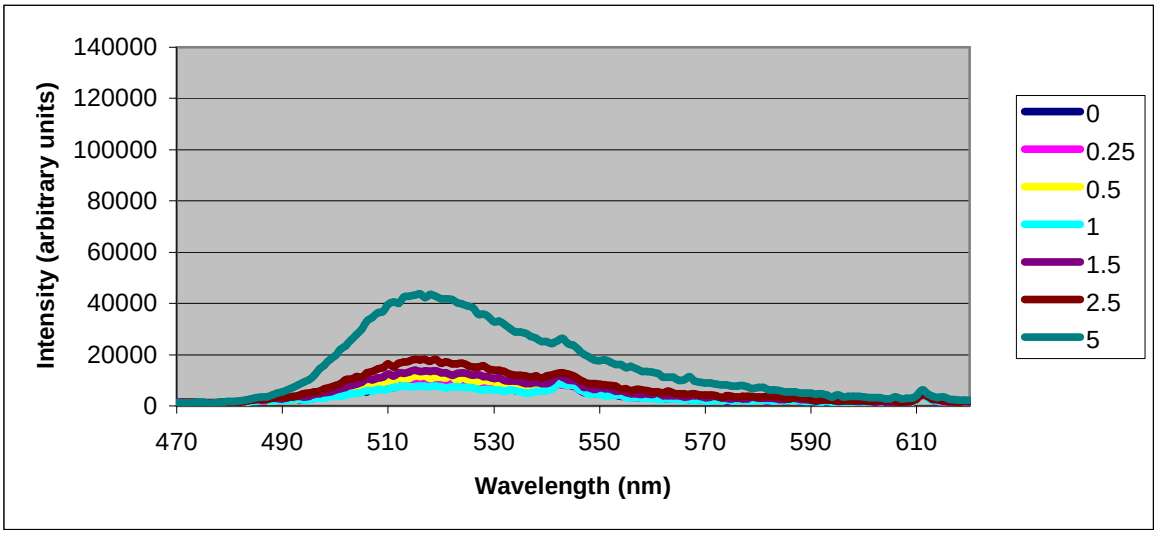

Figure B.12 Percent Release verses Osmotic Pressure Curve

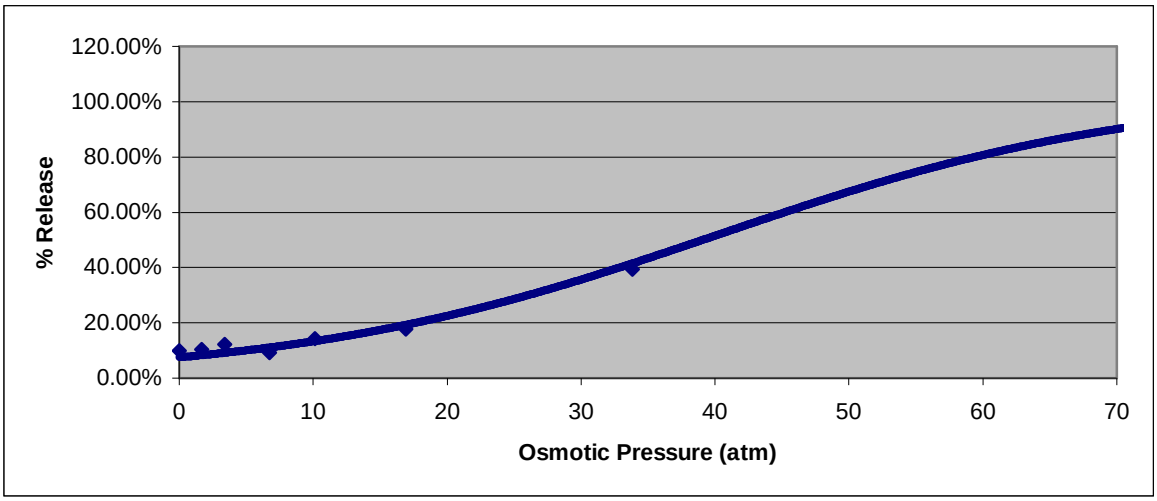

Table B.6 Fitting Constants

A	11.0182
B	10.6194
C	236.3987
D	-0.0634
E	-0.5540
R^2	0.999998992

Figure B.13 Sample 6 Fluorescent Intensity

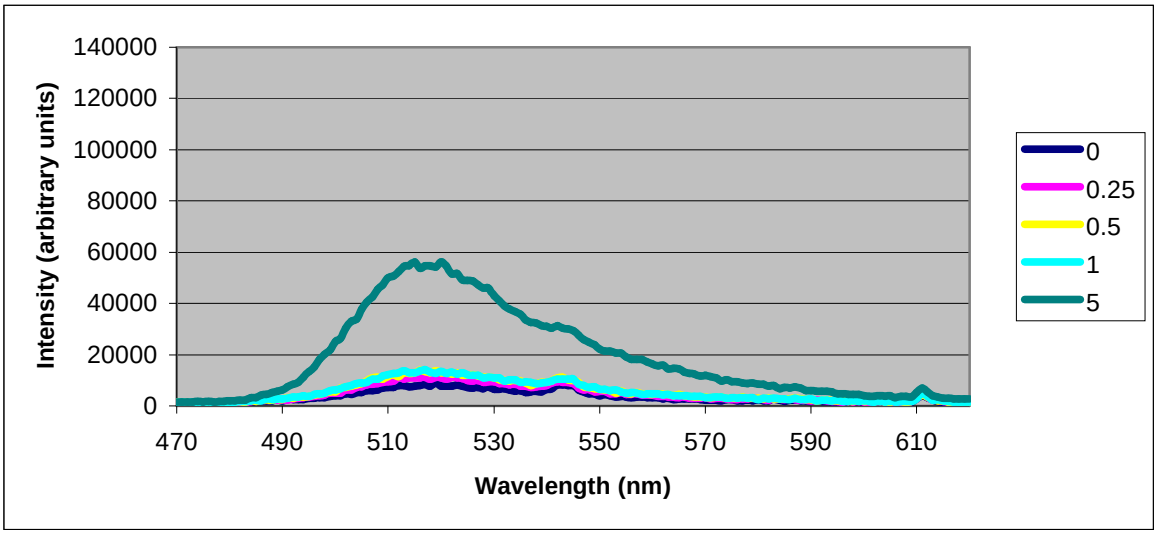

Figure B.14 Percent Release verses Osmotic Pressure Curve

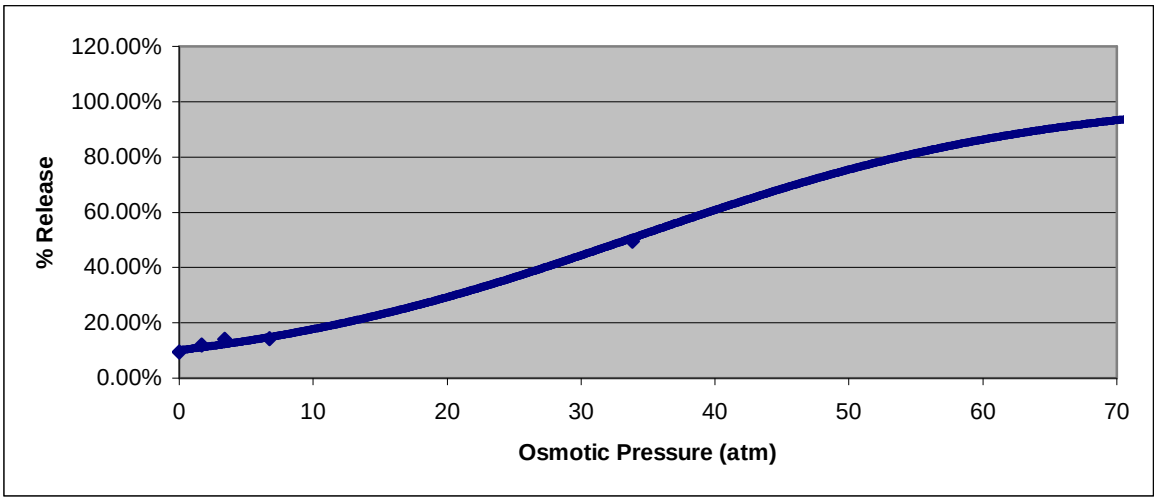

Table B.7 Fitting Constants

A	10.9708
B	10.7066
C	236.3973
D	-0.0648
E	-0.8823
R^2	0.999999909

Appendix C Resistance Kinetics Calculations

Figure C.1 Bare Liposomes 15 Minutes

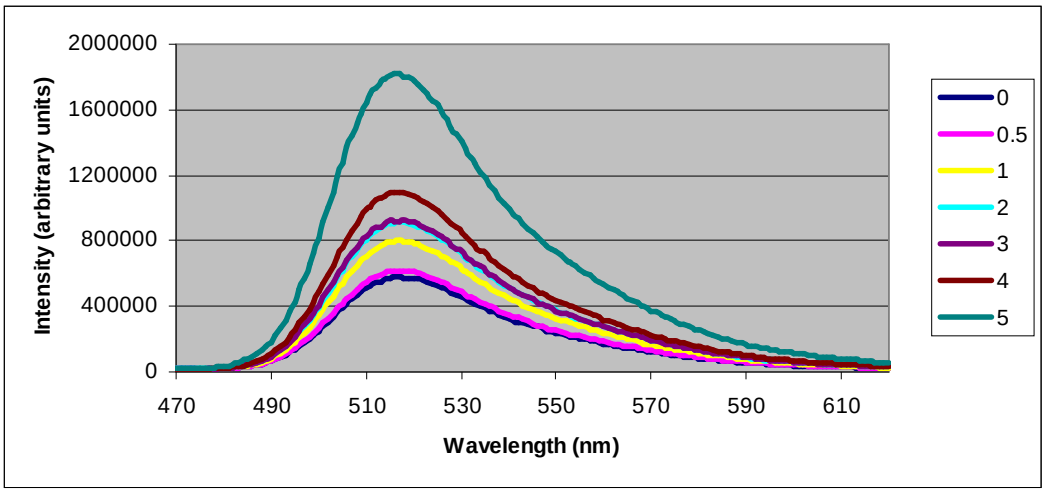

Figure C.2 Percent Release verses Osmotic Pressure Curve

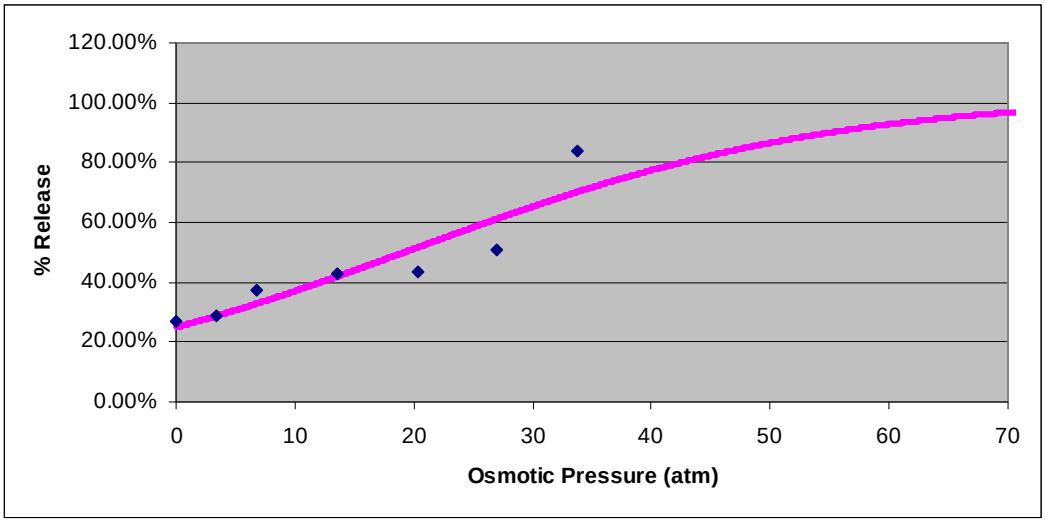

Table C.1 Fitting Constants

A	11.0155
B	10.7478
C	236.3928
D	-0.0566
E	-1.9564
R^2	0.99999666

Figure C.3 Bare Liposomes 2 Hours

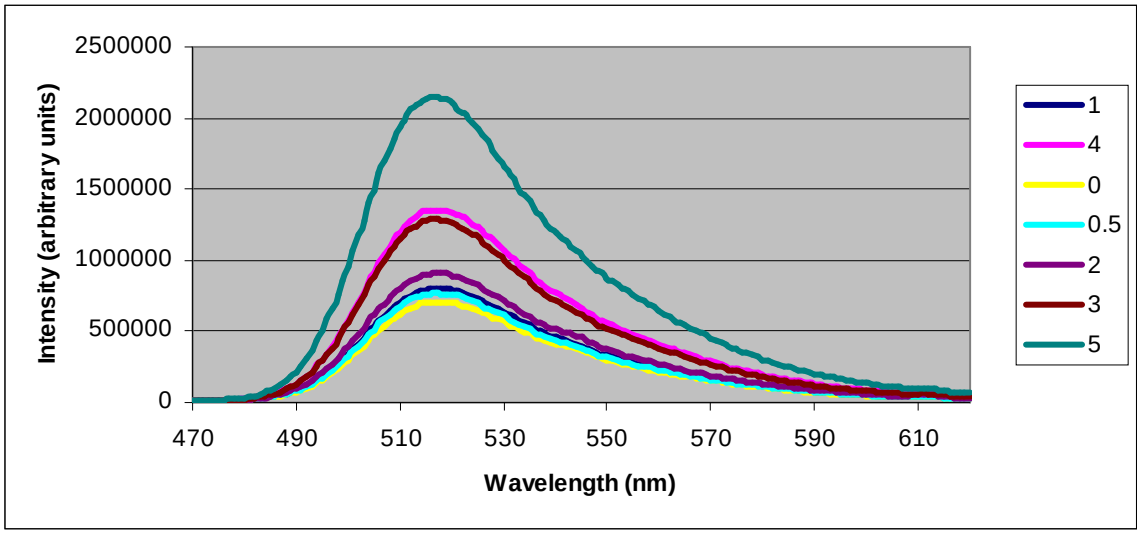

Figure C.4 Percent Release verses Osmotic Pressure Curve

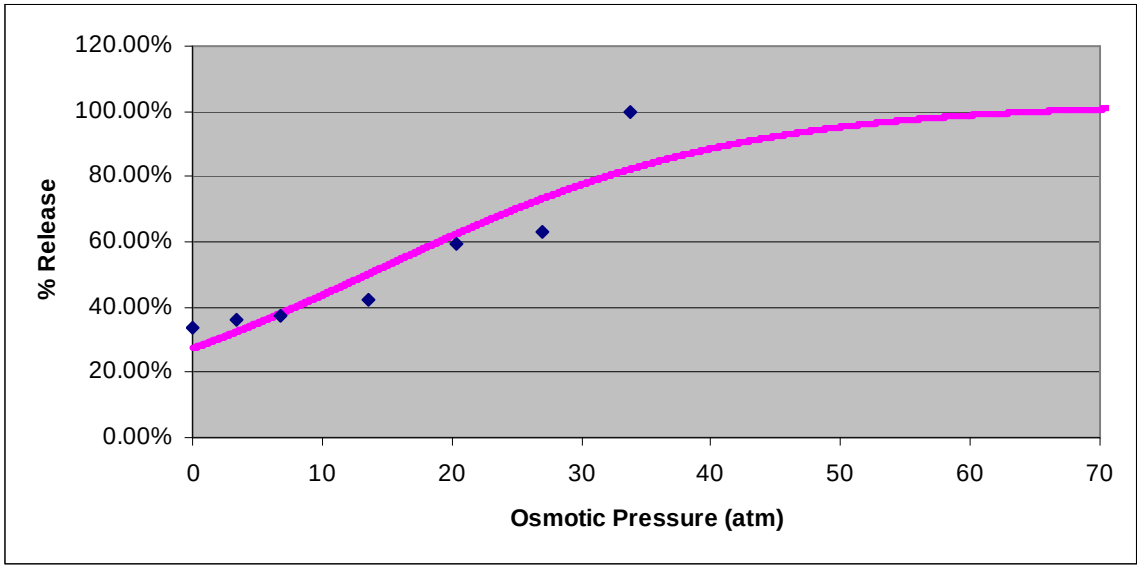

Table C.2 Fitting Constants

A	11.0250
B	10.7513
C	236.3923
D	-0.0715
E	-2.0768
R^2	0.99999666

Figure C.5 Bare Liposomes 5 Hours

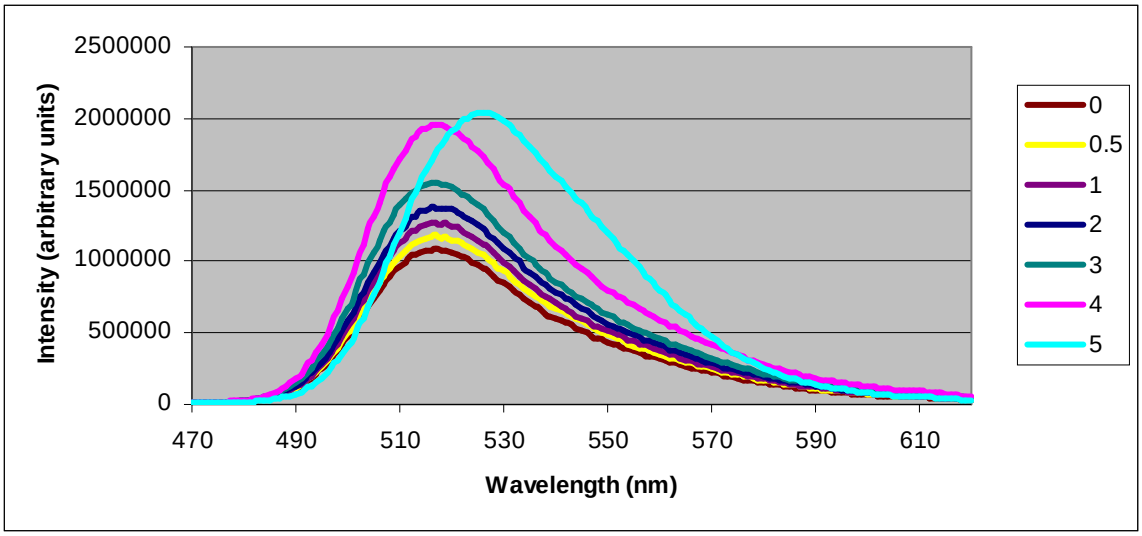

Figure C.6 Percent Release verses Osmotic Pressure Curve

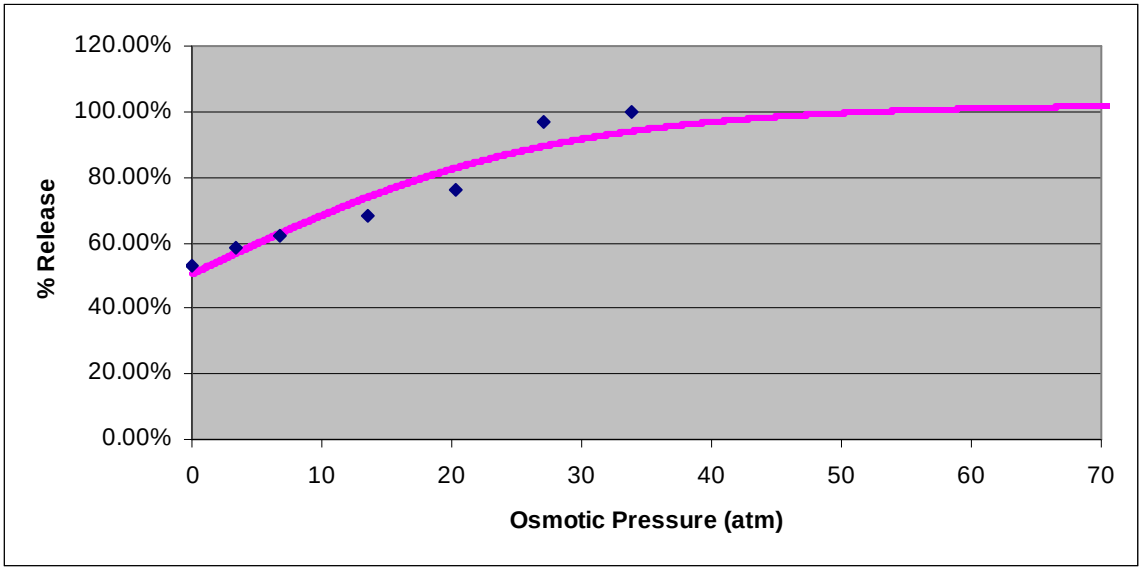

Table C.3 Fitting Constants

A	11.0545
B	10.8115
C	236.3881
D	-0.0727
E	-3.0599
R^2	0.999998869

Figure C.7 Bare Liposomes 24 Hours

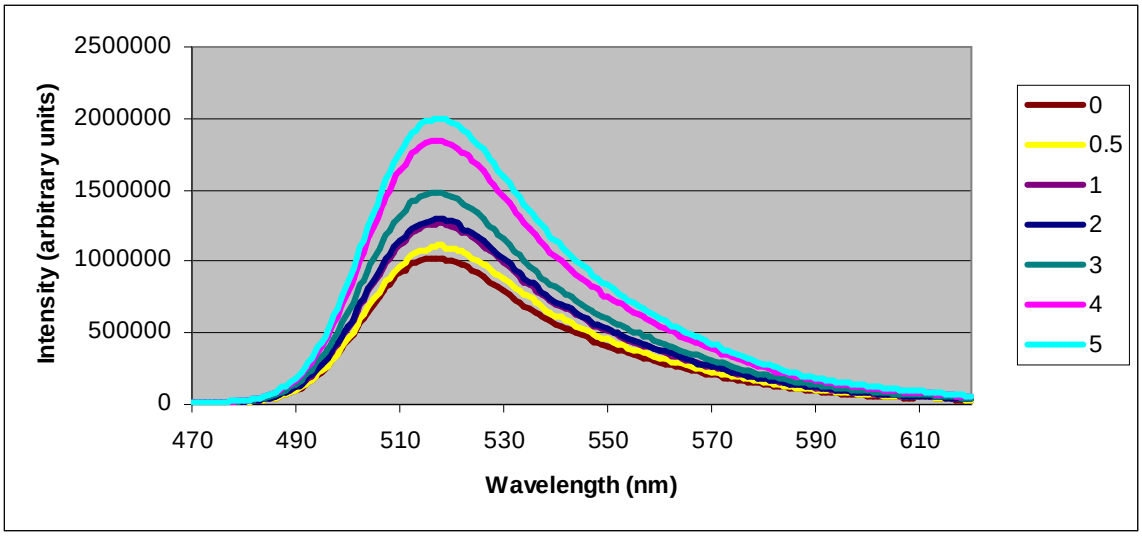

Figure C.8 Percent Release verses Osmotic Pressure Curve

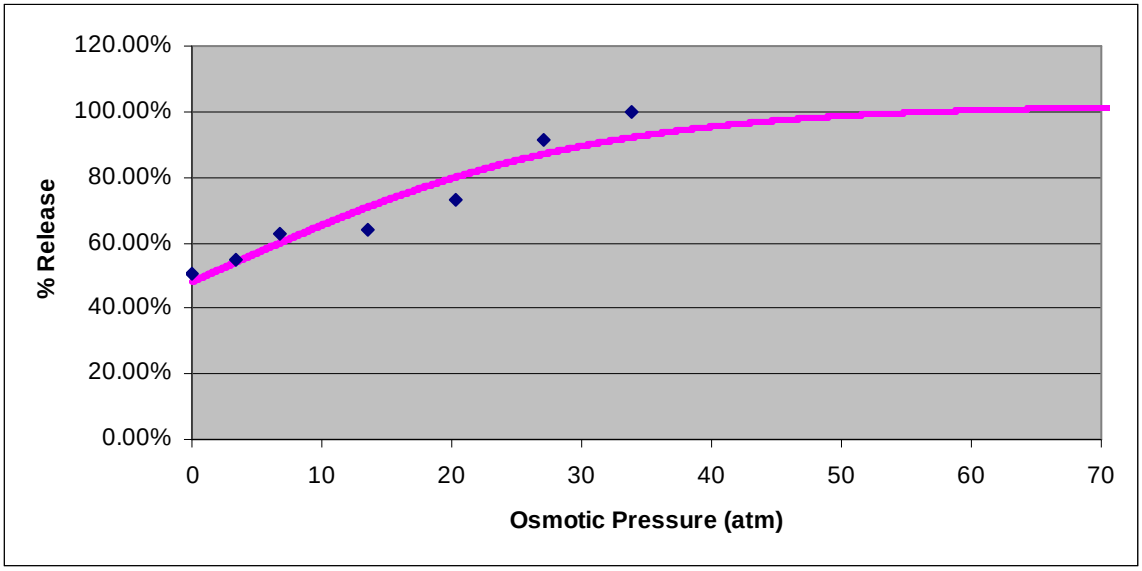

Table C.4 Fitting Constants

A	11.0451
B	10.8126
C	236.3885
D	-0.0691
E	-2.9678
R^2	0.999998799

Figure C.9 Polymer Caged Liposomes 15 Minutes

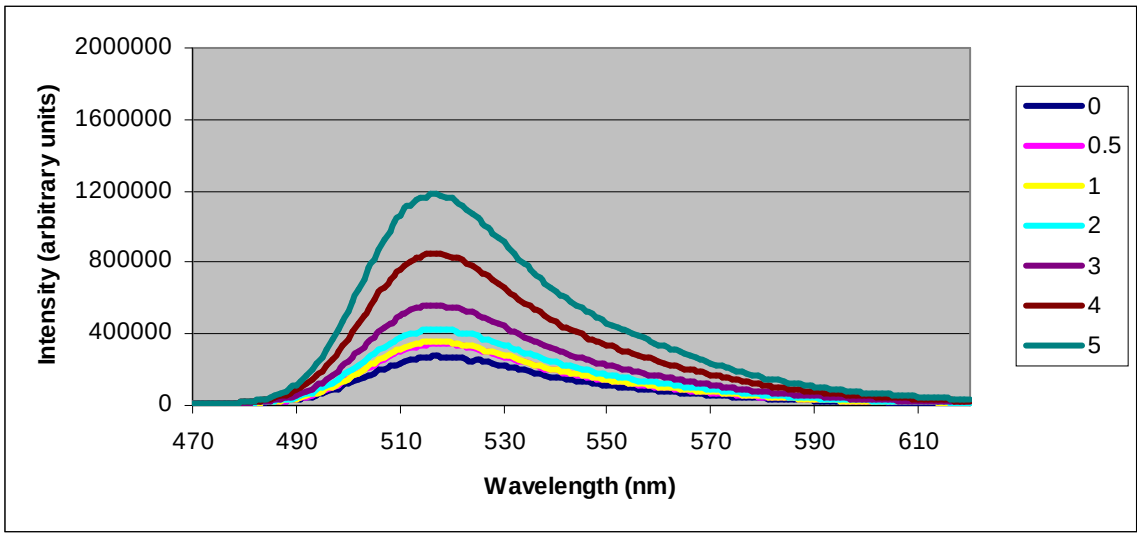

Figure C.10 Percent Release verses Osmotic Pressure Curve

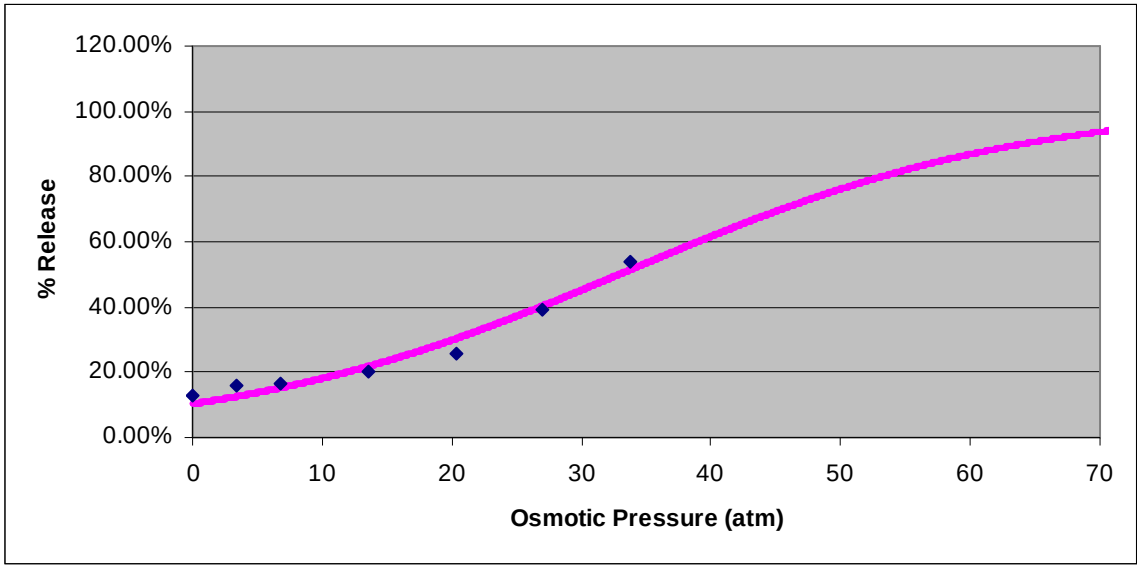

Table C.5 Fitting Constants

A	8.2079
B	8.0049
C	236.3933
D	-0.0650
E	-1.1973
R^2	0.999999617

Figure C.11 Polymer Caged Liposomes 2 Hours

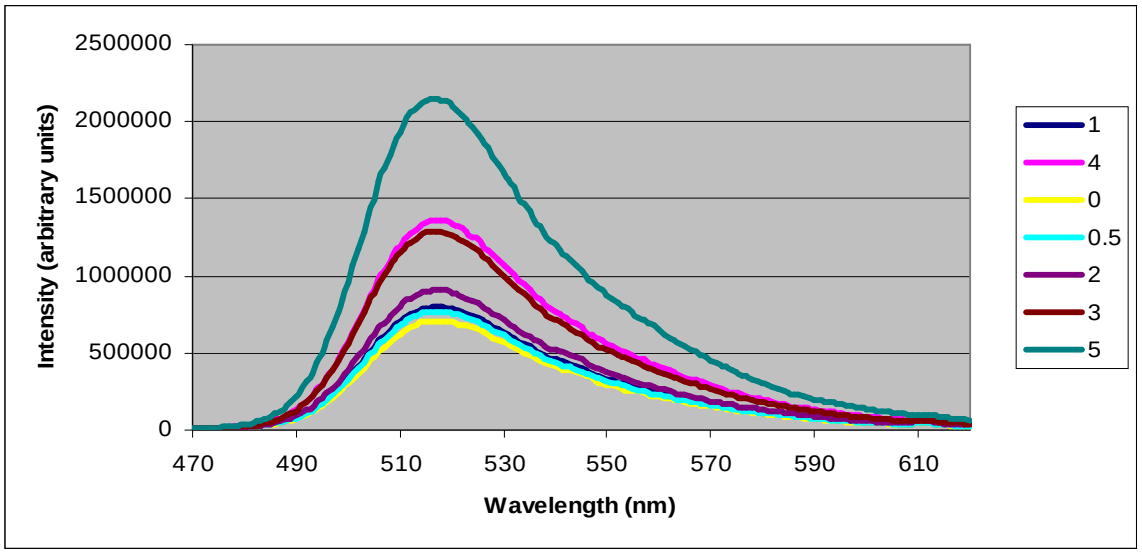

Figure C.12 Percent Release verses Osmotic Pressure Curve

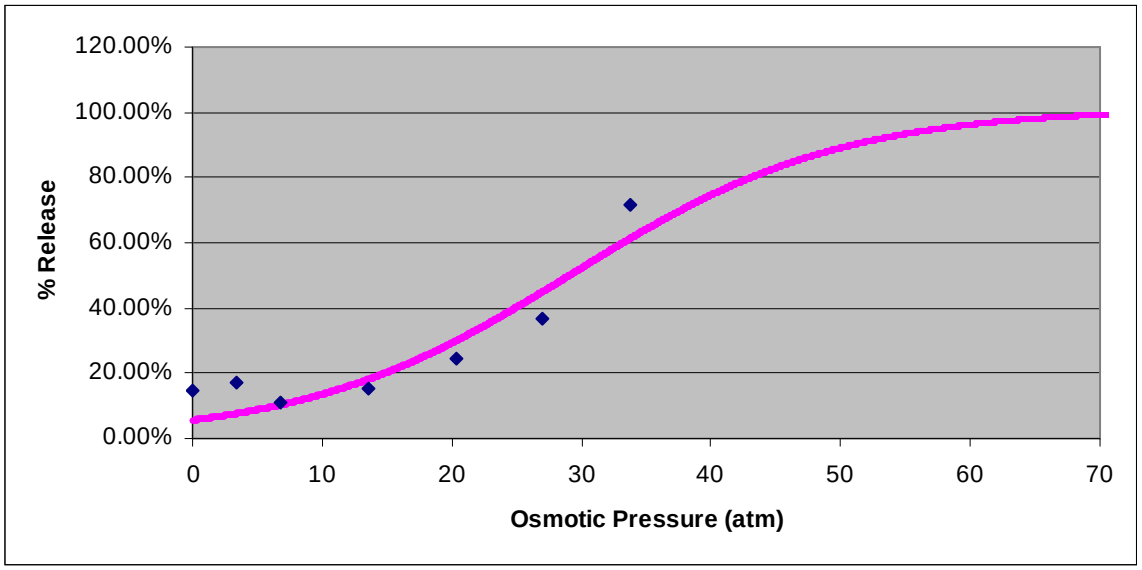

Table C.6 Fitting Constants

A	10.8813
B	10.7531
C	236.4000
D	-0.0966
E	-0.2614
R^2	0.999997645

Figure C.13 Polymer Caged Liposomes 5 Hours

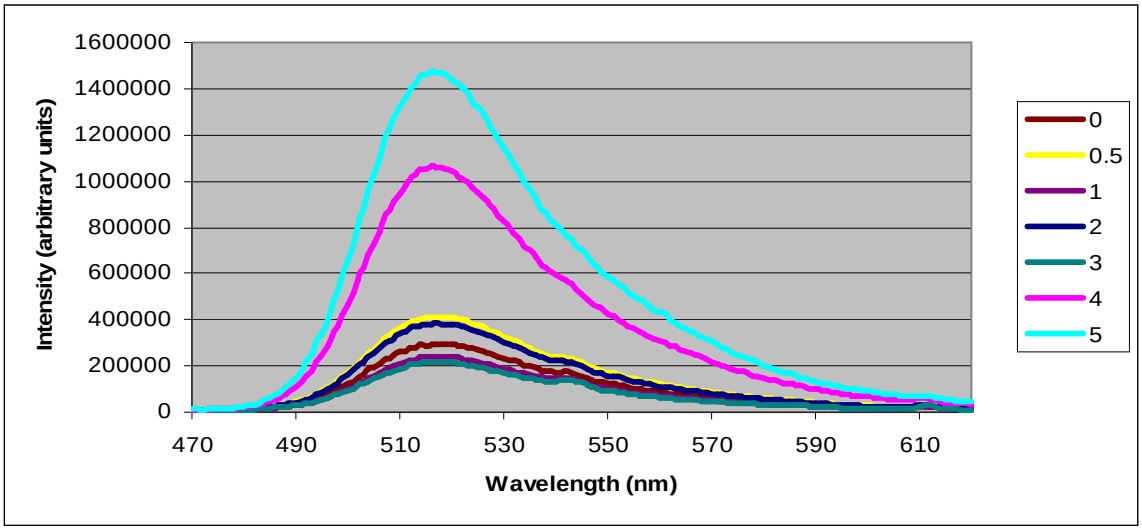

Figure C.14 Percent Release verses Osmotic Pressure Curve

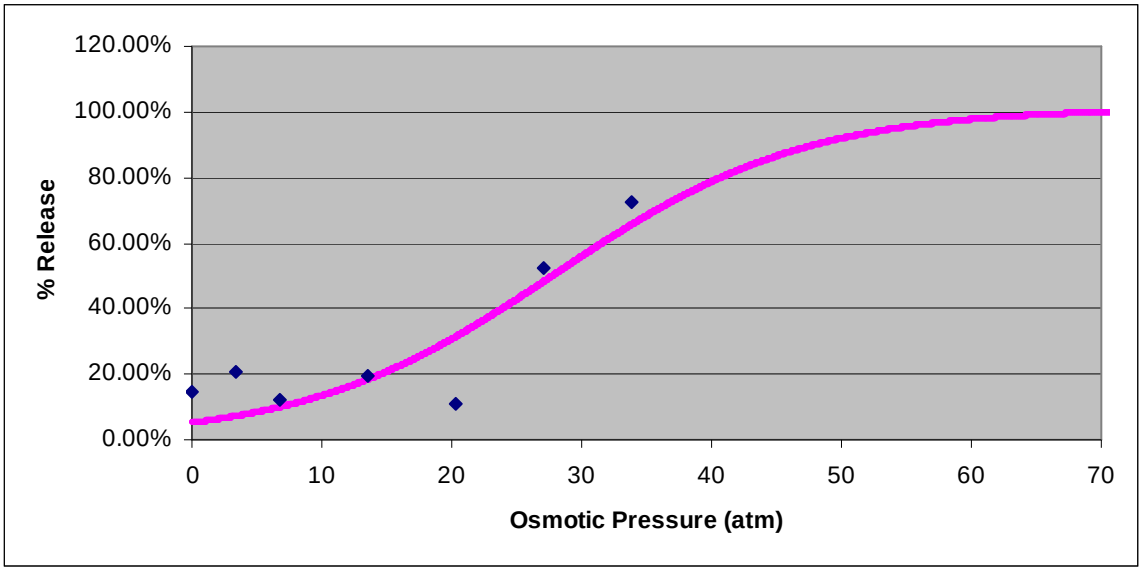

Table C.7 Fitting Constants

A	11.0451
B	10.8126
C	236.3885
D	-0.0691
E	-2.9678
R^2	0.999998799

Figure C.15 Polymer Caged Liposomes 24 Hours

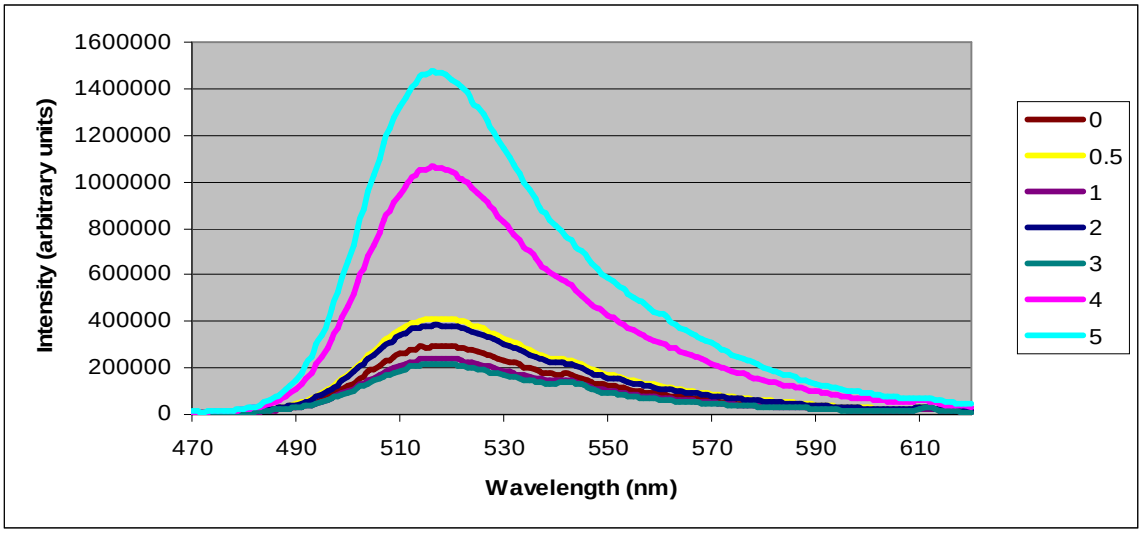

Figure C.16 Percent Release verses Osmotic Pressure Curve

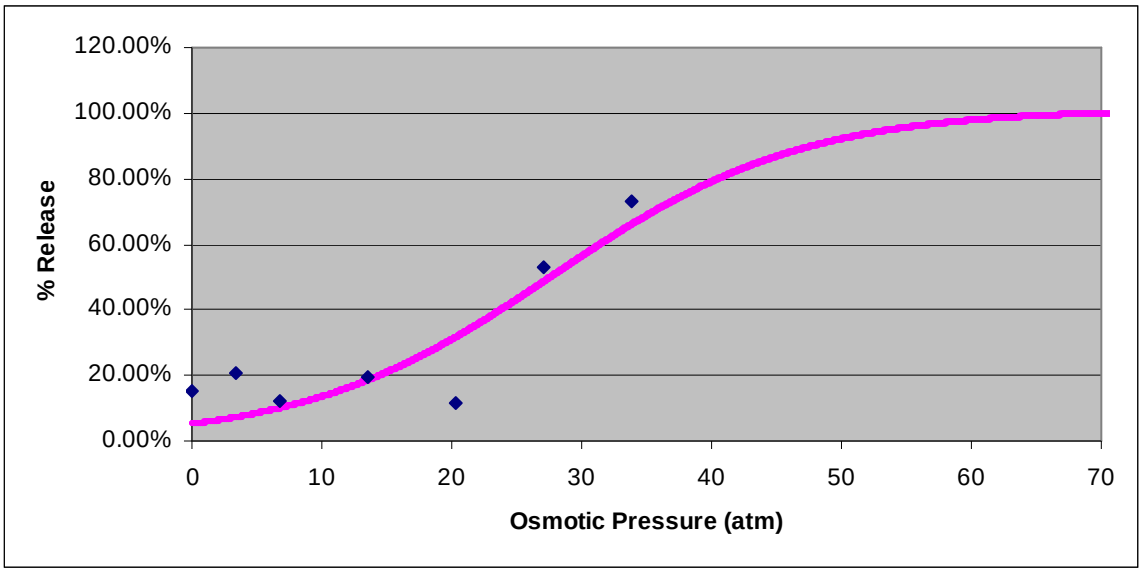

Table C.8 Fitting Constants

A	10.8987
B	10.7597
C	236.4003
D	-0.1045
E	-0.1824
R^2	0.999995247

Appendix D Oleic Acid Effect Calculations

Figure D.1 3.7% Oleic Acid Bare Liposomes

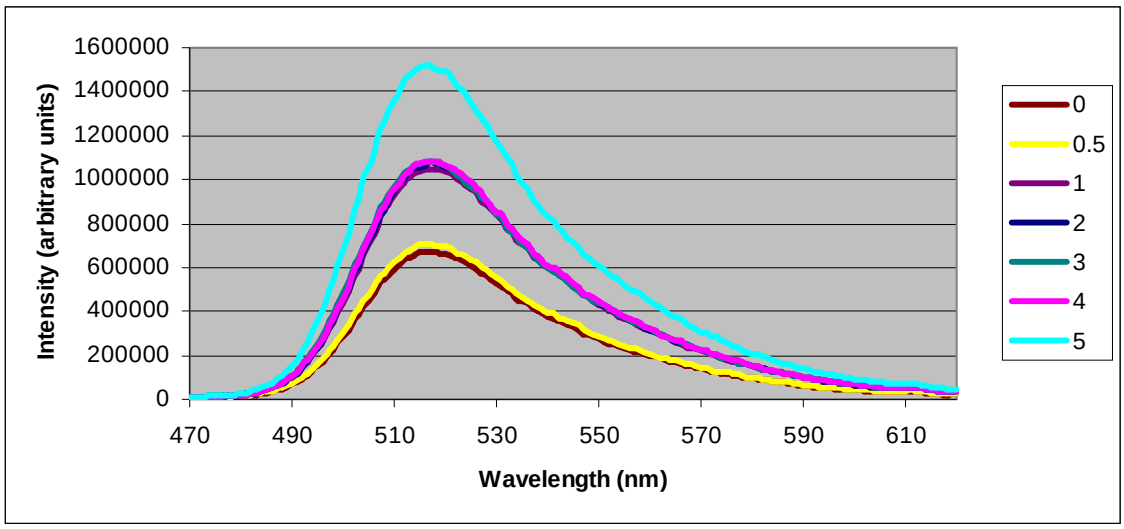

Figure D.2 Percent Release verses Osmotic Pressure Curve

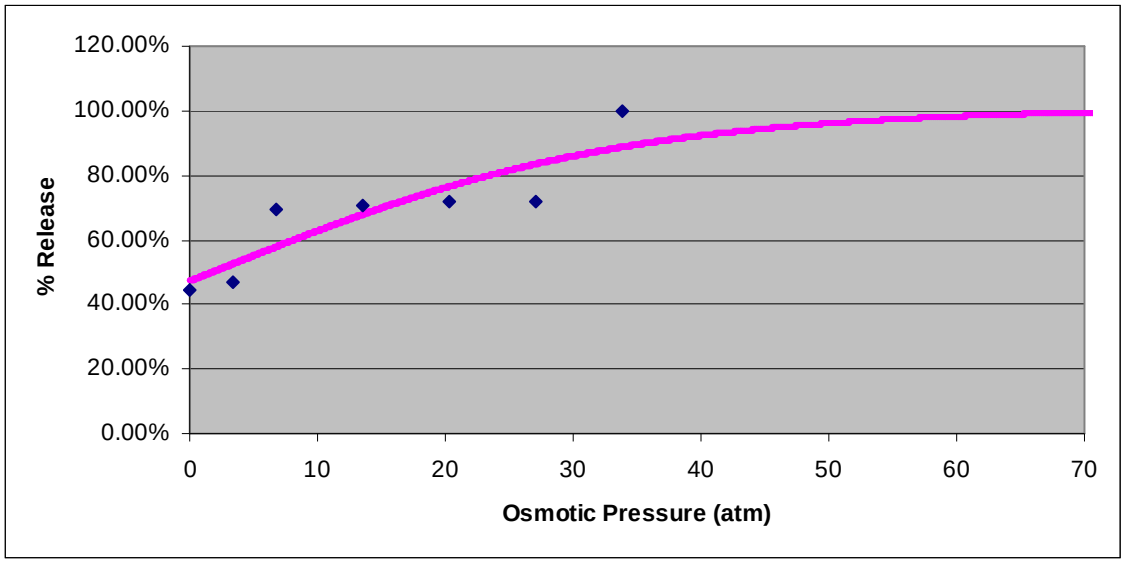

Table D.1 Fitting Constants

A	10.9754
B	10.8820
C	236.3886
D	-0.0627
E	-2.9522
R^2	0.999997076

Figure D.3 2.5% Oleic Acid Bare Liposomes

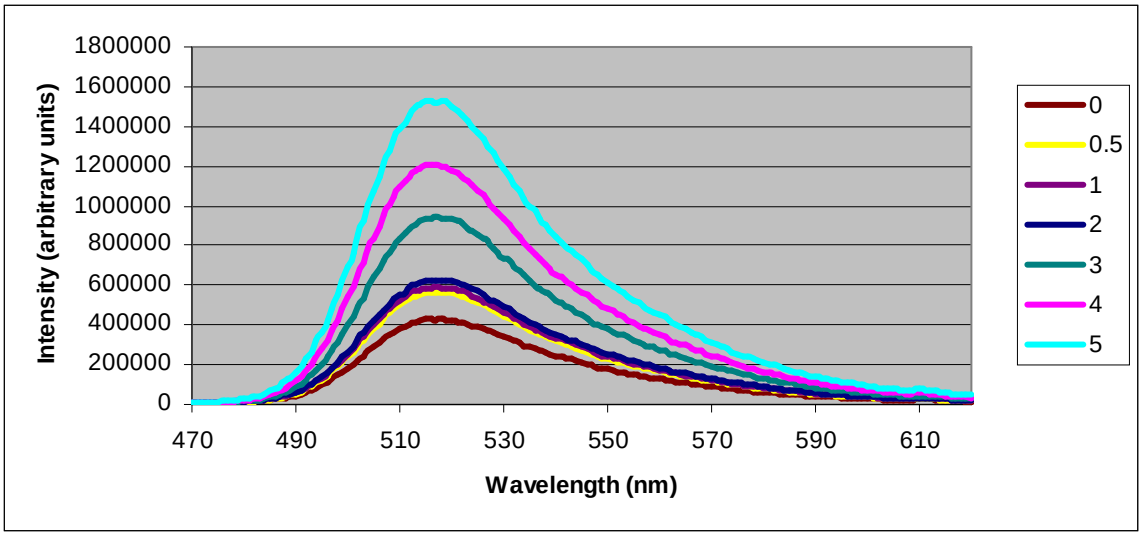

Figure D.4 Percent Release verses Osmotic Pressure Curve

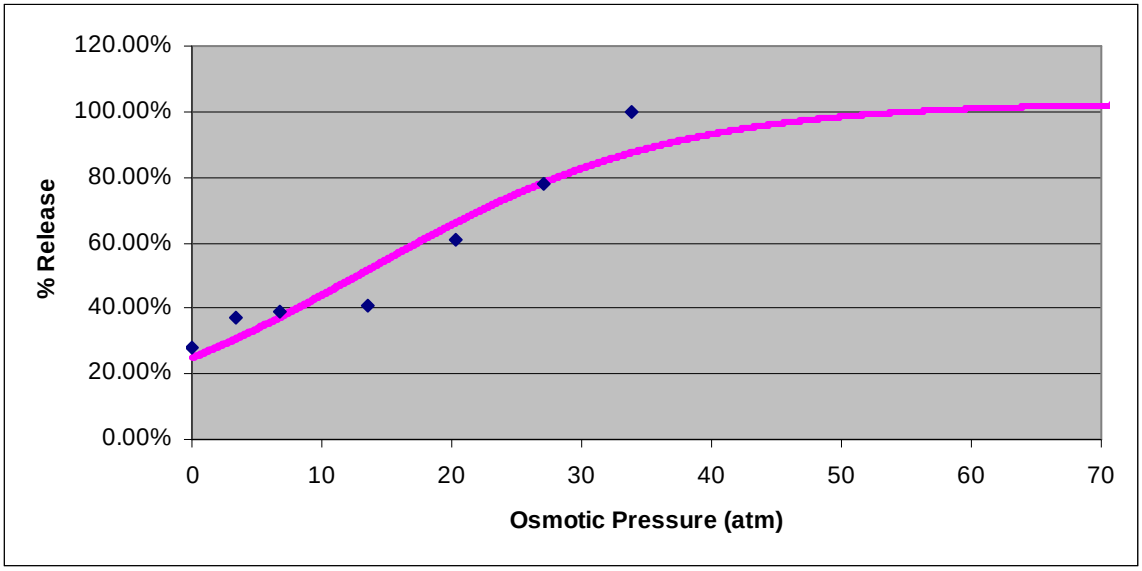

Table D.2 Fitting Constants

A	11.0323
B	10.7320
C	236.3928
D	-0.0852
E	-1.9513
R^2	0.999997744

Figure D.5 1.2% Oleic Acid Bare Liposomes

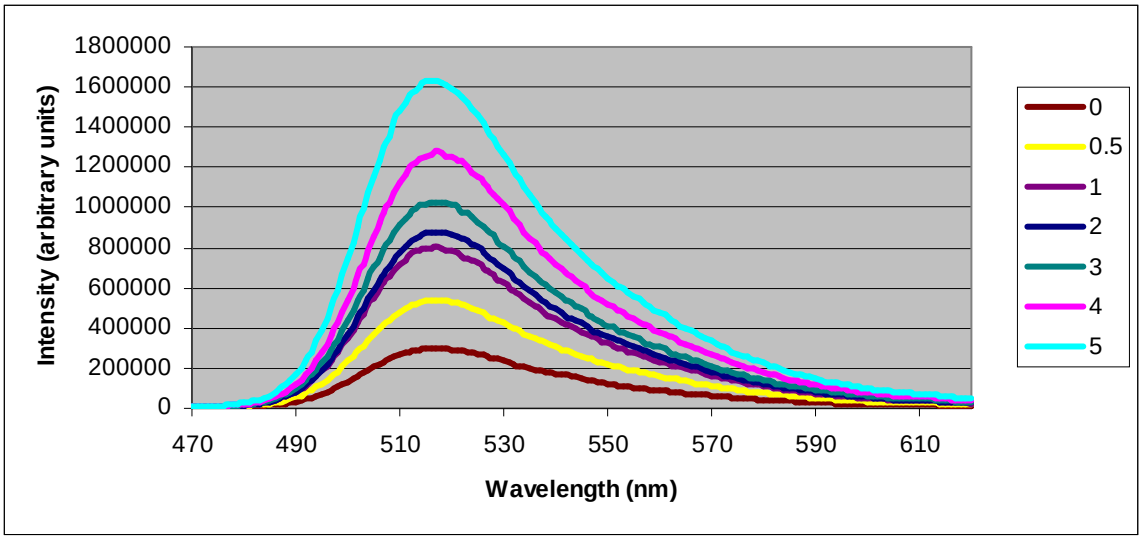

Figure D.6 Percent Release verses Osmotic Pressure Curve

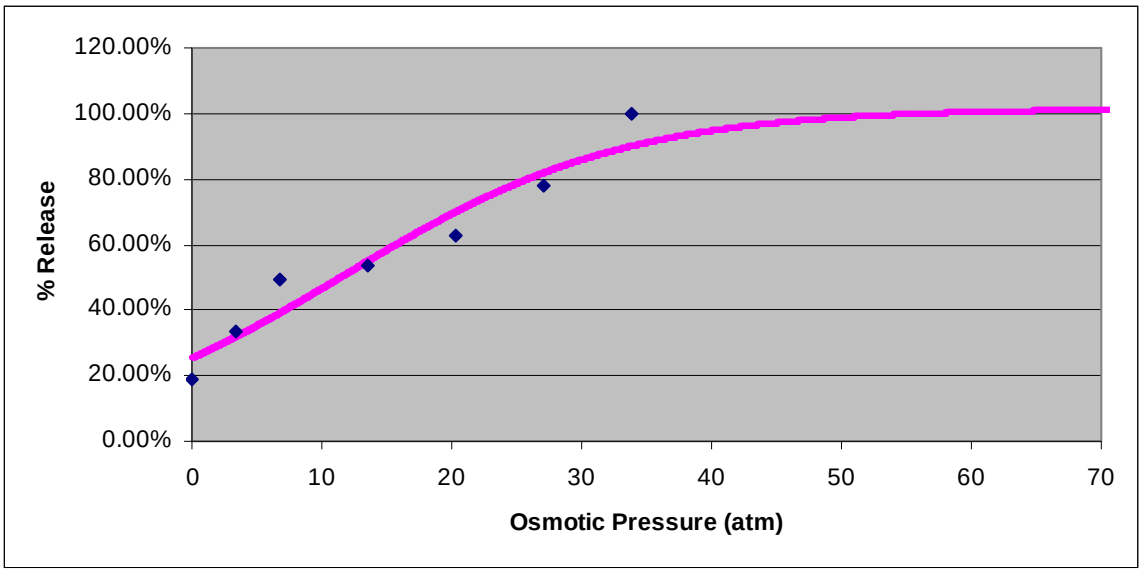

Table D.3 Fitting Constants

A	10.9677
B	10.8020
C	236.3927
D	-0.0933
E	-1.9888
R^2	0.999998044

Figure D.7 3.7% Oleic Acid Polymer Caged Liposomes

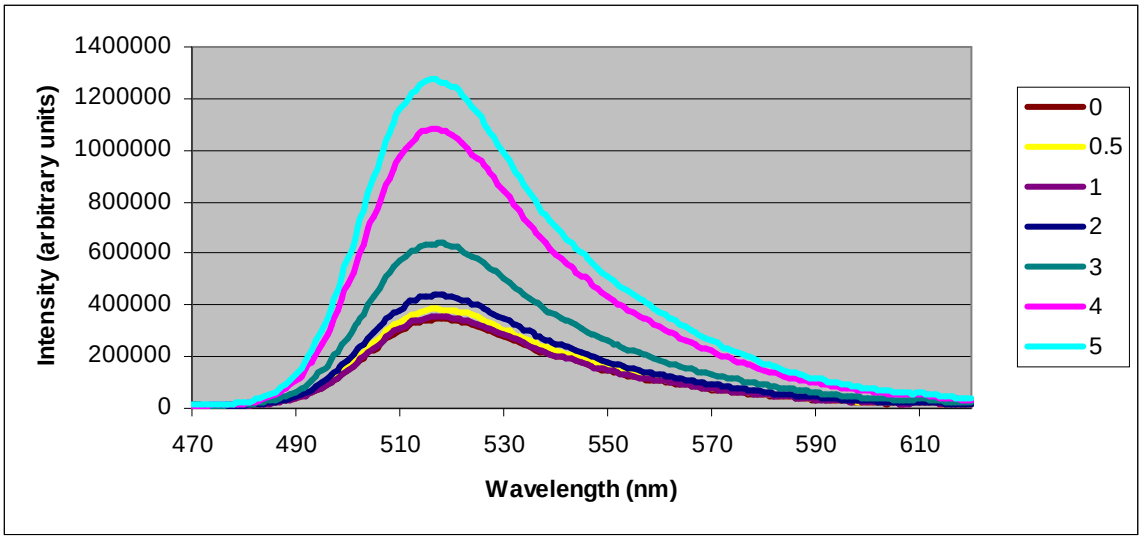

Figure D.8 Percent Release verses Osmotic Pressure Curve

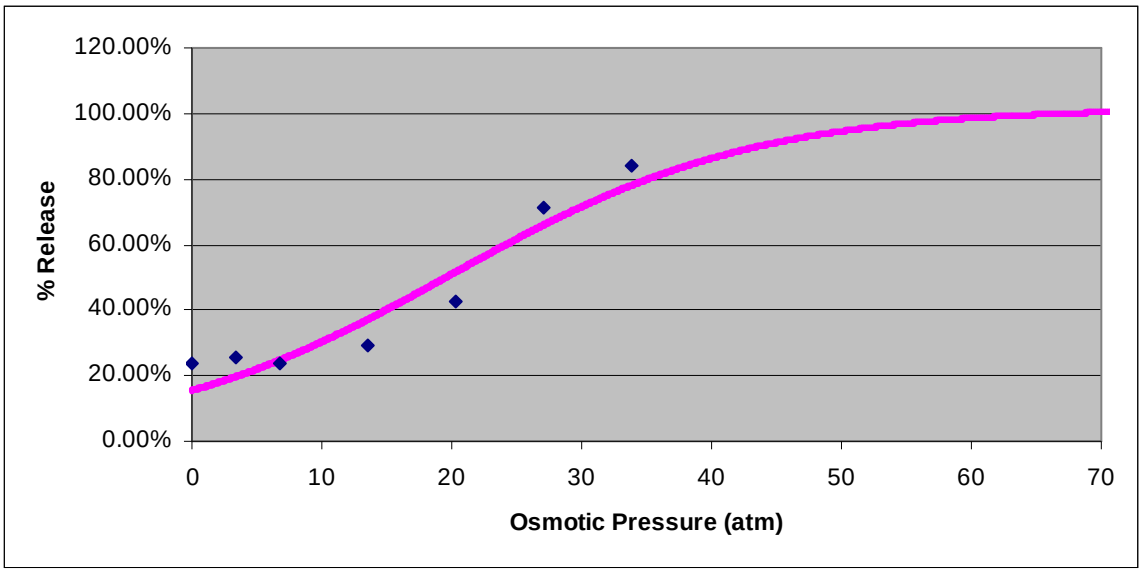

Table D.4 Fitting Constants

A	10.9487
B	10.7659
C	236.3953
D	-0.0860
E	-1.3751
R^2	0.999998045

Figure D.9 2.5% Oleic Acid Polymer Caged Liposomes

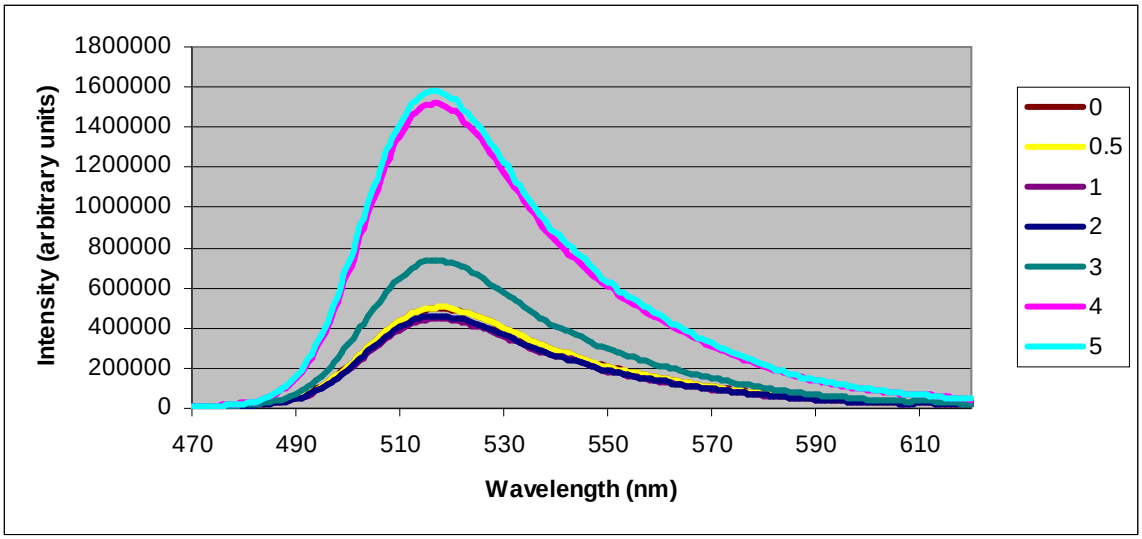

Figure D.10 Percent Release verses Osmotic Pressure Curve

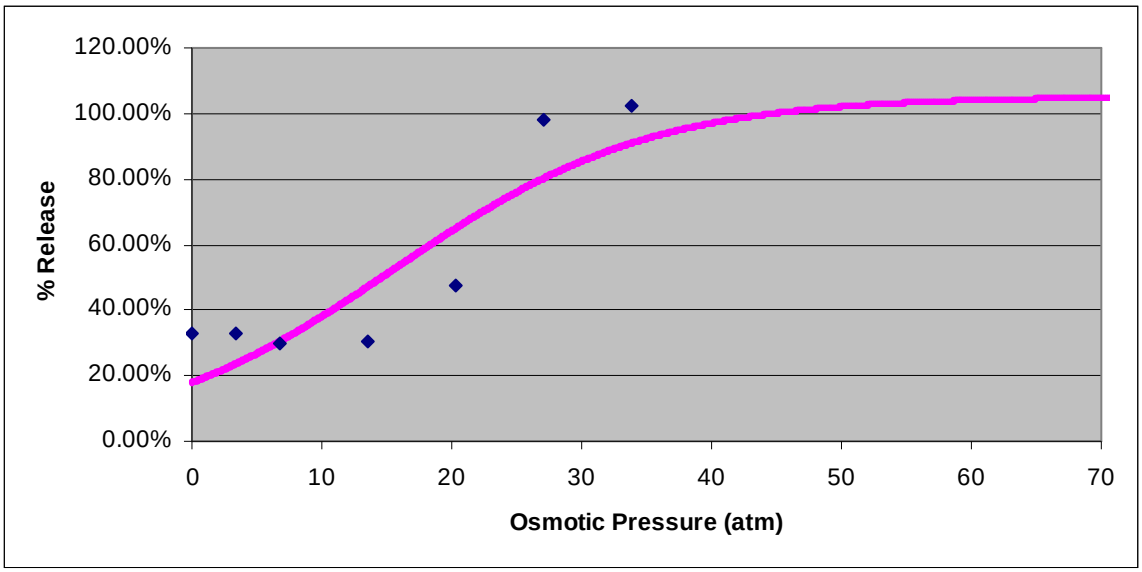

Table D.5 Fitting Constants

A	2.0289
B	1.9293
C	235.9896
D	-0.1016
E	-3.2253
R^2	0.999991258

Figure D.11 1.2% Oleic Acid Polymer Caged Liposomes

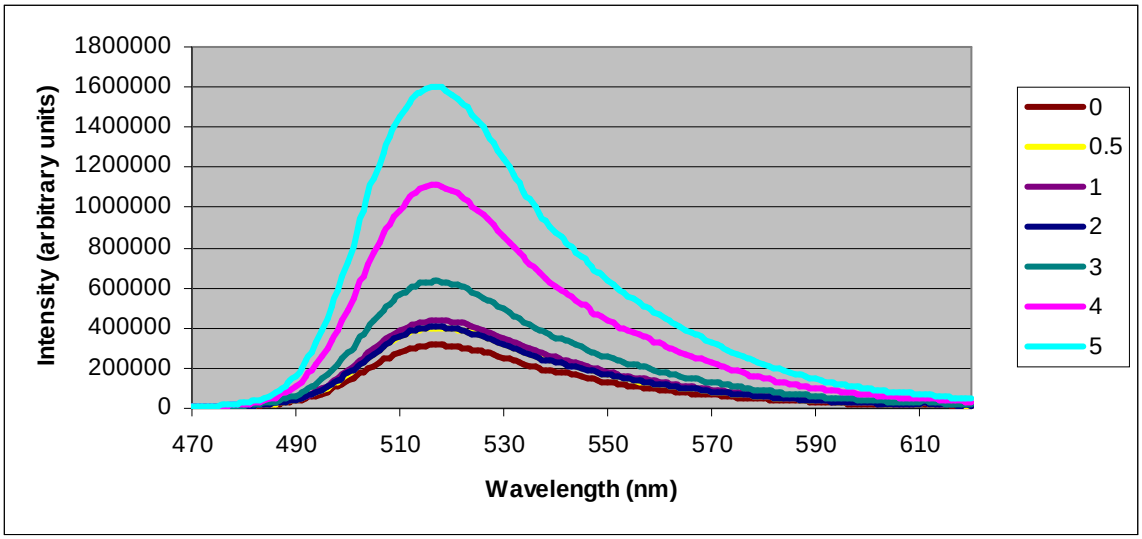

Figure D.12 Percent Release verses Osmotic Pressure Curve

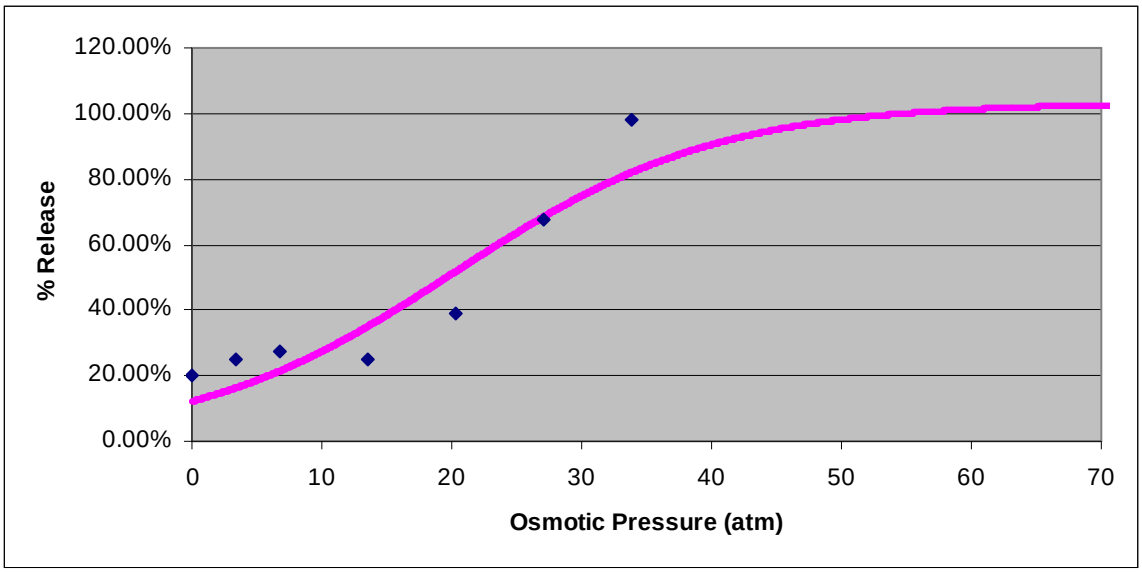

Table D.6 Fitting Constants

A	1.9076
B	1.8484
C	235.9912
D	-0.0993
E	-2.8404
R^2	0.999995579

Appendix E Cholesterol Effect Calculations

Figure E.1 20% Cholesterol – Bare Liposomes

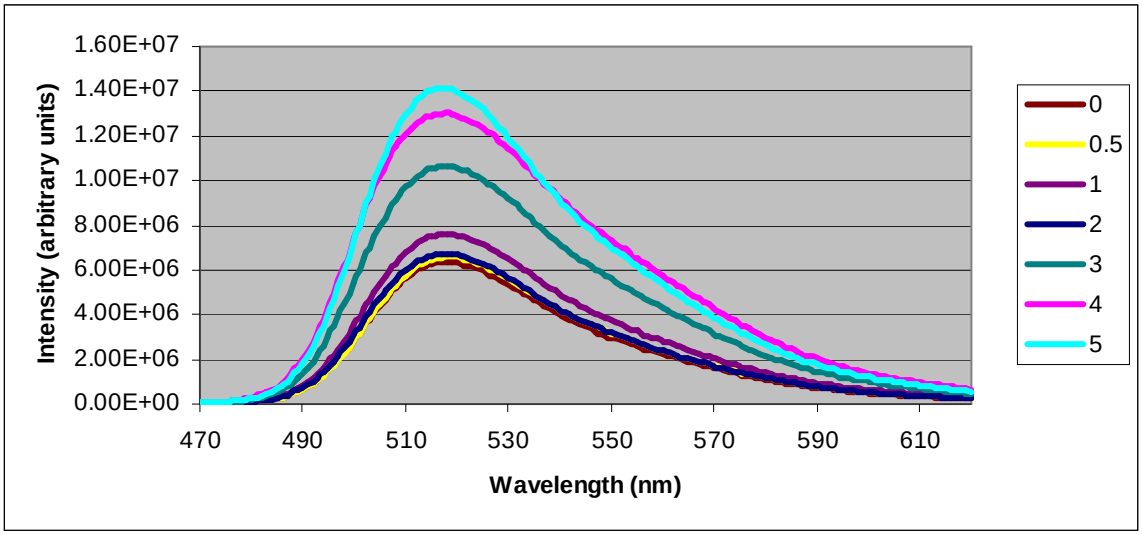

Figure E.2 Percent Release verses Osmotic Pressure Curve

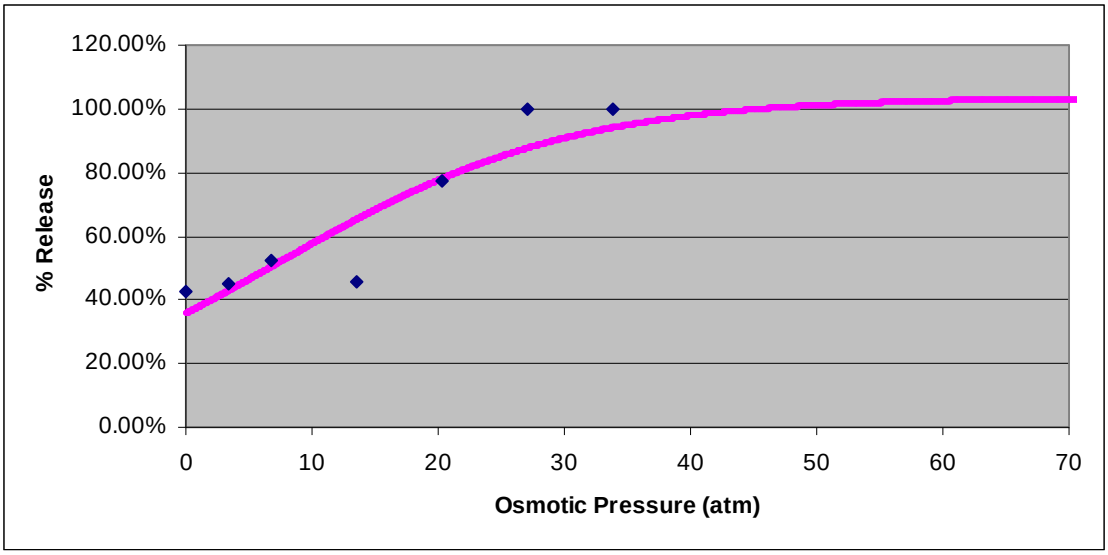

Table E.1 Fitting Constants

A	11.1022
B	10.7098
C	236.3907
D	-0.0867
E	-2.4542
R2	0.999995969

Figure E.3 45% Cholesterol – Bare Liposomes

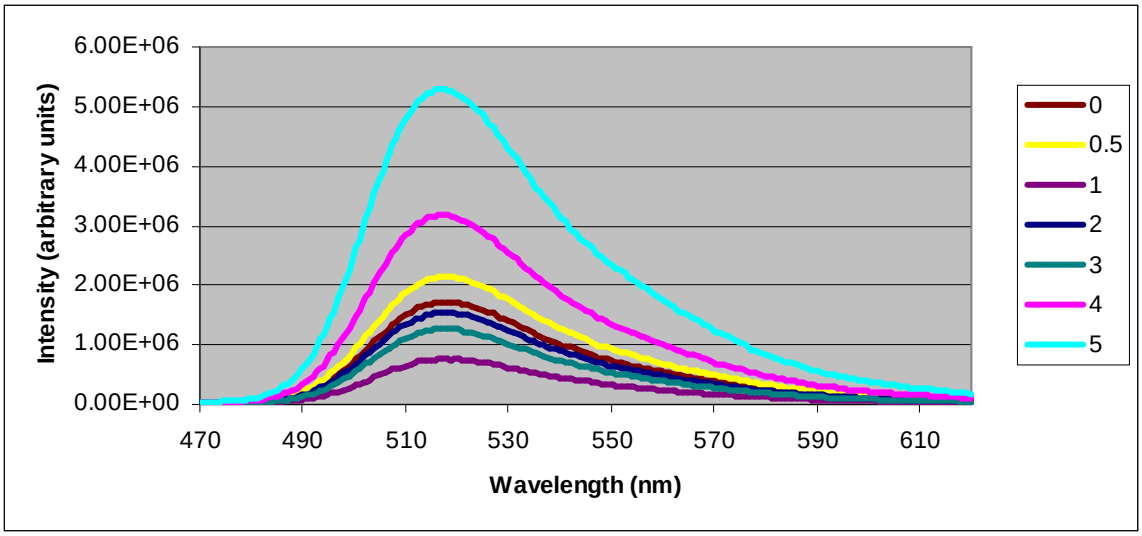

Figure E.4 Percent Release verses Osmotic Pressure Curve

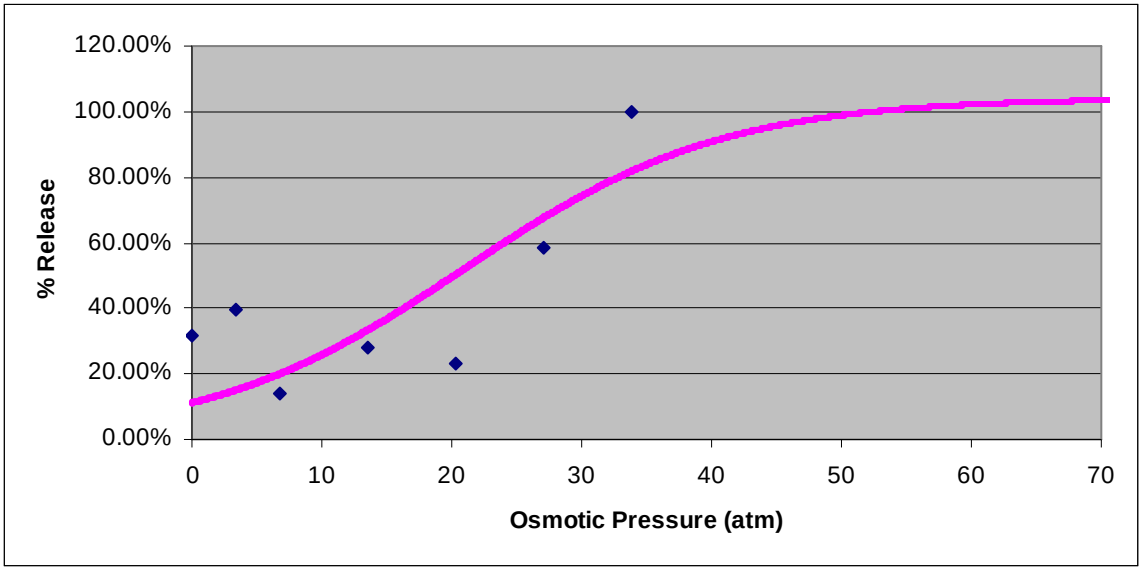

Table E.2 Fitting Constants

A	11.0612
B	10.6192
C	236.3969
D	-0.1010
E	-0.9850
R2	0.99999815

Figure E.5 20% Cholesterol – Polymer Caged Liposomes

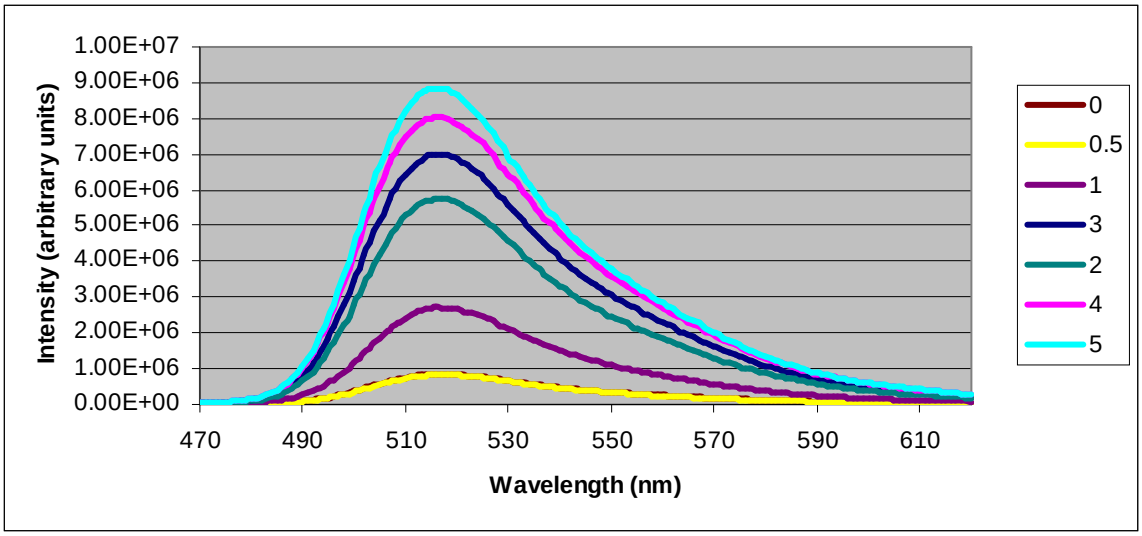

Figure E.6 Percent Release verses Osmotic Pressure Curve

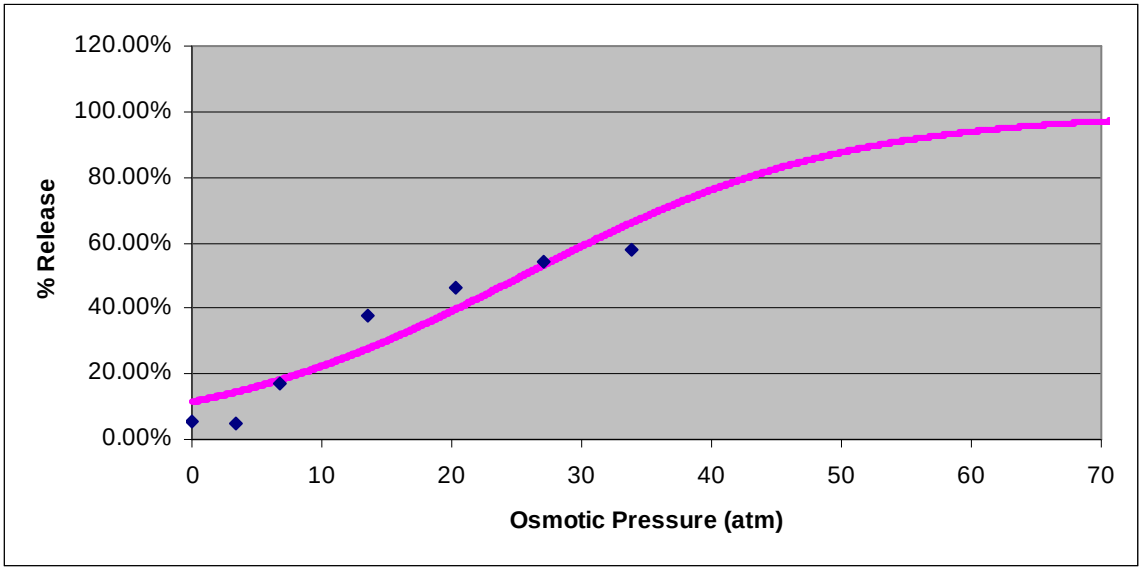

Table E.3 Fitting Constants

A	10.8296
B	10.8595
C	236.3967
D	-0.0804
E	-1.0361
R2	0.99999795

Figure E.7 45% Cholesterol – Polymer Caged Liposomes

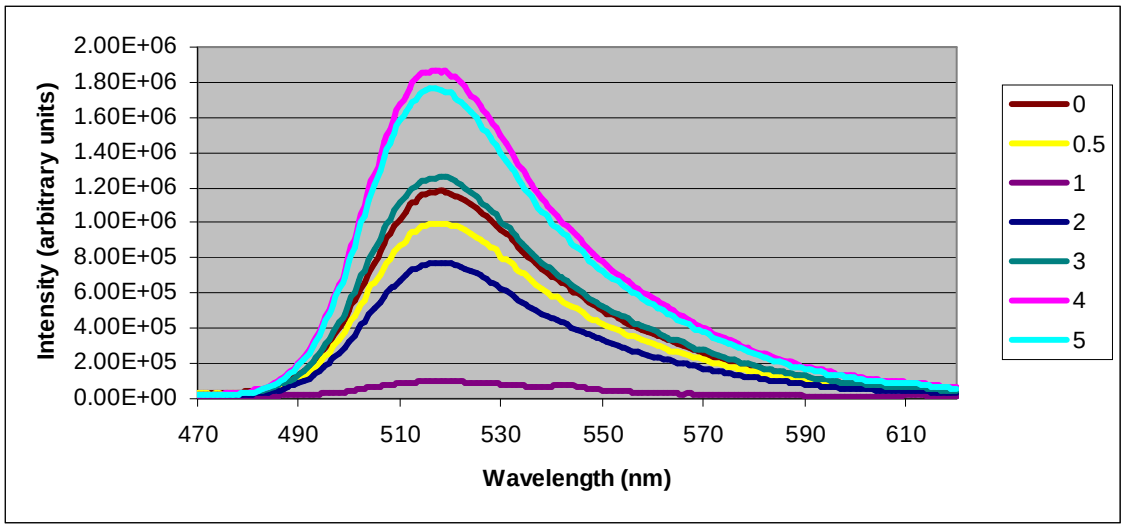

Figure E.8 Percent Release verses Osmotic Pressure Curve

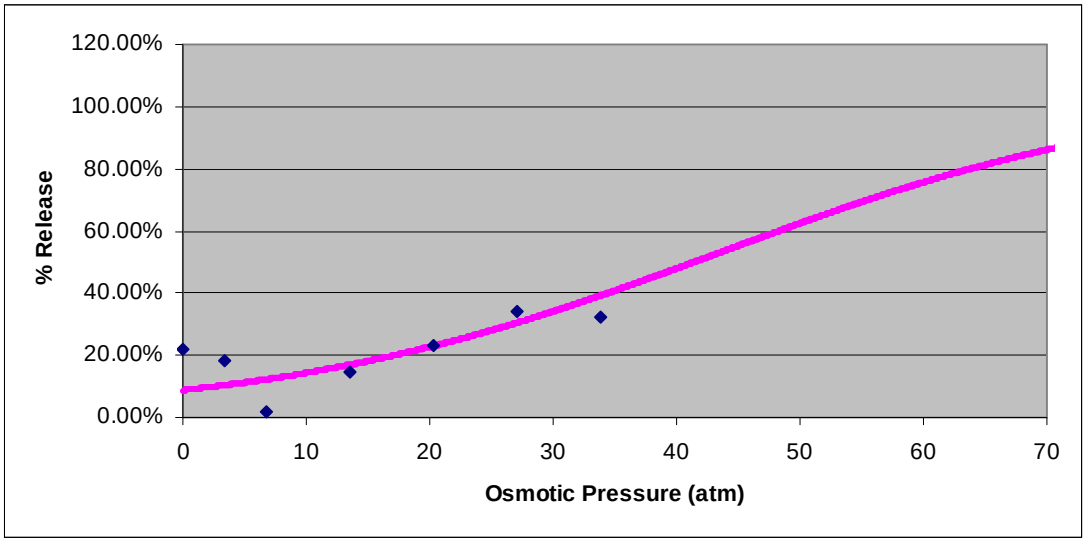

Table E.4 Fitting Constants

A	11.1366
B	10.5138
C	236.3981
D	-0.0554
E	-0.7073
R2	0.999997088

Appendix F Revisiting Polymer Content and Crosslinking

Figure F.1 Bare Liposomes Fluorescence

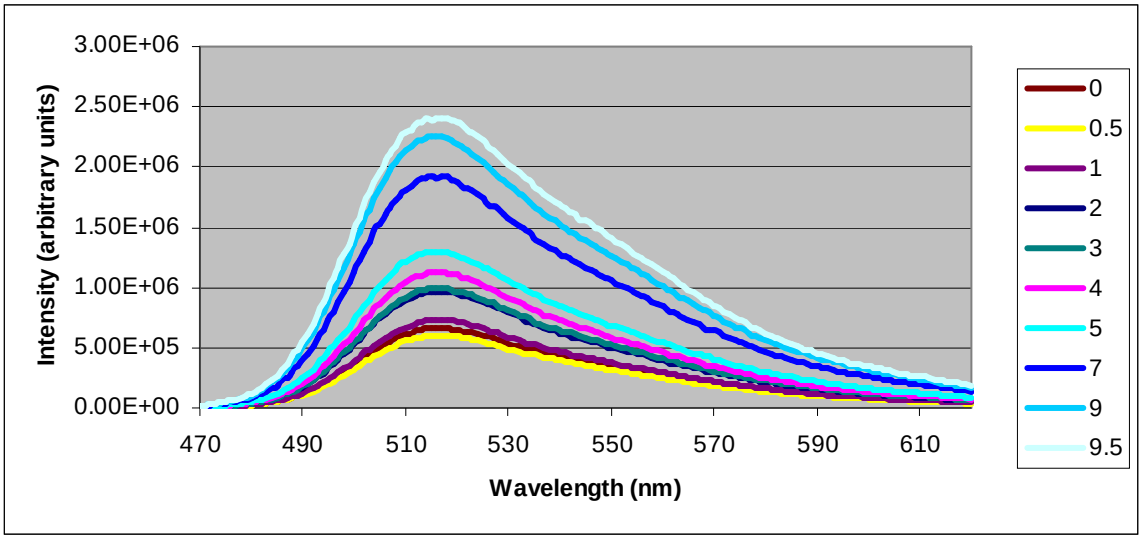

Figure F.2 Percent Release verses Osmotic Pressure Curve

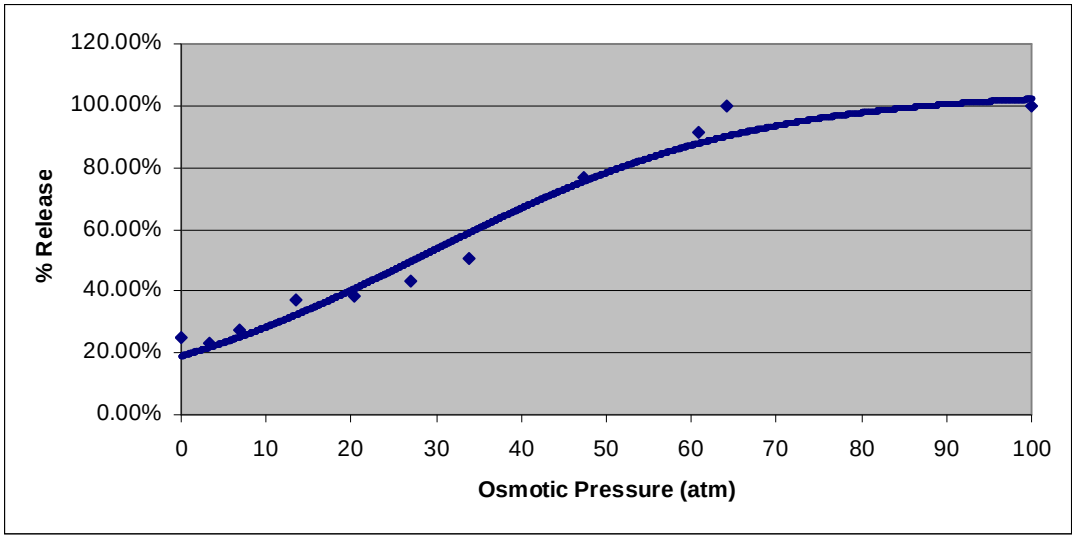

Table F.1 Fitting Constants

A	13.4547
B	12.8522
C	236.3951
D	-0.0519
E	-1.4063
R^2	0.999999068

Figure F.3 0.6% Polymer 50% Crosslinking Fluorescence

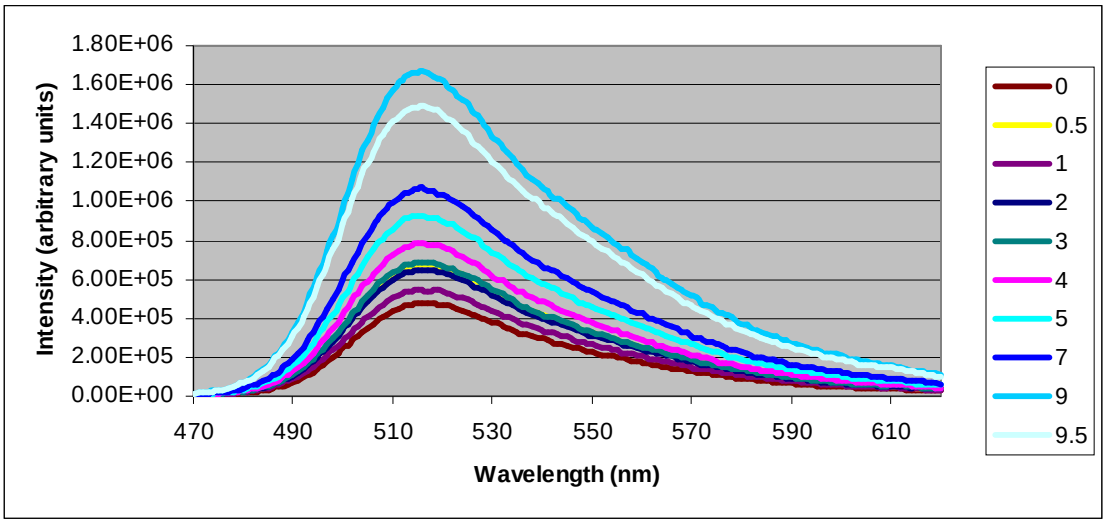

Figure F.4 Percent Release verses Osmotic Pressure Curve

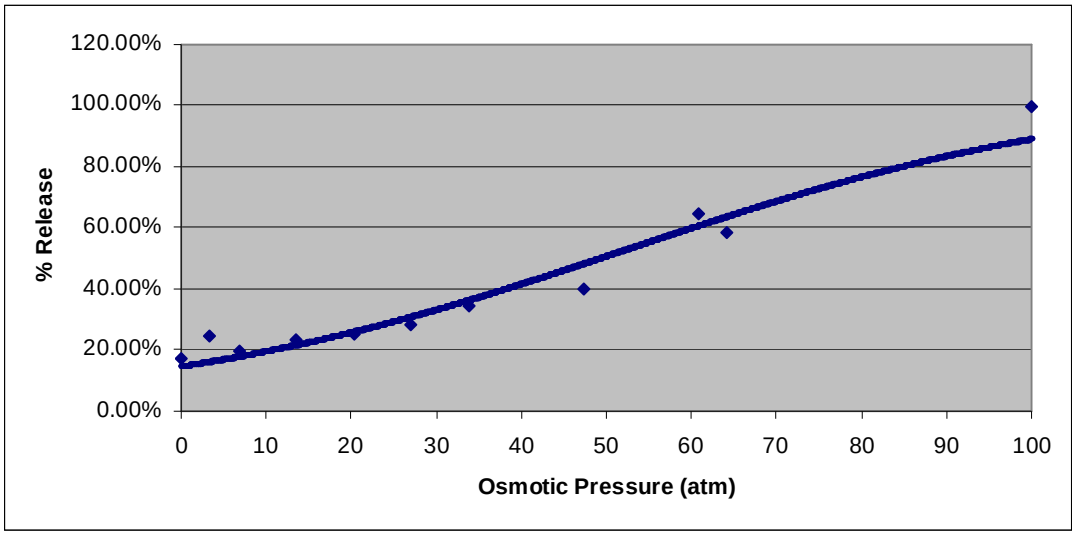

Table F.2 Fitting Constants

A	13.5202
B	12.7588
C	236.3965
D	-0.0349
E	-1.0863
R^2	0.999998988

Figure F.5 0.6% Polymer 75% Crosslinking

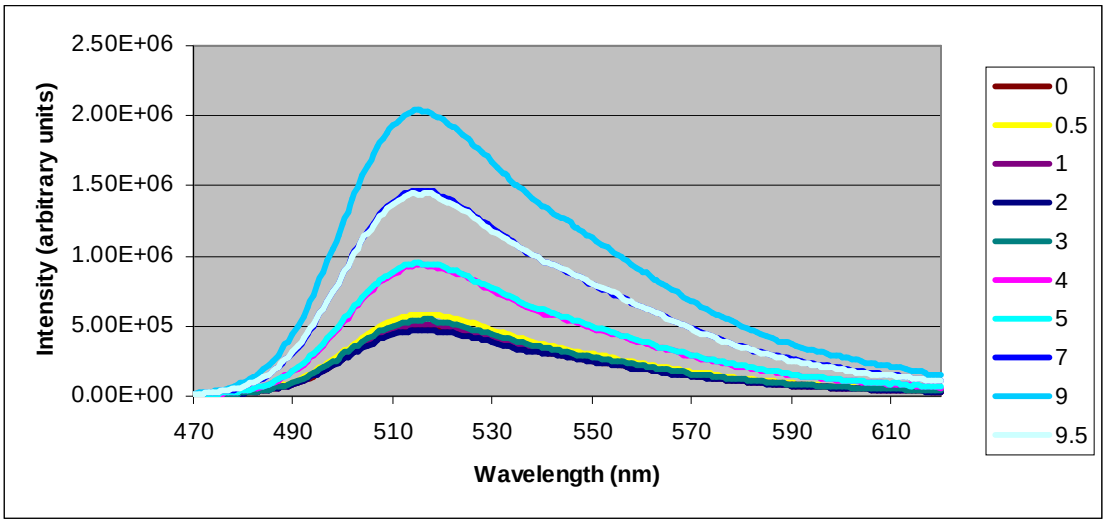

Figure F.6 Percent Release verses Osmotic Pressure Curve

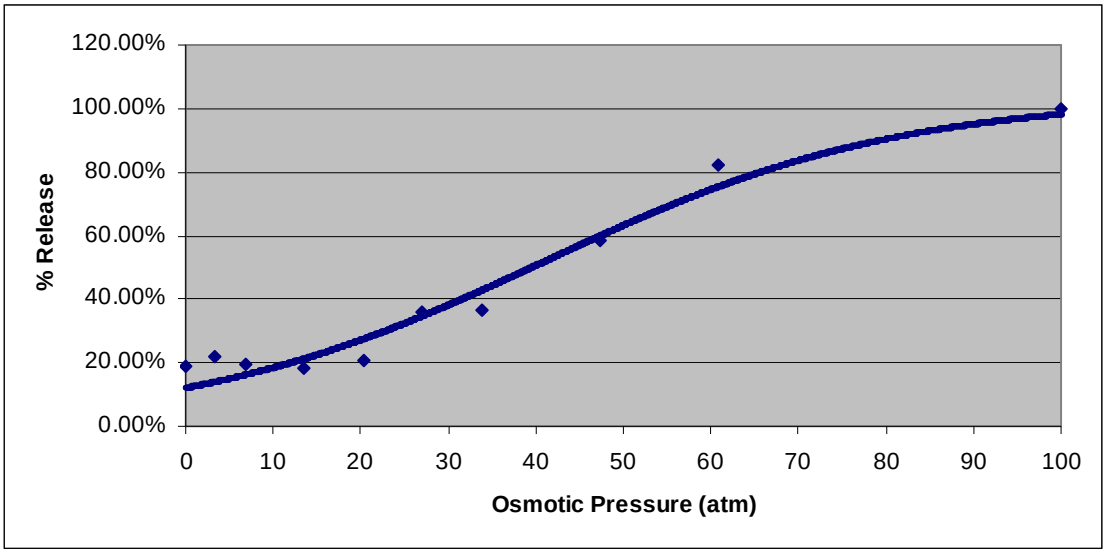

Table F.3 Fitting Constants

A	13.3590
B	12.9129
C	236.3973
D	-0.0495
E	-0.8853
R^2	0.999999211

Figure F.7 0.6% Polymer 100% Crosslinking

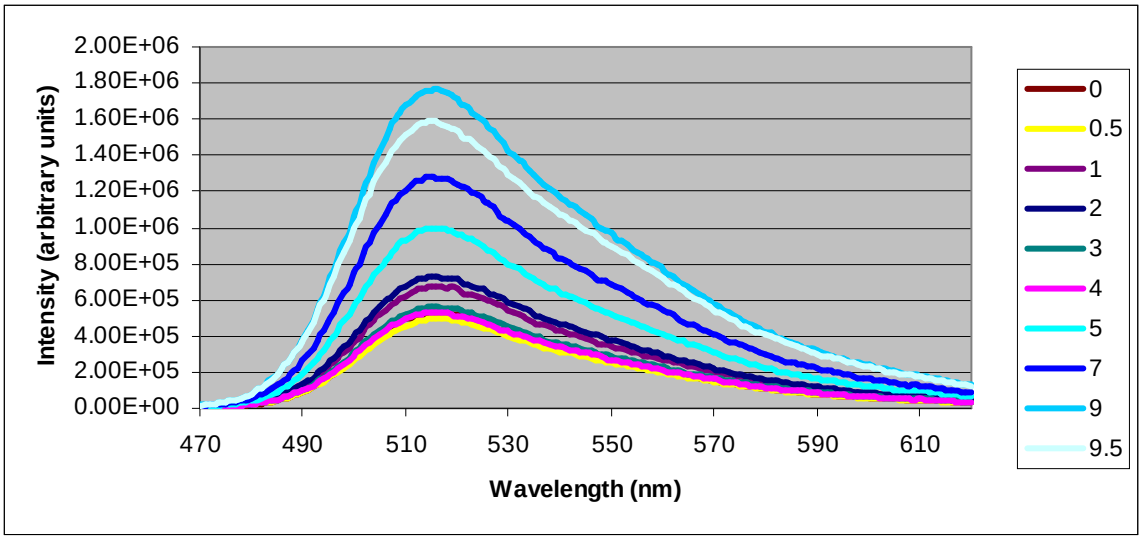

igure F.8 Percent Release verses Osmotic Pressure Curve

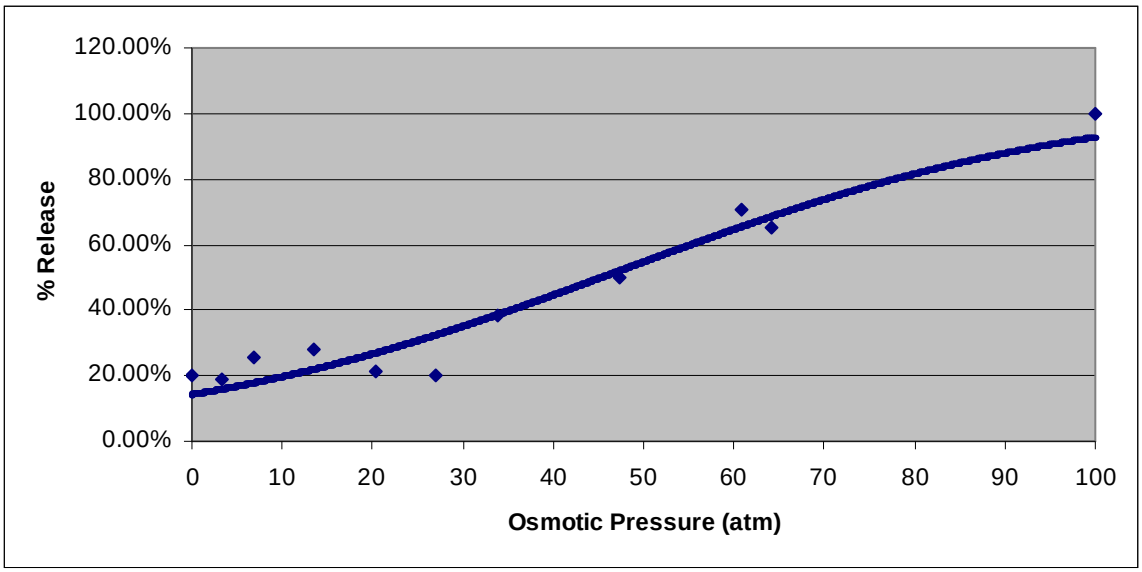

Table F.4 Fitting Constants

A	13.4649
B	12.8154
C	236.3966
D	-0.0387
E	-1.0627
R^2	0.99999877

Figure F.9 1.3% Polymer 50% Crosslinking

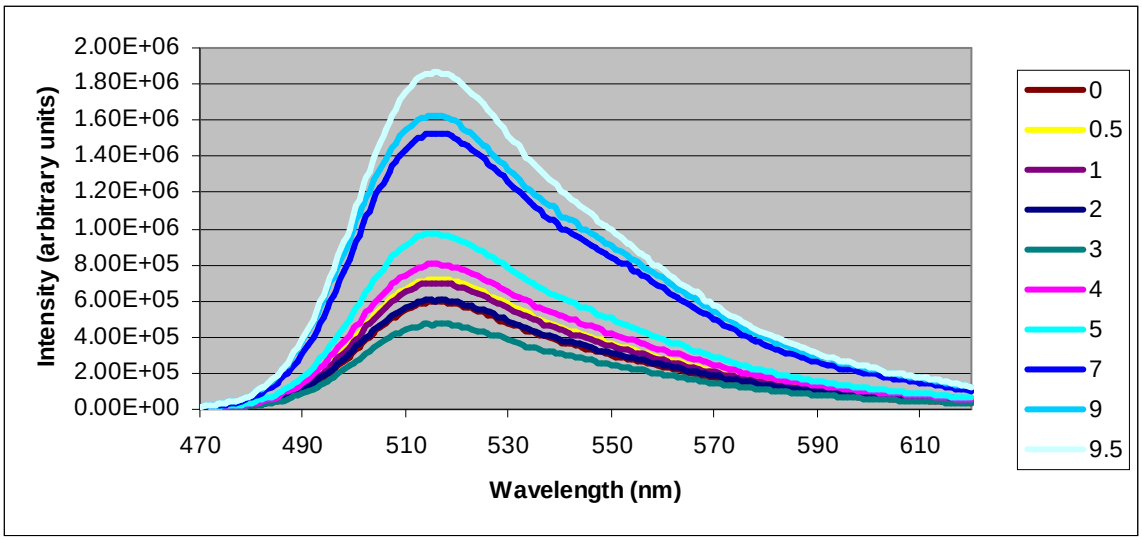

Figure F.10 Percent Release verses Osmotic Pressure Curve

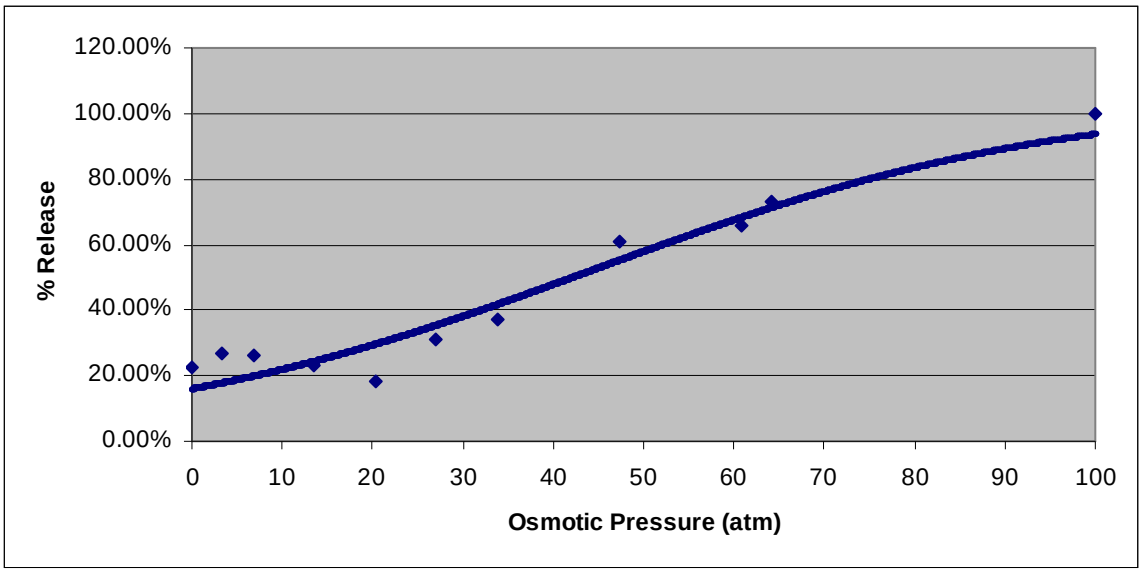

Table F.5 Fitting Constants

A	13.4523
B	12.8394
C	236.3960
D	-0.0385
E	-1.2011
R^2	0.999998748

Figure F.11 1.3% Polymer 75% Crosslinking

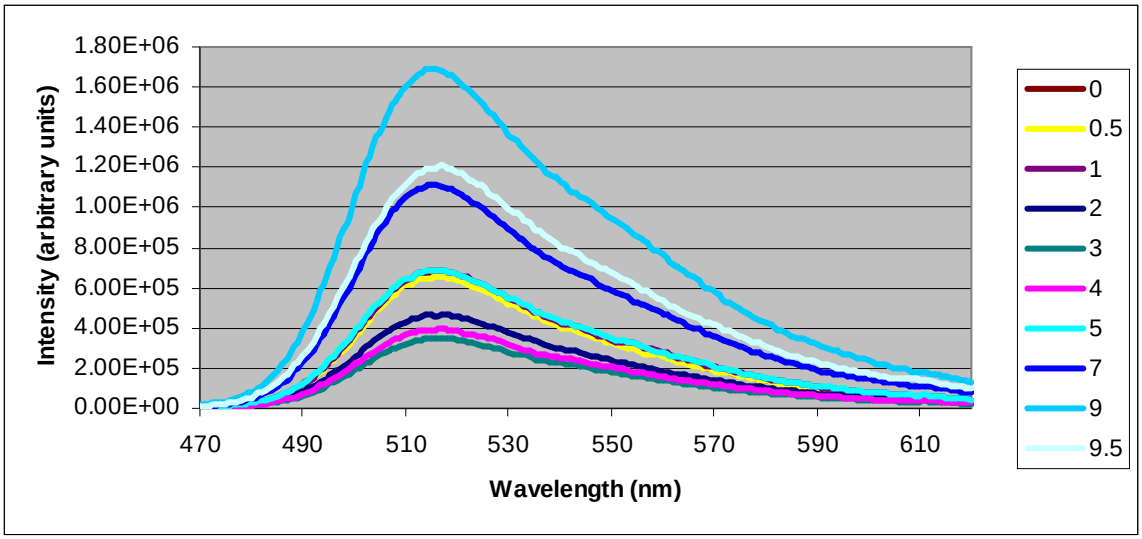

Figure F.12 Percent Release verses Osmotic Pressure Curve

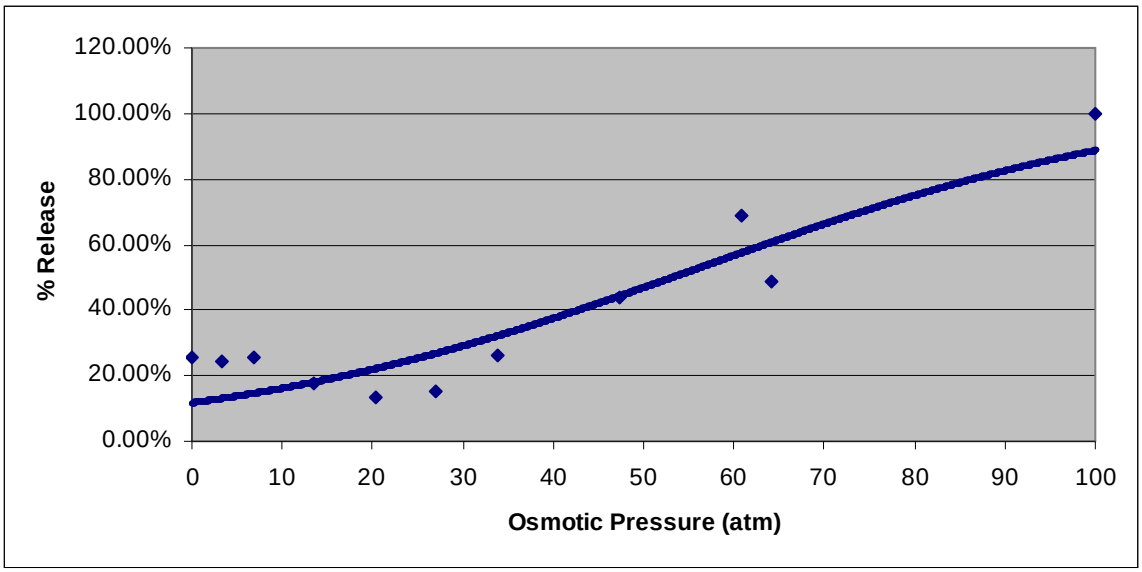

Table F.6 Fitting Constants

A	13.5403
B	12.7184
C	236.3976
D	-0.0369
E	-0.8366
R^2	0.999996771

Figure F.13 1.3% Polymer 100% Crosslinking

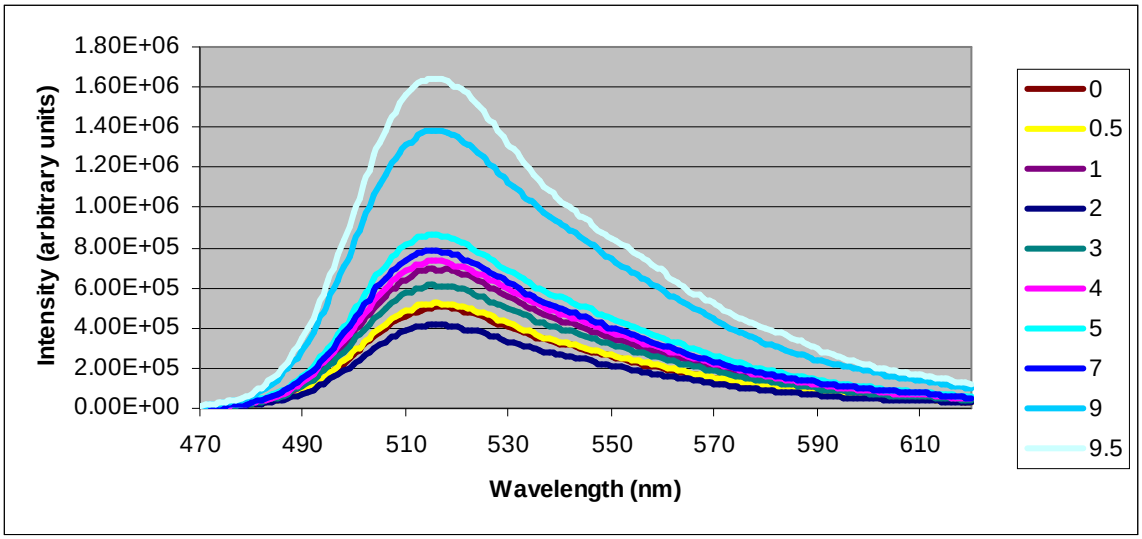

Figure F.14 Percent Release verses Osmotic Pressure Curve

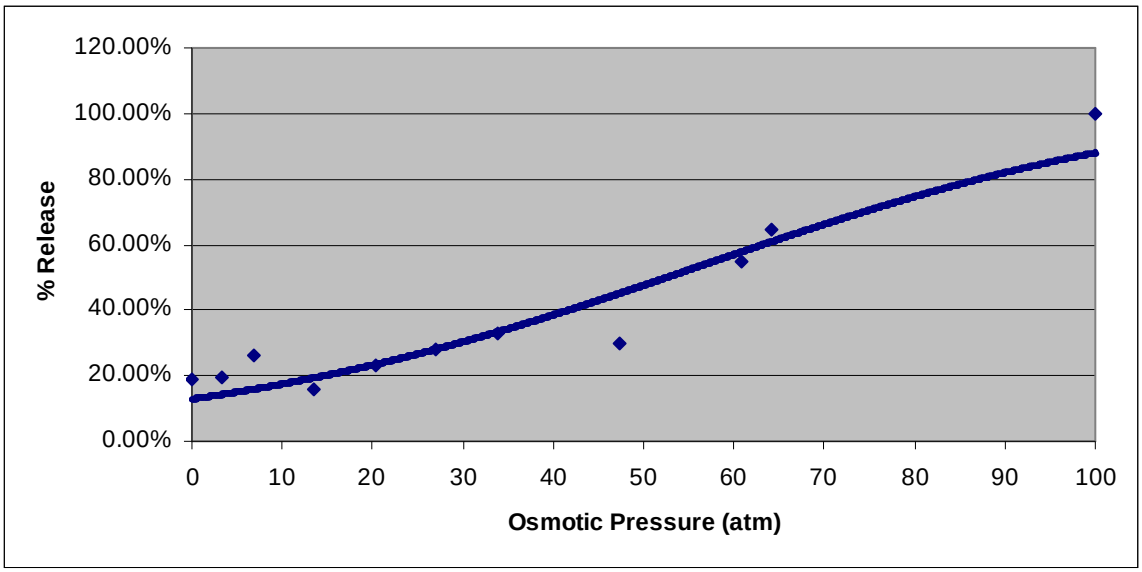

Table F.7 Fitting Constants

A	16.5264
B	15.4923
C	236.3980
D	-0.0354
E	-0.7421
R^2	0.999998231

Figure F.15 5.3% Polymer 50% Crosslinking

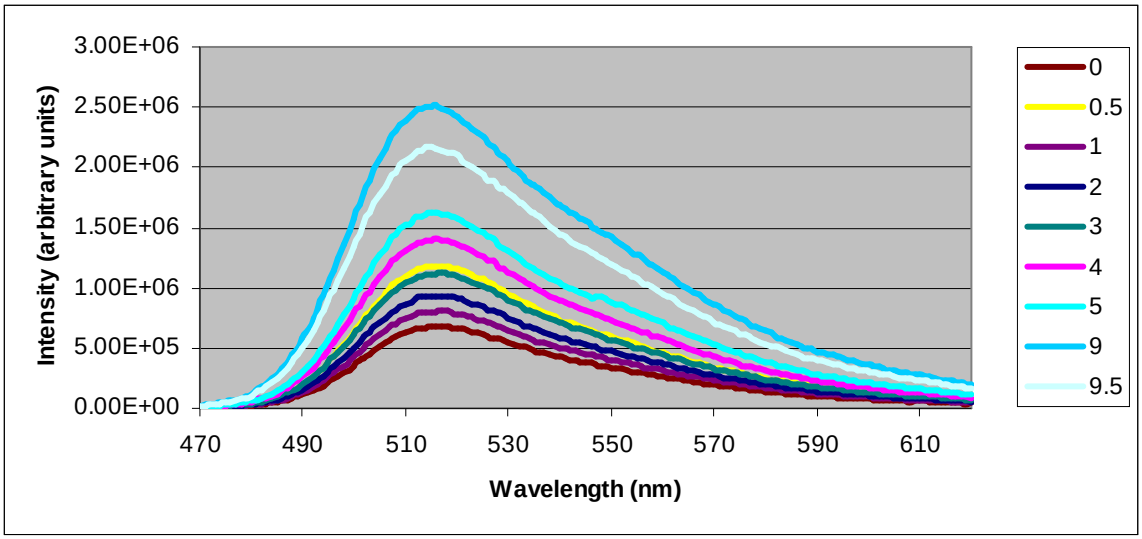

Figure F.16 Percent Release verses Osmotic Pressure Curve

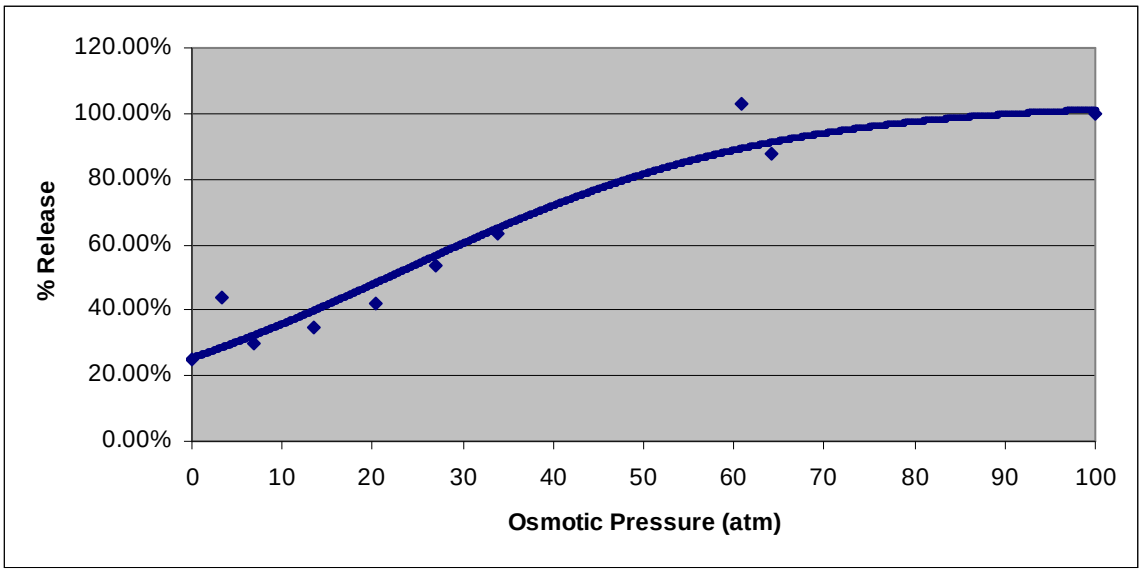

Table F.8 Fitting Constants

A	16.3310
B	15.7604
C	236.3944
D	-0.0486
E	-1.5848
R^2	0.999998514

Figure F.17 5.3% Polymer 75% Crosslinking

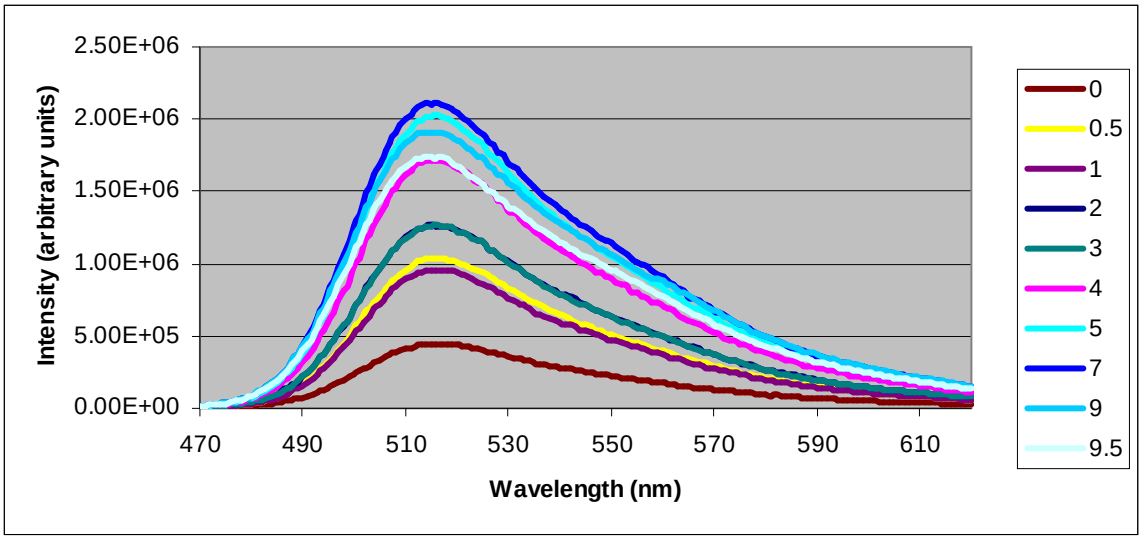

Figure F.18 Percent Release verses Osmotic Pressure Curve

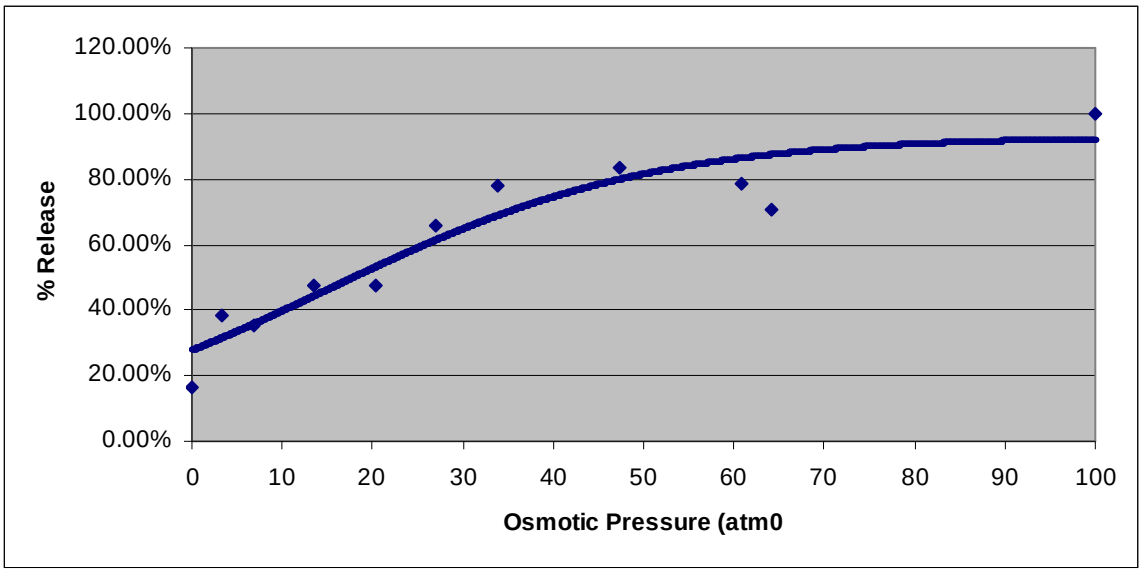

Table F.9 Fitting Constants

A	15.4834
B	16.6370
C	236.3935
D	-0.0562
E	-1.8014
R^2	0.99999774

Figure F.19 5.3% Polymer 100% Crosslinking

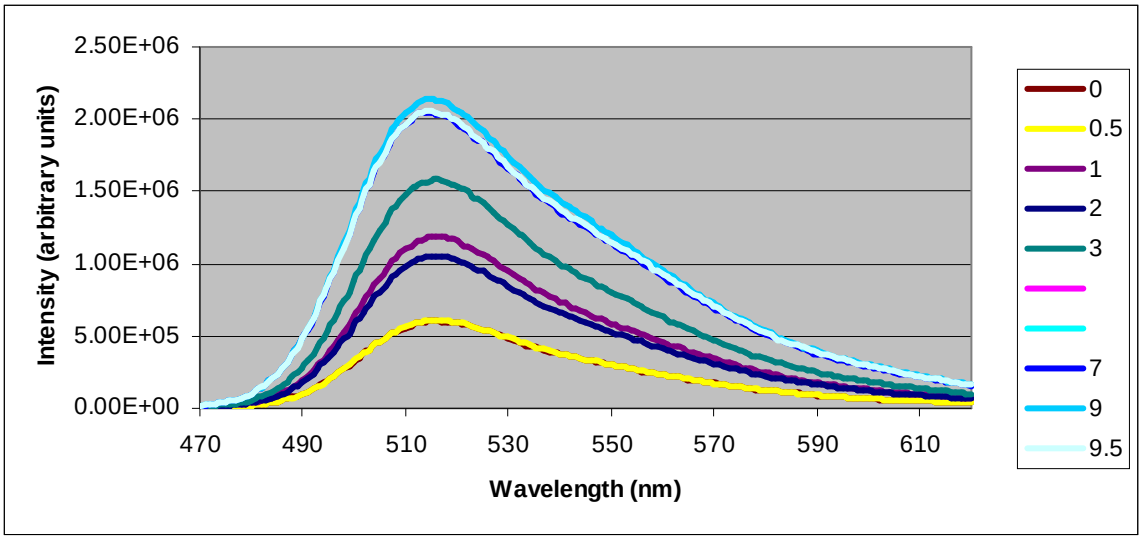

Figure F.20 Percent Release verses Osmotic Pressure Curve

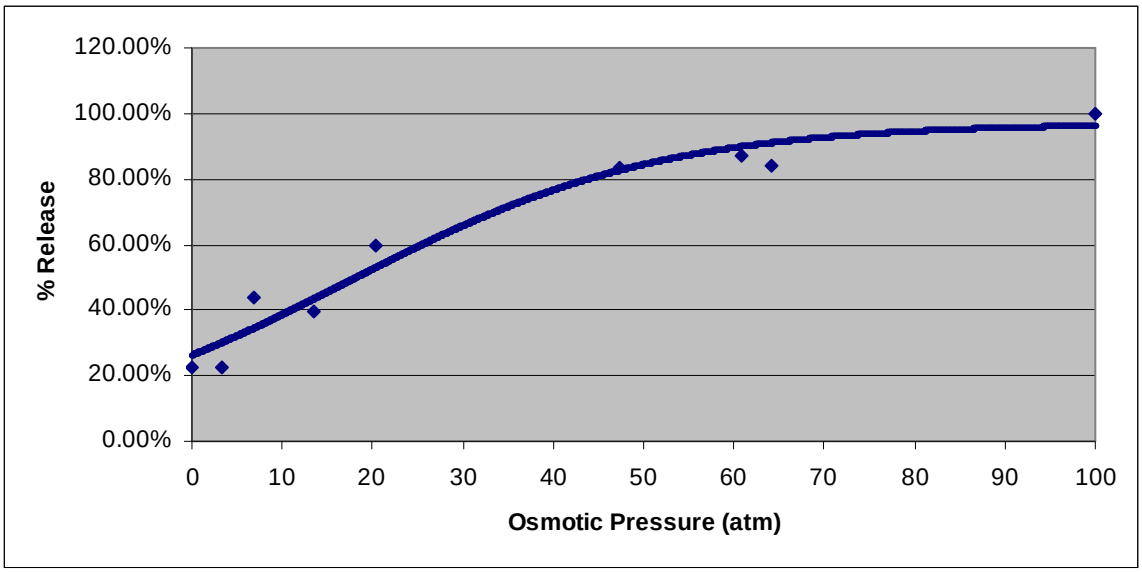

Table F.10 Fitting Constants

A	15.8163
B	16.2978
C	236.3940
D	-0.0579
E	-1.6845
R^2	0.999999097

Appendix G Protease Sensitivity First Test

Figure G.1 No uPA Fluorescent Intensity

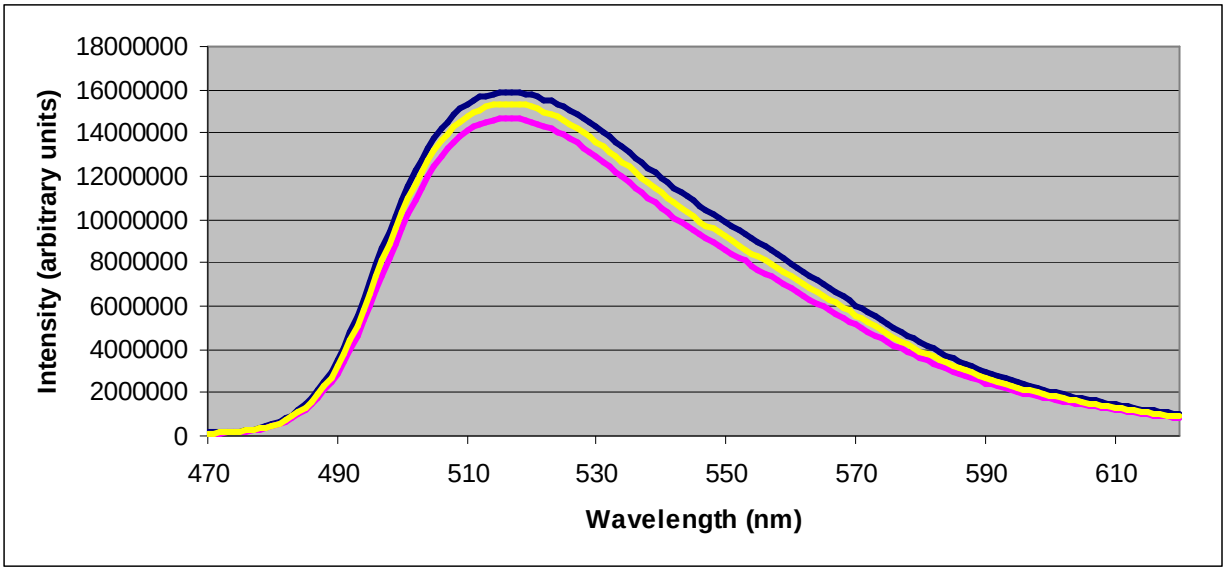

Figure G.2 + uPA Fluorescent Intensity

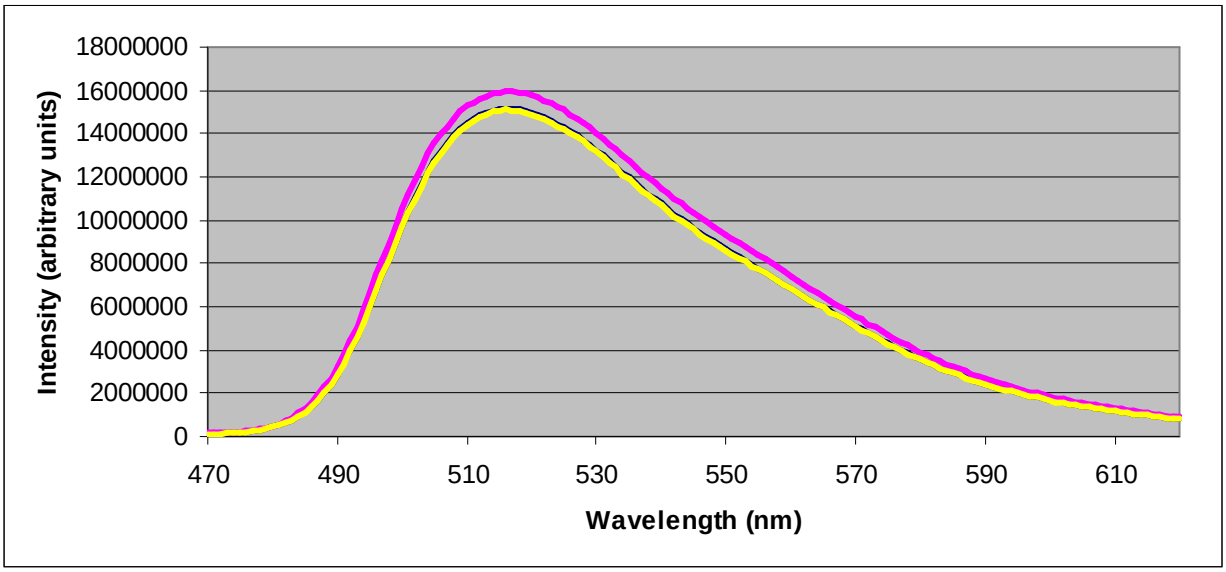

Appendix H Protease Sensitivity Second Test

Figure H.1 Baseline Fluorescent Intensity

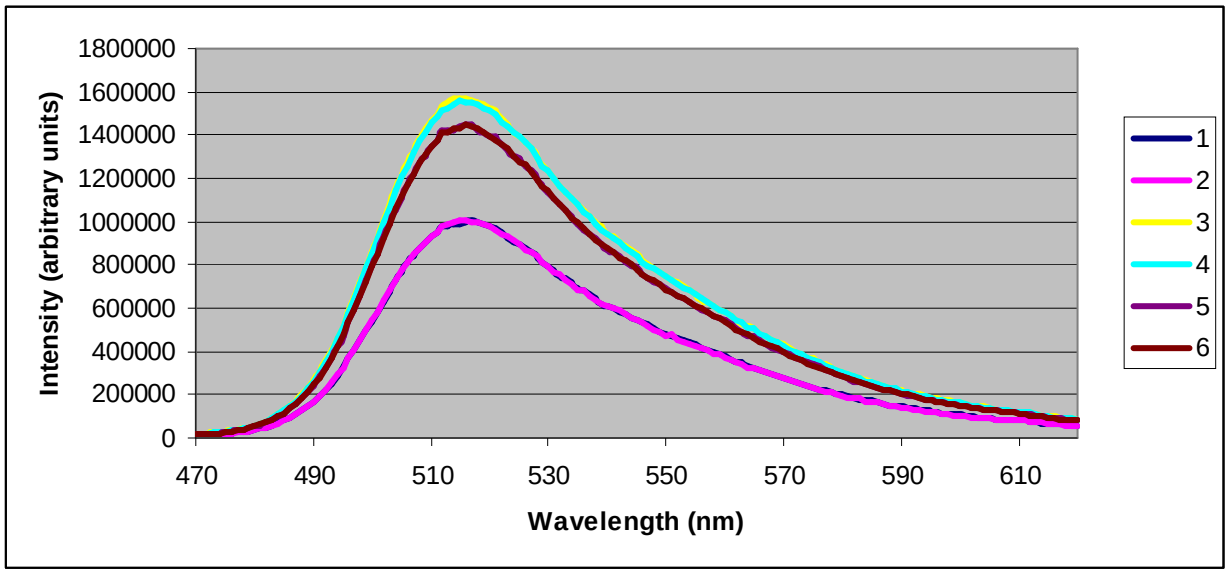

Figure H.2 – uPA Fluorescent Intensity

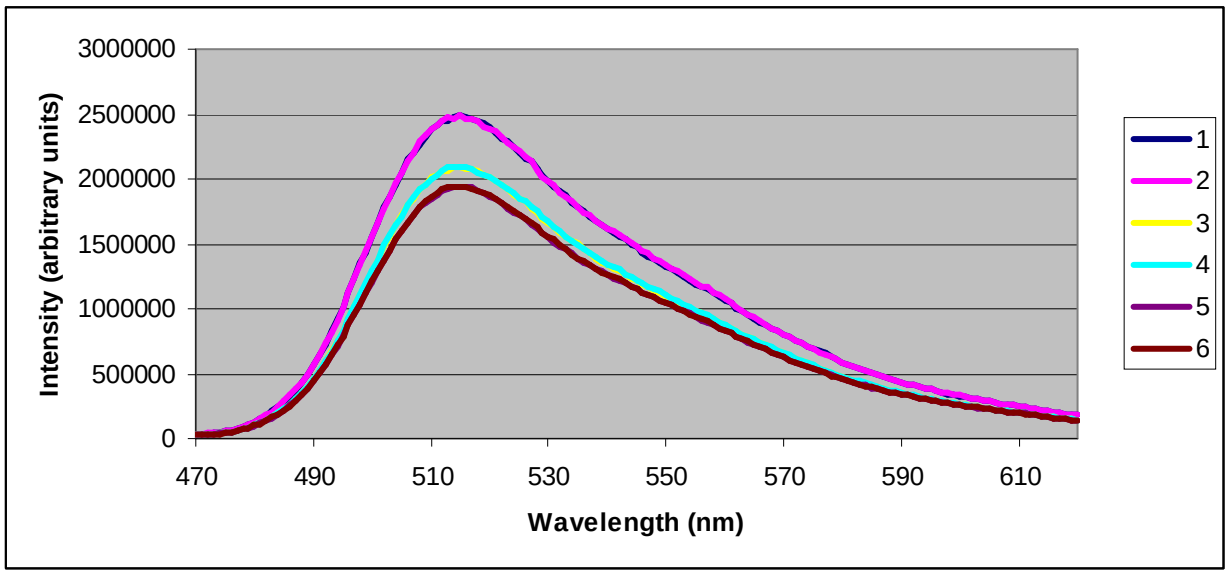

Figure H.3 + uPA Fluorescent Intensity

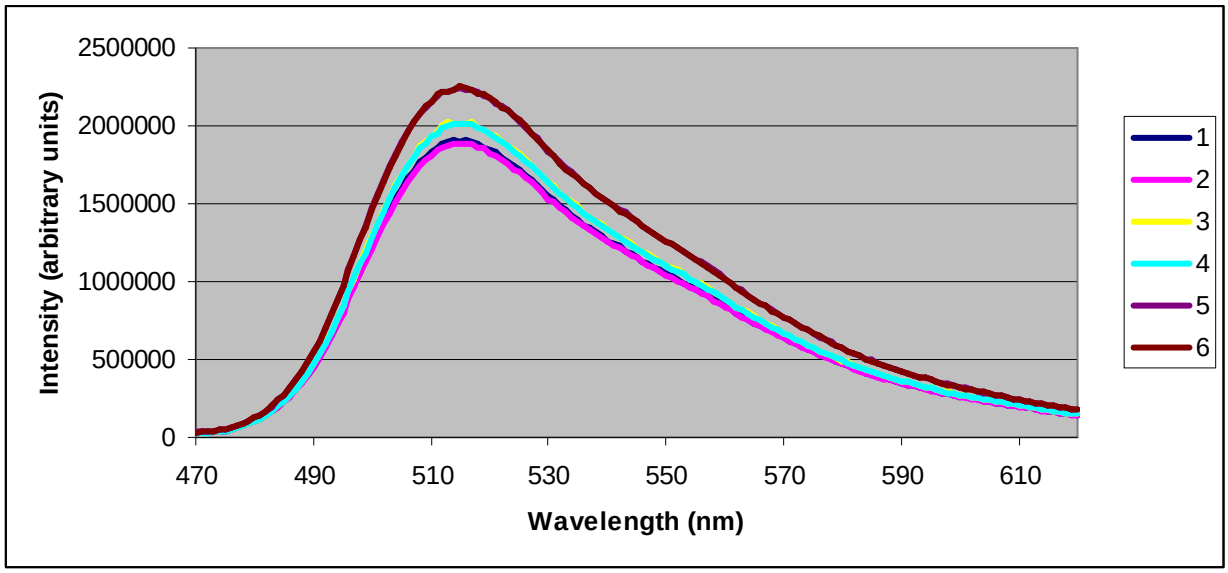

Appendix I Statistical Calculations

All statistics in this dissertation were done using a student's t-test to determine how likely the two samples being compared are the same. Equal variances were not assumed. The calculations used are as follows:

$$\sigma = \sqrt{\frac{\sum\left(x-\bar{x}\right)}{n-1}}$$

where σ is standard deviation, x is the measured value, xbar is the mean of the sample, and n is the number of measurements.

The t value is calculated as follows:

$$t = \frac{\overline{x_1} - \overline{x_2}}{s_{\overline{x_1}-\overline{x_2}}}$$

$$s_{\overline{x_1}-\overline{x_2}} = \sqrt{\frac{\sigma_1^2}{n_1} + \frac{\sigma_2^2}{n_2}}$$

where t is the t value. The degrees of freedom (D.F.) can also be calculated by:

$$D.F. = \frac{\left(\sigma_1^2/n_1 + \sigma_2^2/n_2\right)^2}{\left[\left(\sigma_1^2/n_1\right)^2/(n-1)\right] + \left[\left(\sigma_2^2/n_2\right)^2/(n_2-1)\right]}$$

The t value and the degrees of freedom can then be used to calculate the p value by plugging into a p value calculator. P values less than 0.05 are generally thought of as significant, and P values less than 0.01 are considered very significant. Significance increases with decreasing P value after this.